UNIVERSIDADE FEDERAL DE PERNAMBUCO
CENTRO DE TECNOLOGIA E GEOCIÊNCIAS
PROGRAMA DE PÓS-GRADUAÇÃO EM ENGENHARIA CIVIL

YANE COUTINHO LIRA

IMPACT OF AAR-REACTIVE FILLERS ON ASR-INDUCED DEVELOPMENT

Recife
2025

YANE COUTINHO LIRA

IMPACT OF AAR-REACTIVE FILLERS ON ASR-INDUCED DEVELOPMENT

Thesis presented to the Civil Engineering Graduate Program of the Universidade Federal de Pernambuco, as a requirement to obtain the title of Ph.D in Civil Engineering.
Concentration area: Structures with emphasis in Civil Construction.

Supervisor: Prof. Dr. Arnaldo Manoel Pereira Carneiro

Co-supervisor: Prof. Dr. Leandro Francisco Moretti Sanchez

Recife

2025

YANE COUTINHO LIRA

IMPACT OF AAR-REACTIVE FILLERS ON ASR-INDUCED DEVELOPMENT

Thesis presented to the Civil Engineering Graduate Program of the Universidade Federal de Pernambuco, Center of Technology and Geoscience, as a partial requirement to obtain the title of Ph.D in Civil Engineering, area of Structures with emphasis in Civil Construction.

.

Approved in 25/07/2025

Supervisor: Prof. Dr. Arnaldo Manoel Pereira Carneiro, Universidade Federal de Pernambuco

Co-supervisor: Prof. Dr. Leandro Francisco Moretti Sanchez, University of Ottawa

EXAMINATION BOARD

participation by videoconference
Prof. Dr. Diego Jesus de Souza (External Examiner)
Technical University of Denmark

participation by videoconference
Prof. Dr. Isabel Fernandes (External Examiner
University of Lisbon

participation by videoconference
Prof. Dr. Medhat Shehata (External Examiner)
Toronto Metropolitan University

participation by videoconference
Prof. Dr. Cassandra Trottier (External Examiner)
College la Cité

participation by videoconference
Prof. Dr. Nicole Hasparyk (External Examiner)
Consultant

To my mom, for everything, always.

.Catalogação de Publicação na Fonte. UFPE - Biblioteca Central

Lira, Yane Coutinho.
Impact of AAR-Reactive Fillers on ASR-Induced Development / Yane Coutinho Lira. - Recife, 2025.
181f.: il.

Tese (Doutorado) - Universidade Federal de Pernambuco, Centro de Tecnologia e Geociências, Programa de Pós-Graduação em Engenharia Civil, 2025.
Orientação: Arnaldo Manoel Pereira Carneiro.
Coorientação: Leandro Francisco Moretti Sanchez.
Inclui referências e apêndices.

1. Alkali-aggregate reaction; 2. Alkali-silica reaction; 3. Aggregate mineral fillers; 4. AAR-reactive AMFs; 5. ASR-reactive AMFs; 6. Multilevel assessment. I. Carneiro, Arnaldo Manoel Pereira. II. Sanchez, Leandro Francisco Moretti. III. Título.

UFPE-Biblioteca Central

ACKNOWLEDGEMENTS

The journey to complete the Ph.D was long and difficult, but I was lucky to have by my side the most wonderful people, to whom I will always be grateful.

First, I would like to thank my supervisor, Prof. Arnaldo Carneiro, for guiding me since the Master's program and supporting me in moments I was driven by curiosity, as well as in my objective to go abroad.

I would also like to thank my co-supervisor, Prof. Leandro Sanchez, who believed in the project and received me in his research group, guided me and supported me to complete a bold research program considering the time available. Thank you for all the discussions and for all the engineering and life lessons.

In this important moment in my research career, I could not forget to mention the one who led me into the research path, professor Milton Bezerra das Chagas Filho. More than a former professor and supervisor, he is a lifelong mentor and friend that has taught much more than Engineering but precious life lessons that shaped me into a better person.

Thank you to all colleagues of Labtag, in particular Priscilla and Igor, who have dedicated several hours to help me with tests and analyses.

I also acknowledge the contribution of professors Lauro Montefalco, Nathália Lima, and Pedro Guzzo, in Brazil, and of St. Marys Cement, in Canada, for the collaboration to perform tests in their laboratories.

My deepest thanks to all the colleagues in the μStructure group, which became for me a family in Canada. Thank you for all the discussions, all the help, and all the shared moments in the laboratory.

Thank you to my great friends Kai, Rennan, and Yuri for all the long hours of batching, measurements, DRI, SDT, and the good moments shared. Special thanks to Rennan and Monica, who were there for me since the very first moment in Ottawa, and Kai, who was always with me in every situation, supporting me, listening to me, giving me advice, and sharing good food.

I could not forget my friends in Brazil that shared half of the journey in person and half virtually. Thank you Danilo, Fernanda, Sophia, and Thalissa for your presence in my life.

I would like to recognize the important role of the technical officers of the Materials and Structures laboratory at uOttawa, Concrete laboratory at UFPE, and

Laboratory of Mineral Technology at UFPE, Drs. Muslim Majeed and Gamal Elnabelsya, Rinaldo Catunda, and Marcelo Gomes. They were essential during the experimental program. A special thanks to Gamal and Nadinho, for making rough places, such as Structures laboratories, a light work environment.

I cannot thank enough my mom, who raised me by overcoming unimaginable difficulties and has always supported me in all my dreams. I would not be the person I am without her.

Thank you for the Coordination for the Improvement of Higher Education Personnel (CAPES), for the financial support by means of a PhD scholarship (88887.814410/2023-00**)** and PRINT grant (88887.900098/2023-00), which enabled me to have full dedication to the research and expand the scope of the study with the exchange to the University of Ottawa.

“The truth, however ugly in itself, is always curious and beautiful to seekers after it.”

Agatha Christie

ABSTRACT

The NetZero target has stimulated studies focused on reducing CO_2 emissions in several industries. In the cement industry, one of the approaches is the use of supplementary cementitious materials and aggregate mineral fillers (AMFs) to partially replace cement. However, some of the rocks used to produce AMFs may be susceptible to alkali-aggregate reaction (AAR), a harmful distress mechanism affecting critical concrete infrastructure, and their impact in concrete durability remains unclear. Considering this context, this study aimed to contribute to comprehending the effect of AAR-reactive AMFs on AAR-induced damage in concrete. Initially, a thorough literature review was conducted to understand the current state of the art and identify knowledge gaps concerning the use of AAR-reactive AMFs, focusing on the roles of mineralogy, particle size distribution (PSD), replacement content, and the test methods used to assess AAR kinetics, ultimate expansion, and associated microscopic and mechanical deterioration. Based on the gaps found, an experimental program was designed to assess the influence of alkali-silica reaction (ASR)-reactive AMFs on ASR-induced damage in concrete when used to replace cement in systems with reactive and non-reactive aggregates. Three systems were evaluated: one with non-reactive aggregates (mixtures A), one with reactive coarse aggregates (mixtures B, Springhill), and one with reactive fine aggregates (mixtures C, Texas sand). Two reactive rocks were used to produce fillers, one moderately reactive mylonite and one highly reactive greywacke, with varying PSDs (i.e., <150 μm and <75 μm) and used at cement replacement rates of 10% and 20%. The concrete prism test (CPT) was adopted to monitor expansions and kinetics. To evaluate the deterioration process, the multilevel assessment was applied by means of microstructural (i.e., damage rating index – DRI) and mechanical (i.e., stiffness damage test – SDT) evaluations at 1, 3, and 6 months. For the systems with reactive aggregates, results indicated that ASR-reactive AMFs altered the kinetics of the systems in different ways, which was related to the competition for alkalis at early ages. The expansion rate reduced, tending to stabilization from 180 and 60 days for mixtures B and C, respectively. Mechanical degradation remained significant, as evidenced by increased stiffness damage index values and reduced modulus of elasticity over time. In general, the introduction of ASR-reactive AMFs in a system with reactive coarse aggregates did not alter the ultimate expansion and degradation when compared to a system with the same aggregate with

no fillers. For a system with reactive fine aggregates, the ultimate expansion was reduced but the degradation level was significant when compared to a system with no fillers. For the system with non-reactive aggregates, the filler reactivity, PSD, and percentage significantly affected expansion behavior, with finer PSD materials (<75 μm) promoting higher expansions. Despite some expansion, the values remained in general below the threshold set by standards. Moreover, negligible physical damage was observed. The findings indicate that ASR-reactive AMFs can be a viable alternative for blended cements and suggest that CPT combined with multilevel assessment is a reliable approach for evaluating ASR-reactive AMFs.

Keywords: alkali-aggregate reaction; alkali-silica reaction; aggregate mineral fillers; AAR-reactive AMFs; ASR-reactive AMFs; multilevel assessment.

RESUMO

A meta NetZero tem estimulado pesquisas com foco em reduzir as emissões de CO_2 em diversas indústrias. Na indústria cimenteira, uma das estratégias é a substituição parcial do cimento por materiais cimentícios suplementares e fílers minerais de aggregados (FMA). Contudo, algumas das rochas utilizadas para produzir FMAs podem ser suscetíveis à reação álcali-agregado (RAA), um mecanismo de deterioração que afeta infraestruturas de concreto, e seu impacto na durabilidade de concreto ainda não está claro. Desta forma, este estudo teve como objetivo contribuir para a compreensão do efeito de fílers reativos à RAA nos danos causados pela RAA em concreto. Inicialmente, foi realizada uma revisão bibliográfica aprofundada para mapear o estado da arte e identificar lacunas relacionadas ao uso de fílers reativos à RAA, com foco na influência da mineralogia, distribuição granulométrica (DG), teor de substituição e métodos de ensaio para avaliação da cinética da RAA, expansão final e danos microscópicos e mecânicos associados. Com base nas lacunas identificadas, foi elaborado um programa experimental para avaliar o impacto de fílers reativos à reação álcali-sílica (RAS) nos danos causados pela RAS em concretos, quando utilizados substituindo o cimento em três sistemas distintos: i) com agregados não reativos (misturas A), ii) com agregado graúdo reativo (misturas B, Springhill), e iii) com agregado miúdo reativo (misturas C, Texas sand). Duas rochas reativas foram utilizadas para a produção dos fílers: um milonito moderadamente reativo e uma grauvaca altamente reativa, com diferentes DGs (i.e., <150 µm, <75 µm), empregados em teores de substituição de cimento de 10% e 20%. O ensaio de prismas de concreto (CPT) foi adotado para monitorar as expansões e a cinética da reação. A avaliação multinível foi aplicada para avaliar o processo de deterioração, por meio de análises microestruturais (i.e., índice de deterioração – DRI) e mecânicas (i.e., ensaio de deterioração de rigidez – SDT) nas idades de 1, 3 e 6 meses. Nos sistemas com agregados reativos, os fílers reativos à RAS alteraram a cinética da reação de maneiras distintas, o que pode estar relacionado à competição por álcalis nas idades iniciais. As taxas de expansão diminuíram tendendo à estabilização a partir de 180 (misturas B) e 60 dias (misturas C). A degradação mecânica permaneceu significativa, conforme evidenciado pelo aumento dos índices de deterioração de rigidez e pela redução do módulo de elasticidade ao longo do tempo. De modo geral, a introdução de fílers reativos à RAS em um sistema com agregado graúdo reativo não alterou a

expansão final nem a degradação, em comparação com um sistema semelhante sem fílers. Para o sistema com agregado miúdo reativo, a expansão final foi reduzida, mas o nível de degradação permaneceu significativo em relação ao sistema sem fílers. No sistema com agregados não reativos, a reatividade dos fílers, a DG e o teor de substituição influenciaram significativamente o comportamento expansivo, com partículas mais finas (<75 μm) promovendo maiores expansões. Apesar disso, os valores permaneceram, em geral, abaixo dos limites normativos, e os danos físicos foram considerados desprezíveis. Os resultados indicam que fílers reativos à RAS podem ser uma alternativa viável para cimentos compostos, desde que suas características sejam controladas. Ademais, o CPT, combinado com a avaliação multinível, mostrou-se eficaz na avaliação desses materiais.

Palavras-chave: reação álcali-agregado; reação álcali-sílica; fílers minerais de agregado; fílers reativos à RAA; fílers reativos à RAS; avaliação multinível.

LIST OF FIGURES

LIST OF TABLES

LIST OF ABBREVIATIONS AND ACRONYMS

AAR	Alkali-aggregate reaction
ACI	American Concrete Institute
ACPT	Accelerated concrete prism test
ACR	Alkali-carbonate reaction
AMBT	Accelerated mortar bar test
ANOVA	Analysis of variance
ASTM	American Society for Testing and Materials
AMF	Aggregate mineral filler
ASR	Alkali-silica reaction
BET	Brunauer–Emmett–Teller
CA	Coarse aggregate
CPT	Concrete prism test
CSA	Canadian Standards Association
D10 / D50 / D90	Percentile sizes in particle distribution curves (10%, 50%, 90%)
DF	Degrees of freedom
DRI	Damage rating index
F (ANOVA)	Fisher statistic
FA	Fine aggregate
GU	General use (cement type)
LOI	Loss on ignition
MS	Mean square
NR	Non reactive
NS	Not significant
PDI	Plastic deformation index
PSD	Particle size distribution
P-value	Probability value
R	Reactive
RH	Relative humidity
S	Significant
SCM	Supplementary cementitious material
SDI	Stiffness damage index

SDT	Stiffness damage test
SH	Springhill
SSA	Specific surface area
TX	Texas sand
XRD	X-ray diffraction
XRF	X-ray fluorescence

LIST OF SYMBOLS

Al_2O_3	Aluminum oxide
CaO	Calcium oxide
CH, $Ca(OH)_2$	Calcium hydroxide
CO_2	Carbon dioxide
C-S-H	Calcium silicate hydrate
Fe_2O_3	Iron (III) oxide
K_2O	Potassium oxide
MgO	Magnesium oxide
MnO	Manganese (II) oxide
Na_2O	Sodium oxide
Na_2O_{eq}	Alkali equivalent
P_2O_5	Phosphorus Pentoxide
SiO_2	Silicon dioxide
TiO_2	Titanium dioxide

TABLE OF CONTENTS

CHAPTER 1 – INTRODUCTION

Sustainable measures to reduce the carbon footprint have led to an increasing interest in alternative construction materials. Concrete, in particular, has been the focus of numerous studies as it is the most used construction material worldwide (HANZIC; HO, 2017). The demand for concrete is forecasted to increase from the current 14 bn m^3 to 20 bn m^3 per year by 2050 (GCCA, 2021).

The Net-Zero carbon emissions target, which consists of reaching a balance between emissions of greenhouse gas and removal from the atmosphere by 2050, has set a new scenario in the construction industry (IEA, 2021). This mainly affects the production of cement, which was estimated to generate 0.6 tons of CO_2 per ton of cement produced, from which two-thirds are from calcination reactions to produce clinker (IEA, 2021). Reducing the clinker-to-cementitious materials ratio by partially replacing cement with a supplementary cementitious material (SCM) or fillers is a viable alternative to reduce CO_2 emissions in the short term (AMRAN *et al*., 2022; BALLAN; PAONE, 2014; DAMTOFT *et al*., 2008; EUROPEAN CEMENT RESEARCH ACADEMY, 2017; GARTNER; HIRAO, 2015; IEA, 2020; LOTHENBACH; SCRIVENER; HOOTON, 2011; LUDWIG; ZHANG, 2015; MILLER *et al*., 2021; SCRIVENER *et al*., 2018; SCRIVENER; JOHN; GARTNER, 2018; VON GREVE-DIERFELD *et al*., 2020).

In this regard, as conventional SCMs are byproducts of some industries, their supply tends to decrease in the coming years, which requires the study of alternative materials. Fillers are chemically inert materials that contribute to improving concrete properties via improved packing and introduction of nucleation sites for hydration products (AQEL; PANESAR, 2016; KORPA; KOWALD; TRETTIN, 2008; LI *et al*., 2018; LOTHENBACH; SCRIVENER; HOOTON, 2011; MOOSBERG-BUSTNES; LAGERBLAD; FORSSBERG, 2004). Among the materials commonly used, limestone has been widely adopted owing to its low cost and availability worldwide (BERGMANN *et al*., 2024; WANG *et al*., 2018; XIA; BERGMANN; SANCHEZ, 2024). The percentage of this material that can be used varies from 11% to 35% (ABNT, 2018a; CAC, 2023). In Brazil, the maximum amount allowed is 25%, whereas in Canada this value is 15% (ABNT, 2018a; CAC, 2023).

Considering this scenario, the use of aggregate mineral fillers (AMFs), defined as finely divided inorganic materials produced in crushing operations of rocks (ACI, 2020), has also been considered as an alternative to be used replacing cement. The main characteristics of AFMs that affect concrete properties are particle morphology and size, particle size distribution (PSD), mineralogy, deleterious materials, and density (ACI, 2020).

AFMs from different sources, including quartzite (CRAEYE *et al*., 2010; KADRI *et al*., 2010; POPPE; DE SCHUTTER, 2005; RAHHAL; TALERO, 2005), alumina (POPPE; DE SCHUTTER, 2005), basalt (DOBISZEWSKA; SCHINDLER; PICHÓR, 2018; LI *et al*., 2021; SOROKA; SETTER, 1977; XIE *et al*., 2024; ZHU *et al*., 2024), diabase (ZHU *et al*., 2024), tuff (ZHU *et al*., 2024), dolomite (SOROKA; SETTER, 1977), marble (MULTON *et al*., 2010; VARDHAN *et al*., 2015), and granite (COUTINHO; MONTEFALCO; CARNEIRO, 2024; MÁRMOL *et al*., 2010; RAMOS *et al*., 2013), have been studied.

Among the rocks used to produce AMFs, some may be susceptible to alkali-aggregate reaction (AAR). AAR refers to a chemical reaction between certain mineral phases in the aggregates and the alkalis present in the concrete pore solutions (FOURNIER; BERUBÉ, 2000; LEEMANN *et al*., 2024a; NIXON; SIMS, 2016). This reaction is commonly divided into two main mechanisms: alkali-silica reaction (ASR) and alkali-carbonate reaction (ACR) (FOURNIER; BÉRUBÉ, 2011). ASR involves the interaction between metastable siliceous phases in the aggregate and hydroxyl ions in the pore solution. This reaction forms a hydrophilic expansive gel (i.e., ASR gel) that has a surface charge opposite to that of the aggregate, generating a repulsive force at the interface, leading to progressive expansion and deterioration of the affected concrete (LEEMANN *et al*., 2024a). ASR has been reported to affect critical concrete infrastructure worldwide (SIMS; POOLE, 2017). In contrast, the mechanism of ACR remains under debate and has only been identified in a limited number of countries (GRATTAN-BELLEW *et al*., 2010; KATAYAMA, 1992, 2010; KATAYAMA; GRATTAN-BELLEW, 2012; LEEMANN *et al*., 2024b; MEDEIROS; SANCHEZ; DOS SANTOS, 2024; THOMAS; FOURNIER; FOLLIARD, 2013).

Fillers from AAR-reactive rocks have been used in several studies to evaluate their effects in different concrete properties, as well as their mitigation potential to ASR expansions (ALVES et al., 1997; BRAGA *et al*., 1991; CARLES-GIBERGUES *et al*.,

2008; COUTINHO; MONTEFALCO; CARNEIRO, 2024; CYR; RIVARD; LABRECQUE, 2009; LI; HE; HU, 2015; OLIVEIRA; SALLES; ANDRIOLO, 1995; TAPAS *et al*., 2023). The most commonly used tests are the accelerated mortar bar test (ABMT) and concrete prism test (CPT). However, these traditional tests were developed to assess aggregates and their effectiveness in evaluating the behaviour of AAR-reactive fillers is still unknown. In fact, conflicting results have been reported for the same conditions when using AMBT and CPT in systems with AAR-reactive AMFs (CASTRO *et al*., 1997; COUTINHO; MONTEFALCO; CARNEIRO, 2024; OLIVEIRA; SALLES; ANDRIOLO, 1995; PEDERSEN, 2004; TAPAS *et al*., 2023). This highlights the need to critically examine whether existing test methods are appropriate for assessing the impact of AAR-reactive fillers in concrete.

As AAR-reactive rocks can be found worldwide, the use of fillers from crushing of rocks replacing cements in the production of concrete can be a viable alternative in both sustainable and economic perspectives, considering the current scenario of reduction of CO_2 emissions. However, a more in-depth study is necessary to better understand the effect of this material on AAR expansions considering both reactive and non-reactive systems. In this regard, some parameters related to the use of reactive fillers, such as mineralogy, PSD, and replacement percentage need to be further studied. Moreover, the type of test applied should also be assessed, as it is still unclear whether current methods to evaluate aggregate reactivity can be used to assess the effect of AAR-reactive fillers. Therefore, this study aims to contribute to the understanding of ASR-reactive fillers action on ASR-induced damage in concrete.

1.1. OBJECTIVES

The objectives of the present study are described as follows.

1.1.1. General objective

This study aims to contribute to a better understanding of the effect of ASR-reactive AMFs when used partially replacing cement in different systems (i.e., reactive and con-reactive) and considering various parameters (i.e., type of fillers, PSD, and cement replacement percentage) in ASR-induced damage in concrete.

1.1.2. Specific objectives

The specific objectives of the thesis are:

- Establish the current state of the art and identify knowledge gaps concerning the use of ASR-reactive AMFs;
- Evaluate the impact of adding ASR-reactive AMFs in reactive systems with either coarse or fine reactive aggregates, considering parameters such as type of AMF, PSD, and cement replacement percentage, and assess the adequacy of the CPT to test systems with ASR-reactive AMFs;
- Analyze the impact of adding ASR-reactive AMFs in non-reactive systems considering parameters such as type of AMF, PSD, and percentage, and assess the adequacy of the CPT to test systems non-reactive systems with ASR-reactive AMFs.

1.2. STRUCTURE OF THE THESIS

The thesis is structured into seven chapters. Chapters 4 to 6 report results and discussion in paper format for submission to journals.

Chapter 1 introduces the topic studied, indicating its importance and relevance. The objectives and structure of the thesis are also presented.

Chapter 2 is a literature review of the study, with a discussion about the use of fillers in concrete. The state of the art on the use of AAR-reactive fillers in concrete is discussed and knowledge gaps are identified. The gaps identified based the definition of the approach and experimental program proposed.

Chapter 3 describes the materials, characterization, and methods used in this study.

Chapter 4 is presented in the form of a literature review paper on the use of AAR-reactive fillers in concrete, focusing on the tests that have been used, evaluation of the deterioration process, as well as the role of filer mineralogy, PSD, and replacement content, highlighting gaps to be addressed in future studies.

Chapter 5 presents the evaluation of the action of AAR-reactive fillers when used in reactive systems. The parameters assessed were type of filler, PSD, and replacement percentage. The CPT was conducted to determine the AAR-induced expansion and

the multilevel assessment was applied to evaluate the AAR-induced deterioration in reactive systems.

Chapter 6 provides a further analysis regarding the effect of AAR-reactive AMFs in concrete. In this chapter, the focus is on non-reactive systems with ASR-reactive AMFs to understand the individual influence of the fillers used. Expansions were monitored using CPT and the AAR-induced deterioration was assessed through the multilevel assessment. The results are discussed.

Chapter 7 presents the final considerations of the study, with conclusions and recommendations for future studies.

CHAPTER 2 – LITERATURE REVIEW

2.1 AGGREGATE MINERAL FILLERS

A filler can be defined as a particulate product that is inert or almost chemically inert when mixed with cement (ACI, 2020; JOHN *et al.,* 2018). The American Concrete Institute defines AMFs as a finely divided inorganic material produced in crushing operations of rocks (ACI, 2020). In this regard, limestone is treated separately, as its production undergoes a more controlled process and the final product is more consistent, whereas other AMFs have different characteristics depending on their source rock and crushing and separation processes. Any material that is volumetrically stable when exposed to cement hydration products and does not negatively influence durability can be used as filler (SCRIVENER; JOHN; GARTNER, 2018).

The use of limestone replacing Portland cement dates to the latter part of the 19th century, when it was considered an adulteration of cement (MAYFIELD, 1990). The use of limestone in cement was only included in standards in the 1980s as a means to reduce energy consumption owing to the uncertainty caused by the oil crisis in the 1970s (MAYFIELD, 1990). The first reported use of AFMs was in the construction of Elephant Butte and Arrowrock Dams from 1912 to 1916. In these dams, 48% and 45% of the binder was replaced by sandstone and granite, respectively. The AFMs were milled in a ball mill and subsequently interground with cement until 90% of the mixture was <75 μm (MEISSNER, 1950). Both dams are still operating, and no major interventions have been reported (US BUREAU OF RECLAMATION, n. d.).

Fillers considerably affect the hydration of the clinker phases, the chemical structure of the cement paste and concrete, and, consequently, fresh and hardened state properties of concrete (LOTHENBACH; SCRIVENER; HOOTON, 2011; MOOSBERG-BUSTNES; LAGERBLAD; FORSSBERG, 2004; TIA; CHUNG; SUBGRANON, 2021). The actions of fillers in concrete are mainly physical, consisting of the modification of the PSD, heterogeneous nucleation, and dilution (KORPA; KOWALD; TRETTIN, 2008; MOOSBERG-BUSTNES; LAGERBLAD; FORSSBERG, 2004; TIA; CHUNG; SUBGRANON, 2021). In particular, limestone also has a chemical effect as it reacts with calcium aluminate to form calcium monocarboaluminate (AQEL; PANESAR, 2016; BONAVETTI; RAHHAL; IRASSAR, 2001; DE WEERDT *et al.,* 2011; LI *et al.,* 2018; LOTHENBACH *et al.,* 2008).

The modification of PSD results in improved compactness of the concrete owing to the reduced size of the grains that fill the spaces between large particles (AQEL; PANESAR, 2016). The extra surface provided by fillers acts as nucleation sites for the precipitation of hydration products (AQEL; PANESAR, 2016; LI *et al.,* 2018; LOTHENBACH; SCRIVENER; HOOTON, 2011; MOOSBERG-BUSTNES; LAGERBLAD; FORSSBERG, 2004). Dilution refers to the reduction of binder concentration because of replacement by inert material, which consequently reduces the rate of hydration product development (AQEL; PANESAR, 2016; JOHN *et al.,* 2018).

The dilution effect is compensated at early ages by the improved PSD and nucleation (AQEL; PANESAR, 2016). At later ages, this effect can be compensated by reducing the amount of mixing water, which can be achieved by improving particle packing and consequently reducing the space that should be filled by water (JOHN *et al.,* 2018). The increased packing can promote maintenance of mechanical properties of concrete while requiring less cement. In this case, most of the water is adsorbed on the surface of grains, and the use of admixtures is essential to keep the same water/binder ratio, with a good homogenization of cement and fillers, and an adequate workability (MOOSBERG-BUSTNES; LAGERBLAD; FORSSBERG, 2004).

The optimization of the PSD and consequent reduction of water content can be achieved by using particle packing models (PPMs) (DE GRAZIA; SANCHEZ, 2024). The combined use of PPMs and limestone can lead to a reduction of cement content by >50% (PALM *et al.,* 2016; SCRIVENER; JOHN; GARTNER, 2018) while maintaining performance and durability (PALM *et al.,* 2016). These strategies enable the use of fillers in high percentages replacing cement. However, further evaluations on durability aspects, as well as on the use of other AMFs, are necessary.

2.1.1 Influence of AMFs on Concrete Properties

The use of AMFs in concrete affects the hydration kinetics as well as properties such as setting time, permeability, and porosity, which influence the mechanical performance of concrete and, consequently, its resistance against deterioration mechanisms.

The hydration kinetics seems to be influenced by the type of AMF as well as the fineness (CRAEYE *et al.,* 2010; KADRI *et al.,* 2010). Limestone, for instance, promotes an acceleration of the hydration kinetics at early ages, with a reduction of the induction period (CRAEYE *et al.,* 2010; KUMAR *et al.,* 2013; POPPE; DE SCHUTTER, 2005; YE *et al.,* 2007). This is because the extra surface promotes faster precipitation of hydration products, also resulting in early age strength gain (CRAEYE *et al.,* 2010). Alumina filler also had an acceleration effect for particles ≤1.5 μm in the first hours of reaction, related to the nucleation effect. The same was observed for basalt filler, with a less intense acceleration compared to that of limestone (XIE *et al.,* 2024). In contrast, quartzite filler had only a slight influence on the hydration kinetics, regardless of its PSD (CRAEYE *et al.,* 2010; KADRI *et al.,* 2010; POPPE; DE SCHUTTER, 2005). Moreover, limestone also leads to an increase of the maximum hydration production rate, whereas quartzite does not alter this parameter (POPPE; DE SCHUTTER, 2005).

Regarding setting times, a higher percentage of limestone replacing cement leads to a shorter initial setting time given that the limestone particles are finer than those of cement (BOUASKER *et al.,* 2008; KUMAR *et al.,* 2013; WANG *et al.,* 2018). This is in agreement with results on hydration kinetics, in which reactions are accelerated in the first hours of hydration. For particles coarser than those of cement, no significant influence is observed (KUMAR *et al.,* 2013). In contrast, when using marble powder as filler up to 50% of replacement, initial and final setting times increase, indicating delayed hydration (VARDHAN *et al.,* 2015).

Permeability, which is the ease with which a fluid permeates a porous medium under a pressure gradient, is directly influenced by the pore structure (AMERICAN CONCRETE INSTITUTE, 2016). The connectivity of pores rather than their size is the most important aspect in the transport of ions as it increases permeability (LI *et al.,* 2018). Therefore, a disconnected network of pores is preferred to slow ions transport. When using cement with limestone, a lower water/cement ratio is necessary to achieve disconnected porosity (BENTZ; WEISS, 2009).

At early ages for mortars, up to 30% of limestone reduces porosity and the mean pore diameter. This is related to the filling effect, hydration acceleration, and stabilization of ettringite, with consequent higher volume of hydration products compared to ordinary Portland cement (OPC) concrete, as ettringite is more voluminous than monosulfate (DE WEERDT *et al.,* 2011; LI *et al.,* 2018). The reduction in porosity also influences

the compressive strength (DE WEERDT *et al.,* 2011; LOTHENBACH *et al.,* 2008). In contrast, for high limestone contents (>30%), both porosity and pore size are higher than those of OPC concrete, although higher fineness is beneficial to these parameters. The porosity and pore size increase with the use of water/solids ratio instead of water/cement ratio, as expected (LI *et al.,* 2018). The use of granite has no effect on porosity until 7.5% of replacement, above which the porosity increases (ABD ELMOATY, 2013).

For the compressive strength, the dilution of the binder can reduce strength because of increased porosity if the water content remains the same (JOHN *et al.,* 2018). This effect can be compensated with the increase in cement fineness. Moreover, because of the lower specific gravity of limestone, the paste volume is larger, improving the rheological behavior of concrete and allowing a reduction in the water/cement ratio, also compensating for the dilution effect (JOHN *et al.,* 2018).

Considering the acceleration of hydration at early ages, a compressive strength higher than that of OPC would also be expected. For quartzite fillers, with no acceleration effect, a 10% replacement level resulted in compressive strength lower than that of reference OPC mortars at early ages (<28 days), even when using very fine particles (~2.6 μm), which is consistent. For later ages (≥28 days), mortars with finer quartzite particles reached a compressive strength slightly higher than that of reference mortars (KADRI *et al.,* 2010). In contrast, percentages of 30% and 45% led to a reduction in compressive strength of approximately 20% and 40%, respectively (DU; PANG, 2020). Low percentages of limestone led to no significant differences, whereas a 20% replacement resulted in an increase of 25% in the compressive strength at 28 days (XIE *et al.,* 2024).

As for alumina fillers replacing 10% of cement, the compressive strength at 1 day was higher than that of OPC mortar, consistent with its influence on the hydration kinetics, and reduced with time, being lower than that of OPC mortar for all posterior ages regardless of the particle size (KADRI *et al.,* 2010). Basalt powder in 10% and 20% replacement levels slightly increased the compressive strength of pastes at 7 and 28 days (XIE *et al.,* 2024), whereas a reduction was observed for replacements levels of 15%, 30%, and 45% for ultra-high performance concrete even with increased fineness (LI *et al.,* 2021). Similarly, replacement levels of 10%, 20%, and 30% led to reductions in compressive strength until 60 days, and similar values at 90 days (ZHU *et al.,* 2024).

This behaviour was also observed for diabase and tuff (ZHU *et al.,* 2024). Basalt fillers replacing sand in replacement levels up to 30% increased the compressive strength of concrete (DOBISZEWSKA; SCHINDLER; PICHÓR, 2018), which is related to the better packing provided by the fines and maintenance of cement content and w/c ratio. For marble fillers, the increase in replacement percentage up to 50% for mortar resulted in a decrease in compressive strength (VARDHAN *et al.,* 2015). Granite fillers replacing up to 15% of cement led to a reduction in compressive strength except for 5%, in which an increase of approximately 8% was observed. However, a reduction of the water amount could counterbalance the negative effect in compressive strength (ABD ELMOATY, 2013).

Based on the results discussed, the characteristics and durability of concrete produced with AMFs are directly influenced by the type of AMF, PSD, and replacement percentage used. Therefore, studies on the use of AMFs should consider the effect of these parameters.

2.1.2 AAR-reactive AMFs

AMFs of different mineralogies, including quartzite (CRAEYE *et al.,* 2010; KADRI *et al.,* 2010; POPPE; DE SCHUTTER, 2005; RAHHAL; TALERO, 2005), alumina (POPPE; DE SCHUTTER, 2005), basalt (DOBISZEWSKA; SCHINDLER; PICHÓR, 2018; LI *et al.,* 2021; SOROKA; SETTER, 1977; XIE *et al.,* 2024; ZHU *et al.,* 2024), diabase (ZHU *et al.,* 2024), tuff (ZHU *et al.,* 2024), dolomite (SOROKA; SETTER, 1977), marble (MULTON *et al.,* 2010; VARDHAN *et al.,* 2015), granite (COUTINHO, 2019; MÁRMOL *et al.,* 2010; RAMOS *et al.,* 2013), have been studied. However, limited information is available regarding the durability aspect of concrete produced with AMFs.

Among the rocks used to produce AMFs, some may be reactive to AAR. AAR refers to a chemical reaction between certain mineral phases in the aggregates and the alkalis present in the concrete pore solutions (FOURNIER; BERUBÉ, 2000; LEEMANN *et al*., 2024a; NIXON; SIMS, 2016). This mechanism is commonly divided into two main mechanisms: ASR and ACR (FOURNIER; BERUBÉ, 2000).

AAR poses a significant challenge to the long-term durability of concrete infrastructure and is among the most harmful deterioration mechanisms affecting concrete infrastructure around the globe, compromising both their durability and serviceability.

As rehabilitation of AAR-affected structures is complex and costly, preventive approaches are generally more effective and economical.

AAR-reactive fillers have been mainly used to investigate their mitigation potential to AAR-induced expansions (ALVES *et al.,* 1997; BRAGA *et al.,* 1991; CARLES-GIBERGUES *et al.,* 2008; COUTINHO, 2019; CYR; RIVARD; LABRECQUE, 2009; LI; HE; HU, 2015; OLIVEIRA; SALLES; ANDRIOLO, 1995; TAPAS *et al.,* 2023). Considering the availability of reactive rocks worldwide, they can be an option to replace cement, being sustainably and economically viable. However, the use of AAR-reactive fillers raises concerns as their long-term behavior in concrete remains insufficiently understood.

2.2 APPRAISING AAR-REACTIVE AMFs IN CONCRETE

2.2.1 ASR-induced expansion and deterioration

ASR involves the interaction between metastable siliceous phases in the aggregates and hydroxyl ions in the pore solution. This reaction forms a hydrophilic expansive gel (i.e., ASR gel) with an opposite surface charge to that of the aggregate, and generates repulsive forces at the interface of the aggregate and the gel, leading to progressive expansion and deterioration of the affected concrete (LEEMANN et al., 2024). This mechanism has been reported to affect critical concrete infrastructure worldwide (SIMS; POOLE, 2017). In contrast, the mechanism of ACR remains under debate and has only been identified in a limited number of countries (GRATTAN-BELLEW *et al*., 2010; KATAYAMA, 1992, 2010; KATAYAMA; GRATTAN-BELLEW, 2012; LEEMANN *et al*., 2024b; MEDEIROS; SANCHEZ; DOS SANTOS, 2024; THOMAS; FOURNIER; FOLLIARD, 2013).

Considering ASR, the expansion level in concrete affects the damage development, as it is related to the reduction in mechanical properties and loss in physical integrity and durability associated with the net cracking extent (SANCHEZ *et al.*, 2017). In this regard, Sanchez et al. (2015) proposed a descriptive model for the ASR damage development in concrete as a function of expansion considering internal cracking initiating from the aggregate (Figure 2.1). Type A cracks (sharp cracks) could be closed cracks originated in the processing operation of aggregates or porous zones, whereas type B cracks (onion cracks) could be formed with no preexisting type A crack.

Figure 2.1 – Qualitative AAR damage model vs. levels of expansion between 0.05 and 0.30%.

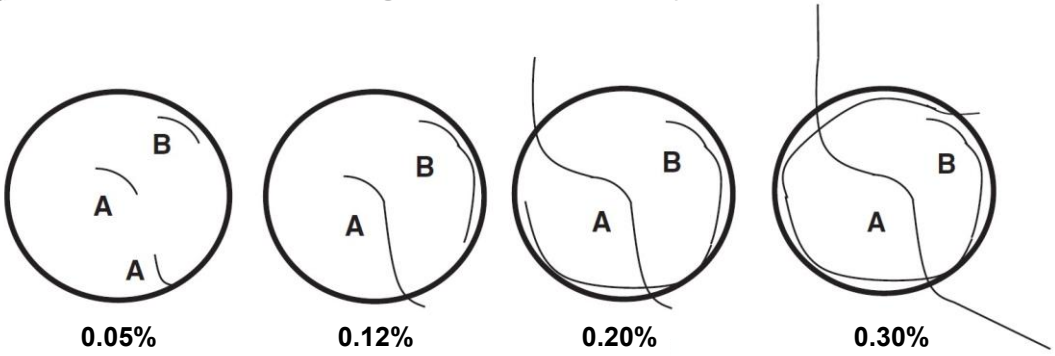

Source: Sanchez *et al.* (2015).

At the start of the reaction, cracks are mainly generated in the aggregates (expansion levels up to 0.05%). For moderate expansion levels (i.e., up to 0.12%), new cracks are developed, and the existing cracks lengthen and start connecting within the aggregate. Moreover, cracks in the aggregate start reaching the cement paste. Further progress of the reaction to high levels of expansion (i.e., up to 0.20%) results in connection of cracks and their continuous extension to the cement paste. At high expansion levels (i.e., ≥ 0.30%), the cracks start connecting in the cement paste forming a network, resulting in considerable impact on the mechanical properties of the concrete (SANCHEZ *et al.*, 2015).

This model was also correlated with mechanical properties of concrete affected by ASR and indices to evaluate ASR-induced deterioration (i.e., stiffness damage index – SDI and damage rating index – DRI), providing ranges that allow the classification of the ASR damage degree (Table 2.1) (further discussion in Section 2.2.3).

Table 2.1 – Classification of damage in concrete due to ASR.

Classification of ASR damage degree	**Reference expansion level (%)[a]**	**Assessment of ASR**				
		Stiffness loss (%)	**Compressive strength loss (%)**	**Tensile strength loss (%)**	**SDI**	**DRI**
Negligible	0.00–0.03	–	–	–	0.06–0.16	100–155
Marginal	0.04 ± 0.01	5–37	(–)10–15	15–60	0.11–0.25	210–400
Moderate	0.11 ± 0.01	20–50	0–20	40–65	0.15–0.31	330–500
High	0.20 ± 0.01	35–60	13–25	45–80	0.19–0.32	500–765
Very high	0.30 ± 0.01	40–67	20–35	–	0.22–0.36	600–925

[a] These expansion levels should not be considered as strict limits between the various classes of damage degree but as indicators/reference levels for which comparative analysis of petrographic and mechanical data was conducted allowing to highlight significant damage due to ASR progress.

Source: Sanchez *et al.* (2017).

2.2.2 Test methods to assess AAR-induced expansion

The most widely used test procedures to appraise the potential reactivity of aggregates are the accelerated mortar bar test (ABMT) (ABNT, 2018a; ASTM, 2023a) and concrete prism test (CPT) (ABNT, 2018b; ASTM, 2023b; CSA, 2024). From these tests, ASR kinetics (i.e., expansion rate over time) and ultimate expansion (i.e., maximum expansion resulting from ASR for the duration of the test) can be obtained. These parameters can help assess the effects of AAR-reactive AMFs in systems with reactive or non-reactive aggregates. In reactive systems, the type of the reactive aggregate, whether coarse or fine, must also be analyzed separately. In general, most of the studies focused on the use of AMFs with reactive coarse aggregates.

The AMBT is commonly adopted given its fast duration (i.e., 16 days – ASTM C1260 (ASTM, 2023a) and CSA A23.2-25A (CSA, 2024), 30 days – Brazilian standard NBR 15577-4 (ABNT, 2018a), 56 days – Norwegian standard). However, the test is conducted in mortar, requiring crushing of aggregates, which may affect its reactive potential, and the conditions are harsh (i.e., samples immersed in a 1N NaOH solution, 80 ºC), leading to misclassification of some aggregates (BÉRUBÉ; FOUNIER, 2003; DEMERCHANT; FOURNIER; STRANG, 2000; GOLMAKANI; HOOTON, 2016; GRATTAN-BELLEW, 1997; IDEKER *et al*., 2012; THOMAS *et al*., 2006). The CPT (ASTM C1260 (ASTM, 2023b), CSA A23.2-14A (CSA, 2024), and NBR 15577-6 (ABNT, 2018b)) is considered more reliable compared to the AMBT owing to more realistic storage conditions (i.e., 38 ºC, high relative humidity (RH)). However, the duration of the test is one year, and some challenges remain to be addressed, such as alkali leaching (IDEKER *et al*., 2010; LINDGÅRD *et al.,* 2012). Other tests have been developed to address some shortcomings of these tests, such as the accelerated CPT (ACPT, RILEM AAR 4.1 (NIXON; SIMS, 2016) and NBR 15577:7 (ABNT, 2018c)). This test has a reduced duration (i.e., 180 days) compared to the CPT, increased particle size distribution (PSD) compared to that used in the AMBT (AASHTO, 2022; LINDGÅRD *et al*., 2011; THOMAS; FOURNIER; FOLLIARD, 2013), and intermediate conditions (i.e., 60 ºC, 100% RH).

The following sections present literature data on the use of AMBT, CPT, and ACPT to evaluate reactive and non-reactive systems containing AAR-reactive AMFs incorporating i) reactive coarse, ii) reactive fine, and iii) non-reactive aggregates.

2.2.2.1 Accelerated mortar bar test (AMBT)

Figure 2.2 depicts the AMBT expansion curves available in the literature for systems containing reactive coarse aggregates and reactive AMFs. The solid lines represent results of control mixtures, and dashed lines represent results of mixtures containing ASR-reactive AMFs. Each color represents a family of results for the same coarse aggregate used.

As observed, the ultimate expansion was reduced for all the AMFs used. The expansions reduced up to 74% for greywacke AMFs (GF), 56% for dacite AMFs (DF, greywacke coarse aggregate), 72% and 91% for sandstones AMFs (SF) Capanda and Formosa, respectively, 61% for basalt AMFs (BF), and 74% for orthogneiss AMFs (OF). Differences in the effect on ultimate expansion were observed for different parameters evaluated, such as the reactivity degree of the aggregate and percentage of AMFs, which will be further discussed in the coming sections.

Figure 2.2 – Expansion results of systems with reactive coarse aggregate and reactive filler (SF: Sandstone filler; DF: Dacite filler; GF: Greywacke filler; BF: Basalt filler; OF: Orthogneiss filler).

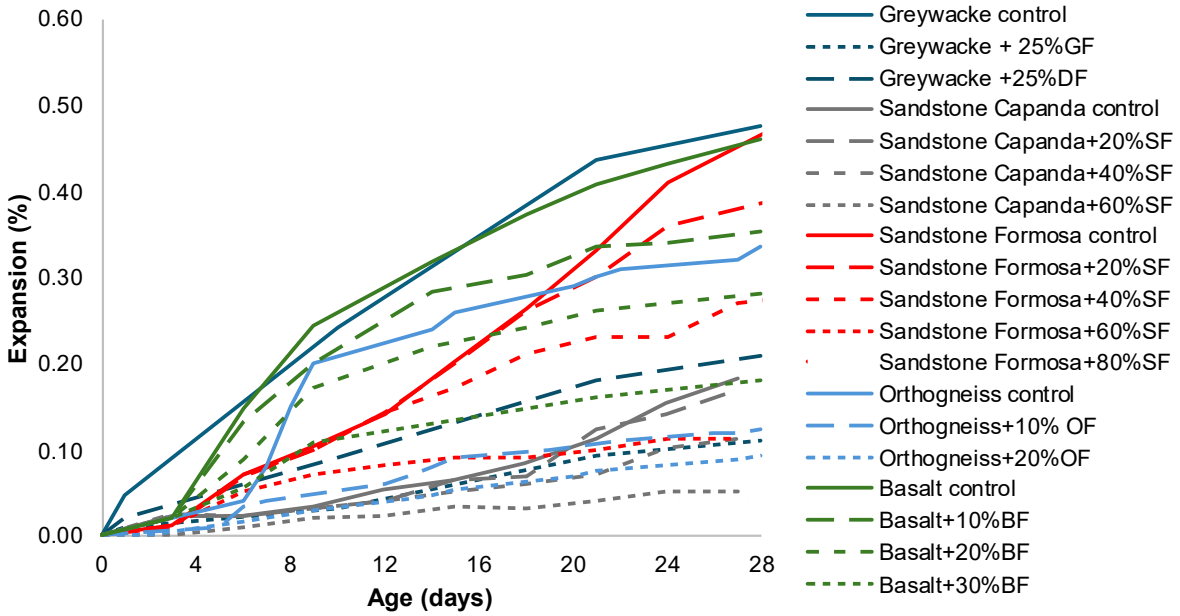

Source: Adapted from CASTRO *et al.* (1997); COUTINHO; MONTEFALCO; CARNEIRO (2024); OLIVEIRA; SALLES; ANDRIOLO (1995); TAPAS *et al.* (2023).

In a robust study by Pedersen (2004), several parameters were appraised using both the AMBT and CPT following Norwegian standards. The AMBT results are shown in Figure 2.3.

Figure 2.3 – AMBT expansion results using reactive aggregate AMFs (Norwegian standard).

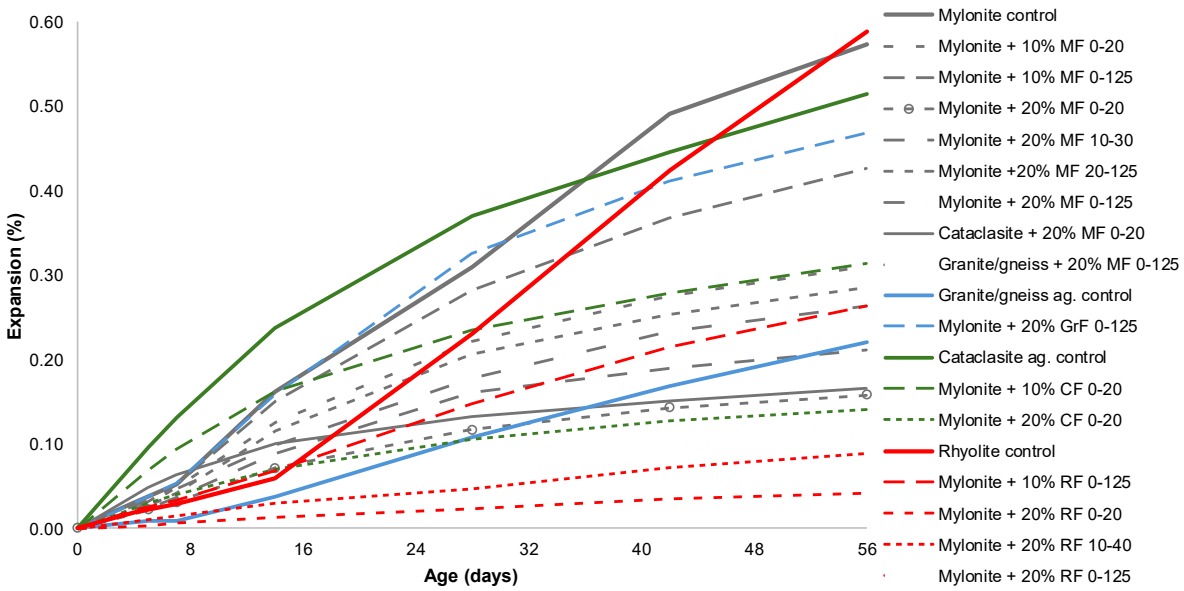

Source: Adapted from PEDERSEN (2004).

As observed, the AMBT results obtained with the Norwegian standard were similar to those obtained using the ASTM standard (Figure 2.2), that is, lower expansions with the use of AMFs. The parameters evaluated were type of AMFs (i.e., mylonite (MF), granite (GF), cataclasite (CF), rhyolite (RF)), PSD (i.e., 0–20 μm, 10–30 μm, 10–40 μm, 20–125 μm, 0–125 μm), and percentages (i.e., 10% and 20%). The mixtures with reactive AMFs (dashed lines) resulted in reduced ultimate expansion compared to the control curves (solid lines). The exception was the mixture with mylonite as aggregate and 20% GF, with higher expansions than the control mixture.

Few studies evaluated systems with fine reactive aggregates (ANTUNES, 2021; TAPAS *et al*., 2023). In this regard, the AMBT was used to assess a combination with reactive Waikato natural river sand and reactive AMFs produced from a greywacke (GF), and replacing 25% of cement (Figure 2.4). Fine reactive aggregates usually exhibit a faster rate of reaction (SANCHEZ *et al*., 2018), reaching considerable expansion levels at early ages, as observed in the figure by the steep inclination of the control curve. When using GF in Figure 2.4, the rate of reaction was slowed. Moreover, the maximum expansion was reduced from 0.47% to 0.12%, representing a reduction of approximately 74%.

Figure 2.4 – AMBT results for a system with reactive fine aggregate.

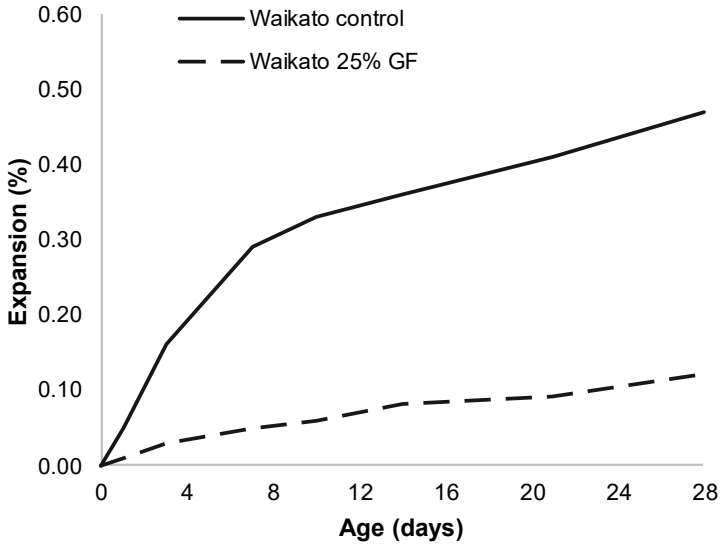

Source: Adapted from TAPAS *et al.* (2023).

2.2.2.2 Concrete prism test (CPT)

Figure 2.5 shows expansion results obtained through the CPT. In general, the kinetics and ultimate expansions of the combinations were similar to those of the control mixture, except for the combination with RF, in which the expansion was considerably reduced. In this case, the type of AMFs may have played a significant role, as RF has been reported to have pozzolanic activity (PEDERSEN, 2004).

Figure 2.5 – CPT expansion results using reactive AMFs (Norwegian version).

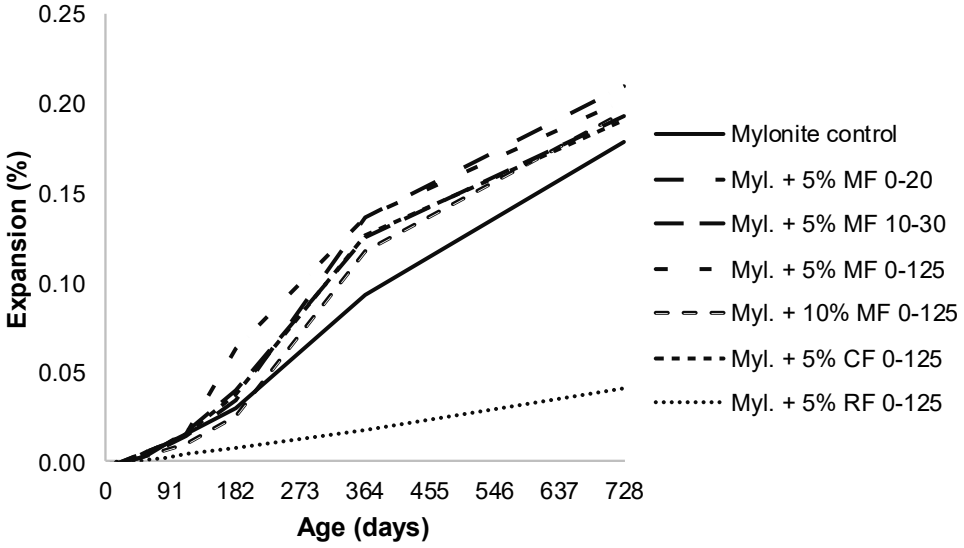

Source: Adapted from PEDERSEN (2004).

In addition to systems with reactive aggregates, the study of non-reactive systems, in which reactive AMFs and non-reactive aggregates are used, is very important but has

not been extensively addressed in previous studies. This analysis was found in one study in which a limestone AMF was used in percentages of 15% and 30% (50% replacing cement and 50% replacing sand) (GUÉDON-DUBIED *et al.,* 2000). As observed in Figure 2.6, the use of the reactive AMFs resulted in increased expansions. Despite the different percentages, the expansions after 1 year for both replacement levels were similar. However, compared to the control curve, the average ultimate expansion was twice as much higher.

These results indicate the potential impact of reactive AMFs in non-reactive systems. Further studies should focus on different lithologies of aggregates to be used as AMFs. Moreover, both cement and sand were replaced by AMFs, hindering the identification of individual effects. The type of replacement, whether by cement or sand, must be tested separately to identify the corresponding influences on the kinetics, ultimate expansion, and concrete deterioration process.

Figure 2.6 – Expansion of non-reactive systems containing reactive aggregate AMFs.

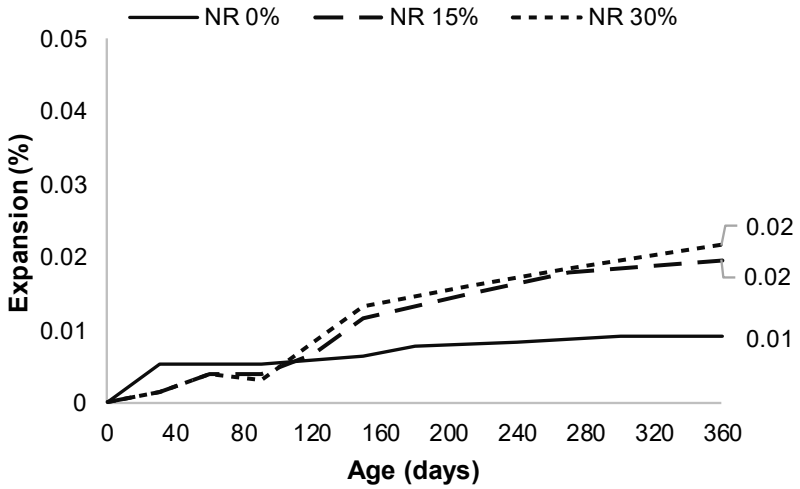

Source: Adapted from GUÉDON-DUBIED *et al.* (2000).

2.2.2.3 Accelerated concrete prism test (ACPT)

Figure 2.7(a) shows expansion results of mixtures with AAR-reactive AMFs using the ACPT. As observed, combinations with reactive coarse aggregates (greywacke – SH), two AMFs (greywacke – SH and dolomitic argillaceous limestone – K, ASR- and ACR-reactive, respectively), and replacing sand (15% SH) and cement (15% SH-C) resulted in similar or slightly higher ultimate expansions. For the combination with SH AMFs replacing sand, the kinetics was also accelerated. The above outcomes contradict the

AMBT results, in which the use of AAR-reactive AMFs led to reduced expansions, but are in agreement with the CPT results (Figure 2.5).

Moreover, the ACPT was utilized to evaluate a system incorporating a highly reactive sand (i.e., Texas sand – TX), and AMFs from a greywacke (SH) and a limestone (K), which are ASR- and ACR-reactive, respectively, replacing 15% of cement and sand (Figure 2.7(b)).

Combinations with reactive fine aggregates or reactive coarse aggregates incorporating AAR-reactive AMFs exhibited similar or slightly higher ultimate expansions and similar or accelerated kinetics compared to combinations without AAR-reactive AMFs (Figure 2.7(a)). The type of test and the aggregate features (i.e., reactivity degree, PSD) may have influenced the results. To better understand the effect of AAR-reactive AMFs in systems with fine reactive aggregates, a long-term evaluation coupled with continuous assessment of the deterioration, that is, evaluating samples at different ages to understand how the deterioration is progressing, is essential.

Figure 2.7 – (a) ACPT results for combinations with AAR-reactive AMFs and reactive coarse aggregate. (b) ACPT results for systems with reactive fine aggregate (TX) (ANTUNES, 2021). (SH: Springhill, reactive greywacke aggregate; K: Kingston, limestone associated with ACR occurrences).

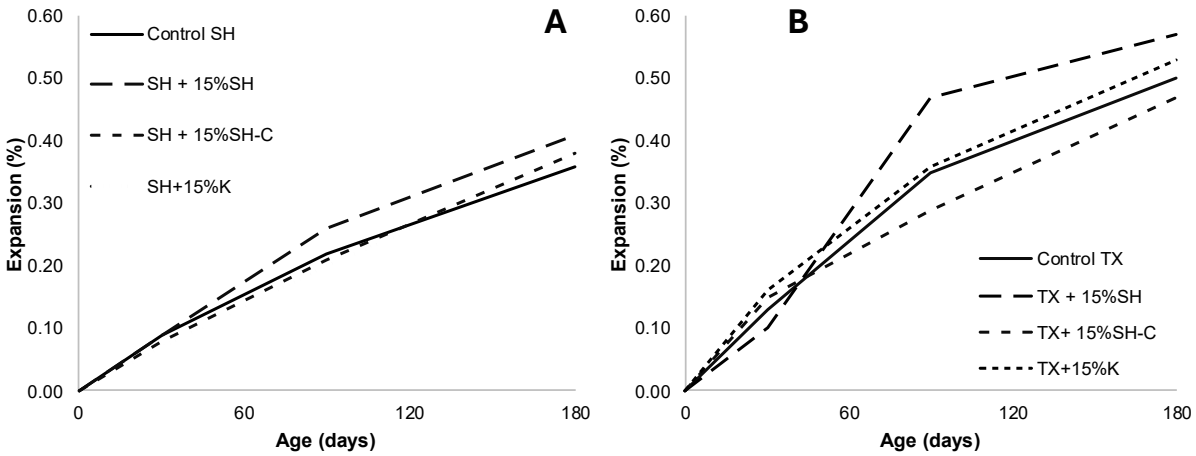

Source: Adapted from ANTUNES (2021).

The use of reactive AMFs with reactive coarse aggregates (ANTUNES, 2021; CASTRO *et al*., 1997; COUTINHO; MONTEFALCO; CARNEIRO, 2024; OLIVEIRA; SALLES; ANDRIOLO, 1995; PEDERSEN, 2004; TAPAS *et al*., 2023), reactive fine aggregates (ANTUNES, 2021; TAPAS *et al*., 2023), and non-reactive aggregates (GUÉDON-DUBIED *et al.,* 2000) was analyzed using either AMBT, CPT, or ACPT.

However, there is no comprehensive evaluation of the effect of the same AMFs in these three different systems, which would be beneficial for a better understanding of the AMFs action. Moreover, several studies were conducted using test methods and/or conditions that are not applied anymore, with different sample sizes, temperatures, and durations (CARLES-GIBERGUES *et al.,* 2008; GUÉDON-DUBIED *et al.,* 2000; HOBBS; GUTTERIDGE, 1979; SHAO *et al*., 2000; ZHANG *et al.,* 1999; ZHANG; GRAVEST, 1990). In addition, tests in mortar were more used, such as the AMBT (ALVES *et al*., 1997; RAMYAR; TOPAL; ANDIÇ, 2005; SALLES; OLIVEIRA; ANDRIOLO, 1997; SHAFAATIAN *et al*., 2013; SHAYAN, 1992). Temperature is an aspect that can affect the results of tests when using AMFs (PEDERSEN, 2004). Therefore, a comprehensive study using a long-term test at a lower temperature compared to that of accelerated tests, such as the CPT, could provide a better understanding of the action of reactive AMFs in concrete.

2.2.3 Test methods to assess AAR-induced deterioration

Few methods were used to evaluate the deterioration progress of systems with AAR-reactive AMFs. A surface cracking evaluation (CARLES-GIBERGUES *et al*., 2008) was conducted in prisms of 7×7×28 cm stored at 60 ºC with 20% AMFs replacing sand were stored and 34 weeks. As observed in Figure 2.8, a drastic reduction in surface cracking was observed for samples with a reactive aggregate and 20% of sand replaced by AMFs derived from the same aggregate (i.e., metaquartzite (o): 100% reduction, siliceous limestone (t): approximately 90% reduction, opaline aggregate (b): 100% reduction, crushed waste glass (g): 100% reduction).

Figure 2.8 – Influence of the use of AMFs on surface cracking of concrete prisms. O, T, B, G refer to the aggregates and O-o, T-t, B-b, G-g samples with the use of the corresponding reactive AMFs.

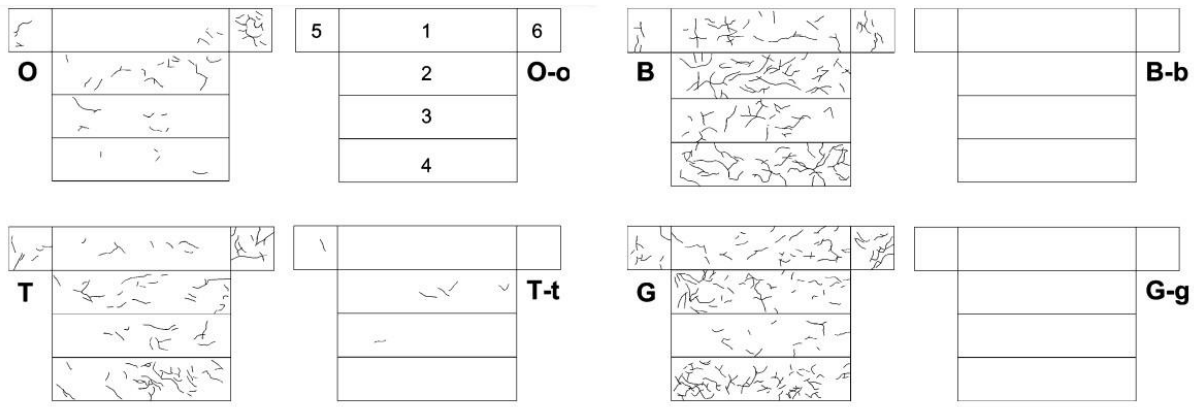

Source: CARLES-GIBERGUES *et al*. (2008).

The multilevel assessment, combining microstructural (i.e., DRI) and mechanical (i.e., stiffness damage test (SDT)) evaluations, enables a more accurate appraisal of the extent and progress of damage over time (SANCHEZ *et al.*, 2017).

The DRI was developed by Grattan-Bellew and Danay (1992) and modified by Villeneuve (2011). It consists of a microscopy tool conducted on a stereomicroscope (15–16× magnification) in which distress features are counted in a 1 cm^2 grid drawn on the surface of a polished and reflective concrete section (SANCHEZ, 2014) Figure 2.9 (a). Each distress feature has a weight, as indicated in Table 2.2 and shown in Figure 2.9 (b). Cracks with a length ≥ 1 mm are counted. The DRI is calculated by averaging the features found multiplied by the corresponding weights and normalized for an area of 100 cm^2. The weights of the features indicate their relative importance.

Table 2.2 – DRI deterioration features and corresponding weights.

Distress Features		**Weighting factors**
Closed crack in the aggregate	CCA	0.25
Open crack in the aggregate	OCA	2
Open crack in the aggregate with reaction product	OCA-RP	2
Debonded aggregate	CAD/Debon	3
Disaggregate/corroded particle	DAP	2
Crack in the cement paste	CCP	3
Crack in the cement paste with reaction product	CCP-RP	3

Source: Sanchez et al. (2016); Villeneuve (2011).

Figure 2.9 – (a) DRI test. (b) DRI features.

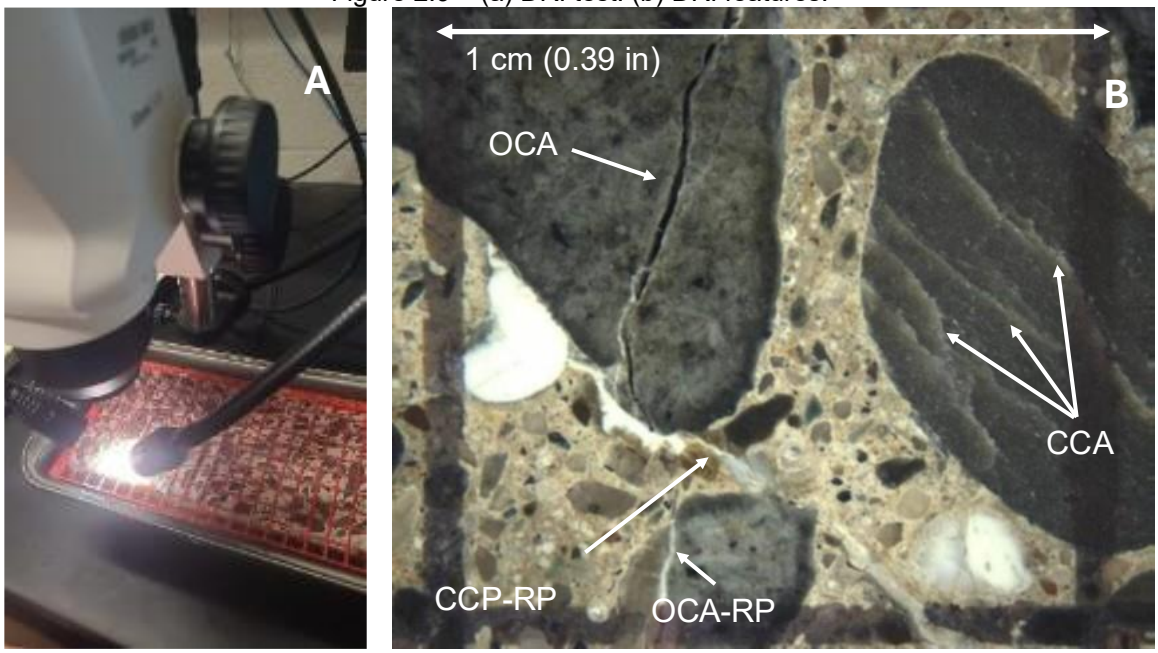

Source: (a) Author (2025), (b) Sanchez et al. (2016).

The stiffness damage test (SDT) was first devised by Walsh (1965) for rock testing by observing a correlation between loading cycles and crack density. The methodology was adapted by Chrisp et al. (1993) for concrete cores. The test consists of applying cyclic loads in compression to concrete specimens, and the parameters of the test such as the load and loading rate have been modified over time (CHRISP; WALDRON; WOOD, 1993; SANCHEZ *et al*., 2014; SMAOUI *et al*., 2004). In the current version of the test, five cycles are conducted, the load applied generally corresponds to 40% of the compressive strength at 28 days representing the elastic range limit, and the loading rate is 0.10 MPa/s (SANCHEZ *et al*., 2014) (Figure 2.10(a)). The outcomes of the test are the modulus of elasticity, SDI, and plastic deformation index (PDI). The SDI represents the ratio of dissipated energy to the total energy, whereas the PDI is the ratio of plastic deformation to the total deformation over the five loading/unloading cycles (Sanchez *et al*., 2014), as illustrated in Figure 2.10(b) and shown in Equations 1 and 2, respectively:

Figure 2.10 – (a) SDT test. (b) Calculation of SDI and PDI.

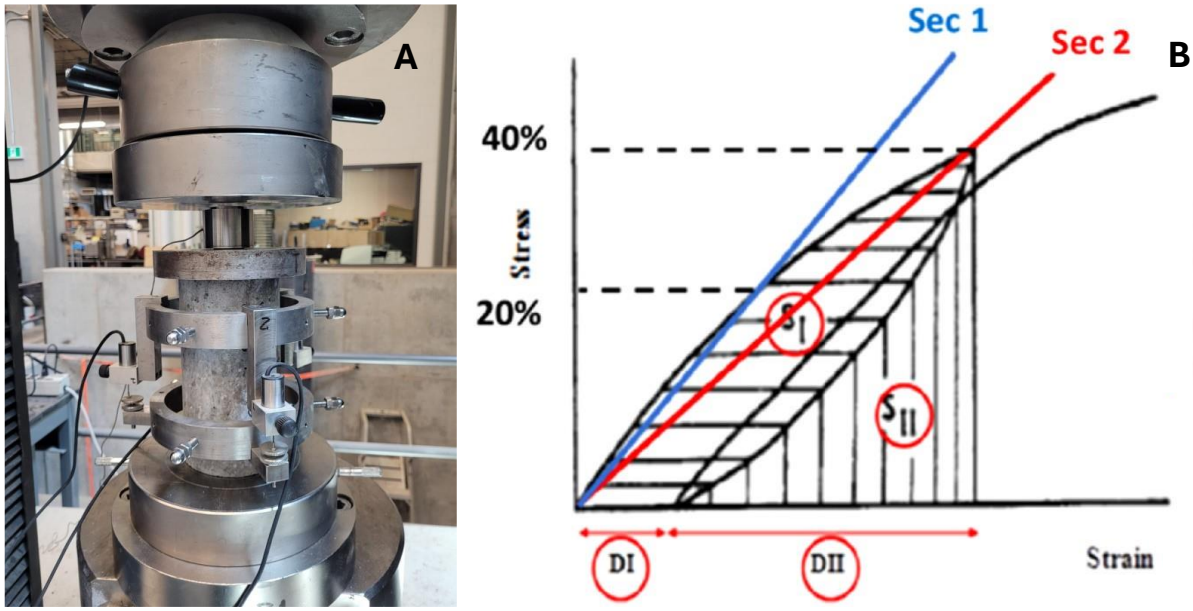

Source: (a) Author (2025), (b) ZHU *et al.* (2021).

$$SDI = \frac{SI}{(SI + SII)} \quad (1)$$

$$PDI = \frac{DI}{(DI + DII)} \quad (2)$$

The higher the SDI and PDI, the higher the damage in the sample. Therefore, they are important indices to evaluate damage both for laboratory specimens and cores and have been applied in many studies (DE SOUZA; SANCHEZ; BIPARVA, 2024; SANCHEZ *et al.*, 2017; SANCHEZ *et al.*, 2018; ANTUNES, 2021; SOUZA, 2022).

The DRI and SDT were adopted to evaluate systems containing 15% greywacke and dolomitic argillaceous limestone AMFs (i.e., ASR- and ACR-reactive, respectively) with reactive coarse and reactive fine aggregates. When the greywacke AMFs replaced cement, the DRI values were lower (ANTUNES, 2021), but a replacement by sand led to similar to or higher DRI numbers compared to the DRI for a system with no AMFs. Replacing 15% of dolomitic argillaceous limestone AMFs by sand resulted in similar DRI for systems with reactive coarse aggregate and lower DRI for systems with reactive fine aggregates. The main difference that caused this variation in the DRI was the number of cracks in the cement paste with and without reaction product, which is directly influenced by the use of AMFs. The DRI number also exhibited a very good correlation with the expansion level of the samples.

For the SDT, replacement of cement by AMFs led to slightly higher SDI values. In contrast, sand replacement led to similar or lower SDI values compared to systems without AMFs. The modulus of elasticity reduction exhibited different behaviours depending on the type of reactive aggregate used. For reactive coarse aggregates, the reduction was lower than that observed for systems with no AMFs for both types of replacement. For reactive fine aggregates, the reductions were higher for the greywacke AMFs, being more prominent when cement was replaced. For the dolomitic argillaceous limestone AMF, the reduction was considerably lower.

In the studies discussed, the AAR-induced deterioration was evaluated at the end of the expansion measurement period (i.e., 34 weeks for the surface cracking and 180 days for the multilevel assessment). Therefore, assessing the deterioration progress at different ages or expansion levels could provide insights into the process when using AAR-reactive AMFs.

2.2.4 Influential Parameters

The impact of some physiochemical properties of AAR-reactive AMFs, such as the mineralogy and PSD, as well as the replacement strategy, on the behavior against

ASR should be better studied, as previously indicated. In the following sections, these parameters are discussed in detail.

2.2.4.1 Role of AMFs mineralogy on AAR

Several reactive aggregates with different lithologies and, consequently, different degrees of reactivity have been used to evaluate the influence of reactive AMFs on AAR expansion. The type of rock used (i.e., texture, mineralogy, and microcracks (RÄISÄNEN; MERTAMO, 2004)), as well as the crushing process, directly influence the morphology of particles produced (BOUQUETY; DESCANTES, 2007; DIÓGENES *et al.,* 2021), which also influences the action of AMFs produced from these rocks. These aspects impact the dispersion of mineral phases that compose the rocks, as the propagation of microcracks is different depending on the mineral and their structure (ÅKESSON et al., 2003; PANG *et al*., 2010). This was observed when using AMFs from the same rock but crushed by different types of crusher, in which the specific surface areas (SSAs) were different and resulted in distinct effects on AAR-induced expansions (COUTINHO; MONTEFALCO; CARNEIRO, 2022). Moreover, aggregates from different types of rocks also result in distinct expansion tendencies when produced using the same crushing methods, highlighting the influence of the rock characteristics on expansion results (COUTINHO; MONTEFALCO; CARNEIRO, 2022; VALDUGA, 2007). However, the crushing procedure to produce AMFs is frequently not disclosed in studies on the topic. Moreover, studies on the morphology of AMFs, directly related to the source rock characteristics, are still limited and should be further explored.

In addition to physical aspects, chemical aspects related to the composition of the rock also influence the effect of corresponding AMFs. Reactive AMFs were indicated to exhibit pozzolanic activity (CASTRO *et al.*, 1997; PEDERSEN, 2004; SALLES; OLIVEIRA; ANDRIOLO, 1997; TAPAS *et al*., 2023), with differences observed in terms of amount of reaction products formed, Si/Ca ratio, and dissolved silica (TAPAS et al., 2023). As results were different depending on the type of AMFs used, their effect may not be limited to cement dilution and can be also influenced by the lithotype and chemical composition of the rock used to produce the filler, which should be further examined. This can also be influenced by the temperature of the test adopted, as AMFs derived from rocks containing siliceous minerals may exhibit pozzolanic activity at high

temperatures (i.e., 80 ºC) (PEDERSEN, 2004). The efficacy of the filler was also indicated to be directly related to the alkali content, with a lower alkali level requiring lower replacement levels to reduce expansions (QINGHAN *et al*., 1996; SALLES; OLIVEIRA; ANDRIOLO, 1997). However, the contribution of alkalis from the AMFs should also be considered.

The alkali release by the aggregate may have a role when considering the effects of reactive AMFs (LEEMANN; HOLZER, 2005), and it varies depending on the type of rock (MENÉNDEZ *et al.*, 2022; WANG et al., 2008). Feldspars are one of the major sources of alkalis from the aggregate (BERUBÉ *et al*., 2002; FERRAZ *et al.*, 2017; MENÉNDEZ *et al*., 2022; SOARES *et al*., 2016). However, the contribution of alkalis from aggregates remains unclear. The size of particles and the alkali solution interfere in the release of alkalis by the aggregate, with smaller sizes resulting in more release (SOARES *et al*., 2016). Moreover, the K^+ release is more intense in 1 N NaOH solutions (SOARES *et al*., 2016). Thus, considering the importance of the lithology of the rock on the AMF produced, a petrographic analysis of the rock could provide interesting insights into the effect of the AMF in concrete.

2.2.4.2 Role of particle size of AAR-reactive fillers

The similarity between ASR and pozzolanic reaction has been acknowledged (HOU; STRUBLE; KIRKPATRICK, 2004; THOMAS, 2011). Taylor (TAYLOR, 1997) affirmed that the chemical mechanisms of these reactions are the same, with different effects owing to different particle sizes of siliceous materials. These reactions also differ in their timescale and occurrence of expansion. This effect is considerably affected by the size of reactive particles of the aggregate. For small particles, the dissolution of ASR gel is rapid, and the dissolved silicate groups can react with calcium ions to produce C-S-H, contributing to strength development (DYER, 2014; PEDERSEN; WIGUM; LINDGÅRD, 2016). In contrast, large aggregates lead to accumulation of the gel (PEDERSEN; WIGUM; LINDGÅRD, 2016). This can be exemplified considering the use of silica fume, which is the most effective SCM to counteract ASR; yet, when agglomerated, it can have the opposite effect, triggering ASR (BODDY; HOOTON; THOMAS, 2003; DIAMOND, 1997; GUDMUNDSSON; OLAFSSON, 1999; MARUSIN; SHOTWELL, 2000), which can also be related to the silica content (BODDY; HOOTON; THOMAS, 2003).

Stanton (STANTON, 1940) studied a siliceous magnesium limestone containing opal and chalcedony and determined that if this aggregate is sufficiently fine (< 180 μm), no expansion occurs. In his work, he also indicated that when the aggregate has a reduced size, the gel dissipates in the cementitious matrix such that no tension is generated, and the reaction terminates before final setting of concrete. In contrast, Vivian (VIVIAN, 1951) found that expansions increase with the reduction of particle size until it reaches 50 μm, from which no expansion is observed, as shown in Figure 2.11.

Figure 2.11 – Expansion of mortars with different contents of reactive component vs mean size of reactive particles.

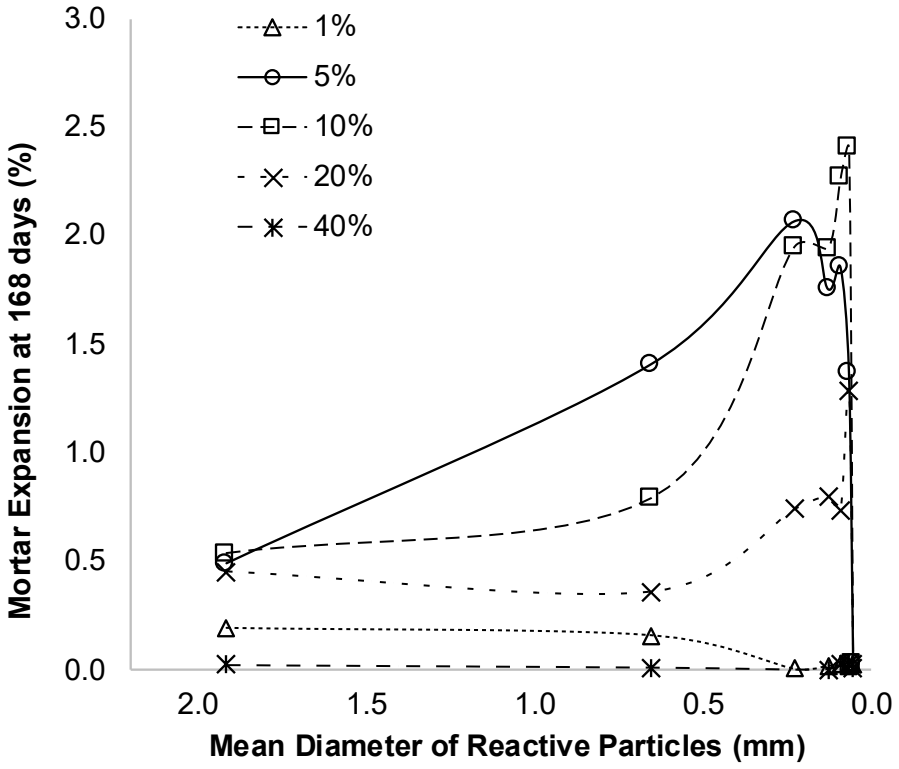

Source: Adapted from VIVIAN (1951).

The amount of reactive particles is considered to affect the number and width of the cracks formed, which influences expansion (VIVIAN, 1951). The volume of a particle would determine its capacity to generate cracks. If the diameter of the particle is below a certain threshold, the corresponding increase in volume after reaction can be accommodated by the pores in the surrounding area. Moreover, larger particles would be expected to generate wider cracks and a more pronounced local expansion compared to small particles. However, the core of the particle may react slowly, which limits this behavior, indicating that not all the reactive portion of a particle may

contribute to expansions (VIVIAN, 1951). By increasing the number of reactive particles in cementitious materials, the number of cracks also increases, followed by an increase in expansion. Nevertheless, there is a limit for the number of reactive particles of a certain size, above which no additional cracks are generated. This limit number of cracks tends to increase as the particle size reduces. In addition, by increasing the number of particles, their distribution becomes more uniform, leading to uniformity of crack width. The increase in the number of reactive particles may not result in increased expansions because the amount of alkalis acts as a limiting factor. Therefore, the expansion in cementitious materials with reactive AMF can be a result of the effects of volume, SSA, number and distribution of reactive particles (VIVIAN, 1951).

The size effect may also be related to the reaction on the surface of the aggregate, which acts to produce ASR gel, and the dissolution of silica, which acts to reduce ASR gel (DYER, 2014). Therefore, the ASR rate is defined by the rate of these two processes. In small particles, the reactive portion is completely converted to gel, meaning that posterior dilution will contribute to reducing expansions. For big particles, the smaller SSA and volume mean that only a part of the reactive components will react, as illustrated in Figure 2.12.

Figure 2.12 – Effect of a relatively fast rate of ASR gel formation and a slow rate of gel dissolution over a period t1. Large particles (a) produce relatively large volumes of gel as they react. Smaller particles (b) become entirely converted to gel, which then gradually dissolves. Very small particles (c) are dissolved entirely in a relatively short period of time.

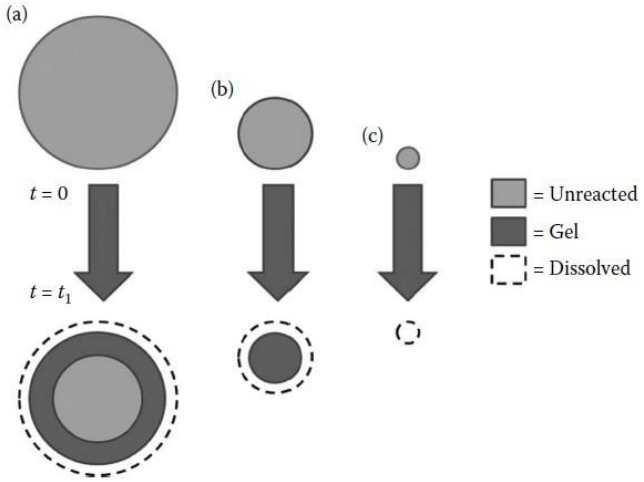

Source: DYER (2014).

Considering the size effect, different size ranges of marble and siliceous limestone sands were used to evaluate ASR, and higher expansions were obtained for coarse particles (630–1250 μm) and no expansion for fine particles (0–160 μm) (MULTON *et al.*, 2010). In contrast, the use of opal in ranges from 125 μm to 20 μm led to increased expansions for all ranges, with maximum expansions in the range from 30 μm to 20 μm (DIAMOND; THAULOW, 1974). A similar study using opal also obtained higher expansions for the finer fraction (150 to 300 μm) (HOBBS; GUTTERIDGE, 1979). The effect of the size of particles, considering the fractions of the AMBT, has also been analyzed by using a non-reactive aggregate and replacing each fraction by a reactive aggregate. Although the results indicate lower expansions for the coarser and finer fractions (2.0 to 4.0 mm and 0.125 to 0.250 mm, respectively), the percentages of these fractions are also lower than those of intermediate fractions, which may have influenced the results (RAMYAR; TOPAL; ANDIÇ, 2005).

These conflicting results may be related to the pessimum effect, which is the intensification of the reaction in a certain size range, whereas above and below this size range expansions reduce (QIU *et al.*, 2022). Some explanations have been proposed for this behavior. For instance, the pessimum silica content is considered to be directly related to the pessimum content (DIAMOND; THAULOW, 1974; KUO; SHU, 2015; QIU *et al.*, 2022; SEKRANE; ASROUN, 2014). The pessimum SiO_2/Na_2O ratio varies with the size and nature of the aggregate and the amount of accessible SiO_2 (ZHANG; GRAVEST, 1990). In another model, the gel formed is divided into two types: the gel deposited into the interface pores and the gel that permeates into the surrounding pores in the cement paste. The first type does not cause expansion and is governed by dilution, whereas the second type generates interface pressure and causes expansion. In this case, the aggregate size and porosity of the paste influence the amount of the first type of gel, and the permeation rate influences the amount of the second type (SUWITO *et al.*, 2002). Given a fixed volume of aggregate, small particles lead to higher expansions because of the higher surface area, which is the dilution process. If the particles are sufficiently small such that the volume of gel formed is comparable to the volume of pores in the surrounding paste, the pressure is released and expansions are reduced, which is the permeation process. For a particle sufficiently small such that the gel can be completely held in the interfacial pore space,

no expansion occurs. According to this model, the pessimum size is that at which these diffusion processes are balanced (SUWITO *et al*., 2002).

Fracture mechanics was also used to explain this behavior (PEDERSEN; WIGUM; LINDGÅRD, 2016). In this case, particles below a certain size will not cause cracks even if the expansion caused by the aggregate is higher than the strain capacity of the paste (BAŽANT; ZI; MEYER, 2000; GOLTERMANN, 1995). This is because the energy released from a crack propagating from a particle with radius R is proportional to R^3, whereas the necessary fracture energy is proportional to R^2 (GOLTERMANN, 1995). Cracks propagate when the energy released is higher than the fracture energy required to propagate the crack. Therefore, for a given system, there is a critical particle size below which no crack propagation occurs (GOLTERMANN, 1995).

Certain aggregates may also exhibit a pessimum content, which is a range in which the expansions are pronounced (BEKTAS *et al*., 2004). Despite the variable methods and aggregates used, the nature and composition of aggregates considerably influence the results, particularly considering rapid and slow reactive aggregates (DYER, 2014; MULTON *et al*., 2010). Moreover, the pessimum effect is still not fully understood. However, the observations related to the reduced or nonexistent expansions from a certain size of particle motivated studies on the use of this material as AMF, either replacing fine aggregate or cement.

In this regard, several parameters were used to indicate the particle size of the AMFs, such as maximum dimension, range, D10, D50, D90 (i.e., particle diameters at which 10%, 50%, and 90% of the cumulative mass of the sample passes, respectively), and also parameters related to SSA, such as Blaine fineness and Brunauer-Emmett-Teller (BET) method.

When examining the influence of the fineness of reactive AMFs on the expansion results, a fineness of 800 m^2/kg for andesite powder was determined to be the minimum value required to effectively reduce expansions (QINGHAN *et al.,* 1996). As for powders from three natural aggregates and glass with different SSAs, measured by means of Blaine fineness, and used to replace sand in mortars, an increase in SSA resulted in reduced expansions for all percentages analyzed (CARLES-GIBERGUES *et al*., 2008).

In contrast, samples using reactive powders with different Blaine fineness values (210 m^2/kg, 400 m^2/kg, 610 m^2/kg, 860 m^2/kg) exhibited very similar expansions even for different replacement levels (LI; HE; HU, 2015). The concentration of soluble alkalis varied with the SSA of the powder particles. By studying sandstone powder, the Na^+ concentration increased until reaching a certain value of SSA where the K^+ concentration surpassed that of Na^+. As higher K^+/Na^+ ratios have been related to higher expansions (LEEMANN; LOTHENBACH, 2008), this is a factor that should be considered when evaluating this material. The alkali bonding ability also followed the same tendency, decreasing until reaching a specific SSA value and then increasing again. The alkali binding behavior may be explained by the pozzolanic activity and nucleation effects. Considering that C-S-H is the only phase that can bind alkalis and taking CH content as an indicator of the hydration degree, when the activity effect is dominant, CH is consumed, whereas when the nucleation effect is dominant, the CH content increases. Therefore, the SSA influences the alkali bonding and liberation ability (LI; HE; HU, 2015).

The influence of the particle size on the AAR results was also evaluated (PEDERSEN, 2004), and some of the results are shown in Figure 2.13.

As observed, different particle size ranges resulted in differences in expansion for the same coarse aggregate, AMF, and replacement percentage used. In the AMBT, the finer the AMF, the lower the expansion. The combination with fraction 0–20 μm resulted in the lowest expansion, followed by the combination with fraction. 0–30 μm. The combination with fraction 0–125 μm exhibited a slightly higher expansion than that with fraction 20–125 μm, which indicates that the finer fraction removed in the last fraction mentioned played an influential role in the result. In contrast, for the CPT, the expansions for combinations with reactive AMF were higher than those of the reference sample and very similar.

Based on the exposed, in which different tendencies were observed when varying the particle size, other parameters might affect the results, such as the pessimum content previously described. Therefore, more studies are necessary to better understand the influence of the PSD on AAR expansions, also considering the deterioration process, which has not been studied so far, taking into account this parameter.

Figure 2.13 – Influence of particle size on AAR expansion results considering (a) AMBT and (b) CPT tests (ranges in μm).

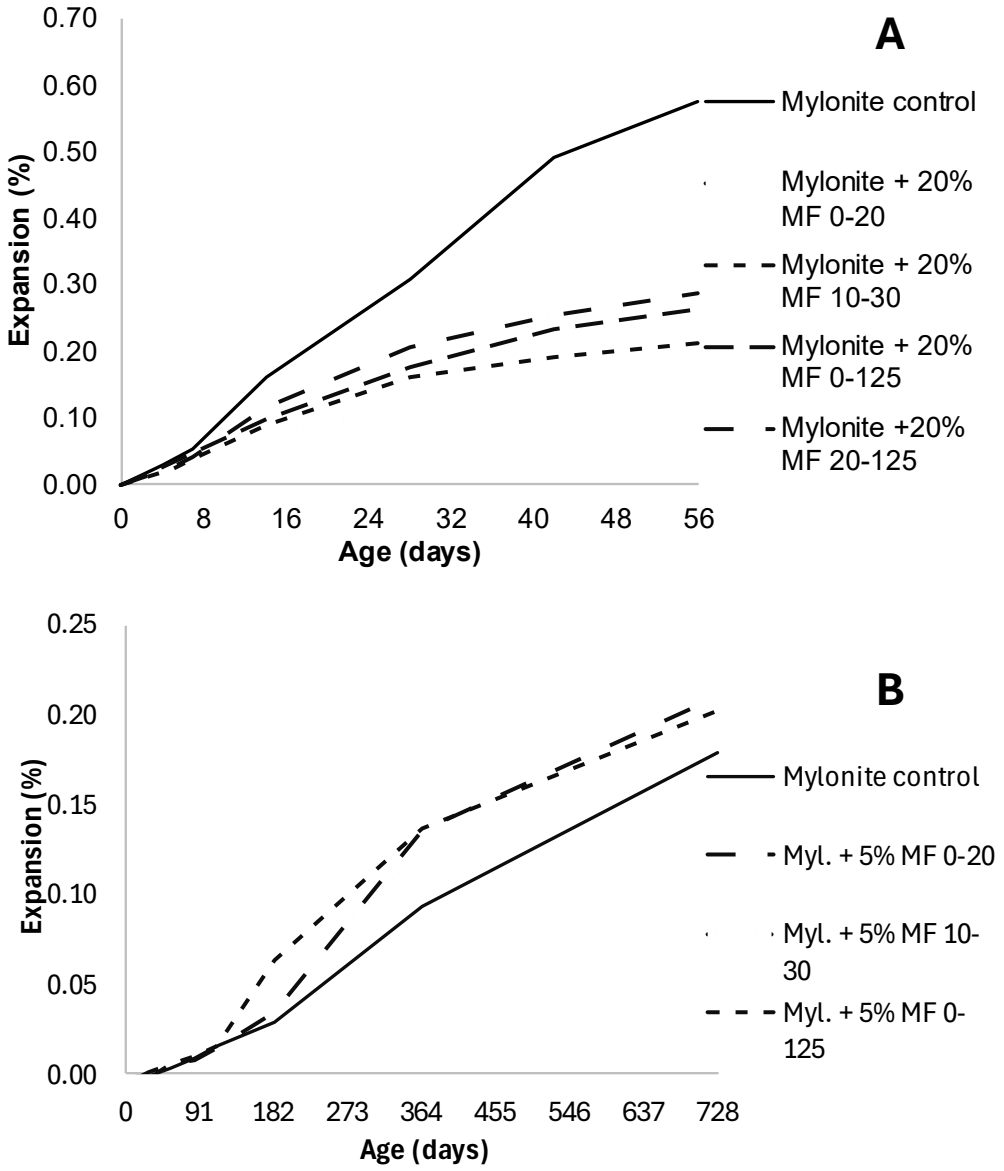

Source: Adapted from PEDERSEN (2004).

2.2.4.3 Role of replacement content

The replacement content has a direct influence on AAR-induced expansion when cement is replaced considering the reduction in alkali content. Replacing cement by SCMs and AMFs has been an important strategy as a means to reduce CO_2 emissions to achieve the NetZero target (SCRIVENER; JOHN; GARTNER, 2018). Considering this scenario, recent studies examining the use of reactive aggregate AMFs have focused on replacing cement by such AMFs. However, former studies also adopted

the replacement of sand. Figure 2.14 shows a summary of the impact of the replacement content on AAR expansions.

Figure 2.14 – Impact of replacement content on AAR expansions.

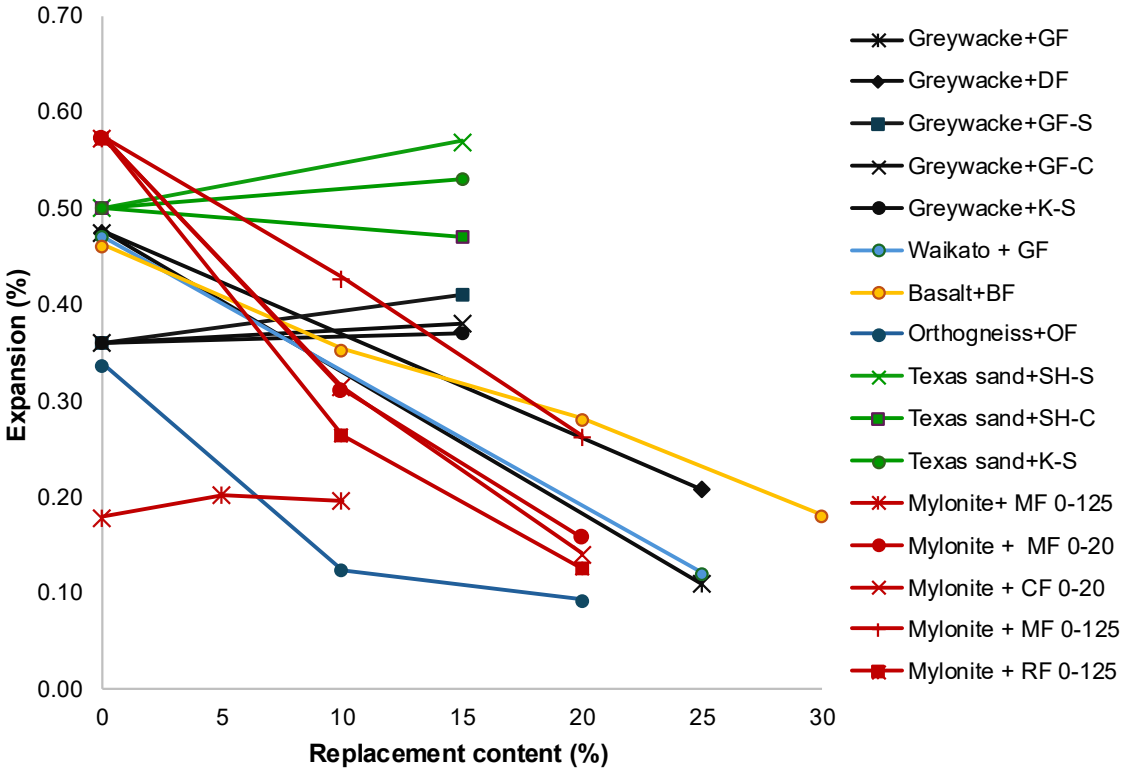

Source: Adapted from ANTUNES (2021); COUTINHO; MONTEFALCO; CARNEIRO (2024); OLIVEIRA; SALLES; ANDRIOLO (1995); PEDERSEN (2004); TAPAS *et al.* (2023).

As observed, most of the results indicate a reduction in expansions with the increase in the replacement percentage. Some of the curves show the opposite tendency, with increased expansions with the increase in the replacement percentage, all of which were tested by means of longer tests compared to the AMBT, such as ACPT and CPT. Moreover, for some of these curves, sand was replaced, which indicates that the replacement content has different roles depending on the material the AMF replaces. Figure 2.15 shows expansion results evaluating the influence of the replacement percentage by cement coupled with different parameters.

Figure 2.15 – Influence of replacement percentage of cement by reactive AMFs.

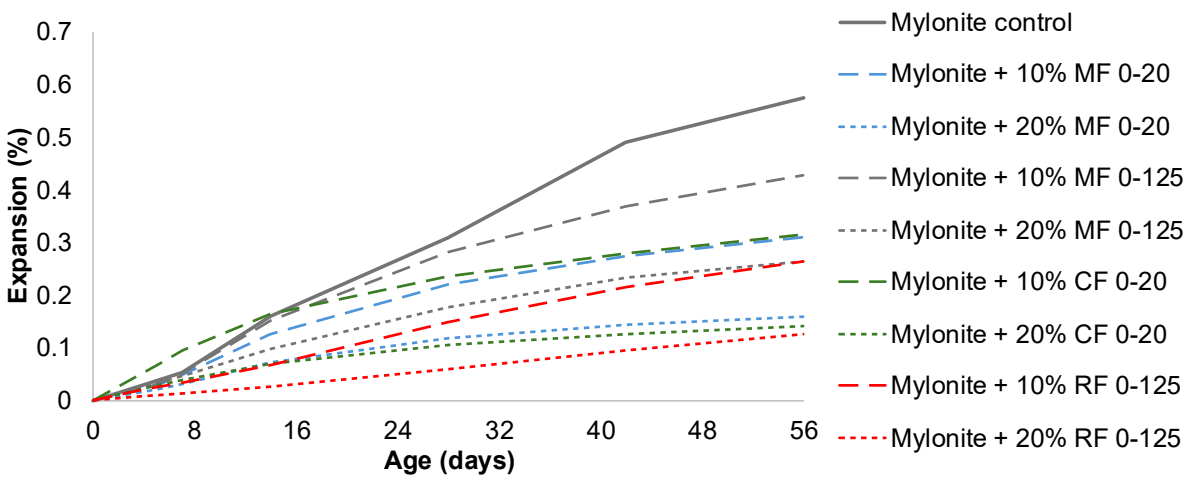

Source: Adapted from PEDERSEN (2004).

As observed, when varying t he replacement percentage while maintaining other parameters fixed such as coarse reactive aggregate, type of AMF, and PSD of the AMF, the expansions reduce by increasing the content.

2.2.5 Considerations

Considering the exposed, despite the promising results obtained, the variability of conditions and parameters applied hinders the understanding of reactive AMFs action in concrete and their practical application. Several tests have been used that differ in many aspects such as sample size, duration, temperature, and immersion conditions. Moreover, many parameters have been evaluated, such as reactivity degree of the aggregate, type of replacement, percentage, and PSD. When combined, all these differences among studies hinder the comparison of results, which also hinders the building of a strong knowledge regarding the topic, making the results isolated and disconnected.

There is considerable room for improvement, considering the advances in techniques and methodologies developed throughout the years that can be applied. Advanced techniques such as DRI and SDT can be used to evaluate the progression of ASR in concretes with AMFs and corresponding effects in mechanical aspects such as the modulus of elasticity. Moreover, a better characterization when it comes to the fineness of the material, as well as consideration of the mineralogy and replacement strategy, may enable comparative analyses.

CHAPTER 3 – RESEARCH PROGRAM

This chapter describes the materials and experimental program adopted in the study. To accomplish the objectives proposed, four parameters were evaluated: type of mixture, reactivity degree of the aggregate to produce AMFs, particle size distribution (PSD), and percentage, as illustrated in Figure 3.1.

Figure 3.1 – Parameters and methods of the study (NR: non-reactive, R: reactive).

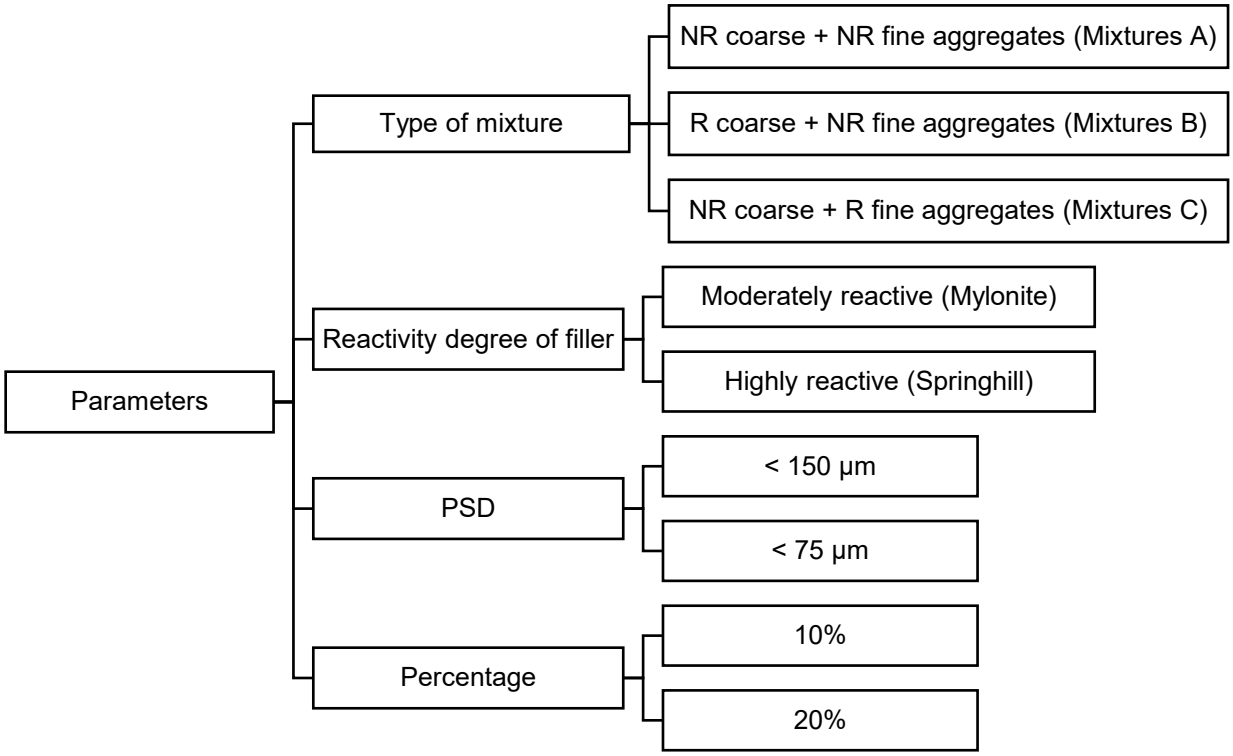

Source: Author (2025).

Regarding the type of mixture, three mixtures were produced: Mixtures A, with non-reactive coarse and fine aggregates, Mixtures B, with reactive coarse and non-reactive fine aggregates, and Mixtures C, with non-reactive coarse and reactive fine aggregates. To evaluate the influence of the reactivity degree of the filler, two types of aggregates were used to produce the fillers: a moderately reactive from Brazil and a highly reactive from Canada. Both aggregates are associated with several ASR cases in Brazil and Canada (Figure 3.2). Moreover, two PSDs (< 150 µm and < 75 µm) and replacement percentages (10% and 20%) were adopted. The following sections describe the materials and methods used.

Figure 3.2 – Structures affected by ASR in which the aggregates evaluated in this study were used. (a) Paulo Guerra bridge, Recife, Brazil (Mylonite). (b) Mactaquac dam, New Brunswick, Canada (Springhill).

(a) (b)

Source: (a) FIGUEIRÔA, ANDRADE (2007); (b) Mactaquac Dam (2015).

3.1 MATERIALS

The cement used was a conventional Portland cement GU type (equivalent to ASTM type I). The fillers used were produced from two reactive rocks, a moderately reactive mylonite from Brazil (Mylonite) and a highly reactive greywacke from Canada (Springhill). The chemical composition was determined by X-ray fluorescence (XRF) using a Rigaku Supermini200 WDXRF Spectrometer. The X-ray diffraction was conducted using a Rigaku Ultima IV Diffractometer. The results of the XRF for the cement and AMFs and diffractograms of the AMFs are presented in Table 3.1 and Figure 3.3, respectively.

Table 3.1 – Chemical composition of cement and AMFs.

Chemical composition	Cement (%)	Mylonite (%)	Springhill (%)
SiO_2	19.64	59.06	51.72
Al_2O_3	4.53	13.48	10.76
CaO	62.04	5.17	8.69
K_2O	0.97	3.58	2.70
Na_2O	0.42	3.45	1.45
MgO	2.64	3.22	5.59
Fe_2O_3	3.69	8.34	4.97
TiO_2	0.23	1.50	0.60
P_2O_5	0.14	0.89	0.11
MnO	0.05	0.12	0.07
Traces	1.81	0.36	0.33
L.O.I.	3.84	0.84	13.00
Na_2O_{eq}	1.06	5.80	3.23
TOTAL	100.00	100.00	100.00

Source: Author (2025).

Figure 3.3 – Diffractograms of the mylonite and Springhill fillers used.

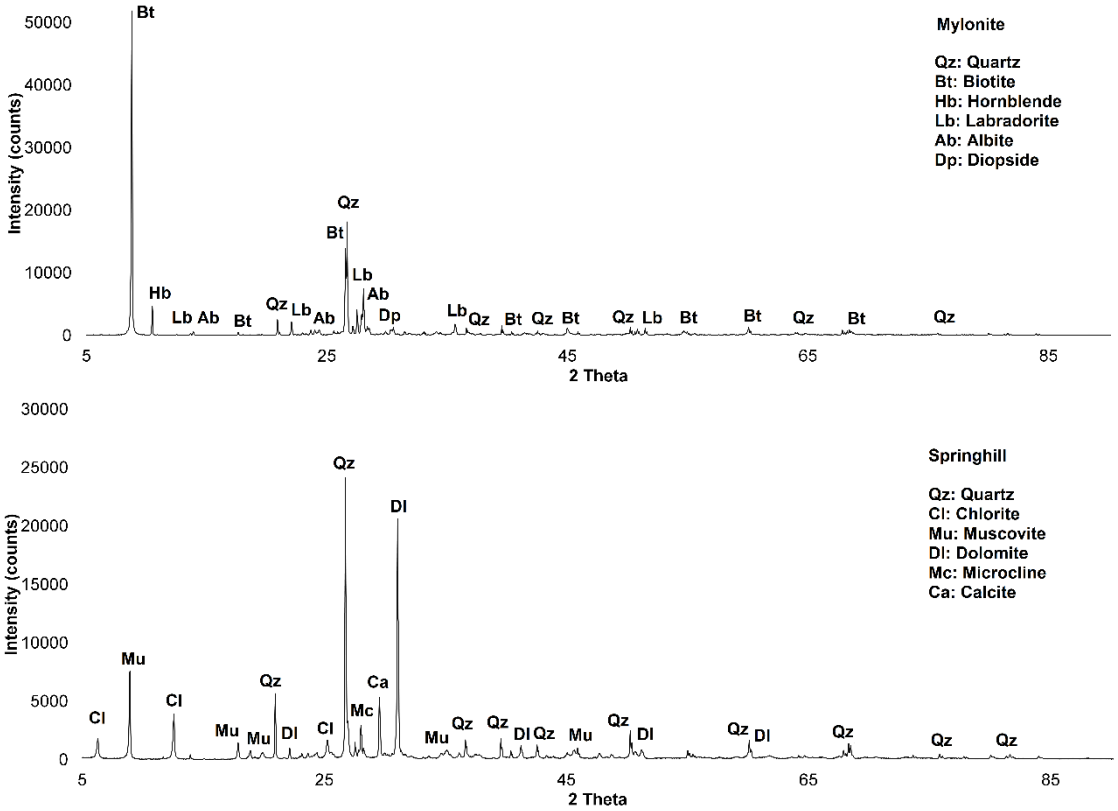

Quartz: SiO_2, Biotite: $(K(Mg,Fe)_3(AlSi_3O_{10})(F,OH)_2)$, Hornblende: $((Ca,Na)_{2\text{-}3}(Mg,Fe,Al)_5(Al,Si)_8O_{22}(OF,F)_2)$, Labradorite: $((Ca,Na)(Si,Al)_4O_8)$, Albite: $(Na,Ca)Al(Si,Al)_3O_8$, Diopside: $(MgCaSi_2O_6)$, Chlorite: $(Mg,Al)_6(Si,Al)_4O_{10}(OH)_8$, Muscovite: $(K,Na)(Al,Mg,Fe)_2(Si_{3.1}Al_{0.9})O_{10}(OH)_2$, Dolomite: $CaMg(CO_3)_2$, Microcline: $K(AlSi_3)O_8$, Calcite: $(Mg_{0.03}Ca0.97)(CO_3)$.
Source: Author (2025).

The aggregates were crushed using a jaw crusher and sieved to obtain powders passing the sieves with openings 150 µm and 75 µm. The use of the < 150 µm opening was based on the fractions adopted in the AMBT test (ASTM, 2023a), still extensively used in laboratories. In this test, the aggregates are crushed and fractions ranging from 4.8 mm to 150 µm are used, and the fraction passing the sieve with opening 150 µm is discarded. Therefore, this fraction was selected as the fraction to test the AMFs because it is indirectly produced. Moreover, to evaluate the effect of the filler PSD, the fraction passing the 75 µm sieve was also adopted. This choice was made considering the physical requirement for type C fillers (byproduct from aggregate crushing operations) of having ≥ 65% passing the 75 µm sieve for use in hydraulic cement concrete, as per the ASTM C1797 (ASTM, 2024). Previous studies have also used these parameters (CASTRO *et al.,* 1997; COUTINHO; MONTEFALCO; CARNEIRO, 2024; SALLES; OLIVEIRA; ANDRIOLO, 1997). The PSD curves of cement and fillers, obtained by laser diffraction, are shown in Figure 3.4.

Figure 3.4 – PSD of cement and fillers.

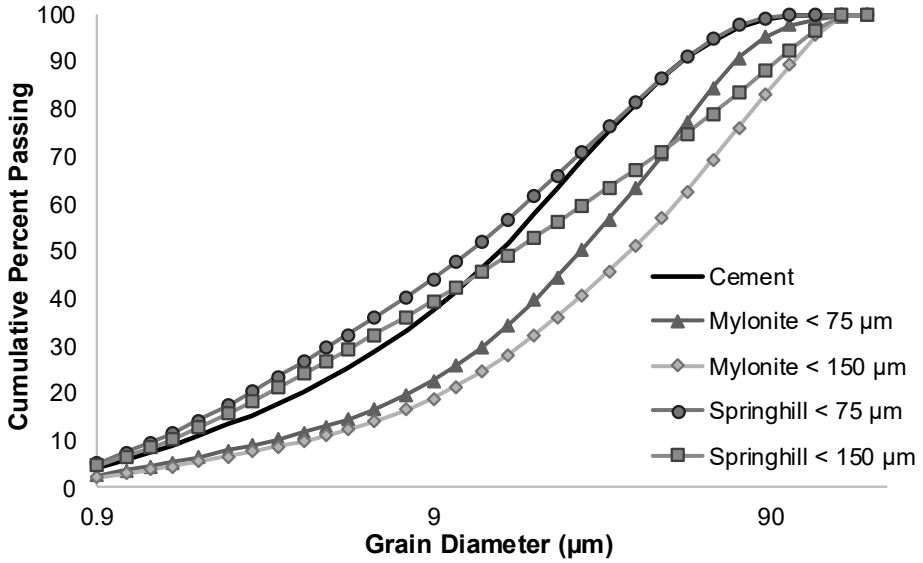

Source: Author (2025).

The percentages adopted were 10% and 20% based on the literature review conducted and the values used in other studies (CARLES-GIBERGUES *et al.,* 2008; COUTINHO; MONTEFALCO; CARNEIRO, 2024; LI; HE; HU, 2015). The replacement was made by cement to reduce the cement consumption considering the NetZero target. The coarse and fine aggregates adopted were reactive and non-reactive, as detailed in Table 3.2.

Table 3.2 – Coarse and fines aggregates used.

Aggregate		**Reactivity**	**Rock Type**	**Specific Gravity**	**Absorption (%)**	**AMBT* (%)**
Coarse	SP	ASR	Greywacke	2.66	0.89	0.33
	LC	NR	Crushed limestone	2.78	0.42	0.02
Fine	TX	ASR	Natural derived from granitic, mixed volcanics, quartzite, chert, quartz)	2.60	0.82	0.81
	NS	NR	Natural sand	2.70	0.40	0.04

* Results of the AMBT test as per ASTM C 1260.

Source: Author (2025).

3.2 EXPERIMENTAL PROGRAM

3.2.1 Production of samples

The CPT was conducted to measure ASR expansions. This test was selected to allow a better representation of field concrete when compared to other tests used such as the AMBT and ACPT. Moreover, previous results indicated that AMFs of rocks containing siliceous mineral phases may exhibit pozzolanic activity at high temperatures such as 80 ºC (PEDERSEN, 2004). Therefore, the use of tests at lower temperatures would be fundamental when assessing AMFs.

Concrete cylinders of 100 × 200 mm were produced in this study. For each type of mixture (mixtures A, B, C), samples were cast using the two fillers adopted (Mylonite and Springhill) and varying the PSD (< 150 µm and < 75 µm) and percentage (10% and 20%), representing 8 families per mixture and a total of 24 families. For each family, four ages were tested, 1, 3, 6, and 9 months. Based on previous studies using these aggregates, the expansions start stabilizing after 6 months (ANTUNES, 2021; BEZERRA, 2021; DE GRAZIA, 2023; REZAIEH, 2021; SOUZA, 2022; ZUBAIDA, 2020). Therefore, tests were conducted at the ages of 1, 3, and 6 months. Six samples were produced for each age for expansion measurements and three additional samples for the compressive strength test, totalling 27 samples per family and 648 for the project. The nomenclature adopted consisted of the type of mixture (A, B, C) followed by the type of filler (M or SP), PSD (150 or 75), and percentage (P10 or P20). Therefore, a sample named BM150P20 would indicate mixture B with mylonite filler, PSD of 150 µm, and percentage of 20%.

The mixture design followed the requirements of ASTM C1293 (ASTM, 2023b). The concrete was boosted with NaOH to reach an alkali equivalent of 5.25 kg/m^3 of concrete. Three fractions of coarse aggregate were used in the same proportion: 19.0–12.5 mm, 12.5–9.5 mm, and 9.5–4.75 mm. The water/cement ratio adopted was 0.45 and the cement + filler content was 420 kg/m^3. The mixture proportions used are listed in Table 3.3.

Table 3.3 – Concrete mixture proportions.

Mixture	Filler	PSD	%	Cement (kg/m^3)	Filler (kg/m^3)	FA – NR* (kg/m^3)	CA – NR* (kg/m^3)	Water (kg/m^3)
A	M	150	10	378.00	42.00	723.07	1133.44	170.10
A	M	150	20	336.00	84.00	723.07	1133.44	151.20
A	M	75	10	378.00	42.00	723.07	1133.44	170.10
A	M	75	20	336.00	84.00	723.07	1133.44	151.20
A	SP	150	10	378.00	42.00	723.07	1133.44	170.10
A	SP	150	20	336.00	84.00	723.07	1133.44	151.20
A	SP	75	10	378.00	42.00	723.07	1133.44	170.10
A	SP	75	20	336.00	84.00	723.07	1133.44	151.20
Mixture	**Filler**	**PSD**	**%**	**Cement**	**Filler**	**FA - NR**	**CA - R**	**Water**
B	M	150	10	378.00	42.00	764.50	1043.70	170.10
B	M	150	20	336.00	84.00	764.50	1043.70	151.20
B	M	75	10	378.00	42.00	764.50	1043.70	170.10
B	M	75	20	336.00	84.00	764.50	1043.70	151.20
B	SP	150	10	378.00	42.00	764.50	1043.70	170.10
B	SP	150	20	336.00	84.00	764.50	1043.70	151.20
B	SP	75	10	378.00	42.00	764.50	1043.70	170.10
B	SP	75	20	336.00	84.00	764.50	1043.70	151.20
Mixture	**Filler**	**PSD**	**%**	**Cement**	**Filler**	**FA - R**	**CA - NR**	**Water**
C	M	150	10	378.00	42.00	696.83	1133.44	170.10
C	M	150	20	336.00	84.00	696.83	1133.44	151.20
C	M	75	10	378.00	42.00	696.83	1133.44	170.10
C	M	75	20	336.00	84.00	696.83	1133.44	151.20
C	SP	150	10	378.00	42.00	696.83	1133.44	170.10
C	SP	150	20	336.00	84.00	696.83	1133.44	151.20
C	SP	75	10	378.00	42.00	696.83	1133.44	170.10
C	SP	75	20	336.00	84.00	696.83	1133.44	151.20

* FA: fine aggregate; CA: coarse aggregate; NR: non-reactive; R: reactive.

Source: Author (2025).

The ends of the samples were drilled and steel gauges were placed using fast-setting cement slurry (Figure 3.5). The samples were allowed to harden for 24 h, after which the initial measurements were taken. The samples were stored in sealed plastic buckets lined with a moist cloth at 38 ºC and 100% relative humidity (RH). The cylinders were regularly measured and taken at the ages of 1, 3, and 6 months for additional tests.

Figure 3.5 – Samples with steel gauges for longitudinal expansion measurements.

Source: Author (2025).

3.2.2 Kinetics and Ultimate Expansion

The kinetics and ultimate expansion, considered as the expansion at the end of the test or from which the expansion stabilize, were evaluated by measuring the expansions at given ages using a measuring arch (Figure 3.6), as per the standard ASTM C1293 (ASTM, 2023b).

Figure 3.6 – Measuring arch for expansion measurements.

Source: Author (2025).

3.2.2 Compressive Strength

The compressive strength test was conducted to determine the test load for the SDT. At least three samples per combination were tested. The samples for compressive strength were wrapped in plastic film and stored in a chamber at 12 ºC to avoid the development of ASR, which can affect the results of the test, as reactive aggregates were used. The samples remained at this temperature for 47 days, which corresponds to 28 days at 20 ºC, as per the maturity concept by ASTM C 1074 (ASTM, 2019). This procedure was validated by Sanchez (2014) and Sanchez et al. (2016).

3.2.3 Stiffness Damage Test

The SDT was performed as per the procedure described in the works of Sanchez and colleagues (SANCHEZ *et al*., 2014, 2017a, 2018). Five cycles of loading/unloading were conducted and the maximum load adopted was 40% of the compressive strength of samples at 28 days with a loading rate of 0.10 MPa/s. The results obtained were an average of three samples tested at each testing period (i.e., 1, 3, and 6 months).

3.2.4 Damage Rating Index

The DRI was calculated as per the method described in Villeneuve (2011) and Sanchez et al. (2016). The samples were axially cut in half and polished using a hand polisher device by means of diamond impregnated rubber disks (nº. 50, 100, 200, 400, 800, 1500, 3000). The analysis was conducted using a stereomicroscope (16× magnification) at the ages of 1, 3, and 6 months. The final DRI number was normalized for an area of 100 cm^2.

3.3. SCIENTIFIC PAPERS

Based on the experimental program implemented to achieve the goals of this study, three scientific papers were produced, as depicted in Figure 3.7.

Figure 3.7 – Scientific papers produced.

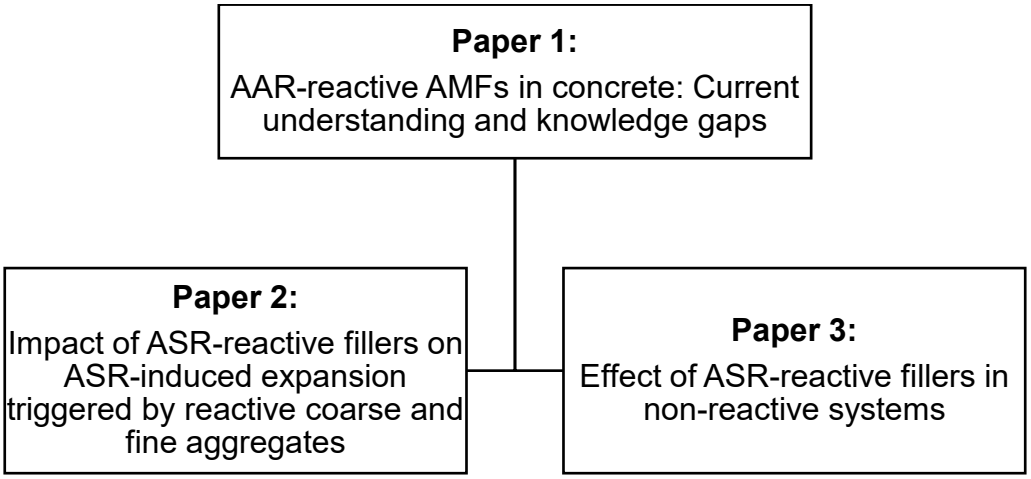

Source: Author (2025).

Paper 1 is a literature review aimed to provide an overview of the use of AAR-reactive mineral fillers in concrete. An extensive analysis was conducted on different uses of mineral fillers, as well as different types of filler, and ultimately focusing on ASR-reactive fillers in concrete and the current understanding of their action in concrete.

The knowledge gap identified in Paper 1 related to the lack of studies evaluating ASR-reactive fillers replacing cement was explored in Papers 2 and 3. In Paper 2, ASR-reactive fillers were used replacing cement in reactive systems, with reactive coarse and non-reactive fine aggregates and with reactive fine and non-reactive coarse aggregates. Two fillers from reactive rocks with different reactivity degrees were used, a moderately reactive Brazilian mylonite and a highly reactive Canadian greywacke (Springhill). Moreover, two particle size distributions (> 150 μm and (> 75 μm) and two replacement percentages (10% and 20%) were evaluated. In contrast, Paper 3 explored the effect of reactive fillers in non-reactive systems (non-reactive course and fine aggregates). The same parameters in Paper 2 were also evaluated in Paper 3. Both papers focused on the impact of ASR-reactive fillers considering ASR-induced expansion (i.e., CPT) and deterioration (multilevel assessment).

CHAPTER 4 – AAR-REACTIVE AMFs IN CONCRETE: CURRENT UNDERSTANDING AND KNOWLEDGE GAPS

This chapter is based on a paper submitted to Buildings.

Yane Coutinho [1, 2, *], Leandro Sanchez [2], and Arnaldo Carneiro [1]

[1] Federal University of Pernambuco, Recife, Brazil.
[2] Department of Civil Engineering, University of Ottawa, Ottawa, Canada.

Abstract: The depletion of natural resources and the increasing interest in reducing CO_2 emissions have heightened the demand for alternative materials in concrete production. A viable approach is to lower the clinker-to-cementitious materials ratio by partially replacing clinker with supplementary cementitious materials (SCMs) and/or alternative materials such as aggregate mineral fillers (AMFs). As the availability of SCMs is expected to decline, AMFs have been increasingly explored, including those derived from aggregates processing and susceptible to alkali-aggregate reaction (AAR). However, the behaviour of AAR-reactive AMFs in concrete remains poorly understood. This paper summarizes the current state of the art and identifies knowledge gaps concerning the use of AAR-reactive AMFs, focusing on the roles of mineralogy, particle size, replacement content, and the test methods used to assess AAR-induced development and associated microscopic and mechanical deterioration. A consistent terminology is also proposed to support future research. Finally, a theoretical foundation to understand the role of AAR-reactive AMFs in mortar and concrete is provided, and the key knowledge gaps are discussed.

Keywords: alkali-aggregate reaction, alkali-silica reaction, aggregate mineral filler, reactive AMF, reactive filler, concrete durability.

4.1. INTRODUCTION

The pursuit to reduce the carbon footprint of concrete construction towards achieving NetZero by 2025 (IEA, 2021) has stimulated studies focusing on reducing the use of cement (i.e., clinker) (IEA, 2020). Reducing the clinker-to-cementitious materials ratio

by partially replacing cement with supplementary cementitious materials (SCM) or mineral fillers is a viable alternative to reduce CO_2 emissions in the short term (AMRAN *et al.*, 2022; BALLAN; PAONE, 2014; DAMTOFT *et al.,* 2008; EUROPEAN CEMENT RESEARCH ACADEMY, 2017; GARTNER; HIRAO, 2015; IEA, 2020; LOTHENBACH; SCRIVENER; HOOTON, 2011; LUDWIG; ZHANG, 2015; MILLER *et al.*, 2021; SCRIVENER *et al.*, 2018; SCRIVENER; JOHN; GARTNER, 2018; VON GREVE-DIERFELD *et al*., 2020). However, conventional SCMs (e.g., blast-furnace slag, silica fume, fly ash, etc.) are byproducts of some industries, which have shown important activity reduction in recent years, prompting investigations into alternative materials (SCRIVENER; JOHN; GARTNER, 2018).

In this context, the use of fillers has gained attention as an alternative material to reduce clicker demand (SCRIVENER; JOHN; GARTNER, 2018). A filler is defined as a particulate product that is inert or almost chemically inert when mixed with Portland cement (ACI, 2020; JOHN *et al.*, 2018). The American Concrete Institute defines aggregate mineral fillers (AMFs) as a finely divided inorganic material produced in crushing operations of rocks (ACI, 2020). The use of AMFs normally enhances concrete properties by means of a physical filling effect (KORPA; KOWALD; TRETTIN, 2008) and extra specific surface area that acts as nucleation sites for the precipitation of clinker hydration products (AQEL; PANESAR, 2016; LI *et al.*, 2018; LOTHENBACH; SCRIVENER; HOOTON, 2011; MOOSBERG-BUSTNES; LAGERBLAD; FORSSBERG, 2004). Considering this potential, AMFs from different sources, including quartzite (CRAEYE *et a*l., 2010; KADRI *et al*., 2010; POPPE; DE SCHUTTER, 2005; RAHHAL; TALERO, 2005), alumina (POPPE; DE SCHUTTER, 2005), basalt (DOBISZEWSKA; SCHINDLER; PICHÓR, 2018; LI *et al.*, 2021; SOROKA; SETTER, 1977; XIE *et al.*, 2024; ZHU *et al.,* 2024), diabase (ZHU *et al.,* 2024), tuff (ZHU *et al.,* 2024), dolomite (SOROKA; SETTER, 1977), marble (MULTON *et al.,* 2010; VARDHAN *et al.,* 2015), granite (COUTINHO, 2019; MÁRMOL *et al.,* 2010; RAMOS *et al.,* 2013), have been studied. However, limited information is available regarding the durability aspect of concrete produced with AMFs.

Among the rocks used to produce AMFs, some may be susceptible to alkali-aggregate reaction (AAR). AAR refers to a chemical reaction between certain mineral phases in the aggregates and the alkalis present in the concrete pore solutions (FOURNIER; BERUBÉ, 2000; LEEMANN *et al*., 2024a; NIXON; SIMS, 2016). AAR is commonly

divided into two main types with different mechanisms: alkali-silica reaction (ASR) and alkali-carbonate reaction (ACR) (FOURNIER; BERUBÉ, 2000). ASR involves the interaction between metastable siliceous phases in the aggregates and hydroxyl ions in the pore solution. This reaction forms a hydrophilic expansive gel (i.e., ASR gel) with an opposite surface charge to that of the aggregate, and repulsive forces at the interface of the aggregate and the gel, leading to progressive expansion and deterioration of the affected concrete (LEEMANN *et al*., 2024a). ASR has been reported to affect critical concrete infrastructure worldwide (SIMS; POOLE, 2017). In contrast, despite being associated with certain dolomitic carbonate rocks, the mechanism of ACR remains under debate and has only been identified in a limited number of countries (GRATTAN-BELLEW *et al*., 2010; KATAYAMA, 1992, 2010; KATAYAMA; GRATTAN-BELLEW, 2012; LEEMANN *et al.*, 2024b; MEDEIROS; SANCHEZ; DOS SANTOS, 2024; THOMAS; FOURNIER; FOLLIARD, 2013).

AAR poses a significant challenge to the long-term durability of concrete infrastructure and is among the most harmful deterioration mechanisms affecting concrete infrastructure around the globe, compromising both their durability and serviceability. As rehabilitation of AAR-affected structures is complex and costly, preventive approaches are generally more effective and economical.

Therefore, considering the importance of alternative materials to reduce the clinker-to-cement ratio as a strategy to reduce CO_2 emissions, the use of AMFs becomes a viable option; however, the use of AAR-reactive AMFs, which are available worldwide, raises concerns as their long-term behaviour in concrete remains insufficiently understood. This paper reviews the current knowledge on using AAR-reactive AMFs in concrete, presenting important questions related to the reaction mechanisms, such as kinetics, ultimate expansion, deterioration, and mitigation potential. A theoretical foundation for understanding the role of AAR-reactive AMFs in mortar and concrete is provided, and the key knowledge gaps are discussed.

4.2. EVALUATION OF SYSTEMS CONTAINING REACTIVE AMFs

4.2.1. Test methods to assess AAR induced expansion

The most widely used test procedures to appraise the potential reactivity of aggregates are the accelerated mortar bar test (AMBT) (ABNT, 2018a; ASTM, 2023a) and concrete prism test (CPT) (ABNT, 2018b; ASTM, 2023b; CSA, 2024). From these

tests, ASR kinetics (i.e., expansion rate over time (SANCHEZ *et al*., 2018)) and ultimate expansion (i.e., maximum expansion resulting from ASR) can be obtained. These parameters can help assess the effects of AAR-reactive AMFs in systems with reactive or non-reactive aggregates. In reactive systems, the type of reactive aggregates, whether coarse or fine, must also be analyzed separately. In general, most of the studies focused on the use of AMFs with reactive coarse aggregates.

The AMBT is commonly adopted given its fast duration (i.e., 16 days – ASTM C1260 (ASTM, 2023a) and CSA A23.2-25A (CSA, 2024), 30 days – Brazilian standard NBR 15577-4 (ABNT, 2018a), 56 days – Norwegian standard). However, the test is conducted in mortar, requiring crushing of aggregates, which may affect its reactive potential, and the conditions are harsh (i.e., samples immersed in a 1N NaOH solution, 80 ºC), leading to misclassification of some aggregates (BÉRUBÉ; FOUNIER, 2003; DEMERCHANT; FOURNIER; STRANG, 2000; GOLMAKANI; HOOTON, 2016; GRATTAN-BELLEW, 1997; IDEKER *et al*., 2012; THOMAS *et al*., 2006). The CPT (ASTM C1260 (ASTM, 2023b), CSA A23.2-14A (CSA, 2024), and NBR 15577-6 (ABNT, 2018b)) is considered more reliable compared to the AMBT owing to more realistic storage conditions (i.e., 38 ºC, high relative humidity (RH)). However, the duration of the test is one year, and some challenges remain to be addressed, such as alkali leaching (IDEKER *et al*., 2010; LINDGÅRD *et a*l., 2012). Other tests have been developed to address some shortcomings of these tests, such as the accelerated CPT (ACPT, RILEM AAR 4.1 (NIXON; SIMS, 2016) and NBR 15577:7 (ABNT, 2018d)). This test has a reduced duration (i.e., 180 days) compared to the CPT, increased particle size distribution (PSD) compared to that used in the AMBT (AASHTO, 2022; LINDGÅRD *et al*., 2011; THOMAS; FOURNIER; FOLLIARD, 2013), and intermediate conditions (i.e., 60 ºC, 100% RH).

The following sections present literature data on the use of AMBT, CPT, and ACPT to evaluate reactive and non-reactive systems containing AAR-reactive AMFs incorporating i) reactive coarse, ii) reactive fine, and iii) non-reactive aggregates.

4.2.1.1. Accelerated mortar bar test (AMBT)

Figure 4.1 depicts the AMBT expansion curves available in the literature for systems containing reactive coarse aggregates and reactive AMFs. The solid lines represent results of control mixtures, and dashed lines represent results of mixtures containing

ASR-reactive AMFs. Each color represents a family of results for the same coarse aggregate used.

As observed, the ultimate expansion was reduced for all the AMFs used. The expansions reduced up to 74% for greywacke fillers (GF), 56% for dacite fillers (DF, greywacke coarse aggregate), 72% and 91% for sandstone fillers (SF) Capanda and Formosa, respectively, 61% for basalt fillers (BF), and 74% for orthogneiss fillers (OF). Differences in the effect on the ultimate expansion were observed for different parameters evaluated, such as the reactivity degree of the aggregate and percentage of AMFs, which will be further discussed in the coming sections.

Figure 4.1 – Expansion results of systems with reactive coarse aggregates and reactive fillers (SF: Sandstone fillers; DF: Dacite fillers; GF: Greywacke fillers; BF: Basalt fillers; OF: Orthogneiss fillers.

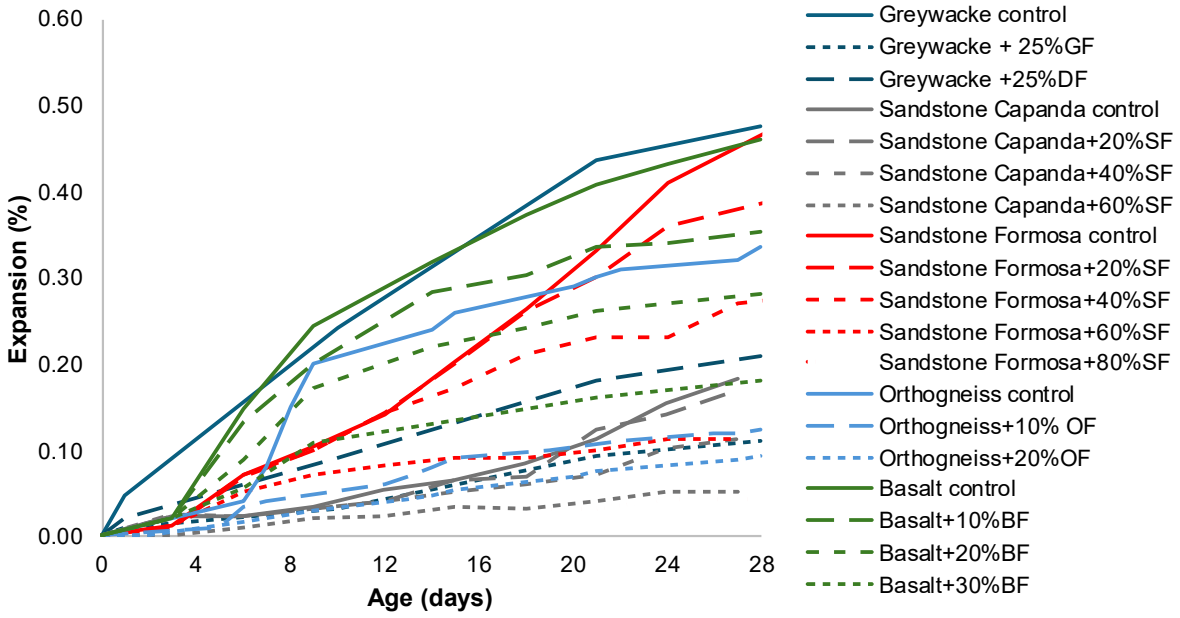

Source: Adapted from CASTRO *et al.* (1997); COUTINHO; MONTEFALCO; CARNEIRO (2024); OLIVEIRA; SALLES; ANDRIOLO (1995); TAPAS et al. (2023).

In a robust study by Pedersen (2004), several parameters were appraised using both the AMBT and CPT following Norwegian standards. The AMBT results are shown in Figure 4.2.

As observed, the AMBT results obtained with the Norwegian standard were similar to those obtained using the ASTM standard (Figure 4.1), that is, lower expansions with the use of AMFs. The parameters evaluated were type of AMFs (i.e., mylonite (MF), granite (GF), cataclasite (CF), rhyolite (RF)), PSD (i.e., 0–20 μm, 10–30 μm, 10–40 μm, 20–125 μm, 0–125 μm), and percentages (i.e., 10% and 20%). The mixtures with

reactive AMFs (dashed lines) resulted in reduced ultimate expansion compared to the control curves (solid lines). The exception was the mixture with mylonite as aggregate and 20% GF, with higher expansions than the control mixture.

Figure 4.2 – AMBT expansion results using reactive AMFs (Norwegian standard).

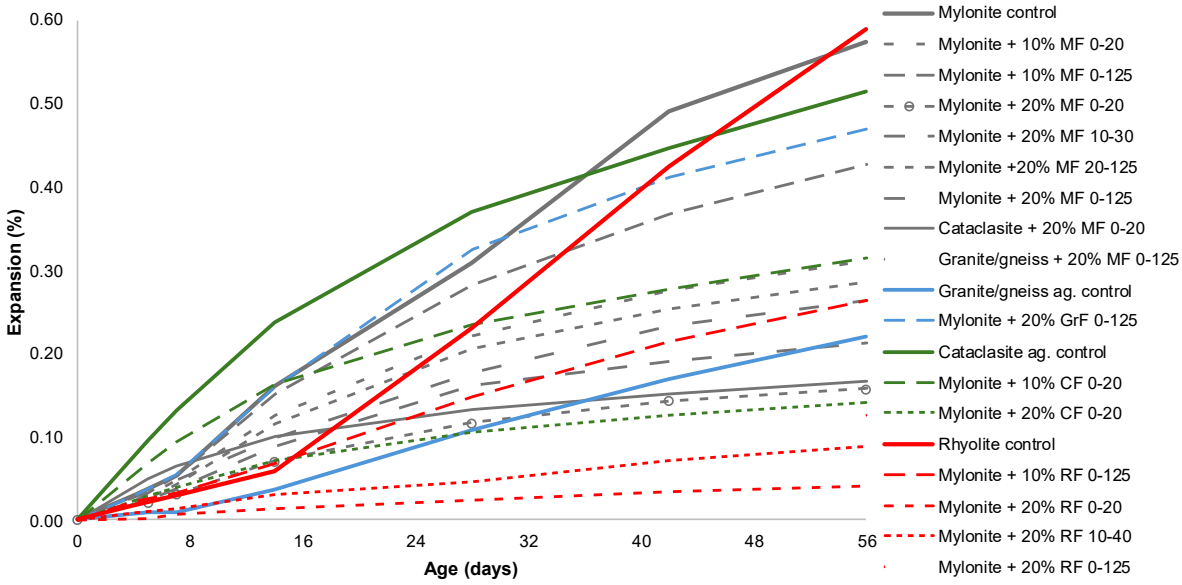

Source: Adapted from PEDERSEN (2004).

Few studies evaluated systems with fine reactive aggregates (ANTUNES, 2021; TAPAS *et al.*, 2023). In this regard, the AMBT was used to assess a combination with reactive Waikato natural river sand and reactive AMFs produced from a greywacke (GF), and replacing 25% of cement (Figure 4.3). Fine reactive aggregates usually exhibit a faster rate of reaction (SANCHEZ *et al.*, 2018), reaching considerable expansion levels at early ages, as observed in the figure by the steep inclination of the control curve. When using GF in Figure 4.3, the rate of reaction was slowed. Moreover, the maximum expansion was reduced from 0.47% to 0.12%, representing a reduction of approximately 74%.

Figure 4.3 – AMBT results for a system with reactive fine aggregates.

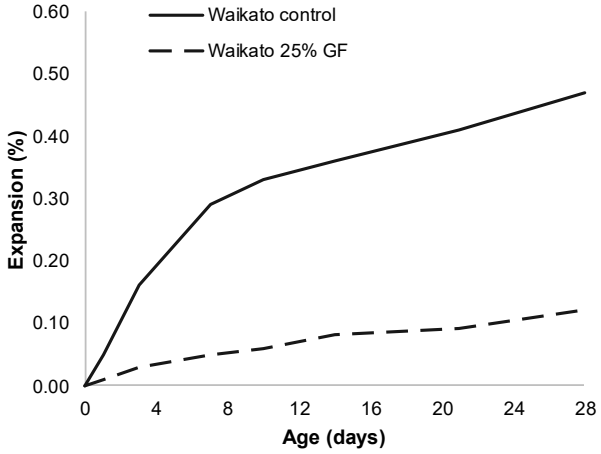

Source: Adapted from TAPAS *et al.* (2023).

Overall, for the AMBT, a lower rate of reaction and maximum expansions were obtained for systems with both reactive coarse and reactive fine aggregates and AAR-reactive AMFs compared to systems without AMFs.

4.2.1.2. Concrete prism test (CPT)

Figure 4.4 shows expansion results obtained through the CPT. In general, the kinetics and ultimate expansions of the combinations were similar to those of the control mixture, except for the combination with RF, in which the expansion was considerably reduced. In this case, the type of AMFs may have played a significant role, as RF has been reported to have pozzolanic activity (PEDERSEN, 2004).

Figure 4.4 – CPT expansion results using reactive AMFs (Norwegian version).

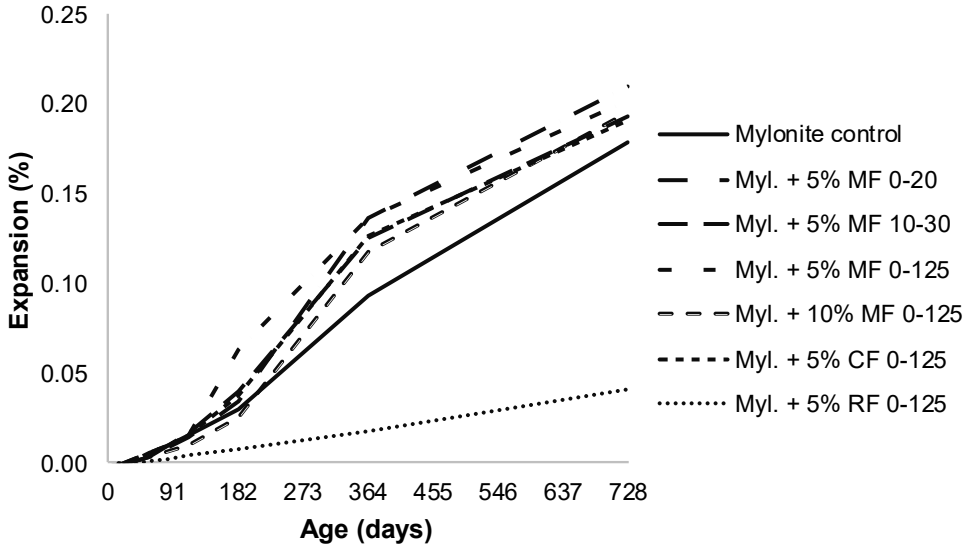

Source: Adapted from PEDERSEN (2004).

In addition to systems with reactive aggregates, the study of non-reactive systems, in which reactive AMFs and non-reactive aggregates are used, is very important but has not been extensively addressed in previous studies. This analysis was found in one study in which limestone fillers were used in percentages of 15% and 30% (50% replacing cement and 50% replacing sand) (GUÉDON-DUBIED *et al.,* 2000). As observed in Figure 4.5, the use of the reactive AMFs resulted in increased expansions. Despite the different percentages, the expansions after 1 year for both replacement levels were similar. However, compared to the control curve, the average ultimate expansion was two times higher.

These results indicate the potential impact of reactive AMFs in non-reactive systems. Further studies should focus on different lithologies of aggregates to be used as AMFs. Moreover, both cement and sand were replaced by AMFs, hindering the identification of individual effects. The type of replacement, whether by cement or sand, should be tested separately to identify the corresponding influences on the kinetics, ultimate expansion, and concrete deterioration process.

Figure 4.5 – Expansion of non-reactive systems containing reactive AMFs.

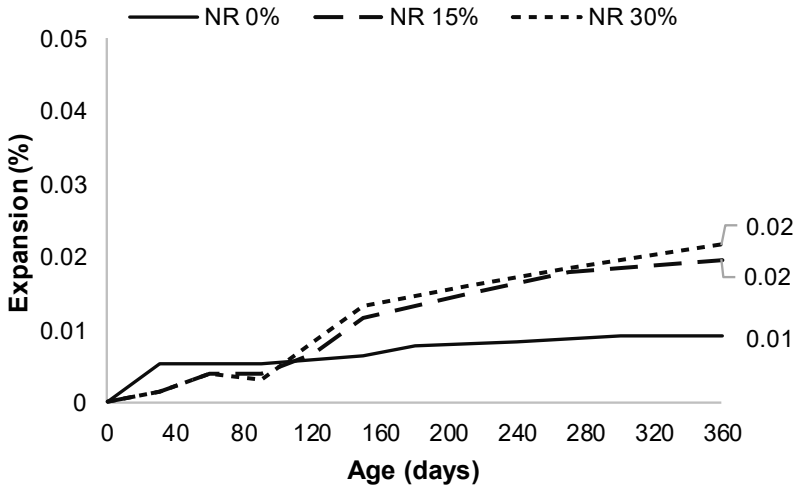

Source: Adapted from GUÉDON-DUBIED et al. (2000).

4.2.1.3. Accelerated concrete prism test (ACPT)

Figure 4.6(a) shows expansion results of mixtures with AAR-reactive AMFs using the ACPT. As observed, combinations with reactive coarse aggregates (greywacke – SH), two AMFs (greywacke – SH and dolomitic argillaceous limestone – K, ASR- and ACR-reactive, respectively), and replacing sand (15% SH) and cement (15% SH-C) resulted

in similar or slightly higher ultimate expansions. For the combination with SH AMFs replacing sand, the kinetics was also accelerated. The above outcomes contradict the AMBT results, in which the use of AAR-reactive AMFs led to reduced expansions, but are in agreement with the CPT results (Figure 4.4).

Moreover, the ACPT was utilized to evaluate a system incorporating a highly reactive sand (i.e., Texas sand – TX), and AMFs from a greywacke (SH) and a limestone (K), which are ASR- and ACR-reactive, respectively, replacing 15% of cement and sand (Figure 4.6(b)).

Combinations with reactive fine aggregates or reactive coarse aggregates incorporating AAR-reactive AMFs exhibited similar or slightly higher ultimate expansions and similar or accelerated kinetics compared to combinations without AAR-reactive AMFs (Figure 4.6(a)). The type of test and the aggregate features (i.e., reactivity degree, PSD) may have influenced the results. To better understand the effect of AAR-reactive AMFs in systems with fine reactive aggregates, a long-term evaluation coupled with continuous assessment of the deterioration, that is, evaluating samples at different ages to understand how the deterioration is progressing, is essential.

Figure 4.6 – (a) ACPT results for combinations with AAR-reactive AMFs and reactive coarse aggregates. (b) ACPT results for systems with reactive fine aggregates (TX). SH: Springhill, reactive greywacke aggregate; K: Kingston, limestone associated with ACR occurrences

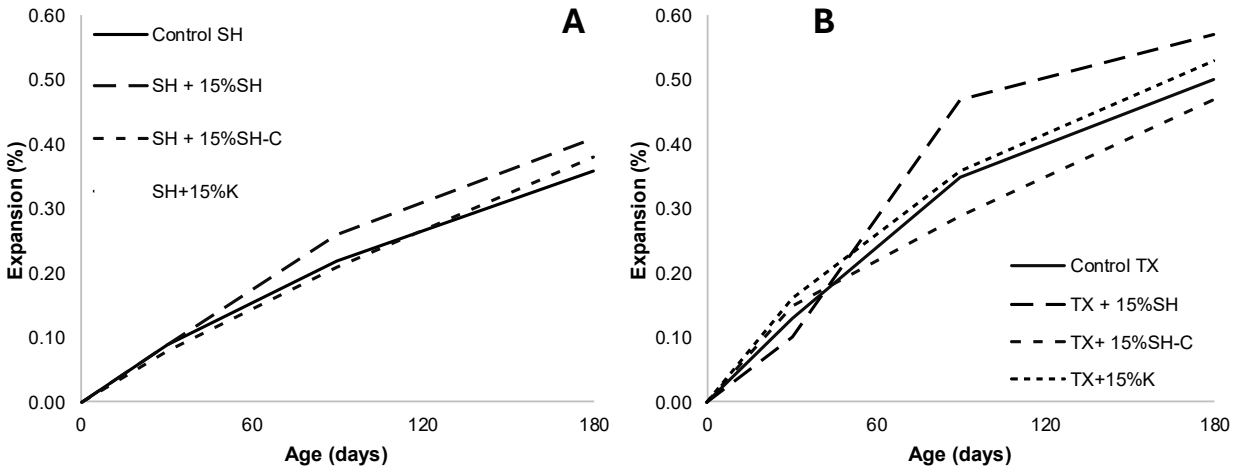

Source: Adapted from ANTUNES (2021).

4.2.2. Test methods to assess AAR-induced deterioration

The methods used to evaluate the deterioration progress of systems with AAR-reactive AMFs were surface cracking (CARLES-GIBERGUES *et al.,* 2008) along with the damage rating index (DRI) and stiffness damage test (SDT) (ANTUNES, 2021). For the surface cracking evaluation, prisms of 7×7×28 cm stored at 60 ºC with 20% AMFs replacing sand were stored for 34 weeks. As observed in Figure 4.7, a drastic reduction in surface cracking was observed for samples with a reactive aggregate and 20% of sand replaced by AMFs derived from the same aggregate (i.e., metaquartzite (o): 100% reduction, siliceous limestone (t): approximately 90% reduction, opaline aggregate (b): 100% reduction, crushed waste glass (g): 100% reduction).

Figure 4.7 – Influence of the use of AMFs on surface cracking of concrete prisms. O, T, B, G refer to the aggregates and O-o, T-t, B-b, G-g to the samples with the use of the corresponding reactive fillers

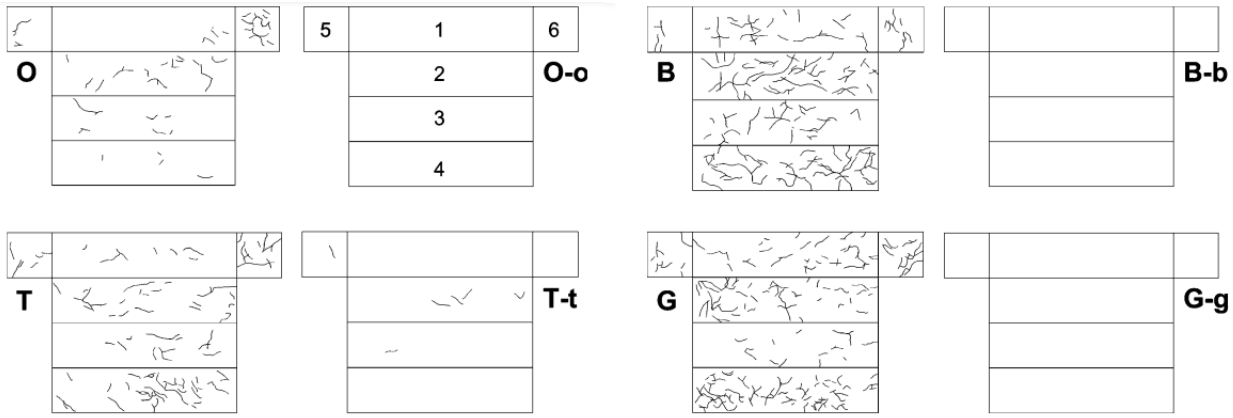

Source: CARLES-GIBERGUES et al. (2008).

The DRI is a petrographic analysis to evaluate the deterioration progress of a concrete sample. Samples are cut, polished, and analyzed using a stereomicroscope (15–16× magnification) (2016b). Deterioration features (i.e., open cracks in aggregate, closed cracks in aggregate, cracks in the cement paste) are counted in a 1 cm^2 grid drawn on the surface of a polished concrete section (SANCHEZ, 2014). Each petrographic feature has a weight. The DRI is calculated by averaging the features found multiplied by the corresponding weights (Figure 4.8) and normalized for an area of 100 cm^2. The SDT provides a correlation between loading cycles and crack density. The test consists of applying five cyclic loads in compression (i.e., generally 40% of the compressive strength at 28 days representing the elastic range limit) to concrete specimens. Some of the outcomes of the test are the stiffness damage index (SDI), which is the ratio of

the dissipated energy to the total energy, and the modulus of elasticity reduction (SANCHEZ *et al*., 2018).

Figure 4.8 – (a) Important features to determine the DRI of a sample (CCP: crack in cement paste; OCA: open crack in aggregate; CCA: closed crack in aggregate) (ANTUNES, 2021). (b) Sample with greywacke AMF replacing 15% of sand.

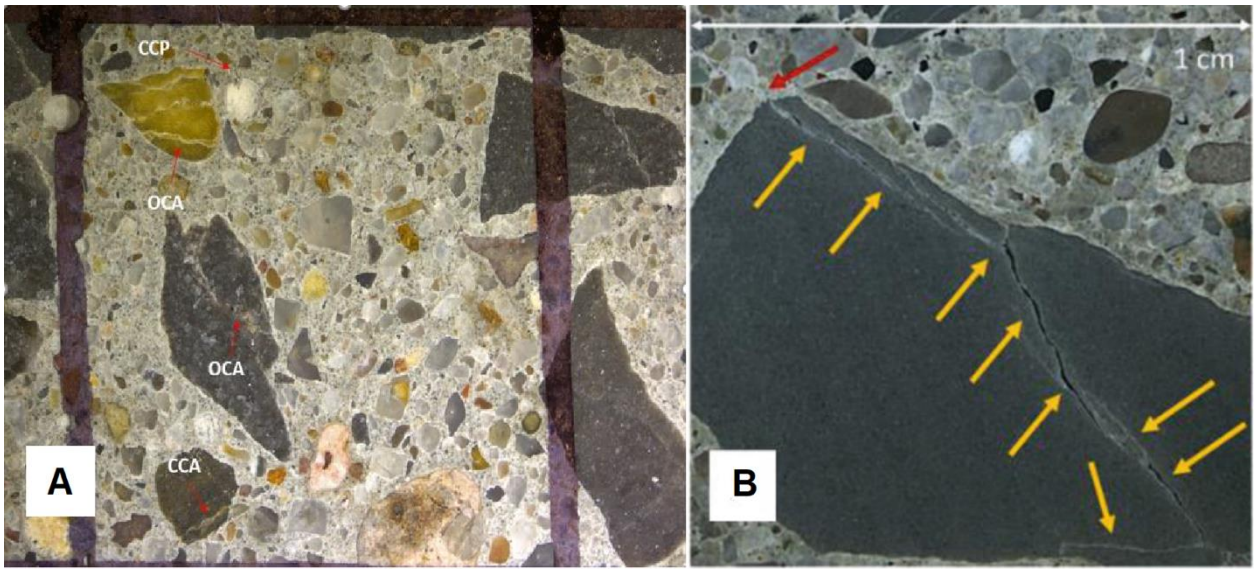

Source: (a) ANTUNES, 2021. (b) DE SOUZA; SANCHEZ; BIPARVA, 2024.

The DRI and SDT were adopted to evaluate systems containing 15% greywacke or dolomitic argillaceous limestone fillers (i.e., ASR- and ACR-reactive, respectively) with reactive coarse and reactive fine aggregates. When the greywacke fillers replaced cement, the DRI values were lower (ANTUNES, 2021), but a replacement by sand led to similar to or higher DRI values compared to the DRI for a system with no AMFs. Replacing 15% of dolomitic argillaceous limestone fillers by sand resulted in similar DRI for systems with reactive coarse aggregates and lower DRI for systems with reactive fine aggregates. The main difference that caused this variation in the DRI was the number of cracks in the cement paste with and without reaction product, which is directly influenced by the use of AMFs. The DRI number also exhibited a very good correlation with the expansion level of the samples.

For the SDT, replacing cement by AMFs led to slightly higher SDI values. In contrast, sand replacement led to similar or lower SDI values compared to systems without AMFs. The modulus of elasticity reduction exhibited different behaviours depending on the type of reactive aggregate used. For reactive coarse aggregates, the reduction was lower than that observed for systems with no AMFs for both types of replacement. For reactive fine aggregates, the values were higher for the greywacke fillers, being more

prominent when cement was replaced. For the dolomitic argillaceous limestone fillers, the value was considerably lower.

In the studies discussed, the AAR-induced deterioration was evaluated at the end of the expansion measurement period (i.e., 34 weeks for the surface cracking and 180 days for the multilevel assessment). Therefore, assessing the deterioration progress at different ages or expansion levels could provide insights into the process when using AAR-reactive AMFs.

4.2.3. Summary of current knowledge

Based on the results presented in the previous sections, the type of test may influence the behaviour of mixtures containing AMFs. AMBT results indicated a more pronounced expansion reduction, whereas CPT and ACPT provided smaller reductions or slight increases, particularly when AMFs were used replacing sand (Table A1 – Appendix A). Some aspects may have led to such discrepancies, influencing test performance and interpretation of results. First, AMFs derived from rocks containing siliceous minerals may exhibit pozzolanic activity at high temperatures such as 80 ºC (PEDERSEN, 2004). Therefore, the use of the AMBT (CASTRO *et al*., 1997; COUTINHO; MONTEFALCO; CARNEIRO, 2024; LI; HE; HU, 2015; SALLES; OLIVEIRA; ANDRIOLO, 1997; TAPAS *et al*., 2023) or tests at elevated temperatures (i.e., 60 ºC) (ANTUNES, 2021; CARLES-GIBERGUES *et al.,* 2008; COUTINHO; MONTEFALCO; CARNEIRO, 2024; GUÉDON-DUBIED *et al.,* 2000) may provide biased results. Second, the tests performed were developed to evaluate aggregates and the efficiency to appraise AMFs is mostly unknown. Third, inconsistent test parameters were used in distinct studies, with varying durations, sample sizes, alkali contents, immersion conditions, and replacement strategies, which hinders comparison across them. Finally, the impact of some physiochemical properties of AMFs, such as mineralogy and PSD, as well as the replacement strategy, on the behaviour against ASR should be better studied.

In the next section, these parameters are discussed in detail.

4.3. DISCUSSION

4.3.1. Role of AMFs mineralogy on AAR

Several reactive aggregates with different lithologies and, consequently, different degrees of reactivity have been used to evaluate the influence of reactive AMFs on AAR expansion. The type of rock used (i.e., texture, mineralogy, and microcracks (RÄISÄNEN; MERTAMO, 2004)) as well as the crushing process, directly influence the morphology of particles produced (BOUQUETY; DESCANTES, 2007; DIÓGENES *et al*., 2021), which also influences the action of AMFs produced from these rocks. These aspects impact the dispersion of mineral phases that compose the rocks, as the propagation of microcracks is different depending on the minerals and their structure (ÅKESSON *et al.,* 2003; PANG *et al.,* 2010). This was observed when using AMFs from the same rock but crushed by different types of crusher, in which the specific surface areas (SSAs) were different and resulted in distinct effects on AAR-induced expansions (COUTINHO; MONTEFALCO; CARNEIRO, 2022). Moreover, aggregates from different types of rocks also result in distinct expansion tendencies when produced using the same crushing methods, highlighting the influence of the rock characteristics on expansion results (COUTINHO; MONTEFALCO; CARNEIRO, 2022; VALDUGA, 2007). However, the crushing procedure to produce AMFs is frequently not disclosed in studies on the topic. Moreover, studies on the morphology of AMFs, directly related to the source rock characteristics, are still limited and should be further explored.

In addition to physical aspects, chemical aspects related to the composition of the rock also influence the effect of corresponding AMFs. Reactive AMFs were indicated to exhibit pozzolanic activity (CASTRO *et al.,* 1997; PEDERSEN, 2004; SALLES; OLIVEIRA; ANDRIOLO, 1997; TAPAS *et al.,* 2023), with differences observed in terms of amount of reaction products formed, Si/Ca ratio, and dissolved silica (TAPAS *et al.,* 2023). As results were different depending on the type of AMFs used, their effect may not be limited to cement dilution and can be also influenced by the lithotype and chemical composition of the rock used to produce the filler, which should be further examined. This can also be influenced by the temperature of the test adopted, as AMFs derived from rocks containing siliceous minerals may exhibit pozzolanic activity at high temperatures (i.e., 80 ºC) (PEDERSEN, 2004). The efficacy of the filler was also indicated to be directly related to the alkali content, with a lower alkali level requiring

lower replacement levels to reduce expansions (QINGHAN *et al.,* 1996; SALLES; OLIVEIRA; ANDRIOLO, 1997). However, the contribution of alkalis from the AMFs should also be considered.

The alkali release by the aggregate may have a role when considering the effects of reactive AMFs (LEEMANN; HOLZER, 2005), and it varies depending on the type of rock (MENÉNDEZ *et al.*, 2022; WANG et al., 2008). Feldspars are one of the major sources of alkalis from the aggregate (BERUBÉ *et al.,* 2002; FERRAZ *et al.,* 2017; MENÉNDEZ *et al.*, 2022; SOARES *et al.,* 2016). The size of particles and the alkali solution interfere in the release of alkalis by the aggregate, with smaller sizes resulting in more release (SOARES *et al.,* 2016). Moreover, the K^+ release is more intense in 1 N NaOH solutions (SOARES *et al.,* 2016). Thus, considering the importance of the lithology of the rock on the AMF produced, a petrographic analysis of the rock could provide interesting insights into the effect of the AMF in concrete.

4.3.2. Role of particle size of AAR-reactive AMFs

The similarity between ASR and pozzolanic reaction has been acknowledged (HOU; STRUBLE; KIRKPATRICK, 2004; THOMAS, 2011). Taylor (TAYLOR, 1997) affirmed that the chemical mechanisms of these reactions are the same, with different effects owing to different particle sizes of siliceous materials. These reactions also differ in their timescale and occurrence of expansion. This effect is considerably affected by the size of reactive particles of the aggregate. For small particles, the dissolution of ASR gel is rapid, and the dissolved silicate groups can react with calcium ions to produce C-S-H, contributing to strength development (DYER, 2014; PEDERSEN; WIGUM; LINDGÅRD, 2016). In contrast, large aggregates lead to accumulation of the gel (PEDERSEN; WIGUM; LINDGÅRD, 2016). This can be exemplified considering the use of silica fume, which is the most effective SCM to counteract ASR; yet, when agglomerated, it can have the opposite effect, triggering ASR (BODDY; HOOTON; THOMAS, 2003; DIAMOND, 1997; GUDMUNDSSON; OLAFSSON, 1999; MARUSIN; SHOTWELL, 2000), which can also be related to the silica content (BODDY; HOOTON; THOMAS, 2003).

Stanton (STANTON, 1940) studied a siliceous magnesium limestone containing opal and chalcedony and determined that if this aggregate is sufficiently fine (< 180 μm), no expansion occurs. In his work, he also indicated that when the aggregate has a reduced size, the gel dissipates in the cementitious matrix such that no tension is

generated, and the reaction terminates before final setting of concrete. In contrast, Vivian (VIVIAN, 1951) found that expansions increase with the reduction of particle size until it reaches 50 μm, from which no expansion is observed, as shown in Figure 4.9.

Figure 4.9 – Expansion of mortars with different contents of reactive component vs mean size of reactive particles

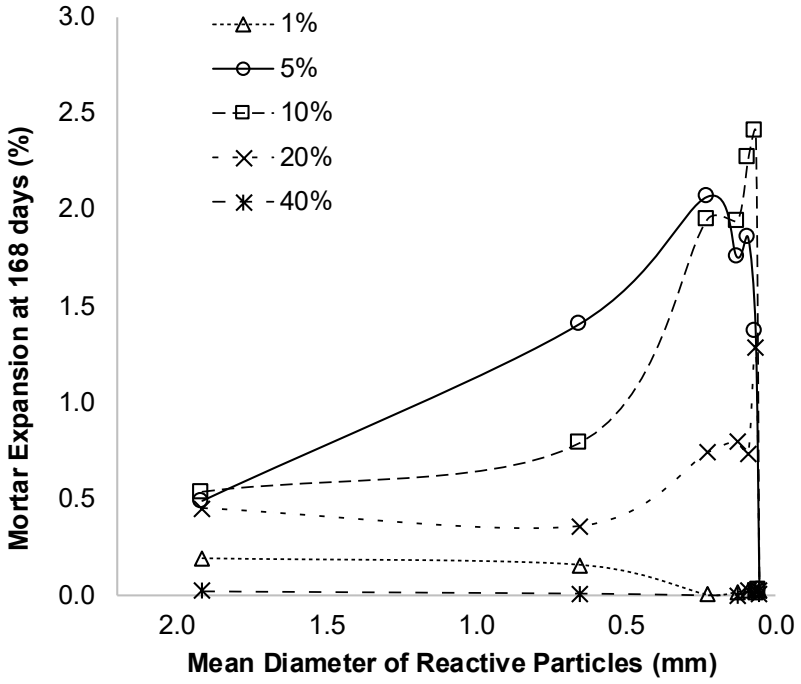

Source: Adapted from VIVIAN (1951).

The amount of reactive particles is considered to affect the number and width of the cracks formed, which influences expansion (VIVIAN, 1951). The volume of a particle would determine its capacity to generate cracks. If the diameter of the particle is below a certain threshold, the corresponding increase in volume after reaction can be accommodated by the pores in the surrounding area. Moreover, larger particles would be expected to generate wider cracks and a more pronounced local expansion compared to small particles. However, the core of the particle may react slowly, which limits this behaviour, indicating that not all the reactive portion of a particle may contribute to expansions (VIVIAN, 1951). By increasing the number of reactive particles in cementitious materials, the number of cracks also increases, followed by an increase in expansion. Nevertheless, there is a limit for the number of reactive particles of a certain size, above which no additional cracks are generated. This limit number of cracks tends to increase as the particle size reduces. In addition, by

increasing the number of particles, their distribution becomes more uniform, leading to uniformity of crack width. The increase in the number of reactive particles may not result in increased expansions because the amount of alkalis acts as a limiting factor. Therefore, the expansion in cementitious materials with reactive AMFs can be a result of the effects of volume, SSA, number and distribution of reactive particles (VIVIAN, 1951).

The size effect may also be related to the reaction on the surface of the aggregate, which acts to produce ASR gel, and the dissolution of silica, which acts to reduce ASR gel (DYER, 2014). Therefore, the ASR rate is defined by the rate of these two processes. In small particles, the reactive portion is completely converted to gel, meaning that posterior dilution will contribute to reducing expansions. For big particles, the smaller SSA and volume mean that only a part of the reactive components will react, as illustrated in Figure 4.10.

Figure 4.10 – Effect of a relatively fast rate of ASR gel formation and a slow rate of gel dissolution over a period t1. Large particles (a) produce relatively large volumes of gel as they react. Smaller particles (b) become entirely converted to gel, which then gradually dissolves. Very small particles (c) are dissolved entirely in a relatively short period of time.

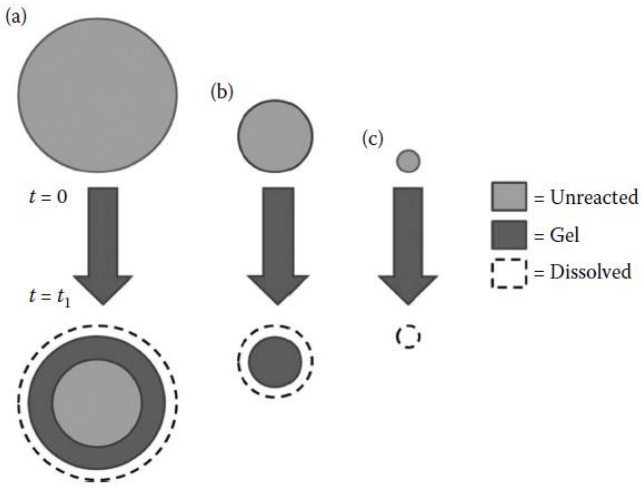

Source: DYER (2014).

Considering the size effect, different size ranges of marble and siliceous limestone sands were used to evaluate ASR, and higher expansions were obtained for coarse particles (630–1250 µm) and no expansion for fine particles (0–160 µm) (MULTON *et al.,* 2010). In contrast, the use of opal in ranges from 125 µm to 20 µm led to increased expansions for all ranges, with maximum expansions in the range from 30 µm to 20 µm (DIAMOND; THAULOW, 1974). A similar study using opal also obtained higher

expansions for the finer fraction (150 to 300 μm) (HOBBS; GUTTERIDGE, 1979). The effect of the size of particles, considering the fractions of the AMBT, has also been analyzed by using a non-reactive aggregate and replacing each fraction with a reactive aggregate. Although the results indicate lower expansions for the coarser and finer fractions (2.0 to 4.0 mm and 0.125 to 0.250 mm, respectively), the percentages of these fractions are also lower than those of intermediate fractions, which may have influenced the results (RAMYAR; TOPAL; ANDIÇ, 2005).

These conflicting results may be related to the pessimum effect, which is the intensification of the reaction in a certain size range, whereas above and below this size range expansions reduce (QIU *et al.,* 2022). Some explanations have been proposed for this behaviour. For instance, the pessimum silica content is considered to be directly related to the pessimum content (DIAMOND; THAULOW, 1974; KUO; SHU, 2015; QIU *et al.,* 2022; SEKRANE; ASROUN, 2014). The pessimum SiO_2/Na_2O ratio varies with the size and nature of the aggregate and the amount of accessible SiO_2 (ZHANG; GRAVEST, 1990). In another model, the gel formed is divided into two types: the gel deposited into the interface pores and the gel that permeates into the surrounding pores in the cement paste. The first type does not cause expansion and is governed by dilution, whereas the second type generates interface pressure and causes expansion. In this case, the aggregate size and porosity of the paste influence the amount of the first type of gel, and the permeation rate influences the amount of the second type (SUWITO *et al*., 2002). Given a fixed volume of aggregate, small particles lead to higher expansions because of the higher surface area, which is the dilution process. If the particles are sufficiently small such that the volume of gel formed is comparable to the volume of pores in the surrounding paste, the pressure is released and expansions are reduced, which is the permeation process. For a particle sufficiently small such that the gel can be completely held in the interfacial pore space, no expansion occurs. According to this model, the pessimum size is that at which these diffusion processes are balanced (SUWITO *et al*., 2002).

Fracture mechanics was also used to explain this behaviour (PEDERSEN; WIGUM; LINDGÅRD, 2016). In this case, particles below a certain size will not cause cracks even if the expansion caused by the aggregate is higher than the strain capacity of the paste (BAŽANT; ZI; MEYER, 2000; GOLTERMANN, 1995). This is because the energy released from a crack propagating from a particle with radius R is proportional

to R^3, whereas the necessary fracture energy is proportional to R^2 (GOLTERMANN, 1995). Cracks propagate when the energy released is higher than the fracture energy required to propagate the crack. Therefore, for a given system, there is a critical particle size below which no crack propagation occurs (GOLTERMANN, 1995).

Certain aggregates may also exhibit a pessimum content, which is a range in which the expansions are pronounced (BEKTAS *et al.,* 2004). Despite the variable methods and aggregates used, the nature and composition of aggregates considerably influence the results, particularly considering rapid and slow reactive aggregates (dyer, 2004; MULTON *et al.,* 2010). Moreover, the pessimum effect is still not fully understood. However, the observations related to the reduced or nonexistent expansions from a certain size of particle motivated studies on the use of reactive fillers, either replacing fine aggregates or cement.

In this regard, several parameters were used to indicate the particle size of the AMFs, such as maximum dimension, range, D10, D50, D90, and also parameters related to SSA, such as Blaine fineness and Brunauer-Emmett-Teller (BET) method, as summarized in Table A2 (Appendix A).

When examining the influence of the fineness of reactive AMFs on the expansion results, a fineness of 800 m^2/kg for andesite powder was determined to be the minimum value required to effectively reduce expansions (QINGHAN *et al.,* 1996). As for powders from three natural aggregates and glass with different SSAs, measured by means of Blaine fineness, and used to replace sand in mortars, an increase in SSA resulted in reduced expansions for all percentages analyzed (CARLES-GIBERGUES *et al.,* 2008).

In contrast, samples using reactive fillers with different Blaine fineness values (210 m^2/kg, 400 m^2/kg, 610 m^2/kg, 860 m^2/kg) exhibited very similar expansions even for different replacement levels (LI; HE; HU, 2015). The concentration of soluble alkalis varied with the SSA of the filler particles. For sandstone fillers, the Na^+ concentration increased until reaching a certain value of SSA where the K^+ concentration surpassed that of Na^+. As higher K^+/Na^+ ratios have been related to higher expansions (LEEMANN; LOTHENBACH, 2008), this is a factor that should be considered when evaluating reactive fillers. The alkali bonding ability also followed the same tendency, decreasing until reaching a specific SSA value and then increasing again. The alkali binding behaviour may be explained by the pozzolanic activity and nucleation effects.

Considering that C-S-H is the only phase that can bind alkalis and taking CH content as an indicator of the hydration degree, when the activity effect is dominant, CH is consumed, whereas when the nucleation effect is dominant, the CH content increases. Therefore, the SSA influences the alkali bonding and liberation ability (LI; HE; HU, 2015).

The influence of the particle size on the AAR results was also evaluated (PEDERSEN, 2004), and some of the results are shown in Figure 4.11.

Figure 4.11 – Influence of particle size on AAR expansion results considering (a) AMBT and (b) CPT tests (ranges in μm).

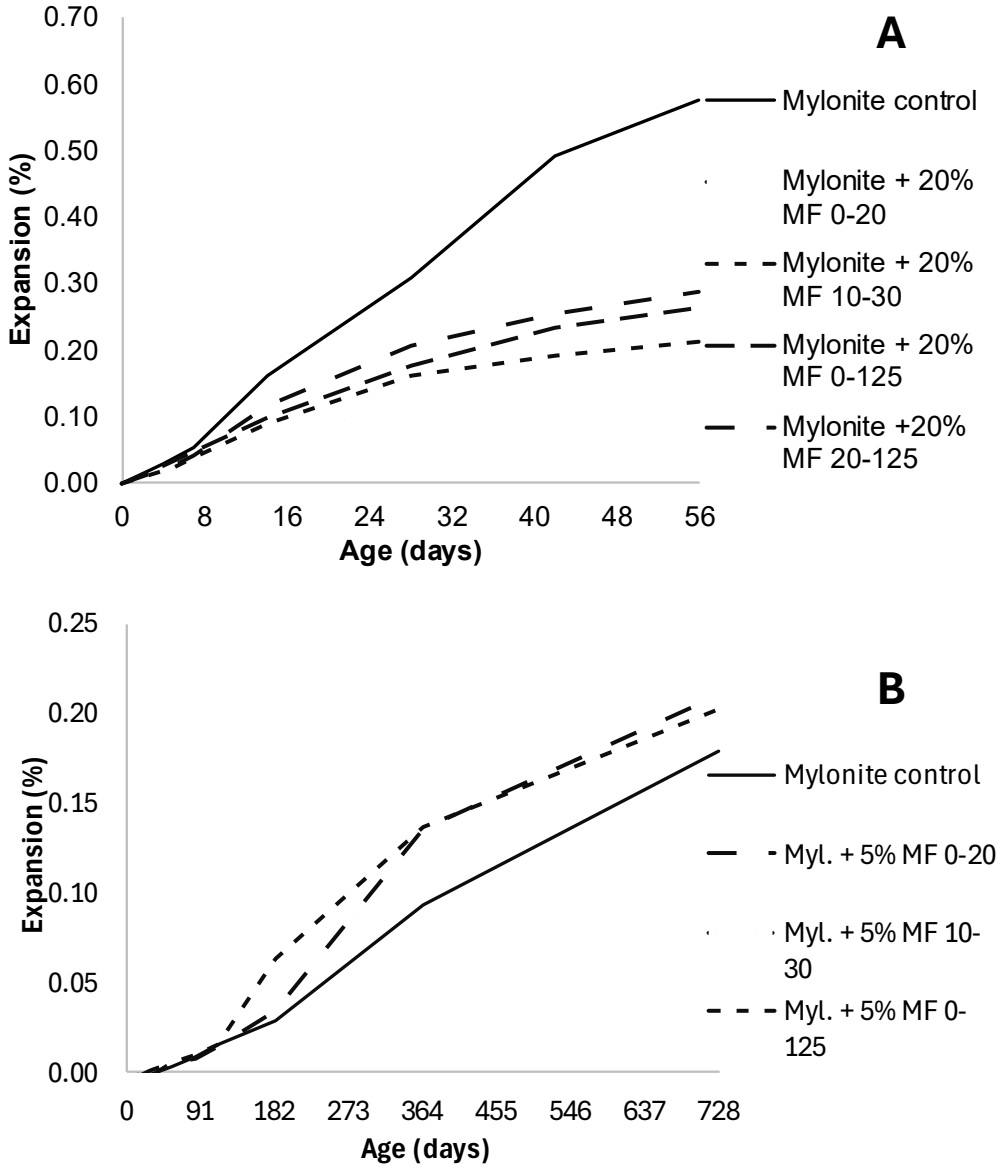

Source: Adapted from PEDERSEN (2004).

As observed, different PSDs resulted in differences in expansion for the same coarse aggregates, AMF, and replacement percentage used. In the AMBT, the finer the AMF, the lower the expansion. The combination with fraction 0–20 μm resulted in the lowest expansion, followed by the combination with fraction. 0–30 μm. The combination with fraction 0–125 μm exhibited a slightly higher expansion than that with fraction 20–125 μm, which indicates that the finer part removed in the latter fraction played an influential role in the result. In contrast, for the CPT, the expansions for combinations with reactive AMFs were higher than those of the control sample and very similar.

Based on the exposed, in which different tendencies were observed when varying the PSD, other aspects might affect the results, such as the pessimum content previously described. Therefore, more studies are necessary to better understand the influence of the PSD on AAR expansions, also considering the deterioration process, which has not been studied so far, taking into account this parameter.

4.3.3. Role of replacement content

The replacement content has a direct influence on AAR-induced expansion when cement is replaced considering the reduction in alkali content. Replacing cement by SCMs and AMFs has been an important strategy as a means to reduce CO_2 emissions to achieve the NetZero target (SCRIVENER; JOHN; GARTNER, 2018). Considering this scenario, recent studies examining the use of reactive AMFs have focused on replacing cement by such AMFs. However, former studies also adopted the replacement of sand. Figure 4.12 shows a summary of the impact of the replacement content on AAR expansions.

Figure 4.12 – Impact of replacement content of cement by reactive AMFs on AAR expansions.

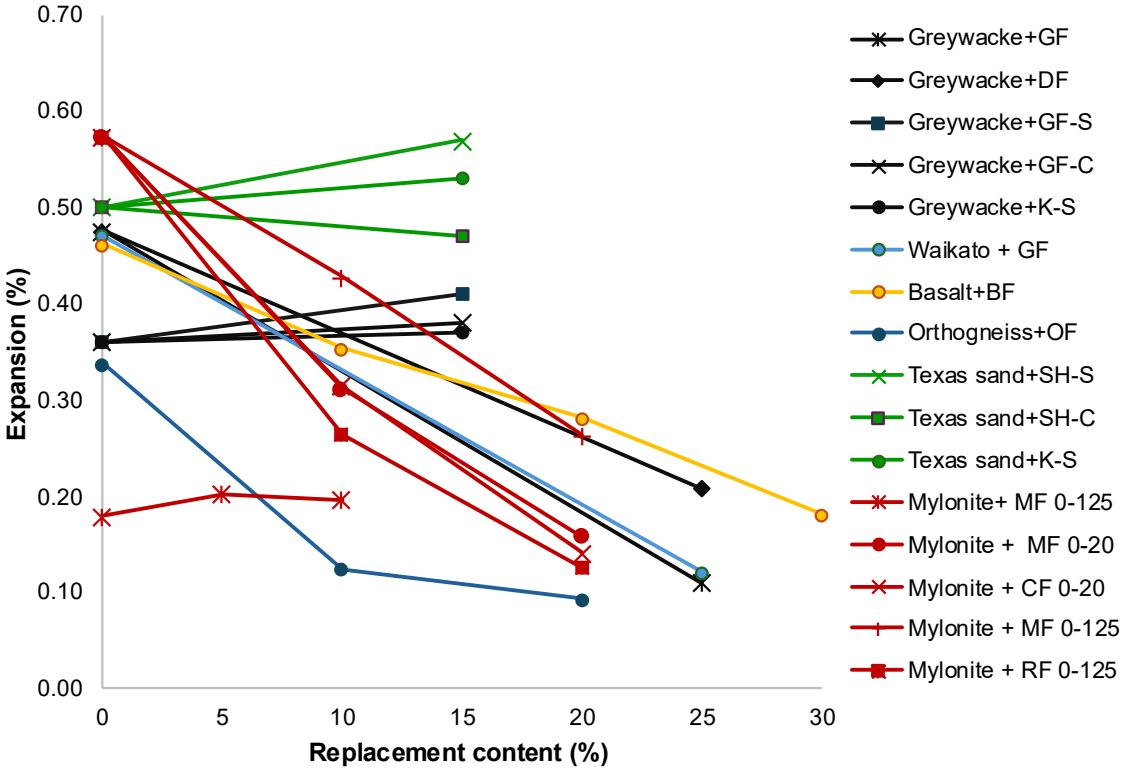

Source: Adapted from ANTUNES, 2021; COUTINHO; MONTEFALCO; CARNEIRO, 2024; OLIVEIRA; SALLES; ANDRIOLO, 1995; PEDERSEN, 2004; TAPAS et al., 2023.

As observed, most of the results indicate a reduction in expansions with the increase in the replacement percentage. Some of the curves show the opposite tendency, with increased expansions with the increase in the replacement percentage, all of which were tested by means of longer tests compared to the AMBT, such as ACPT and CPT. Moreover, for some of these curves, sand was replaced, which indicates that the replacement content has different roles depending on the material the AMF replaces. Figure 4.13 shows expansion results evaluating the influence of the percentage replacing cement coupled with different parameters.

Figure 4.13 – Influence of replacement percentage of cement by reactive AMFs.

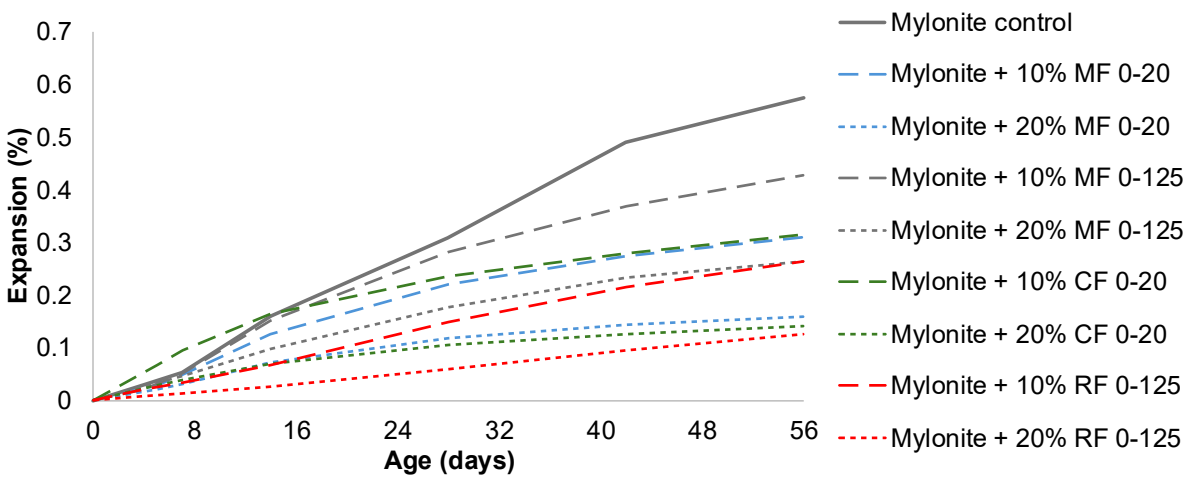

Source: Adapted from PEDERSEN (2004).

As observed, when varying the replacement percentage while maintaining other parameters fixed such as coarse reactive aggregates, type of AMFs, and PSD of the AMFs, the expansions reduce by increasing the content.

4.3.4. Current gaps and research perspectives

Several studies have addressed the effect of reactive aggregate AMFs on AAR, whose parameters adopted are summarized in Table 4.1. However, some limitations hinder a comprehensive evaluation of this material and comparative analysis.

The use of reactive AMFs with reactive coarse aggregates (ANTUNES, 2021; CASTRO et al., 1997; COUTINHO; MONTEFALCO; CARNEIRO, 2024; OLIVEIRA; SALLES; ANDRIOLO, 1995; PEDERSEN, 2004; TAPAS *et al.,* 2023), reactive fine aggregates (ANTUNES, 2021; TAPAS *et al.,* 2023), and non-reactive aggregates (GUÉDON-DUBIED *et al.,* 2000) has been analyzed. However, there is no comprehensive evaluation of the effect of the same AMFs in these three different systems, which would be beneficial for a better understanding of the AMF action. The evaluation of the deterioration progress when using reactive AMFs would also provide interesting insights, mainly when considering different ages and expansion levels.

Table 4.1 – Summary of studies using reactive AMFs.

Year	AMF	Dimension	Crushing process	%	Tests	Nomenclature	Ref.	Observation
1996	Andesite	Blaine fineness: 780 m^2/kg	-	30, 40, 50, 60, and 70% replacing cement	Autoclave (mortar)	Ground reactive aggregate powder	QINGHAN *et al*., 1996	Reduction in expansions
1997	Basalt	<75 µm	-	10, 20, 30% replacing cement	NBRI method	Aggregate powder	SALLES; OLIVEIRA; ANDRIOLO, 1997	Reduction in expansions and pozzolanic activity
1997	Sandstone (Capanda)	<75 µm	-	20, 40, 60% replacing cement	NBRI method	Powdered aggregate	CASTRO *et al*., 1997	Reduction in expansions and pozzolanic activity
	Sandstone (Formoso)			20, 40, 60, 80% replacing cement				
2000	Limestone	<100 µm (D50: ~16 µm) Blaine fineness: 450 m^2/kg	-	15% and 30%, but half replacing cement and half replacing sand	CPT (French standard)	Filler 742	GUÉDON-DUBIED *et al*., 2000	Reduction in expansions
2004	Mylonite	0–20, 10–30, 20–125, 0–125 µm	-	2, 5, and 10% replacing sand in volume	AMBT CPT (Norwegian standards)	Alkali-reactive fillers	PEDERSEN, 2004	Effect of temperature and amorphous silica content on the pozzolanic reactivity of ASR-reactive AMFs
	Cataclasite	0–20, 10–40, 0–125 µm						
	Icelandic Rhyolite	0–20, 10–40, 0–125 µm						

Year	AMF	Dimension	Crushing process	%	Tests	Nomenclature	Ref.	Observation
2008	Metaquartzite, Siliceous limestone, opaline aggregate, Crushed waste glass	80 µm Blaine fineness: 100–650 m^2/kg	-	10% and 20% replacing sand	Autoclave (mortar) Test in concrete (different parameters)	Reactive aggregate powder	CARLES-GIBERGUES *et al.,* 2008	Reduction in expansions
2015	Sandstone	Blaine fineness: 210–860 m^2/kg	-	10, 20, 30, and 40% replacing cement	AMBT	Reactive powder	LI; HE; HU, 2015	Reduction in expansions
2021	Greywacke	D50: 30 µm	Crushing and sieving to obtain particles <150 µm	15% replacing cement and sand	Accelerated CPT	AMF	ANTUNES, 2021	Reduction or similar expansion when replacing cement; higher or similar expansions when replacing sand
	Dolomitic argillaceous limestone	D50: 19 µm						
2023	Greywacke	D50: 30.50 µm	Ring mill for 5 min	25% replacing cement	AMBT	Reactive aggregate powder	TAPAS *et al*., 2023	Reduction in expansions and pozzolanic activity. No contribution to compressive strength development
	Dacite	D50: 41.49 µm						
2024	Orthogneiss	<150 µm D50: 105.36 µm	Crushing and sieving to obtain particles <150 µm	10 and 20% replacing cement and sand	AMBT, MCPT	Reactive aggregate powder	COUTINHO; MONTEFALCO; CARNEIRO, 2024	Reduction in expansions

Source: Author (2025).

Another aspect that has been neglected is the influence of the type of source rock and corresponding lithotype on the AMF action. Reactive AMFs from several types of rocks, such as sandstone, greywacke, and mylonite, have been used. However, this aspect has not been emphasized, with a lack of a more detailed petrographic analysis for a comprehensive assessment of the AMFs. The type of crusher used may also influence the morphology and, consequently, the AMF action (COUTINHO; MONTEFALCO; CARNEIRO, 2022; DIÓGENES *et al*., 2021; KOMBA; MGANGIRA; MOHALE, 2016). Nonetheless, few studies described the crushing method adopted, as seen in Table 4.1.

The alkali release is also dependent on the type of rock and should be considered when analyzing the use of AAR-reactive AMFs (LEEMANN; HOLZER, 2005; WANG et al., 2008). The alkali contents and Na_2O_{eq} of the aggregates used in studies varied considerably, with Na2Oeq values as high as 6.30 (Table A3 – Appendix A). The contribution of feldspars as a source of alkalis has been acknowledged (BERUBÉ *et al*., 2002; FERRAZ et al., 2017; SOARES *et al*., 2016). However, the contribution of alkalis from aggregates remains unclear. Moreover, the size of particles can also interfere in the alkali release (SOARES *et al.*, 2016), which is particularly important considering the use of AMFs. However, this aspect when considering the use of AAR-reactive AMFs coupled with kinetics and deterioration assessment has not been evaluated.

As for the particle size, some results indicated that finer fractions would not cause expansions, whereas intermediate fractions would result in higher expansions (MULTON *et al*., 2010; RAMYAR; TOPAL; ANDIÇ, 2005; SEKRANE; ASROUN, 2014). In a few studies, finer particles resulted in higher expansions (DIAMOND; THAULOW, 1974; HOBBS; GUTTERIDGE, 1979), but the aggregates used contained opal, which is a highly reactive amorphous material that reacts rapidly (THOMAS; FOURNIER; FOLLIARD, 2013). This indicates that the reactivity degree may play a role in the influence of fine particles in concrete. Pozzolanic activity was also identified in reactive AMFs (ALVES *et al*., 1997; BRAGA *et al*., 1991).

Based on Table 4.1, the replacement percentages used considerably varied. Moreover, when considering the PSD, different parameters were used to indicate the fineness of the material, such as particle size, Blaine fineness, and D50, which also hinders comparison.

Furthermore, among the characteristics evaluated in mortars and concretes studied are compressive strength (CARLES-GIBERGUES *et al.,* 2008; QINGHAN *et al.,* 1996; TAPAS *et al.,* 2023), surface cracking (BEKTAS *et al.,* 2004; CARLES-GIBERGUES et al., 2008; HOBBS; GUTTERIDGE, 1979), and pozzolanic reactivity (ALVES et al., 1997; CARLES-GIBERGUES *et al.,* 2008; SALLES; OLIVEIRA; ANDRIOLO, 1997; TAPAS *et al.,* 2023). Other important aspects of the ASR deterioration process have been mostly neglected, such as the development of internal cracks and the impact on the modulus of elasticity and tensile strength, which are more susceptible to AAR progress (MOHAMMADI; GHIASVAND; NILI, 2020).

Many of these studies were also conducted using test methods and conditions that are not applied anymore, with different sample sizes, temperatures, and durations (CARLES-GIBERGUES *et al.,* 2008; GUÉDON-DUBIED *et al.,* 2000; HOBBS; GUTTERIDGE, 1979; SHAO *et al.,* 2000; ZHANG *et al.,* 1999; ZHANG; GRAVEST, 1990). Furthermore, several studies applied only tests in mortar (QINGHAN *et al.,* 1996; RAMYAR; TOPAL; ANDIÇ, 2005), such as the AMBT (ALVES *et al.,* 1997; RAMYAR; TOPAL; ANDIÇ, 2005; SALLES; OLIVEIRA; ANDRIOLO, 1997; SHAFAATIAN *et al.,* 2013; SHAYAN, 1992). Temperature is an aspect that can affect the results of tests when using AMFs (PEDERSEN, 2004). Therefore, a comprehensive study using a long-term test at a low temperature, such as the CPT, and considering varying parameters, such as the ones previously discussed, could provide a better understanding of the action of reactive AMFs in concrete.

In addition to the diverse parameters and conditions adopted in the studies analyzed, an important aspect that should be discussed is the nomenclature. Several terms have been used to describe the AMFs produced by using an AAR-reactive rock, as observed in Table 4.1 (e.g., aggregate powder, alkali-reactive filler, reactive aggregate powder). This makes it difficult for researchers to find studies addressing the topic in current databases and may be an explanation for the variability in parameters adopted that were found in the literature. An established terminology would be beneficial because it would allow researchers to easily find studies on the topic and adopt similar parameters, enabling comparative analysis that would contribute to actually building knowledge, contrary to what has been observed thus far with non-comparable and

disconnected results. Considering the exposed and for clarity, the term AAR-reactive AMFs (which could be ASR- or ACR-reactive AMFs) is suggested.

Among the theories proposed for the action of AAR-reactive AMFs, it can be cited the reduction of alkalis by the replacement of cement, dilution of the total alkalis concentration in the mortar, change in the alkalis distribution in the mortar, reaction of AMFs with alkalis because of broken bonds resulting from grinding, and also a nucleation effect owing to the reduced size (QINGHAN *et al*., 1996; SALLES; OLIVEIRA; ANDRIOLO, 1997). Moreover, the influence of temperature, alkalinity, particle size, and structure of the silica on the solubility of the silica and, consequently, on the AAR and pozzolanic reactions should be considered (PEDERSEN, 2004). The relation between a high availability of calcium and pozzolanic reactions because of the AMF is also highlighted, resulting in lower expansions. However, higher expansions were also observed for a slow-reactive aggregate (mylonite), which was also observed by Diamond and Thaulow (DIAMOND; THAULOW, 1974) for opal, a highly reactive aggregate. These discrepancies prompt more studies to better understand the reaction mechanism in systems with AMFs.

Considering the exposed, despite the promising results obtained, the variability of conditions and parameters applied hinders the understanding of AAR-reactive AMFs action in concrete and their practical application. Several tests have been used that differ in many aspects such as sample size, duration, temperature, and immersion conditions. Moreover, many parameters have been evaluated, such as reactivity degree of the aggregate, type of replacement, percentage, and PSD. When combined, all these differences among studies hinder the comparison of results, which also hinders the building of a strong knowledge regarding the topic, making the results isolated and disconnected.

There is considerable room for improvement, considering the advances in techniques and methodologies developed throughout the years that can be applied. Advanced techniques such as DRI and SDT can be used to evaluate the progression of ASR in concrete with AAR-reactive AMFs and corresponding effects in mechanical aspects such as the modulus of elasticity. Moreover, a better characterization when it comes to the fineness of the material, as well as consideration of the mineralogy and replacement strategy, may enable comparative analyses.

4.4. CONCLUSIONS

Currently, focus has been directed towards the reduction of CO_2 emissions to meet the Net-Zero target. In the construction industry, studies have evaluated the use of alternative materials to replace cement. In this regard, AMFs seem to be an interesting option. However, among AMFs, the current knowledge of the influence of AAR-reactive AMFs in concrete is still insipient, despite the positive impact it could generate as reactive aggregates are available worldwide. Considering previous results, the following conclusions can be drawn:

- The kinetics and ultimate expansion of systems containing AAR-reactive AMFs vary depending on the test used and the mortar/concrete system (e.g., containing reactive coarse aggregates, reactive fine aggregates, or non-reactive aggregates). Therefore, the evaluation of the same AMF in different types of systems and using a long-term test would be beneficial to better understand the influence of AMFs;
- The progress of deterioration has barely been addressed in previous studies, and it has been evaluated only at the ultimate expansion. Therefore, evaluating at different ages would be beneficial to understand the deterioration progress over time;
- Several aspects related to the mineralogy of the source rock need to be considered when evaluating the use of AAR-reactive AMFs, such as the crushing process, which influences the dispersion of mineral grains and morphology of particles, and the alkali release;
- The effect of the size of particles has not been completely understood, as results are conflicting. One hypothesis to explain such behaviour is the pessimum effect, which has also been studied, with some models proposed to explain it. When considering the studies in which AAR-reactive AMFs were used, different parameters were adopted as a measure of particle size, which hinders comparison;
- Considering the percentage of cement replaced, in general, the expansions reduce when the percentage increases, whereas the opposite occurs when the sand is replaced;
- Several tests have been used to assess the effect of AAR-reactive AMFs in mortar and concrete. In general, accelerated results indicated a reduction in

expansion with the use of AMFs, whereas longer tests indicated the same or slightly increased expansions. Moreover, the test methods and parameters tended to vary owing to the different standards applied. Therefore, even when using the same test, the results are not comparable, as the standards and the specifications are different. Thus, a comprehensive evaluation of several aspects previously analyzed while maintaining the same tests and parameters would be essential to better understand the effect of AAR-reactive AMFs;

- An important aspect that may have hindered the development of knowledge in this topic is the nomenclature, as the term used to refer to reactive AMFs varies across studies. Therefore, this study proposes the term AAR-reactive AMFs (which could be ASR- or ACR-reactive AMFs) for clarity.

Considering the exposed, future studies should thoroughly assess the use of AAR-reactive AMFs considering aspects such as lithotype, PSD, percentage, pessimum effect, and using long-term and field evaluation tests.

CHAPTER 5 – IMPACT OF ASR-REACTIVE FILLERS ON ASR-INDUCED EXPANSION TRIGGERED BY REACTIVE COARSE AND FINE AGGREGATES

Yane Coutinho [1, 2, *], Leandro Sanchez [2], and Arnaldo Carneiro [1]

[1] Federal University of Pernambuco, Recife, Brazil.
[2] Department of Civil Engineering, University of Ottawa, Ottawa, Canada.

Abstract: The use of aggregate mineral fillers (AMFs) to replace cement in concrete mixtures has gained attention due to the need to reduce clinker consumption and thus CO_2 emissions. However, when these fillers are produced from alkali-aggregate reaction (AAR)-reactive rocks, their impact on the development of AAR remains unclear. This study aims to investigate the influence of alkali-silica reaction (ASR)-reactive AMFs on ASR-induced expansion and deterioration in concrete. Two reactive systems were evaluated: one with reactive coarse aggregates (mixtures B) and another with reactive fine aggregates (mixtures C). The AMFs were derived from a highly reactive greywacke and a moderately reactive mylonite with two particle size distributions (PSD, <150 µm and <75 µm) and used to replace Portland cement at 10% and 20% levels. The concrete prism test (CPT) was used to monitor expansion, and the multilevel assessment was applied to appraise the deterioration progress by means of microscopy (i.e., damage rating index – DRI) and mechanical (i.e., stiffness damage test – SDT) evaluations. Results indicated that ASR-reactive AMFs altered the induced-expansion kinetics of reactive systems in different ways, which seems to be related to the competition for alkalis consumption at early ages. Mechanical degradation remained significant, as evidenced by increased stiffness damage index and reduced modulus of elasticity over time. In general, the introduction of ASR-reactive AMFs in systems incorporating reactive coarse aggregates did not alter the ultimate expansion and degradation when compared to similar systems without AMFs. However, for systems with reactive fine aggregates, the ultimate expansion and the degradation level were reduced when compared to a system with no AMFs.

Keywords: Alkali-aggregate reaction, ASR-reactive AMFs, reactive systems, multilevel assessment, concrete durability.

5.1 INTRODUCTION

The global effort to reduce CO_2 emissions has intensified the search for alternative construction materials. Concrete, the most consumed construction material worldwide, is projected to increase in demand from 14 to 20 billion m³ annually by 2050, directly challenging efforts to achieve Net-Zero carbon emissions (GCCA, 2021; HANZIC; HO, 2017; IEA, 2021). Portland cement alone was estimated to generate 0.6 tons of CO_2 per ton of cement produced (IEA, 2021). Thus, reducing the clinker-to-cementitious materials ratio by partially replacing cement with supplementary cementitious materials (SCMs) and/or fillers is a viable short-term strategy to lower CO_2 emissions (AMRAN *et al.*, 2022; BALLAN; PAONE, 2014; DAMTOFT *et al.*, 2008; EUROPEAN CEMENT RESEARCH ACADEMY, 2017; GARTNER; HIRAO, 2015; IEA, 2020; LOTHENBACH; SCRIVENER; HOOTON, 2011; LUDWIG; ZHANG, 2015; MILLER et al., 2021; SCRIVENER *et al.*, 2018; SCRIVENER; JOHN; GARTNER, 2018; VON GREVE-DIERFELD *et al.,* 2020).

The supply of conventional SCMs tends to decrease in the coming years, which indicates the need of alternative materials such as fillers. Fillers are chemically “inert” materials that enhance concrete properties via improved packing and introduction of nucleation sites for hydration products (KORPA; KOWALD; TRETTIN, 2008). In this context, aggregate mineral fillers (AMF), which are rock crushing byproducts, present a promising option to replace Portland cement (ACI, 2020). Several AMFs, such as quartzite (CRAEYE *et al.*, 2010; KADRI *et al.*, 2010; POPPE; DE SCHUTTER, 2005; RAHHAL; TALERO, 2005), alumina (POPPE; DE SCHUTTER, 2005), basalt (DOBISZEWSKA; SCHINDLER; PICHÓR, 2018; LI *et al.*, 2021; SOROKA; SETTER, 1977; XIE *et al.*, 2024; ZHU *et al.*, 2024), diabase (ZHU *et al.*, 2024), tuff (ZHU *et al.*, 2024), dolomite (SOROKA; SETTER, 1977), marble (MULTON *et al.*, 2010; VARDHAN *et al.*, 2015), granite (COUTINHO, 2019; MÁRMOL *et al.*, 2010; RAMOS *et al.*, 2013), have been utilized. However, durability aspects of concrete produced with AMFs remain insufficiently addressed.

A related intriguing concern is the use of rocks susceptible to alkali-aggregate reaction (AAR) to produce AMFs. AAR is a chemical reaction between certain mineral phases in the aggregates and the alkalis in the concrete pore solutions (FOURNIER; BERUBÉ, 2000; LEEMANN *et al.*, 2024a; NIXON; SIMS, 2016; SIMS; POOLE, 2017). This reaction, classified as alkali-silica reaction (ASR) and alkali-carbonate reaction (ACR),

affects critical concrete infrastructure worldwide (FOURNIER; BÉRUBÉ, 2011; SIMS; POOLE, 2017). As AAR-susceptible rocks are available worldwide, AAR-reactive AMFs become a viable and widely available option to be used in concrete. However, more studies are necessary to understand the effect of AAR-reactive AMFs on AAR-induced deterioration.

5.2 APPRAISING AAR-REACTIVE AMFS IN CONCRETE

5.2.1 Test methods to assess AAR-induced expansion in concrete

To evaluate AAR-induced expansion in concrete mixtures containing AAR-reactive aggregate mineral fillers (AMFs), three primary test methods have been adopted: the accelerated mortar bar test (AMBT), the concrete prism test (CPT), and the accelerated concrete prism test (ACPT).

The AMBT is favored for its short duration, ranging from 16 to 56 days depending on the standard applied (e.g., ASTM, CSA, Brazilian, Norwegian (ABNT, 2018b; ASTM, 2023a; CSA, 2024)). This method involves severe testing conditions, including crushing of aggregates and immersion in a 1N NaOH solution at 80 °C, which accelerates reaction kinetics but may lead to overestimations and misclassification of aggregate reactivity (BÉRUBÉ; FOUNIER, 2003; DEMERCHANT; FOURNIER; STRANG, 2000; GOLMAKANI; HOOTON, 2016; GRATTAN-BELLEW, 1997; IDEKER *et al*., 2012; THOMAS *et al*., 2006). Despite these limitations, the AMBT results consistently indicated a reduction in expansion when using AAR-reactive AMFs. In systems incorporating reactive coarse aggregates, ultimate expansions were significantly reduced, with reductions varying from 7% to 91% depending on the AMF type and replacement parameters (ABNT, 2018c; CASTRO *et al*., 1997; COUTINHO; MONTEFALCO; CARNEIRO, 2024; OLIVEIRA; SALLES; ANDRIOLO, 1995; TAPAS *et al.,* 2023). Similar behaviour was observed when applying the Norwegian standard, where the use of reactive AMFs generally led to lower expansions compared to control mixtures (PEDERSEN, 2004). Furthermore, in systems with reactive fine aggregates, the use of reactive AMFs resulted in a considerable decrease in both the reaction rate and maximum expansion, as exemplified by a reduction from 0.47% to 0.12% (approximately 74%) (TAPAS *et al*., 2023). Overall, AMBT results consistently demonstrated the potential of AAR-reactive AMFs to mitigate expansion in both coarse and fine reactive aggregate systems.

The CPT, in contrast, offers a more representative assessment of concrete performance, due to its more moderate conditions (i.e., 38 °C and high relative humidity – RH) and longer duration (one year) (ABNT, 2018c; ASTM, 2023b; CSA, 2024). In systems with reactive coarse aggregates, the CPT generally showed kinetics and ultimate expansions comparable to control mixtures, except when using rhyolite filler, which exhibited considerably reduced expansion likely due to its pozzolanic activity (PEDERSEN, 2004). Moreover, in non-reactive systems containing reactive AMFs, expansions were considerably higher than those of control samples, with ultimate expansions approximately twice as large (GUÉDON-DUBIED *et al*., 2000). These findings highlight the critical importance of carefully evaluating the combined effects of AMFs and aggregate type, as reactive fillers can trigger deleterious expansion even when non-reactive aggregates are used.

The ACPT has also been applied to evaluate AAR-reactive fillers (ABNT, 2018d; NIXON; SIMS, 2016). This test was developed as an intermediate approach, with a shorter duration (180 days) and intermediate conditions (60 °C, 100% RH), allowing for the assessment of a larger particle size distribution (PSD) (AASHTO, 2022; LINDGÅRD *et al*., 2011; THOMAS; FOURNIER; FOLLIARD, 2013). Results from the ACPT indicated that in systems with reactive coarse aggregates, the use of reactive AMFs (whether replacing cement or sand) led to similar or slightly higher ultimate expansions, with some combinations showing accelerated reaction kinetics (ANTUNES, 2021). When applied to systems containing reactive fine aggregates, expansions were also similar or slightly higher than those of the controls, and reaction rates were often accelerated (ANTUNES, 2021). These outcomes contrast with the reductions observed in the AMBT but align with the tendency found in CPT evaluations.

In addition to the type of reactive system, other parameters influence the behaviour of AAR-reactive AMFs, such as the PSD. Moreover, the degree of reactivity of AMFs, influenced by mineralogy, affects the results, with highly and moderately reactive fillers providing expansion reductions of up to 93% and 72% in the AMBT, respectively (PEDERSEN, 2004b). Considering the replacement strategy, AAR-reactive AMFs have been used replacing cement (ANTUNES, 2021; CASTRO *et al*., 1997; COUTINHO; MONTEFALCO; CARNEIRO, 2024; LI; HE; HU, 2015; QINGHAN *et al*., 1996; SALLES; OLIVEIRA; ANDRIOLO, 1997; TAPAS *et al*., 2023), sand (ANTUNES,

2021; CARLES-GIBERGUES *et al.*, 2008; PEDERSEN, 2004), and both cement and sand (GUÉDON-DUBIED *et al*., 2000), with replacement percentages ranging from 10% to 80%.

Overall, while the AMBT tends to suggest a clear mitigating effect of AAR-reactive AMFs by indicating reduced expansions, both CPT and ACPT results reveal a more complex and sometimes adverse influence depending on aggregate type, AMFs characteristics, and replacement content. This highlights the need of employing complementary test methods and conducting long-term evaluations to fully understand the behaviour of AAR-reactive AMFs in concrete systems.

5.2.2 Test methods to assess AAR-induced damage in concrete

AAR-induced damage in systems containing AAR-reactive AMFs has been insufficiently addressed. The methods that were previously adopted are the evaluation of surface cracking (CARLES-GIBERGUES *et al*., 2008) and the use of the multilevel assessment (ANTUNES, 2021). The results demonstrated a significant reduction in surface cracking when reactive aggregates were combined with AMFs derived from the same rock source: metaquartzite (100% reduction), siliceous limestone (approximately 90%), opaline aggregate (100%), and crushed waste glass (100%) (CARLES-GIBERGUES *et al*., 2008). However, surface cracking alone is not a good indicator because AAR is an internal mechanism, which means that the concrete deterioration may not be reflected at the surface. In contrast, the multilevel assessment, combining microstructural (i.e., damage rating index – DRI) and mechanical (i.e., stiffness damage test – SDT) evaluations, enables a more accurate appraisal of the extent and progress of damage over time (ANTUNES, 2021).

DRI is a petrographic technique to appraise concrete deterioration. In this method, concrete samples are cut, polished, and examined under a stereomicroscope at 15–16× magnification (2016b). A 1-cm² grid is drawn on the polished surface, and various deterioration features, such as open and closed cracks in aggregates and cracks in the cement paste, are systematically counted (SANCHEZ, 2014). Each feature is assigned a specific weight, and the weighted counts are averaged and normalized to an area of 100 cm². Likewise, the SDT is a mechanical and cyclic procedure that appraises internal damage in concrete. During the test, five compression load cycles (at 40% of the 28-day compressive strength) are applied. Parameters derived from this

test include the stiffness damage index (SDI), which is calculated as the ratio of dissipated energy to total energy, and the loss in modulus of elasticity, both reflecting the extent of internal damage (SANCHEZ *et al*., 2018).

Very few research was conducted on the use of DRI and SDT to appraise the impact of AAR-reactive AMFs on AAR-induced damage. For systems containing 15% greywacke AMFs, the DRI values were generally lower when cement was replaced and similar or higher when sand was replaced, relative to control samples without AMFs. Variations in the DRI were primarily attributed to changes in crack patterns within the cement paste (i.e., cracks in the cement paste with and without reaction product), directly influenced by AMF incorporation (ANTUNES, 2021). Moreover, a good correlation was observed between DRI values and expansion levels.

Regarding SDT outcomes, replacing cement with AMFs tended to slightly increase SDI values, whereas sand replacement produced comparable or reduced SDI values relative to control samples (ANTUNES, 2021). For the modulus of elasticity loss, the behaviour varied by aggregate type: systems with reactive coarse aggregates showed lower losses than control samples regardless of replacement type. In systems with reactive fine aggregates, greywacke AMFs led to higher modulus of elasticity losses, particularly when replacing cement, whereas dolomitic argillaceous limestone AMFs resulted in considerably lower losses (ANTUNES, 2021).

In both evaluations, the deterioration was assessed only at the end of the expansion measurement period. Therefore, evaluating the deterioration progress could provide interesting insights into the behaviour of systems with AAR-reactive AMFs.

5.3 SCOPE OF THE WORK

As demonstrated in previous sections, despite some studies on the influence of AAR-reactive AMFs on AAR, the variability in the parameters assessed and tests used hinder the construction of solid knowledge. To fill this knowledge gap, this study aimed to evaluate the use of ASR-reactive AMFs in reactive systems containing a) reactive coarse and b) reactive fine aggregates. The AMFs were used replacing cement and the variables analyzed were type of filler (highly reactive and moderately reactive), PSD (i.e., < 150 µm and < 75 µm), and percentage (i.e., 10% and 20%). The CPT was adopted and the deterioration progress was assessed by applying the multi-level assessment (DRI and SDT). The results of this study are expected to contribute to a

better understanding of the action of ASR-reactive AMFs considering kinetics and deterioration and how the variables analyzed affect the reaction progress to determine the potential viability of this material to be used in blended cements.

5.4 EXPERIMENTAL PROGRAM

To accomplish the objectives proposed, four parameters were evaluated: type of mixture, reactivity degree of the aggregate to produce AMFs, PSD, and percentage. Regarding the type of mixture, two mixtures were produced: Mixtures B, with reactive coarse and non-reactive fine aggregates, and Mixtures C, with non-reactive coarse and reactive fine aggregates.

5.4.1 Materials for concrete production

A conventional Portland cement GU type was used. This cement is equivalent to ASTM type I. There is no equivalent considering Brazilian cements, but it shares characteristics of CP-V (low percentage of additions) and CP II-F (particle size). The AMFs used were produced from two reactive rocks, a moderately reactive mylonite from Brazil and a highly reactive greywacke from Canada (Springhill). The chemical composition was determined by X-ray fluorescence (XRF) using a Rigaku Supermini200 WDXRF Spectrometer. The X-ray diffraction was conducted using a Rigaku Ultima IV Diffractometer. The results of the XRF for the cement and AMFs and diffractograms of the AMFs are presented in Table 5.1 and Figure 5.1, respectively.

Table 5.1 – Chemical composition of cement and AMFs.

Chemical composition	Cement (%)	Mylonite (%)	Springhill (%)
SiO_2	19.64	59.06	51.72
Al_2O_3	4.53	13.48	10.76
CaO	62.04	5.17	8.69
K_2O	0.97	3.58	2.70
Na_2O	0.42	3.45	1.45
MgO	2.64	3.22	5.59
Fe_2O_3	3.69	8.34	4.97
TiO_2	0.23	1.50	0.60
P_2O_5	0.14	0.89	0.11
MnO	0.05	0.12	0.07
Traces	1.81	0.36	0.33
L.O.I.	3.84	0.84	13.00
Na_2O_{eq}	1.06	5.80	3.23
TOTAL	100.00	100.00	100.00

Source: Author (2025).

Figure 5.1 – Diffractograms of the mylonite and Springhill fillers used

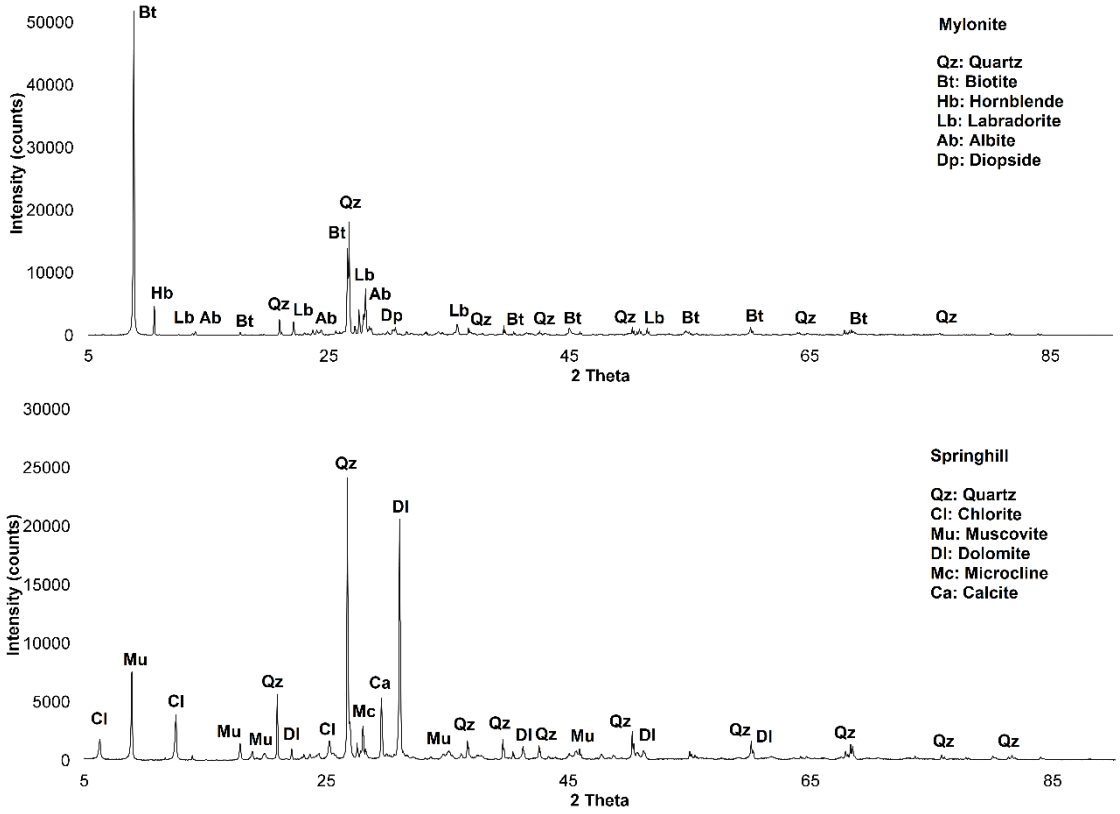

Quartz: SiO_2, Biotite: $(K(Mg,Fe)_3(AlSi_3O_{10})(F,OH)_2)$, Hornblende: $((Ca,Na)_{2-3}(Mg,Fe,Al)_5(Al,Si)_8O_{22}(OF,F)_2)$, Labradorite: $((Ca,Na)(Si,Al)_4O_8)$, Albite: $(Na,Ca)Al(Si,Al)_3O_8$, Diopside: $(MgCaSi_2O_6)$, Chlorite: $(Mg,Al)_6(Si,Al)_4O_{10}(OH)_8$, Muscovite: $(K,Na)(Al,Mg,Fe)_2(Si_{3.1}Al_{0.9})O_{10}(OH)_2$, Dolomite: $CaMg(CO_3)_2$, Microcline: $K(AlSi_3)O_8$, Calcite: $(Mg_{0.03}Ca0.97)(CO_3)$.
Source: Author (2025).

The aggregates were crushed using a jaw crusher and sieved to obtain powders passing the sieves with openings 150 μm and 75 μm. The choice of the <150 μm opening was based on the fractions adopted in the AMBT (ASTM, 2023a), still extensively used in laboratories. In this test, the aggregates are crushed and fractions ranging from 4.8 mm to 150 μm are used, and the fraction passing the sieve with opening 150 μm is discarded. Therefore, this fraction was selected to test the AMFs because it is indirectly produced. Moreover, to evaluate the effect of the AMFs PSD, the fraction passing the 75 μm sieve was also adopted. This choice was made considering the physical requirement for type C fillers (byproduct from aggregate crushing operations) of having ≥ 65% passing the 75 μm sieve for use in hydraulic cement concrete, as per ASTM C1797 (ASTM, 2024). Previous studies have also used these parameters (CASTRO *et al.,* 1997; COUTINHO; MONTEFALCO; CARNEIRO, 2024; SALLES; OLIVEIRA; ANDRIOLO, 1997). The PSD curves of cement and AMFs, obtained by laser diffraction, are shown in Figure 5.2.

Figure 5.2 – PSD of cement and AMFs.

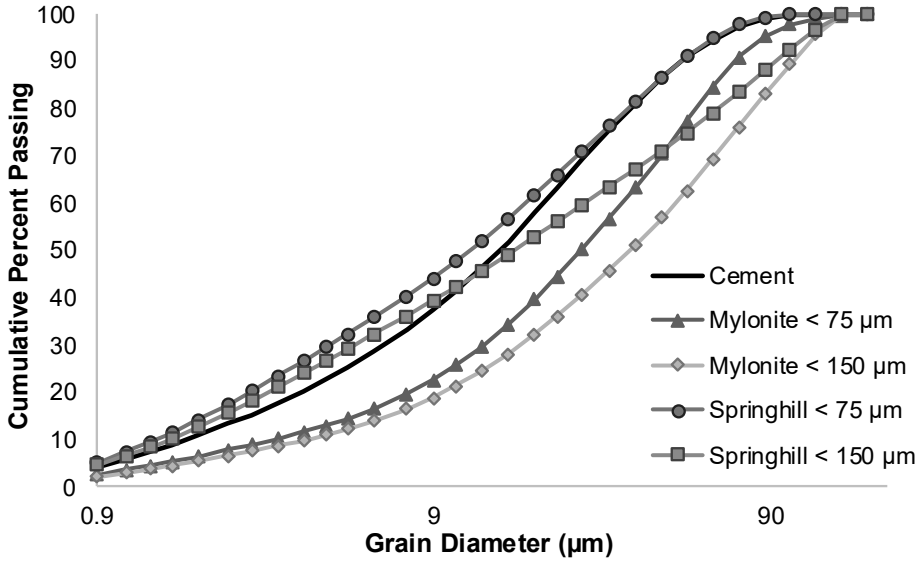

Source: Author (2025).

As observed, mylonite fillers were coarser than cement. Springhill fillers exhibited PSDs closer to that of Portland cement, particularly the <75 µm filler. The AMFs were used replacing cement to reduce the cement consumption considering the Net Zero target. Moreover, the percentages adopted were 10% and 20% based on the literature review conducted (CARLES-GIBERGUES *et al.,* 2008; COUTINHO; MONTEFALCO; CARNEIRO, 2024; LI; HE; HU, 2015).

The coarse and fine aggregates adopted were reactive and non-reactive, as detailed Table 5.2.

Table 5.2 – Coarse and fines aggregates used.

Aggregate		Reactivity	Rock Type	Specific Gravity	Absorption (%)	AMBT[b] (%)
Coarse	SP	ASR	Greywacke	2.66	0.89	0.33
	LC	NR[a]	Crushed limestone	2.78	0.42	0.02
Fine	TX	ASR	Natural derived from granitic, mixed volcanics, quartzite, chert, quartz)	2.60	0.82	0.81
	NS	NR	Natural sand	2.70	0.40	0.04

[a] NR: Non-reactive.
[b] Results of the AMBT as per ASTM C 1260.

Source: Author (2025).

5.4.2 Mixture proportion and production of samples

The CPT was conducted to measure ASR expansions. This test was selected to allow a better representation of field concrete when compared to other tests used such as the AMBT and ACPT. Moreover, previous results indicated that AMFs of rocks containing siliceous mineral phases may exhibit pozzolanic activity at high temperatures such as 80 ºC (PEDERSEN, 2004). Therefore, the use of tests at lower temperatures would be fundamental when assessing AMFs.

Concrete cylinders of 100 × 200 mm were produced in this study. For each of the mixtures (mixtures B and C), samples were cast using the two AMFs adopted (Mylonite and Springhill), two PSDs (< 150 µm and < 75 µm), and two percentages (10% and 20%), representing 16 families. For each family, expansion measurements were conducted until 9 months. Based on previous studies using these aggregates, the expansions start stabilizing after 6 months (ANTUNES, 2021; BEZERRA, 2021; DE GRAZIA, 2023; REZAIEH, 2021; SOUZA, 2022; ZUBAIDA, 2020). Therefore, tests were conducted at the ages of 1, 3, and 6 months. Six samples were produced for each age and three additional samples for the compressive strength tests, totalling 27 samples per family and 432 for the study. The nomenclature adopted consisted of the type of mixture (B and C) followed by the type of filler (M or SP), PSD (150 or 75), and percentage (P10 or P20). Therefore, a sample named BM150P20 would indicate mixture B with mylonite filler, PSD of 150 µm, and percentage of 20%.

The mixture design followed the requirements of ASTM C1293 (ASTM, 2023b). The concrete was boosted with NaOH to reach an alkali equivalent of 5.25 kg/m^3 of concrete. The water/cement ratio adopted was 0.45 and the cement + filler content was 420 kg/m^3. The mixture proportions used are listed in Table 5.3

Table 5.3 – Concrete mixture proportions.

Mixture	Filler	PSD	%	Cement (kg/m^3)	Filler (kg/m^3)	FA – NR* (kg/m^3)	CA – R* (kg/m^3)	Water (kg/m^3)
B	M	150	10	378.00	42.00	764.50	1043.70	170.10
B	M	150	20	336.00	84.00	764.50	1043.70	151.20
B	M	75	10	378.00	42.00	764.50	1043.70	170.10
B	M	75	20	336.00	84.00	764.50	1043.70	151.20
B	SP	150	10	378.00	42.00	764.50	1043.70	170.10
B	SP	150	20	336.00	84.00	764.50	1043.70	151.20
B	SP	75	10	378.00	42.00	764.50	1043.70	170.10
B	SP	75	20	336.00	84.00	764.50	1043.70	151.20

Mixture	Filler	PSD	%	Cement (kg/m³)	Filler (kg/m³)	FA – R (kg/m³)	CA – NR (kg/m³)	Water (kg/m³)
C	M	150	10	378.00	42.00	696.83	1133.44	170.10
C	M	150	20	336.00	84.00	696.83	1133.44	151.20
C	M	75	10	378.00	42.00	696.83	1133.44	170.10
C	M	75	20	336.00	84.00	696.83	1133.44	151.20
C	SP	150	10	378.00	42.00	696.83	1133.44	170.10
C	SP	150	20	336.00	84.00	696.83	1133.44	151.20
C	SP	75	10	378.00	42.00	696.83	1133.44	170.10
C	SP	75	20	336.00	84.00	696.83	1133.44	151.20

* FA: fine aggregate; CA: coarse aggregate; NR: non-reactive; R: reactive.
Source: Author (2025).

The ends of the samples were drilled and steel gauges were placed using fast-setting cement slurry. The samples were allowed to harden for 24 h, after which the initial measurements were taken. Then, they were stored in sealed plastic buckets lined with a moist cloth at 38 ºC and 100% relative humidity (RH). The cylinders were regularly measured and taken at the ages of 1, 3, and 6 months for additional tests.

5.4.3 Assessment of the ASR development in concrete

The kinetics and maximum expansion, considered as the expansion measured at the latest age of the test or from which the expansion stabilize, were evaluated by measuring the expansions as a function of time using a measuring arch, as per the standard ASTM C1293 (ASTM, 2023b)**Error! Reference source not found.**.

5.4.3.1 Compressive Strength

The compressive strength test was conducted to determine the load to be used in the SDT. The samples were wrapped in plastic film and stored in a chamber at 12 ºC to avoid the development of ASR, which can affect the results of the test, as reactive aggregates were used. The samples remained at this temperature for 47 days, which corresponds to 28 days at 20 ºC, as per the maturity concept by ASTM C 1074 (ASTM, 2019). This procedure was validated by Sanchez (2014) and Sanchez et al. (2016).

5.4.3.2 Damage Rating Index

The DRI was calculated as per the method described in Villeneuve (2011) and Sanchez et al. (2016). The samples were axially cut in half and polished using a hand polisher device by means of diamond impregnated rubber disks (nº. 50, 100, 200, 400, 800, 1500, 3000). The analysis was conducted in a stereomicroscope (15–16×

magnification) at the ages of 1, 3, and 6 months. The DRI was calculated based on counting the features, multiplying by weighting factors (Figure 5.3), and normalizing for an area of 100 cm^2.

Figure 5.3 – DRI petrographic features and corresponding weights.

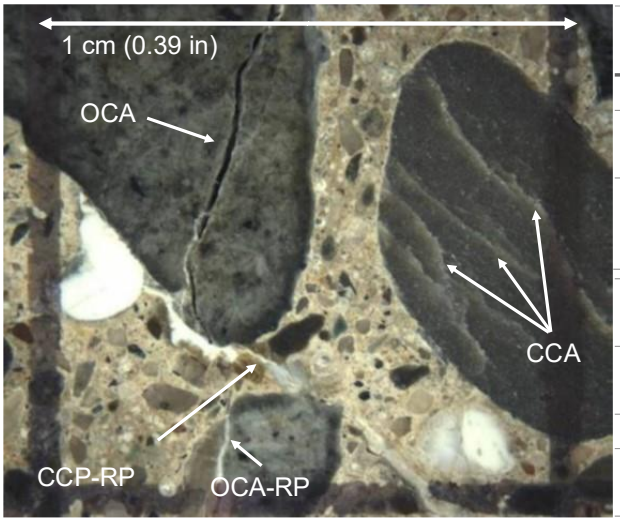

Petrographic Features		Weighting factors
Crack in coarse aggregate	CCA	0.25
Opened crack in coarse aggregate	OCA	2
Crack with reaction product in coarse aggregate	OCA -RP	2
Coarse aggregate debonded	CAD	3
Disaggregate/corroded particle	DAP	2
Crack in cement paste	CCP	3
Crack with reaction product in cement paste	CCP -RP	3

Source: Sanchez *et al.* (2016).

5.4.3.3 Stiffness Damage Test

The SDT was performed as per the procedure described in the works of Sanchez and colleagues (SANCHEZ et al., 2014, 2017, 2018a). Five cycles of loading/unloading were conducted at 40% of the ultimate compressive strength capacity of the samples at 28 days through a loading rate of 0.10 MPa/s. The results obtained and presented in this work are the average of three samples tested at each curing period. The outputs of the test are the SDI, plastic deformation index (PDI), and modulus of elasticity. The SDI and PDI were calculated as the ratios of dissipated energy to total energy and plastic deformation to total deformation implemented in the system, respectively (SANCHEZ *et al*., 2017). The modulus of elasticity was calculated as the average obtained from the second and third cycles of the SDT.

5.4.4 Statistical Analysis

The results obtained were statistically analyzed using multi-factorial analysis of variance (ANOVA) for a significance level of 5%. Shapiro–Wilk and Barlett's tests were applied to verify the normality and homoscedasticity (equal variance) of the data.

5.5 RESULTS

5.5.1 ASR Kinetics

Figure 5.4 shows the expansion kinetics (i.e., average value of four consecutive measurements per sample with standard deviations ranging from 0.01% to 0.07%) obtained by incorporating different types of ASR-reactive AMFs with different PSDs and percentages on mixtures produced using reactive coarse and fine aggregates as a function of time.

Figure 5.4 – ASR kinetics over time for mixtures containing reactive coarse and reactive fine aggregates and reactive AMFs replacing cement.

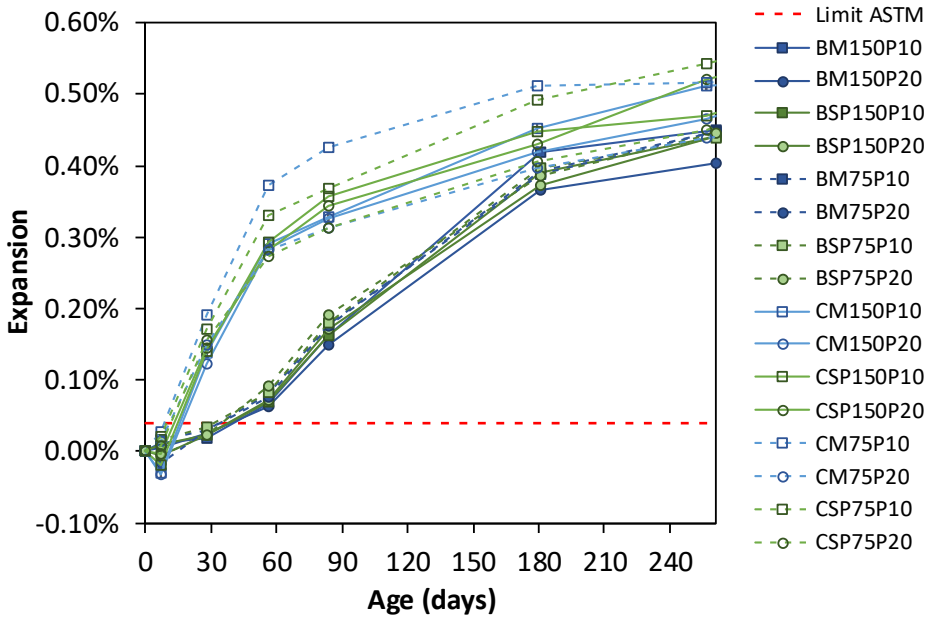

Source: Author (2025).

As observed, the curves are distinctively grouped, indicating the different behaviour of mixtures depending on the type of aggregates used. Mixtures with reactive fine aggregates exhibited faster kinetics, reaching higher expansions earlier than mixtures B, as obtained in other studies (DE SOUZA; SANCHEZ; BIPARVA, 2024). Moreover, given the faster kinetics, the expansion rate considerably reduces at around 60 days, whereas this happens at 180 days for mixtures B. The maximum expansions obtained also reflect the reactivity degree of the aggregates used, where mixtures with Texas sand, an ultra-highly reactive fine aggregate, reached expansions above 0.50% at 270 days, whereas the maximum value obtained for mixtures with Springhiill, a highly reactive aggregate, was 0.45% at the same age.

To better analyze each mixture, the results were separated as in Figure 5.5 (a) and (b) for mixtures B and C, respectively. The corresponding mass variations are shown in Figure 5.6(a) and (b). The grey area encompasses results obtained in previous studies (ANTUNES, 2021; BEZERRA, 2021; DE GRAZIA, 2023; REZAIEH, 2021; SOUZA, 2022; ZUBAIDA, 2020) for mixtures using the same aggregate and no reactive AMFs and represent control values.

Figure 5.5 – (a) ASR kinetics over time for mixtures containing (a) reactive coarse and (b) reactive fine aggregates and ASR-reactive AMFs replacing cement.

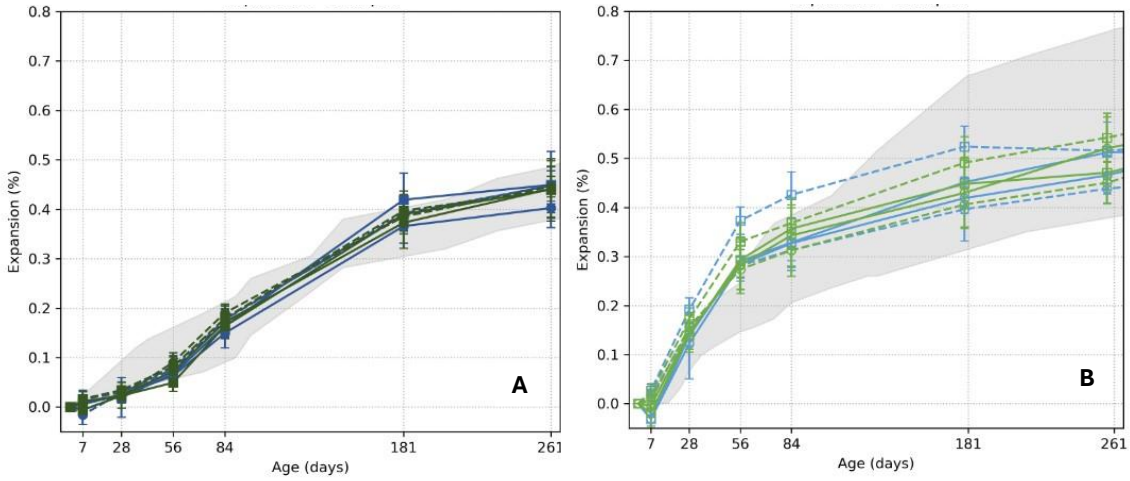

Source: Author (2025).

Figure 5.6 – Mass variation over time of mixtures containing (a) reactive coarse and (b) reactive fine aggregates and reactive AMFs replacing cement.

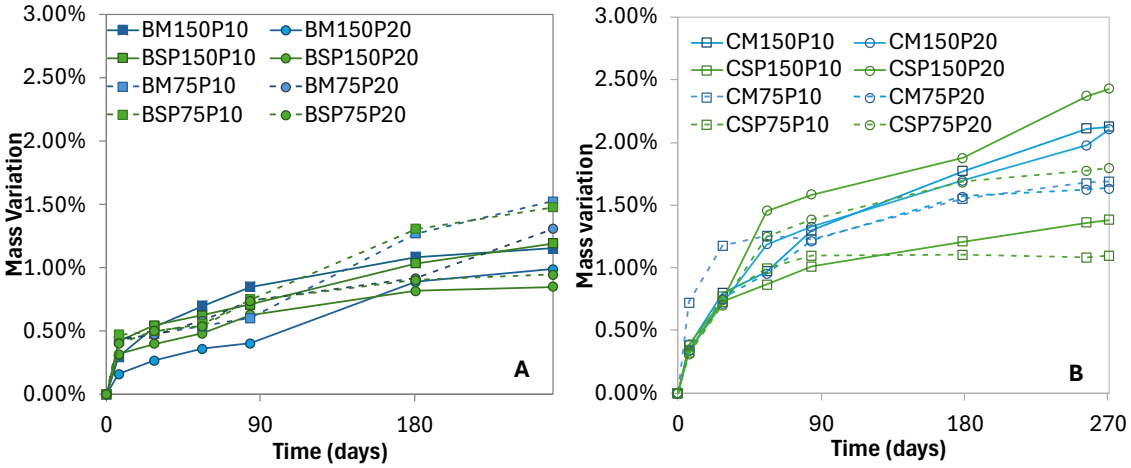

Source: Author (2025).

As observed in Figure 5.5(a), the mixtures with reactive coarse aggregates were mainly outside the envelope consisting of results without reactive AMFs until 28 days, indicating that the expansions were slightly lower during this period. This behaviour was previously observed by Vivian (1951), in which the start of the expansion was

delayed when using reactive particles of a siliceous magnesium limestone. From this point on, all the curves were within the envelope, which indicates that the AMFs did not have a considerable effect on expansion for all the variations analyzed. The combination BM150P10 was the only one that exhibited one value outside the envelope at 180 days, after which the expansion rate tended to reduce. Three distinct behaviours can be observed: initially, until 56 days, the expansions increase at a slow rate, close to and lower than the bottom part of the envelope; in sequence, the expansions increase at a faster rate and become close to the upper part of the envelope and even over it; finally, from 180 days, the expansion rate tends to decrease and the expansions become closer to the bottom part of the envelope. The envelope shows a tendency to continue increasing at a slow rate, whereas the curves seem to start levelling off.

As for mixtures with fine reactive aggregates in Figure 5.5(b), the kinetics were fast in the first 56 days, with all the curves above the envelope of previous results. After 56 days, the expansion rate reduces, and the expansions start levelling off. At 120 days, the expansions are within the envelope and tending to its bottom part.

Moreover, almost no shrinkage occurred in both mixtures, being slightly more pronounced in mixtures with fine reactive aggregates in the first 7 days. The behaviour of the curves was also similar, particularly for the mixtures with reactive coarse aggregates.

For mixtures B, the maximum expansions ranged from 0.40% to 0.45%, indicating no considerable difference despite the varied parameters. The mass gain ranged from 0.85% and 1.52% at the maximum expansion and the behaviour of the curves was similar to that of the expansion curves. For mixtures C with reactive fine aggregates, the maximum expansions were less concentrated, ranging from 0.44% to 0.55%. The mass gain ranged from 1.09% to 2.43% at the maximum expansion level and the behaviour of the curves was also similar to that of the expansion curves.

5.5.2 Damage Rating Index

Figures 5.7 and 5.8 show the DRI values (i.e., average of two specimens per combination) for mixtures B with reactive coarse aggregates and C with reactive fine aggregates, respectively, for the ages of 1, 3, and 6 months and for all combinations analyzed. Reference values were obtained from Zubaida (2020).

Figure 5.7 – DRI values for mixtures B.

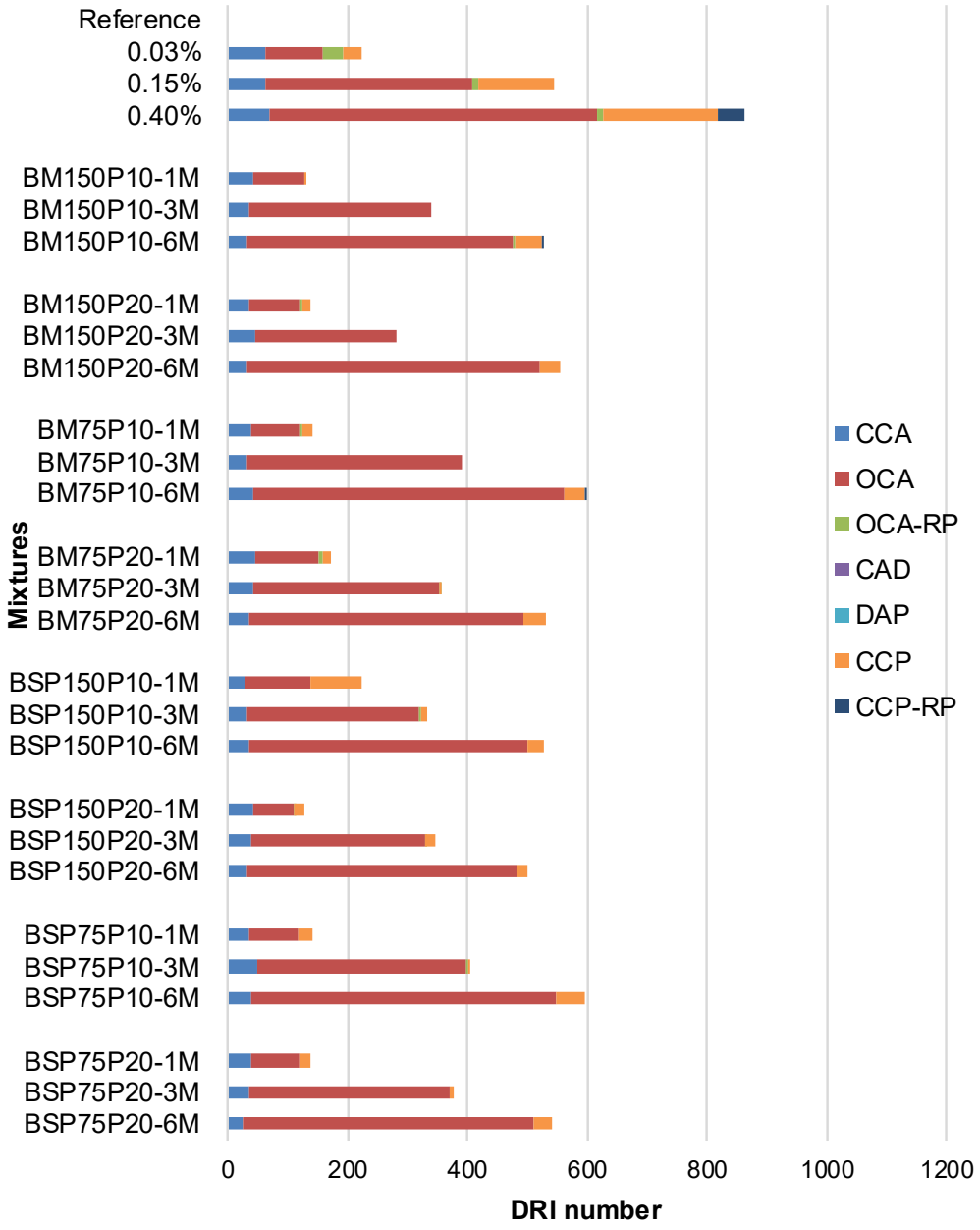

Source: Author (2025)

Figure 5.8 – DRI values for mixtures C.

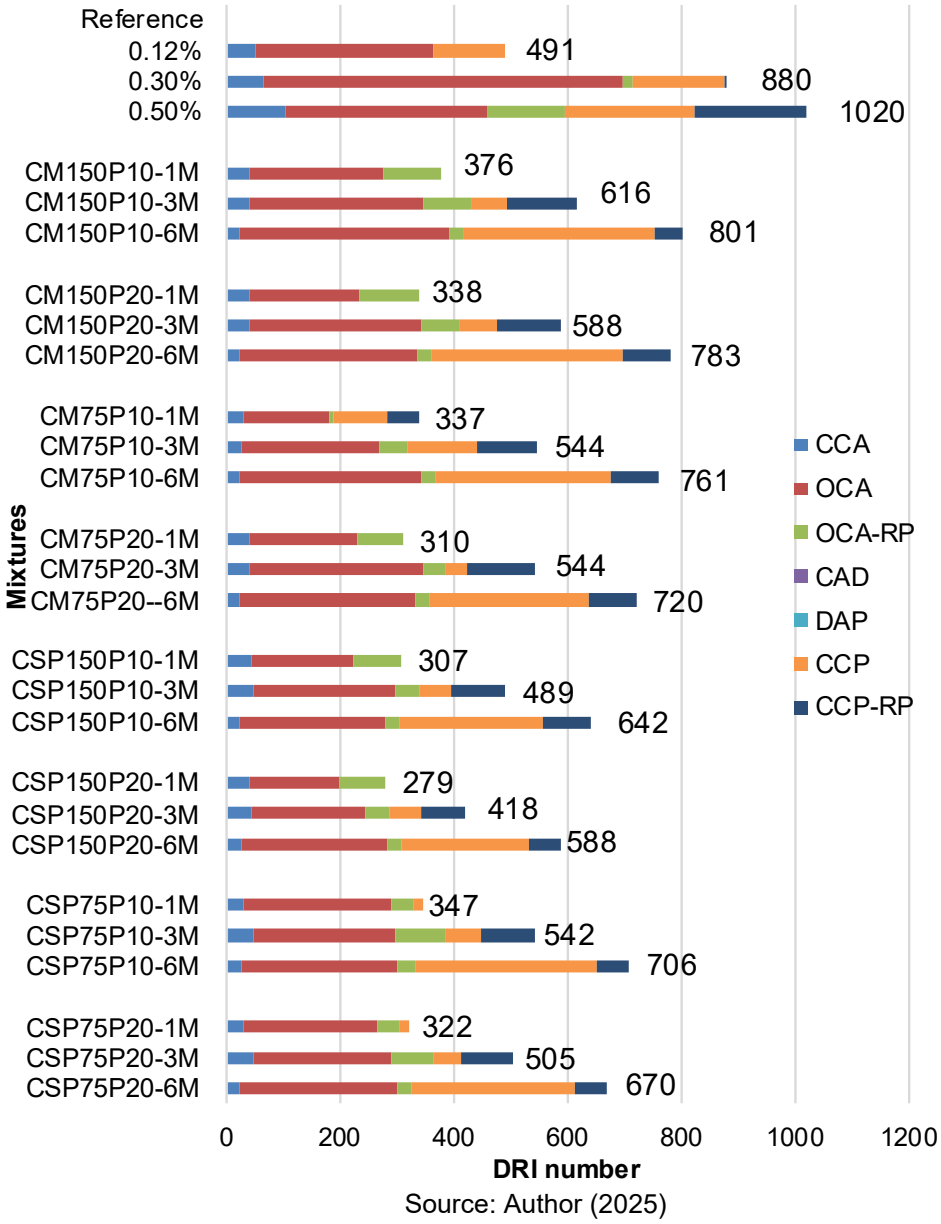

Source: Author (2025)

The DRI numbers ranged from 128 to 600 for mixtures B and from 279 to 801 for mixtures C. At 6 months, the DRI numbers ranged from 499 to 600 for mixtures B and from 588 to 801 for mixtures C, which indicates high and very high damage, respectively, as per the classification of damage degree in concrete due to ASR proposed by Sanchez et al. (2017). The numbers increased with age, which was expected as the deterioration progressed. Compared to the reference values, which were obtained from previous studies in which the same aggregates were used and correspond to a similar expansion level, all mixtures exhibited lower DRI values. The DRI values for mixtures C were, in general, also higher than those for mixtures B,

particularly at one month, indicating more deterioration, which agrees with the higher expansion values and faster kinetics observed for mixtures C.

In general, for mixtures B, the DRI values were similar. For instance, at 6 months, mixtures BM75P10 and BSP150P10 with different types of fillers and same PSD and percentage had DRI values of 600 and 595, respectively. However, when compared to the reference sample, the number of open cracks with reaction product (OCA-RC) is reduced for combinations with AMFs, particularly at 1 month. For all mixtures, a considerable reduction in cracks in the cement paste (CCP) was observed compared to the reference mixture, indicating that the AMFs had an effect on the cement paste.

When analyzing mixtures C with Texas sand, more OCA-RP were observed for mixtures with AMFs at 1 month compared to the reference sample. Only few CCP were observed at 1 month for combinations with AMFs. The number of CCP, with and without reaction product, increased over time. However, compared to the reference results, the contribution related to CCP was higher whereas that of CCP-RP was lower, which may indicate an effect of the AMFs in the formation of reaction product.

5.5.3 Stiffness Damage Test

The results of SDT represent the average obtained from three samples tested. Figures 5.9 and 5.10 show the results of SDI, PDI, and modulus of elasticity for the ages tested for mixtures B and C, respectively.

Figure 5.9 – SDT results for samples with coarse reactive aggregates. (a) SDI. (b) PDI. (c) Modulus of elasticity.

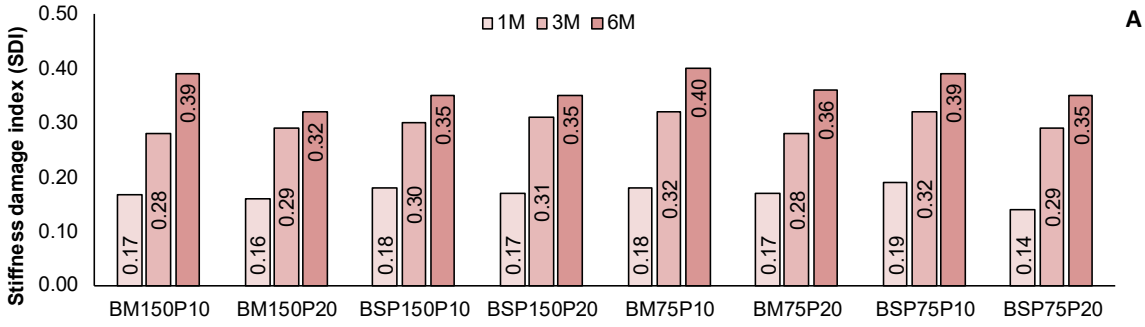

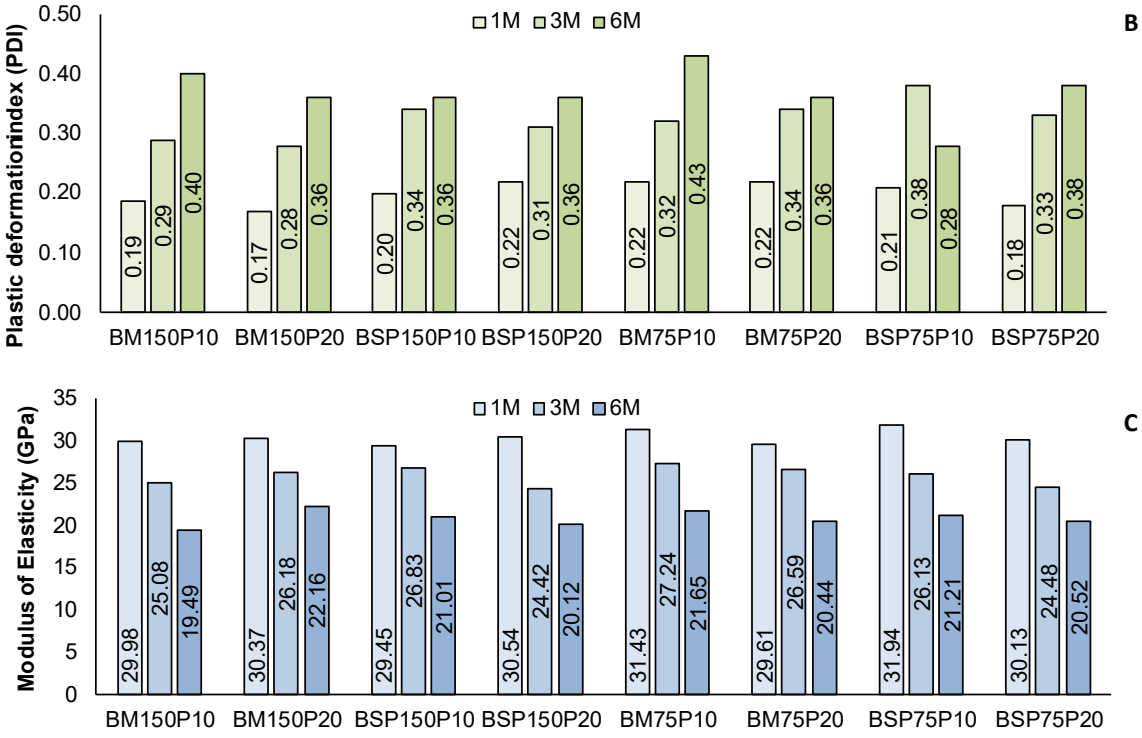

Source: Author (2025).

Figure 5.10 – SDT results for samples with reactive fine aggregates. (a) SDI. (b) PDI. (c) Modulus of elasticity.

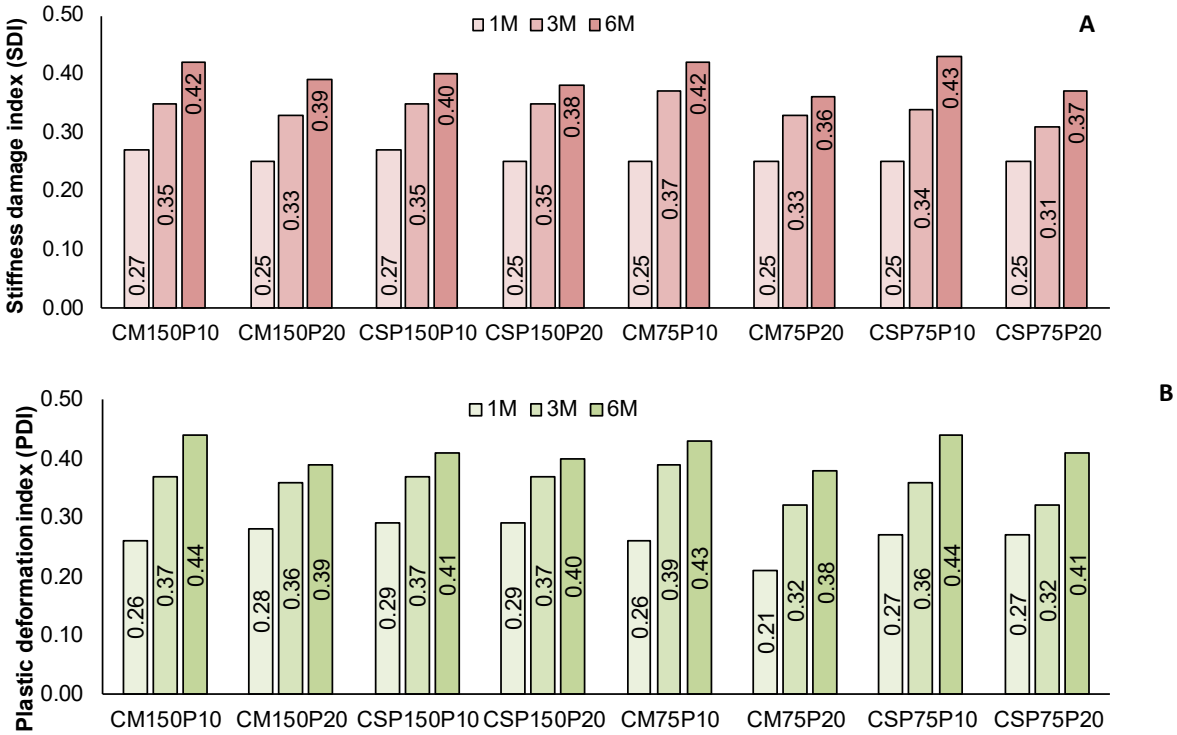

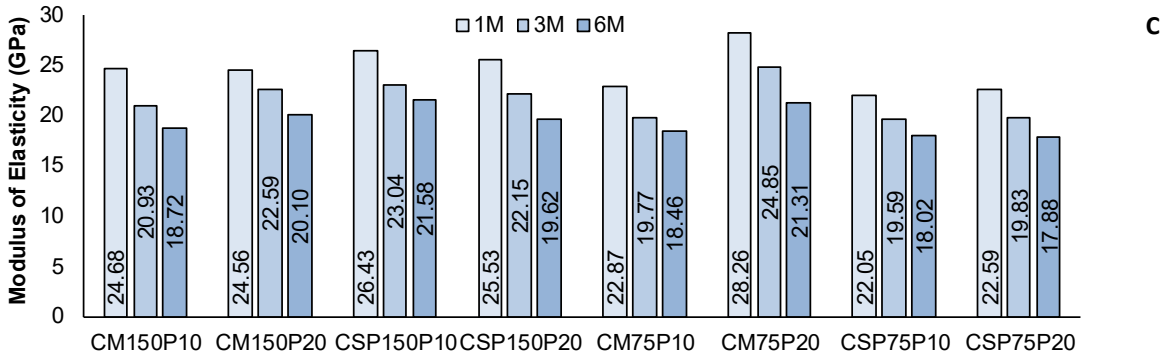

Source: Author (2025).

As observed, the SDI and PDI increased over time, whereas the modulus of elasticity decreased, which was expected as the deterioration progressed. The damage was more pronounced in mixtures C compared to mixtures B as per the higher SDI and PDI values and decrease in modulus of elasticity, which is also in agreement with the higher expansions and DRI values for these mixtures. For mixtures B, the SDI values varied from 0.14 to 0.40 and the PDI values varied from 0.17 to 0.43. For mixtures C, the SDI values varied from 0.21 to 0.43 and the PDI values varied from 0.21 to 0.44. These values indicate that the damage degree at 6 months is very high (SANCHEZ *et al*., 2017).

5.6 DISCUSSION

5.6.1 Effect of parameters evaluated on the kinetics and maximum expansion of the reaction

In this study, two types of mixtures were produced: mixtures B with reactive coarse aggregates (i.e., Springhill) and mixtures C with reactive fine aggregates (i.e., Texas sand). Moreover, three parameters were analyzed for each mixture: type of filler (i.e., Mylonite or Springhill), PSD (< 150 µm or < 75 µm), and percentage (10% and 20%). Figures 5.11(a) and (b) show the expansion development and magnification of the maximum expansions obtained for mixtures B and C, respectively.

Figure 5.11 – Expansions for (a) mixture B and (b) mixture C combinations.

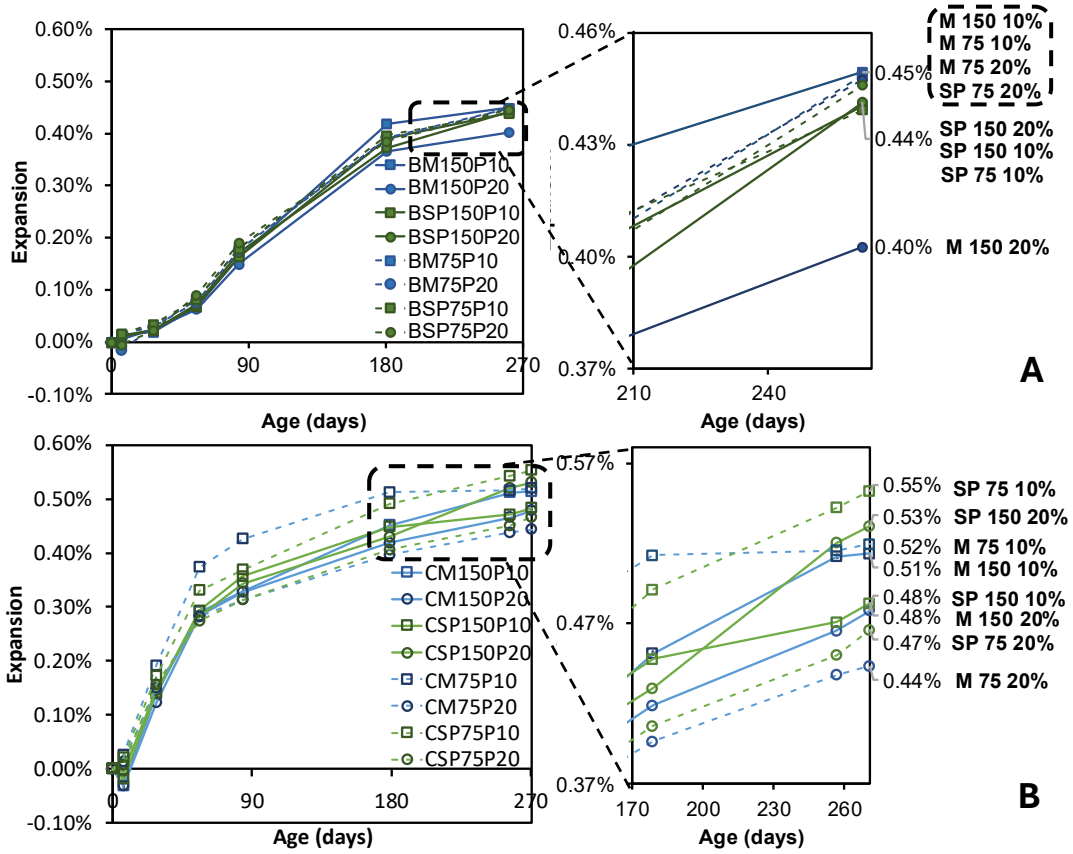

Source: Author (2025).

For mixtures B, the maximum expansions did not vary considerably, ranging from 0.40% to 0.45%. The behaviour of the curves was also very similar. For mixtures C, the maximum expansions varied more within combinations compared to mixtures B, ranging from 0.44% to 0.55%. The behaviour of the curves was also very similar. The curves were very close and even overlapping until 28 days, after which they started spreading.

To better understand the kinetics of the distinct mixtures, the rates of expansion from all curves along with maximum expansion rates were calculated for mixtures B and C and are shown in Figure 5.12.

Figure 5.12 – (a) Expansion rate curves and (b) maximum expansion rates for mixtures B. (c) Expansion rate curves and (d) maximum expansion rates for mixtures C.

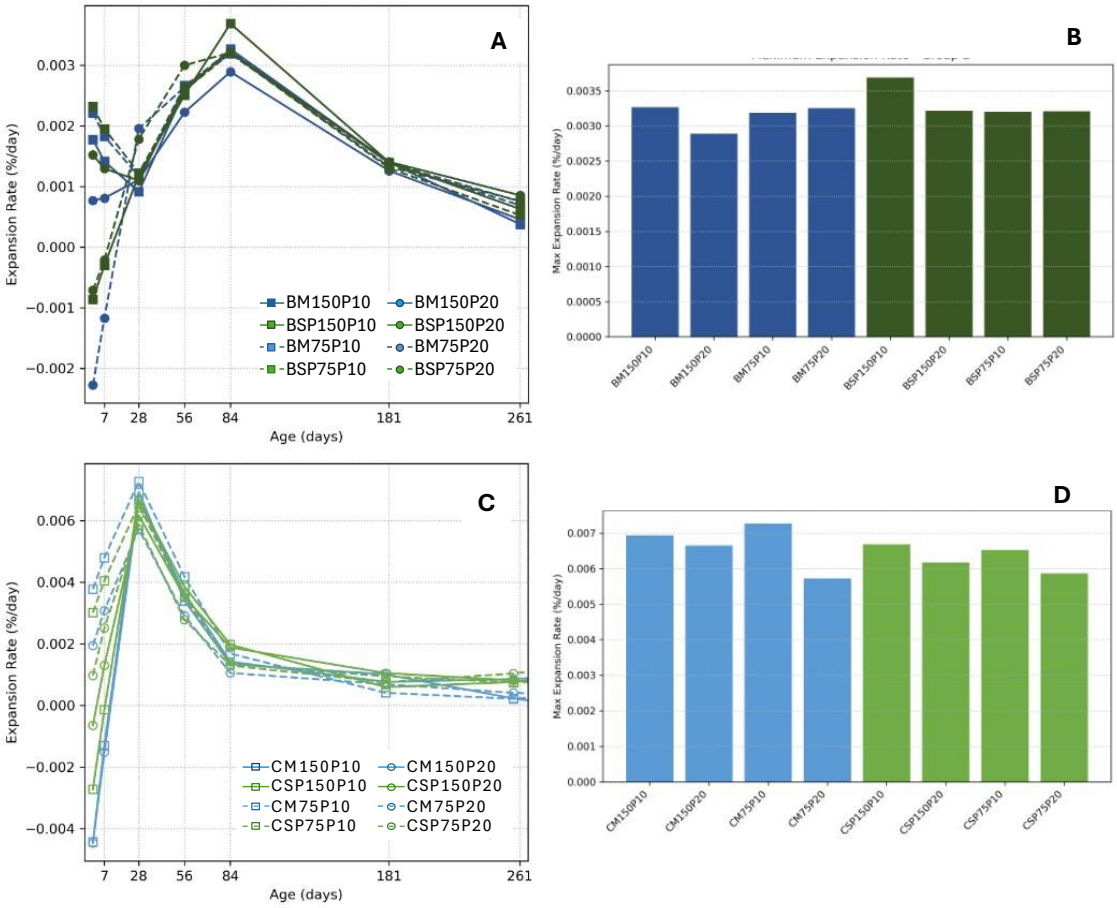

Source: Author (2025).

Mixtures B exhibited a varied behaviour in the first 28 days, some with decreasing and others with increasing expansion rate. They tended to converge to a similar rate at 28 days, after which the expansion rate increases, reaching maximum values at 84 days, ranging from 0.029 to 0.037%/day, followed by a decrease until 180 days and subsequent change in expansion rate.

Mixtures C exhibited a very similar behaviour when it comes to expansion rate. The maximum expansion rate was reached at 28 days and also did not vary considerably, ranging from 0.057 to 0.073%/day.

By comparing Mixtures B and C, mixtures C exhibited a considerably faster expansion rate, with maximum expansion rates approximately twice as higher than those of mixture B. Moreover, the maximum expansion rate was reached after approximately 1 and 3 months for mixtures C and B, evidencing the faster kinetics for mixtures C.

In the following sections, the influence of each parameter analyzed considering the two types of mixture will be discussed in detail.

5.6.1.1 Effect of the type of filler on the kinetics and maximum ASR-induced expansions

Figure 5.13 shows the maximum expansions obtained for mixtures B and C by comparing combinations with different AMFs while maintaining the other parameters.

Figure 5.13 – Maximum expansions obtained considering the type of filler as the focus variable. (a) Mixtures B. (b) Mixtures C.

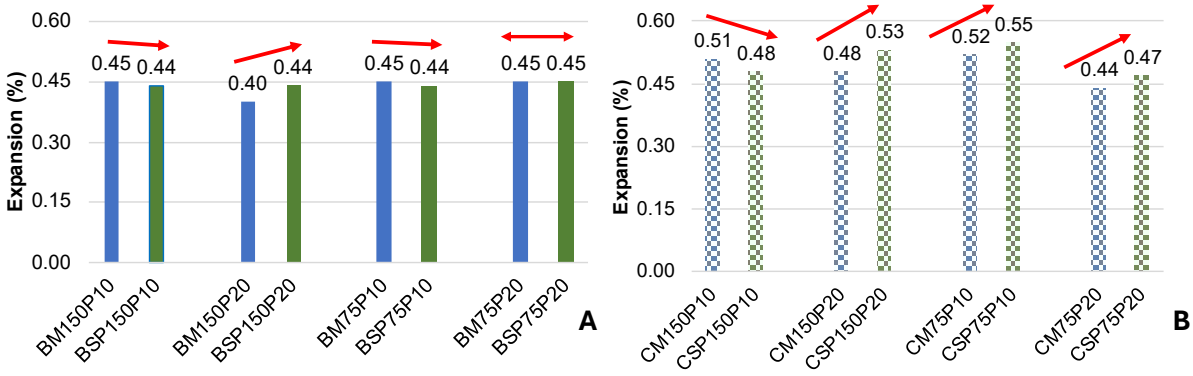

Source: Author (2025).

For mixtures B, when analyzing combinations with all the variables fixed while varying the type of filler, different behaviours were observed. In general, combinations with different fillers exhibited similar expansion. The exception was the combination with Springhill filler, PSD < 150 µm, and 20% replacement, which exhibited a slightly higher expansion (i.e., 0.44%) compared to the combination with the same parameters but mylonite filler (i.e., 0.40%).

For mixtures C, the behaviour of the curves was also similar. However, mixtures with Springhill filler displayed higher maximum expansions when compared to their counterparts with mylonite filler. The exception was the mixture with mylonite filler, PSD < 150 µm, and 10% replacement, whose expansion (i.e., 0.51%) was slightly higher than the combination with the same parameters but Springhill filler (i.e., 0.48%). In this case, the reactivity degree was directly proportional to the maximum expansions obtained.

The results obtained indicate that the type of filler did not have a considerable influence on the system with reactive coarse aggregates, and only a slight effect in the system with reactive fine aggregates.

5.6.1.2 Effect of the filler PSD on the kinetics and maximum ASR-induced expansions

Figure 5.14 shows the maximum expansions obtained for mixtures B and C by comparing combinations with different PSDs of filler (<150 µm and <75 µm) while maintaining the other parameters fixed.

Figure 5.14 – Maximum expansions obtained considering the PSD as the focus variable. (a) Mixtures B. (b) Mixtures C.

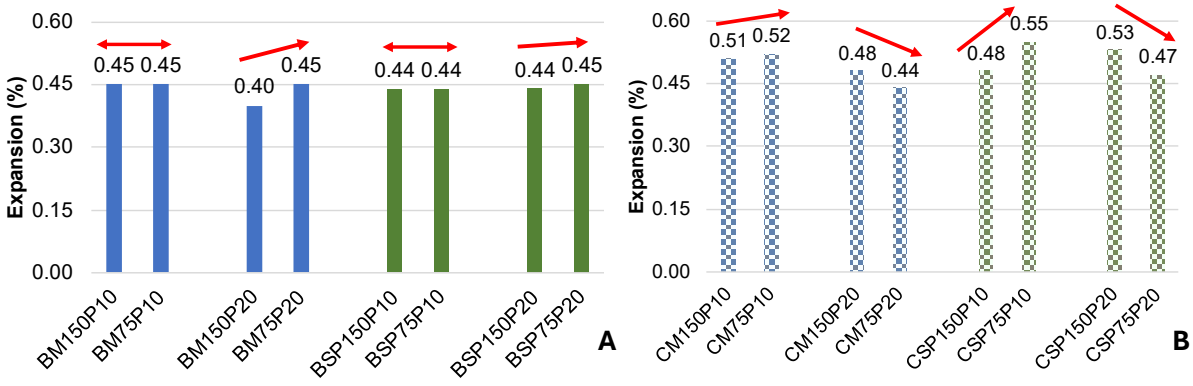

Source: Author (2025).

When analyzing separately the combinations with different PSD, we observed distinct behaviours. For mixtures B and a replacement percentage of 10%, the expansions were the same regardless of the filler used. However, for a replacement percentage of 20%, mixtures with PSD <75 µm resulted in slightly higher expansions. This indicates that the fineness of the AMFs plays a role in intensifying the reaction, but this behaviour is dependent on the percentage of AMFs used. This is contrary to theories on the action of reactive AMFs in the literature, in which finer particles would react fast and the reaction product would dissipate in the cementitious matrix (DYER, 2014). This particular behaviour can be related to the pessimum effect, which is the intensification of the reaction in a certain size range, whereas above and below this content expansions reduce (QIU *et al.,* 2022).

Mixtures C with AMFs with particle size <150 µm exhibited a slight shrinkage at early ages, whereas this was not observed for mixtures with AMFs with particle size <75 µm. Moreover, the influence of the PSD varied depending on the percentage. For combinations with 10% of filler, the expansions increased with the reduction in the PSD, regardless of the type of filler. However, when more filler was added to the system (20%), the reduction in the PSD led to lower expansions. This was the opposite

of what happened for mixtures B, in which more filler resulted in higher expansions. The results also indicate that the effect of PSD is influenced by the percentage used.

5.6.1.3 Effect of the replacement percentage of filler on the kinetics and maximum ASR-induced expansions

Figure 5.15 shows the maximum expansions obtained for mixtures B and C by comparing combinations with different percentages of AMFs replacing cement (10% and 20%) while maintaining the other parameters fixed.

Figure 5.15 – Maximum expansions obtained considering the percentage as the focus variable. (a) Mixtures B. (b) Mixtures C.

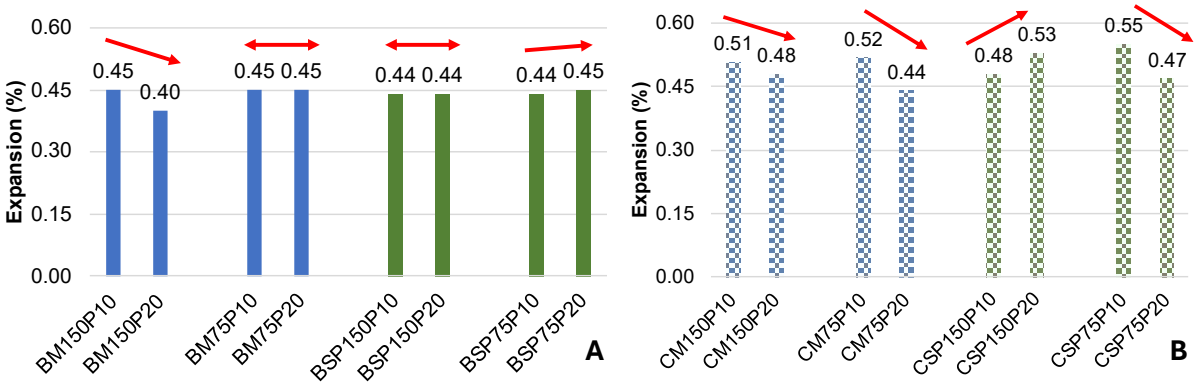

Source: Author (2025).

For mixtures B, the combination with mylonite and PSD <150 µm exhibited a lower expansion for 20% replacement compared to its counterpart with 10%. In contrast, all the other combinations exhibited similar expansions

For mixtures C, the relationship between PSD and percentage is again emphasized. Combinations with PSD <75 µm exhibited lower expansions for higher filler percentages. The results for combinations with PSD <150 µm may have been influenced by the type of AMFs: the combination with mylonite filler exhibited a higher expansion for a 10% percentage (i.e., 0.51%) compared to that with 20% percentage (i.e., 0.48%). The opposite occurred for the combination with Springhill filler, with 0.48% of expansion for 10% and 0.53% for 20%.

5.6.2 Understanding ASR-induced damage development

5.6.2.1 Microscopic assessment

The petrographic deterioration features were analyzed in absolute counts and in percentage of main damage features to evaluate the progress of the ASR-induced

damage, as shown in Figure 5.16. The features were arranged in three groups: Group I, consisting of closed cracks in the aggregate (CCA), Group II, consisting of open cracks in the aggregate, with and without reaction product (OCA and OCA-RP, respectively), and Group III, consisting of cracks in the cement paste, with or without reaction product (CCP and CCP-RP, respectively).

Figure 5.16 – Microscopic deterioration features normalized by 100 cm^2 for mixtures B. (a) Counts. (b) Percentage.

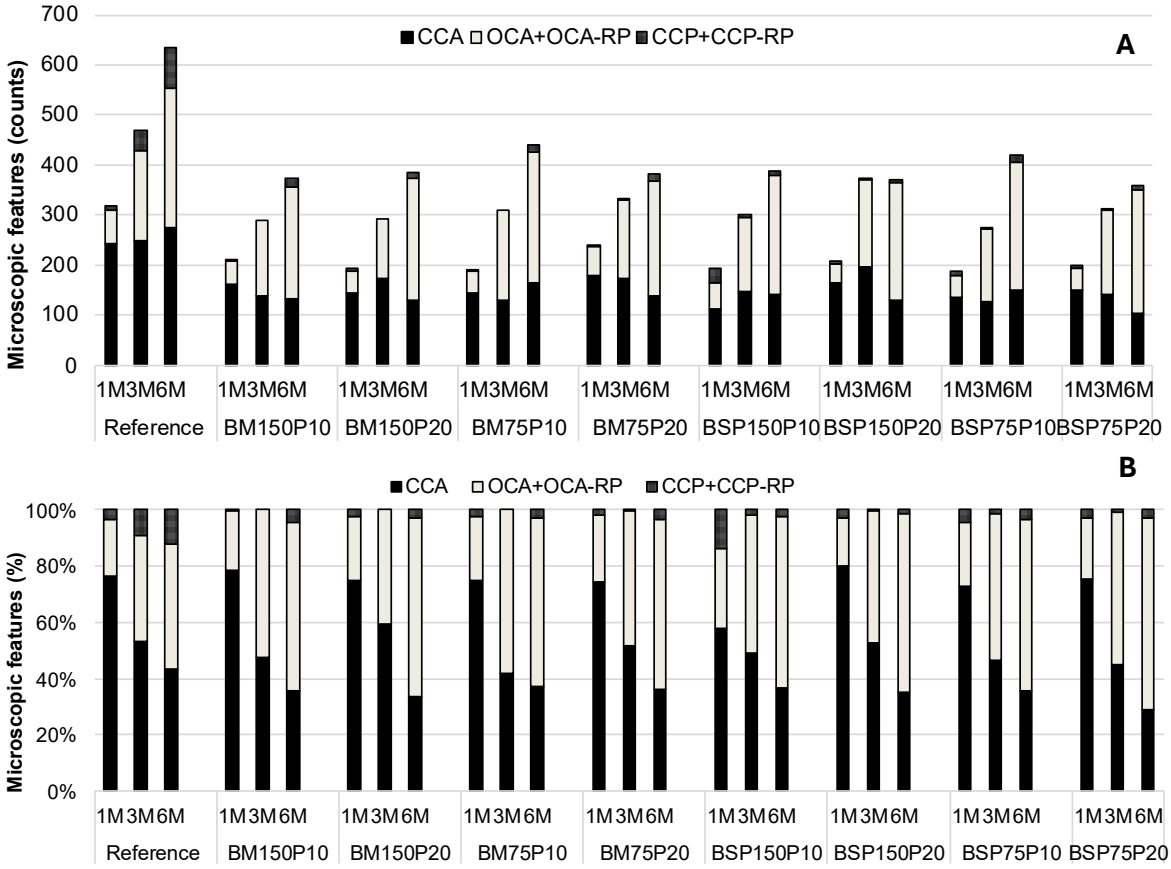

Source: Author (2025).

From Figure 5.16(a), the number of cracks increases with time, but it is lower than that for the reference sample for all combinations and ages analyzed. As observed, the number of CCAs was not considerably altered over time but the percentage contribution reduced because the number of open cracks increased. Moreover, the lower number of cracks in the paste (Group III) compared to the reference is evident. When comparing the combinations, the tendency is similar. Combination BSP150P10 has more group III cracks for the age of 1 month compared to other combinations, which may be attributed to shrinkage. For the ages of 3 and 6 months, the number of

group III cracks is considerably reduced, which may indicate that the filler action was concentrated in early ages.

Considering Figures 5.7 and 5.16, by comparing combinations with different AMFs while the other parameters were kept the same, no considerable difference was found. The exception was for combinations BM150P20 and BSP150P20 with DRI at the age of 6 months of 553 and 499, respectively. For the PSD, mixtures with a finer filler (PSD < 75 μm) exhibited higher DRI values, with exception of combinations BM150P20 and BM75P20, with a slight difference in DRI values at 6 months (553 and 530, respectively). When considering the percentage of AMFs replacing cement, mixtures with 10% filler resulted in higher DRI values, which was also observed for the expansions. The exception was for combinations BM150P10 and BM150P20, with a slight difference at 6 months (526 and 553, respectively).

As previously indicated, the DRI numbers ranged from 499 to 600 for mixtures B at 6 months, which indicates a high damage (SANCHEZ *et al*., 2017). At this level, the cracks in the aggregates are expected to reach the cement paste, forming a dense networking of cracking (SANCHEZ *et al*., 2017). However, this was not the case for the combinations analyzed, as the number of cracks in the paste did not considerably increase. This may evidence the effect of the AMFs by slowing this process.

Figure 5.17 shows the DRI number development for mixtures C with reactive fine aggregates for the ages of 1, 3, and 6 months and for all combinations analyzed.

As observed, there was a considerably lower number of cracks when compared to the reference values obtained in previous studies using the same aggregates and with a similar expansion level. In general, the contribution of group I cracks decreased with time while that of group II remained similar. The number of group III cracks was similar for the reference sample and for combinations with AMFs at the ages of 3 and 6 months. However, at 1 month, few group III cracks were observed in combinations with AMFs. The percentual contribution of group III cracks considerably increased for all the combinations compared to the reference samples for the ages of 3 and 6 months given the lower number of cracks from groups I and II, whereas it decreased for the age of 1 month (exception: sample CM75P10 at 1 month).

When focusing on the influence of the type of AMFs in Figures 5.8 and 5.17, all combinations with mylonite filler exhibited higher DRI values compared to their counterparts with Springhill filler. This is opposed to the expansion results, in which

combinations with Springhill provided higher expansion (exception: CM150P10 and CSP150P10).

Figure 5.17 – Microscopic deterioration features normalized by 100 cm^2 for mixtures C. (a) Counts. (b) Percentage.

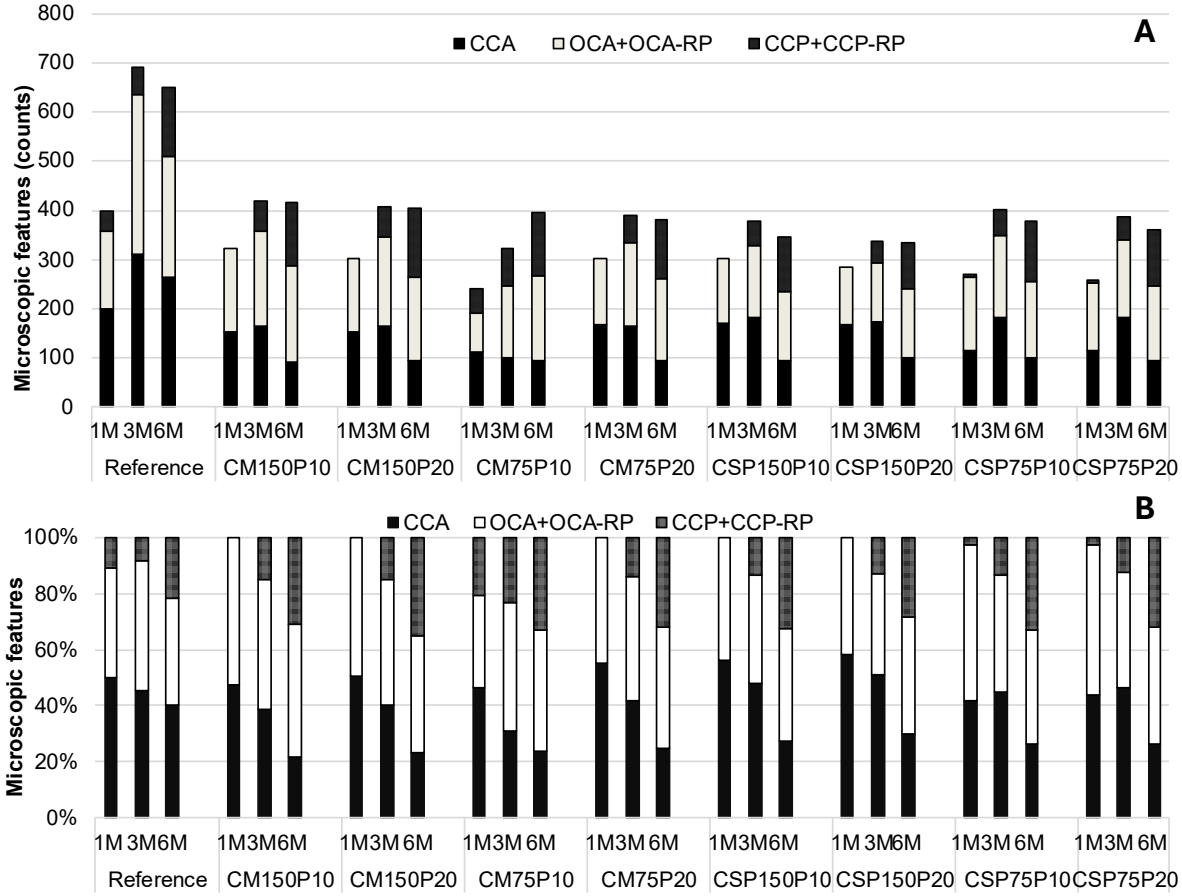

Source: Author (2025).

Considering the PSD, higher DRI values were obtained for mixtures with PSD <150 µm when using mylonite filler. In contrast, the opposite was obtained for combinations with Springhill filler, with higher expansions for a PSD <75 µm. The action of the PSD on expansion and kinetics was influenced by the percentage of AMFs used, and the DRI values indicate that damage progress is influenced by the type of filler. Thus, the parameters analyzed had different effects depending on the characteristic assessed (i.e., expansion or DRI).

Regarding the replacement percentage, a higher percentage resulted in lower DRI values for all combinations analyzed. Considering the expansion, the tendencies observed varied depending on the PSD, which highlights the different effect of parameters depending on the characteristic analyzed.

At 6 months, the DRI numbers ranged from 588 to 801, which indicates a very high damage (SANCHEZ *et al*., 2017). At this level, extensive cracking is expected to be found in the cement paste, connecting the reactive aggregate particles (SANCHEZ *et al*., 2017). Despite observing an increase in the number of CCPs with time, the cracks observed were mainly very thin, as observed in Figure 5.18.

Figure 5.18 – CCP in sample with reactive fine aggregates and ASR-reactive AMFs.

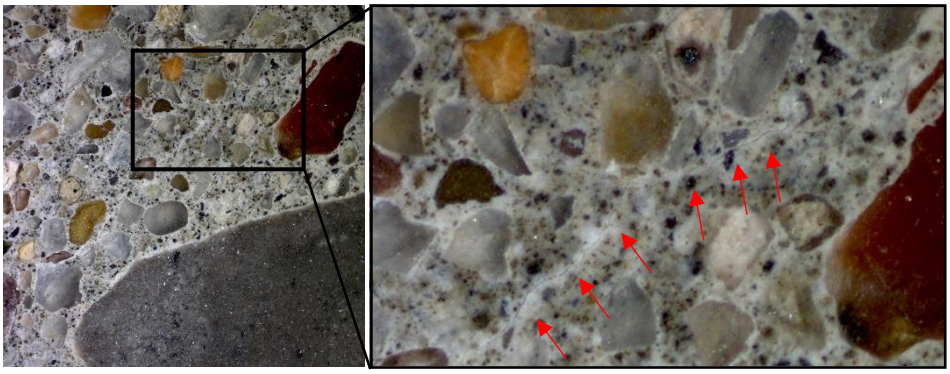

Source: Author (2025).

Figure 5.19 shows the relationship and correlation between DRI number and expansion obtained for mixtures B and C, respectively.

Figure 5.19 – DRI number vs expansion levels for mixtures with reactive (a) coarse and (b) fine aggregates. Correlation between DRI number and expansion for (c) mixtures C and (d) mixtures D.

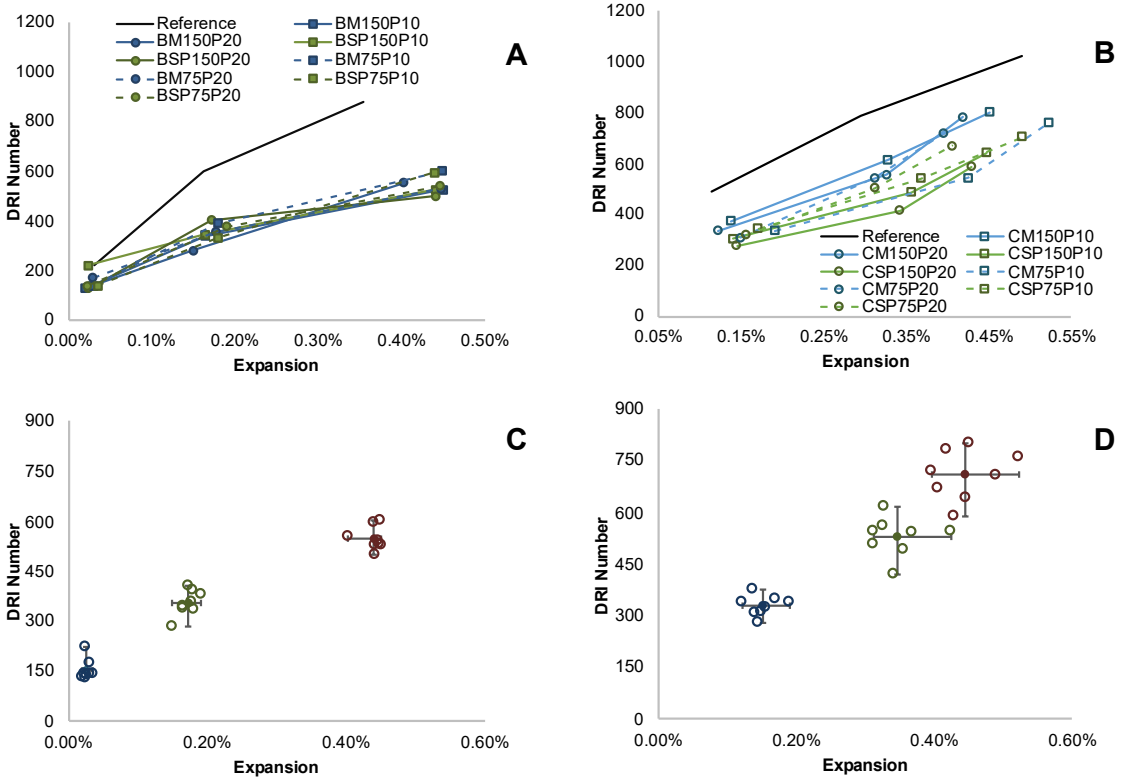

Source: Author (2025)

As observed, all DRI numbers tended to increase linearly with the increase in expansion. For both mixtures B and C, combinations with AMFs tended to provide lower DRI values compared to the reference. This is related to the lower number of cracks in the samples with AMFs, as observed in Figure 5.17(a).

Moreover, for both mixtures, a linear relationship between DRI number and expansion was observed. For mixtures B, the results were more concentrated, whereas for mixtures C the results were more dispersed, as observed in Figures 5.19 (c) and (d), evidencing that the parameters analyzed were more influential in the system with fine reactive aggregates.

5.6.2.2 Mechanical assessment

Figure 5.20(a) and (b) show the SDI values against the expansion values for mixtures B and C, respectively. Reference values were obtained from Souza (2022).

Figure 5.20 – SDI *vs* expansion levels for mixtures with reactive (a) coarse and (b) fine aggregates. Correlation between SDI and expansion for (c) mixtures B and (d) C.

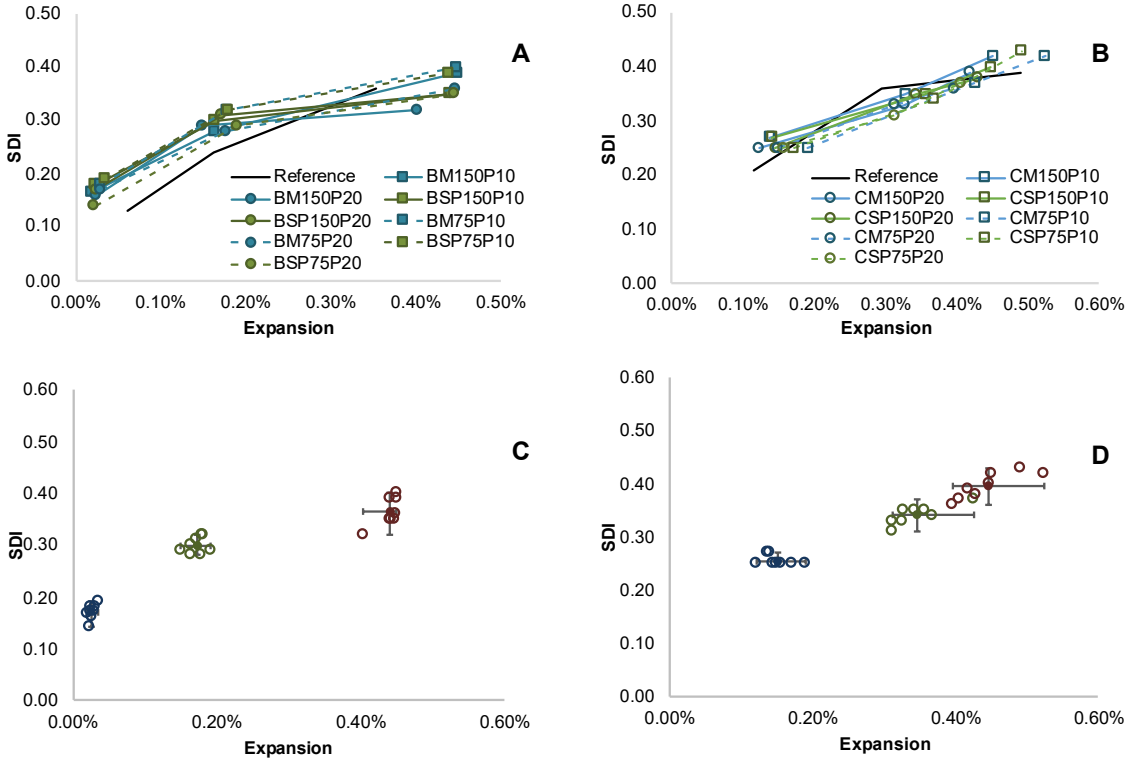

Source: Author (2025)

As observed, a concave tendency was obtained for mixtures B, whereas a rather linear tendency was obtained for mixtures C. For mixtures B, the SDI values ranged from 0.14 (0.02% expansion) to 0.40 (0.39% expansion), whereas they ranged from 0.25

(0.12–0.19% expansion) to 0.43 (0.49% expansion) for mixtures C. Moreover, compared to reference samples with no AMFs and similar expansion, the SDI values with AMFs were higher or similar, which was also observed in a previous study (ANTUNES, 2021) and may be related to the lower amount of cement and, consequently, less hydration products.

Similarly to the DRI results, the SDI results in Figure 5.20(c) and (d) were also more concentrated for mixtures B and more dispersed for mixtures C, indicating more influence of the AMFs in the combinations analyzed when using fine reactive aggregates. Figure 5.21 shows the modulus of elasticity reduction for mixtures B and C. Reference values were obtained from Souza (2022).

Figure 5.21 – Modulus of elasticity reduction for (a) mixtures B and (b) mixtures C.

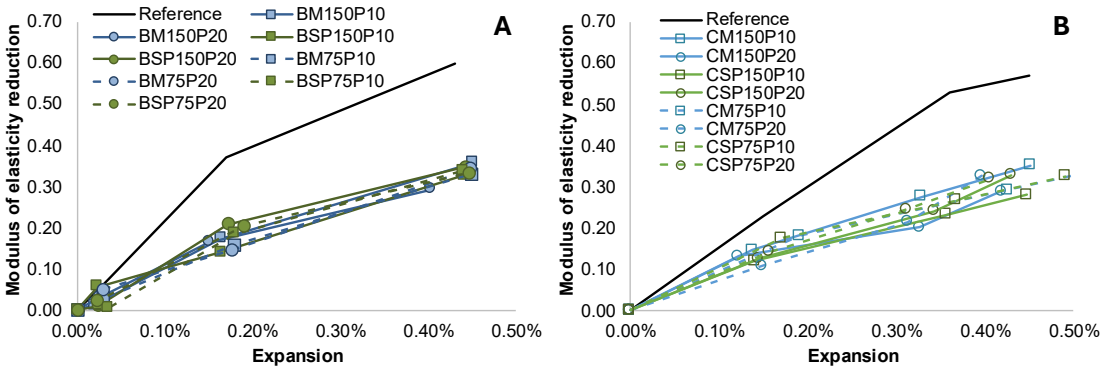

Source: Author (2025).

As observed, the behaviour of the curves was rather linear for both types of mixture. For mixtures B, the reduction ranged from 0.9% to 5.6% at 1 month and from 29.3% to 35.7% at 6 months. These ranges were from 10.7% to 18.1% and from 28.1% to 35.3% for mixtures C, respectively. The modulus of elasticity reduction was similar for both mixtures at 6 months, even considering that mixtures C had higher expansion. This is because of the influential role of the coarse aggregates on the mechanical properties of concrete. The reference samples had a pronounced modulus of elasticity reduction when compared to the mixtures with ASR-reactive fillers. This is in agreement with the DRI results obtained. This indicates that, comparatively, for a given age, the percentual reduction of the modulus of elasticity was lower than that without AMFs, which means that less cracks were formed over time.

5.6.2.3 Multilevel assessment

The multilevel assessment was applied to understand the progression of ASR in combinations containing AAR-reactive AMFs and consists of a coupled evaluation of microscopic features (i.e., DRI) and mechanical properties (i.e., SDT). Along with the expansion results, this thorough evaluation may provide indications of the action of ASR-reactive AMFs in reactive systems.

Mixtures B, containing reactive coarse aggregates, exhibited similar behaviour and expansions for all combinations analyzed. At 1 month, cracks were observed in the aggregates, both open and closed, and few in the cement paste. Compared to a sample with similar expansion and no ASR-reactive AMFs, the number of cracks was reduced for all combinations with AMFs. In particular, OCA-RP, identified in the reference sample, were not observed in combinations with AMFs, which may indicate that the intensity or rate of the reaction was reduced in the aggregates with the use of AMFs. The SDI values varied from 0.14 to 0.19, whereas the modulus of elasticity reduction varied from 0.4% to 5.6%, indicating negligible to marginal damage. These results are in agreement with the expansions observed up until 60 days, which were in the lower part or even below the envelope of expansions for combinations with the same aggregate with no AMFs.

Considering these results, in the first 30 days (i.e., 1 month) there is a competition for alkalis, as both the coarse aggregates and the AMFs are consuming alkalis. The filler particles are uniformly spread in the cementitious matrix around the aggregates and have a higher SSA compared to that of the aggregate particles. Therefore, the filler particles consume preferentially the alkalis in the surrounding of the aggregate particles, resulting in less alkalis available for the coarse aggregates, which leads to less cracks in the aggregates, resulting in less damage and lower expansions. This retardion in alkali migration to aggregates was also indicated by Qinghan *et al.* (1996).

From 30 to 90 days (i.e., 1 to 3 months), the number of cracks in the aggregates considerably increases, particularly open cracks, indicating the reaction is proceeding in the aggregates. However, the number of cracks in the paste is considerably reduced compared to the reference sample, which impacts in the DRI number that is also lower for all combinations with AMFs compared to that of the reference sample. At approximately 90 days (i.e., 3 months), the maximum expansion rate is reached. At 180 days (i.e., 6 months), the expansions ranged from 0.40% to 0.45%, the DRI values

from 499 to 600, the SDI values from 0.32 to 0.40, and the modulus of elasticity loss from 29.3% to 35.7%, which indicates a high damage (SANCHEZ *et al*., 2017). Therefore, despite the lower number of cracks compared to the reference sample, the damage was compatible with the expansions obtained. The lower number of cracks in the paste may be because the propagation of cracks from the coarse aggregates to the cement paste was delayed given the lower availability of alkalis to continue the reaction in the aggregates, as a part was being consumed by the AMFs.

The discrepancy in the count of cracks and the mechanical performance observed (i.e., SDI values) may be related to the formation of cracks in the paste by the AMFs that were thin and too short to be counted in the DRI (only cracks longer than 1 mm are counted). Thus, despite not being counted in the DRI, their impact in the mechanical performance could be measured by the SDI. Moreover, given the lower number of cracks in the aggregate, the impact in the modulus of elasticity was reduced, leading to the lower modulus of elasticity loss.

Based on the findings, the hypothesis that the small particles react fast being completely converted into reactive product that dilutes into the paste and does not contribute to expansions (DYER, 2014; QINGHAN *et al.,* 1996; STANTON, 1940; SUWITO *et al.*, 2002) does not hold. This result can also indicate that the particle sizes used (i.e., < 150 μm and <75 μm) were not sufficiently small to provide this effect. Therefore, for the particle sizes used and for the AMFs adopted (mylonite and Springhill), the factor that governed the effect of the AMFs was the distribution of alkalis, as indicated in previous studies (QINGHAN *et al.,* 1996).

The percentage was also observed to have no considerable effect on crack propagation and mechanical performance, as similar results for DRI, SDI, and modulus of elasticity loss were obtained when using 10% or 20% of filler. This may be explained by a threshold related to the number of reactive particles, which is influenced by the particle size, above which no additional cracks are generated. This hypothesis is supported by the similar number of cracks in Figure 16(a), regardless of the percentage adopted. The SDI values and modulus of elasticity loss were similar to those of mixtures C, in which the expansion and deterioration degree were higher. This is because of the considerable contribution of the coarse aggregates to the mechanical properties of concrete.

For mixtures C, containing fine reactive aggregates, in the first 30 days (i.e., 1 month), few cracks in the paste were observed in the DRI and even less compared to combinations with no AMFs. The maximum expansion rate was also reached at approximately 30 days (i.e., 1 month). The DRI values ranged from 279 to 376, the SDI values ranged from 0.25 to 0.27, and the modulus elasticity reduction ranged from 10.7% to 18.1%, consistent with a marginal to moderate damage (SANCHEZ *et al*., 2017). This is also consistent with the fast kinetics observed, characteristic of reactive fine aggregates and also obtained in previous studies (ANTUNES, 2021; BEZERRA, 2021; DE GRAZIA, 2023; REZAIEH, 2021; SOUZA, 2022; ZUBAIDA, 2020). In the combinations with ASR-reactive AMFs, the reaction progressed even faster, indicating the influence of the AMFs in accelerating ASR. According to Vivian (1951), with the increase in the number of reactive particles, they become more uniformly distributed, leading to uniform crack width. Thus, the cracks at the age of 1 month were probably uniformly distributed and shorter than 1 mm to be counted in the DRI. In contrast, more OCA-RP were identified in samples with AMFs compared to samples with no AMFs. This may indicate that, despite the preferential reaction with the fillers, given the higher SSA of fine aggregate particles compared to that of coarse aggregate particles as in Mixtures B, more alkalis reach the aggregate particles and react intensely, forming reaction product. Moreover, the consumption of alkalis by the AMFs may have delayed the lengthening of cracks by the sand. This is supported by the increase in expansions until approximately 60 days, after which the expansion rate considerably reduces.

In addition, the number of cracks in the paste at 3 and 6 months was similar to that observed for combinations with no AMFs. At 6 months, the expansions ranged from 0.44% to 0.55%, the DRI values from 588 to 801, the SDI values from 0.36 to 0.43, and the modulus of elasticity loss from 28.1% to 35.3%, which indicates a high to very high damage (SANCHEZ *et al*., 2017). However, considering control samples with no AMFs, the DRI values for the combinations with AMFs were considerably reduced, mainly owing to a reduction in the cracks in the aggregates. This may be caused by the consumption of alkalis by the AMFs, resulting in less alkalis available to react with the fine aggregates, and, consequently, in less cracks. Considering that the maximum expansion rate is reached at approximately 30 days, the action of AMFs is reduced after this point. Therefore, the cracks in the cement paste at 3 and 6 months are probably originated in the aggregate and extending to the paste. Similar results were

also obtained for mixtures with AAR-reactive AMFs when applying the accelerated CPT, in which the expansion and DRI values were lower but the SDI value was slightly higher (ANTUNES, 2021). The lower number of cracks in the aggregate over time is also consistent with the lower reduction in modulus of elasticity, as open cracks in the aggregate considerably affect this property in ASR-affected concrete.

In summary, there was an acceleration of the reaction at early ages caused by the AMFs. The competition for alkalis from the AMFs and aggregates led to less observable cracks and lower DRI number. After this initial period, the reaction decelerates owing to the previous intense consumption of alkalis, leading to reduction in expansion rate, increase in the number of cracks in the paste, but less cracks in the aggregates. The mechanical properties were affected by the development of the reaction and also by the lower amount of cement and, consequently, less hydration products. Therefore, in systems with highly reactive fine aggregates, by inserting another source of reactivity such as AAR-reactive AMFs, there is a competition for the consumption of alkalis that leads to reduced damage and tendency to stabilization of expansion at early ages. Considering the high reactivity of the aggregates used, the damage observed was still very high. Further studies with other reactive fine aggregates would be beneficial to understand the competition mechanism for different reactivity degrees of the aggregates.

When comparing the reactive systems analyzed, the main difference observed was the kinetics. Considering that the alkalis acted as a limiting agent in both systems, the difference in kinetics is related to the type of reactive aggregates used, whether coarse or fine, particularly the corresponding SSA. For mixtures with a reactive coarse aggregate and lower SSA, the consumption of alkalis was delayed because the reactive AMFs were also consuming alkalis in the paste, reducing the availability in the surroundings of the aggregate particles. For mixtures with fine reactive aggregates, given the high SSA of aggregate particles compared to that of coarse aggregate particles, the reaction was accelerated, which is also evidenced by the amount of OCA-RP higher than that of samples with no AMFs. After 30 days, with the consumption of alkalis, the expansion rate reduces. The number of cracks in the aggregate at 3 and 6 months remains similar, with an increase in open cracks. The number of cracks in the cement paste increases to a number close to that in samples with no AMFs, which is probably related to cracks in the aggregate extending to the cement paste.

Moreover, for the expansion measurements, the test adopted was the CPT. There is no current indication in standards on the test to adopt when evaluating AAR-reactive AMFs. Based on the results obtained, the CPT was able to capture the expansions and slight differences among the combinations analyzed, and the expansion levels were in agreement with both the deterioration features from the DRI and loss of mechanical properties expected. Therefore, this test can be used to test combinations with AAR-reactive AMFs.

An important aspect that was not evaluated but may have an impact on the results is the contribution of alkalis by the aggregates (LEEMANN; HOLZER, 2005) and, in particular, by the ASR-reactive AMFs used, as the alkali release in influenced by the size of particles (SOARES *et al.*, 2016). The understanding of the contribution of the aggregates and ASR-reactive AMFs to the alkali content available is fundamental to complement the analysis of the filler-induced alkali competition.

Table 5.4 summarizes the findings obtained for mixtures B and C.

Table 5.4 – Summary of results obtained.

	Mixtures B (Reactive coarse aggregate)	**Mixtures C (Reactive fine aggregate)**
Expansion	↔	↓
DRI	↓	↓
SDI	↔	↔
Modulus of elasticity loss	↓	↓
Influential parameters	No	% PSD *vs* %

Note: ↔: Similar values; ↓: Lower values considering as references mixtures without ASR-reactive AMFs.

Source: Author (2025).

5.6.2.4 Statistical analysis

Considering the results obtained and the tendencies observed, it is important to assess whether the differences are statistically significant. A statistical analysis was conducted by means of multi-factorial ANOVA with a significance level of 5%, and the corresponding results are listed in Table 5.5.

Based on the results, no parameter had a significant impact on the expansion results for mixtures B. This confirms the lack of a consistent tendency as indicated in previous discussions. In contrast, for mixtures C, the percentage and the interaction percentage

vs PSD were significant. This indicates that, for mixtures with reactive fine aggregates, which have more contact with the paste, the percentage of fillers influenced the expansion results. Moreover, although the PSD of particles individually did not have a significant effect on expansions, when coupled with the percentage, the influence was significant, indicating that the variation of this parameter may have different effects for different percentages.

Table 5.5 – ANOVA considering expansion results for mixtures B and C.

Mixtures B							
Parameter	**SQ**	**DF**	**MQ**	**F**	**F 0.05**	**p-value**	**Signif.***
Type of fillers	$2.76\ 10^{-8}$	1	$2.76\ 10^{-8}$	0.108	4.013	0.744	NS
PSD	$1.31\ 10^{-7}$	1	$1.31\ 10^{-7}$	0.509	4.013	0.479	NS
Percentage	$9.58\ 10^{-8}$	1	$9.58\ 10^{-8}$	0.373	4.013	0.544	NS
Fillers *vs* Percentage	$2.57\ 10^{-7}$	1	$2.57\ 10^{-7}$	1.003	4.013	0.321	NS
Fillers *vs* PSD	$4.89\ 10^{-7}$	1	$4.89\ 10^{-7}$	1.906	4.013	0.173	NS
Percentage *vs* PSD	$5.87\ 10^{-7}$	1	$5.87\ 10^{-7}$	2.286	4.013	0.136	NS
Fillers *vs* PSD *vs* Percentage	$6.10\ 10^{-8}$	1	$6.10\ 10^{-8}$	0.238	4.013	0.628	NS
Residue	$1.44\ 10^{-5}$	56	$2.57\ 10^{-7}$				
Total	$1.60\ 10^{-5}$	63					
Mixtures C							
Parameter	**SQ**	**DF**	**MQ**	**F**	**F 0.05**	**p-value**	**Signif.**
Type of fillers	$6.21\ 10^{-7}$	1	$6.21\ 10^{-7}$	2.143	4.013	0.145	NS
PSD	$6.25\ 10^{-8}$	1	$6.25\ 10^{-8}$	0.216	4.013	0.644	NS
Percentage	$2.29\ 10^{-6}$	1	$2.29\ 10^{-6}$	7.900	4.013	0.0068	S
Fillers *vs* Percentage	$5.39\ 10^{-7}$	1	$5.39\ 10^{-7}$	1.861	4.013	0.178	NS
Fillers *vs* PSD	$1.56\ 10^{-7}$	1	$1.56\ 10^{-7}$	0.539	4.013	0.466	NS
Percentage *vs* PSD	$3.28\ 10^{-6}$	1	$3.28\ 10^{-6}$	11.327	4.013	0.0014	S
Fillers *vs* PSD *vs* Percentage	$8.67\ 10^{-7}$	1	$8.67\ 10^{-7}$	2.992	4.013	0.089	NS
Residue	$1.62\ 10^{-5}$	56	$2.90\ 10^{-7}$				
Total	$2.40\ 10^{-5}$	63					

*S: Significant; NS: Not significant.

Source: Author (2025).

5.6.2.5 Possible mechanism of ASR-reactive AMFs in reactive systems

Based on the discussed, models were created to illustrate the possible action of ASR-reactive AMFs in the reactive systems analyzed. In this study, the PSDs adopted (<150 µm and <75 µm) did not significantly influence the expansion results. However, smaller particles can have a different effect on reactive systems not explained by the scheme presented. The percentage had a significant influence on the reactive system with fine aggregates, as well as the coupled effect of PSD and percentage. Figure 5.22 shows

the mechanism proposed to illustrate the effect of ASR-reactive AMFs in a period of 180 days for mixtures with reactive coarse aggregates.

Figure 5.22 – Proposed mechanism for reactive systems with reactive coarse aggregates. (a) The filler particles are uniformly distributed in the matrix. (b) Preferential reaction of the AMFs with the alkalis. Less availability of alkalis to the coarse aggregates. (c) Thin and short cracks formed in the cementitious matrix. Closed cracks formed in the aggregate. Reduced expansion rate. (d) Cracks in the aggregate start opening and some cracks in the paste connect. Increased expansion rate. (e) Cracks in the aggregate continue opening and extend to the cement paste.

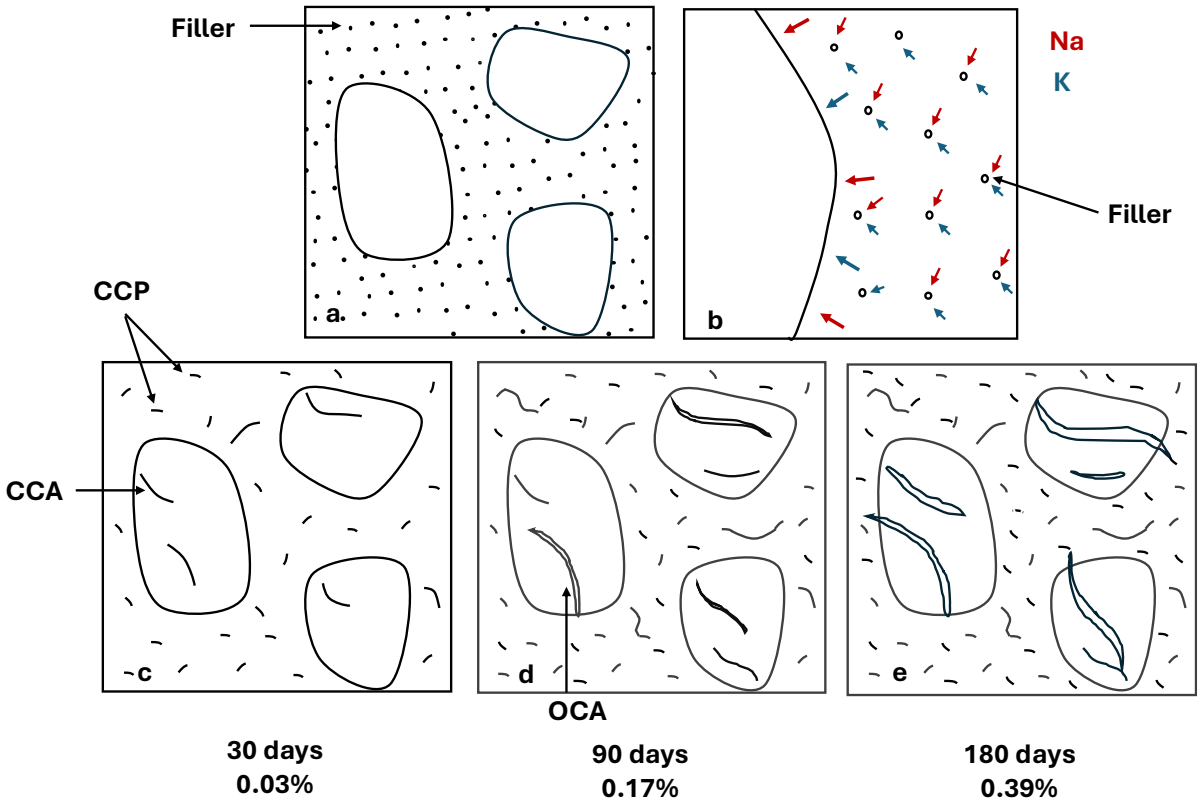

Source: Author (2025).

In a system with reactive coarse aggregates, the filler particles are uniformly distributed in the paste (Figure 5.22(a)). The alkalis start reacting with the AMFs and the coarse aggregates (Figure 5.22(b)). However, given the higher SSA of the AMFs, the reaction proceeds preferentially with the AMFs, and less alkalis diffuse to the coarse aggregates, as evidenced by the reduced number of open cracks and no OCA-RP compared to a system with no reactive fillers. This results in cracks in the cement paste that are thin and too short to be counted in the DRI (Figure 5.22(c)). In this initial period (1 month), the expansion rate is reduced. As the reaction proceeds, the expansions continue increasing slowly until 90 days (i.e., 3 months), when the maximum expansion rate is reached. From this point, the action of AMFs is considered to reduce, and more

alkalis reach the aggregate, leading to expansions and open cracks in the aggregate (Figure 5.22(d)). The reaction continues, with the increase in open cracks in the aggregates. The number of cracks in the cement paste also increases, which is probably related to cracks in the aggregate that extend to the cement paste (Figure 5.22(e)), as the action of AMFs at this point is reduced. The cracks formed by ASR-reactive AMFs are very thin and short and do not considerably impact the expansions, but they affect the mechanical properties of concrete, evidenced by the increase in SDI value and reduction in the modulus of elasticity.

Figure 5.23 shows the model proposed to illustrate the effect of ASR-reactive AMFs in a period of 180 days for mixtures with reactive fine aggregates.

Figure 5.23 – Model for reactive systems with reactive fine aggregate. (a) The filler particles are uniformly distributed in the matrix. (b) The alkalis react with both the fillers and the fine aggregate. (c) Thin and short cracks formed in the cementitious matrix because of the fillers. Open cracks with reaction product formed in the aggregate. Increased expansion rate. (d) Cracks in the aggregate continue opening and extend to the cement paste. Cracks in the cement paste lengthen. Reaction product observed in cracks in the paste. (e) Cracks in the aggregate continue opening and extending to the paste.

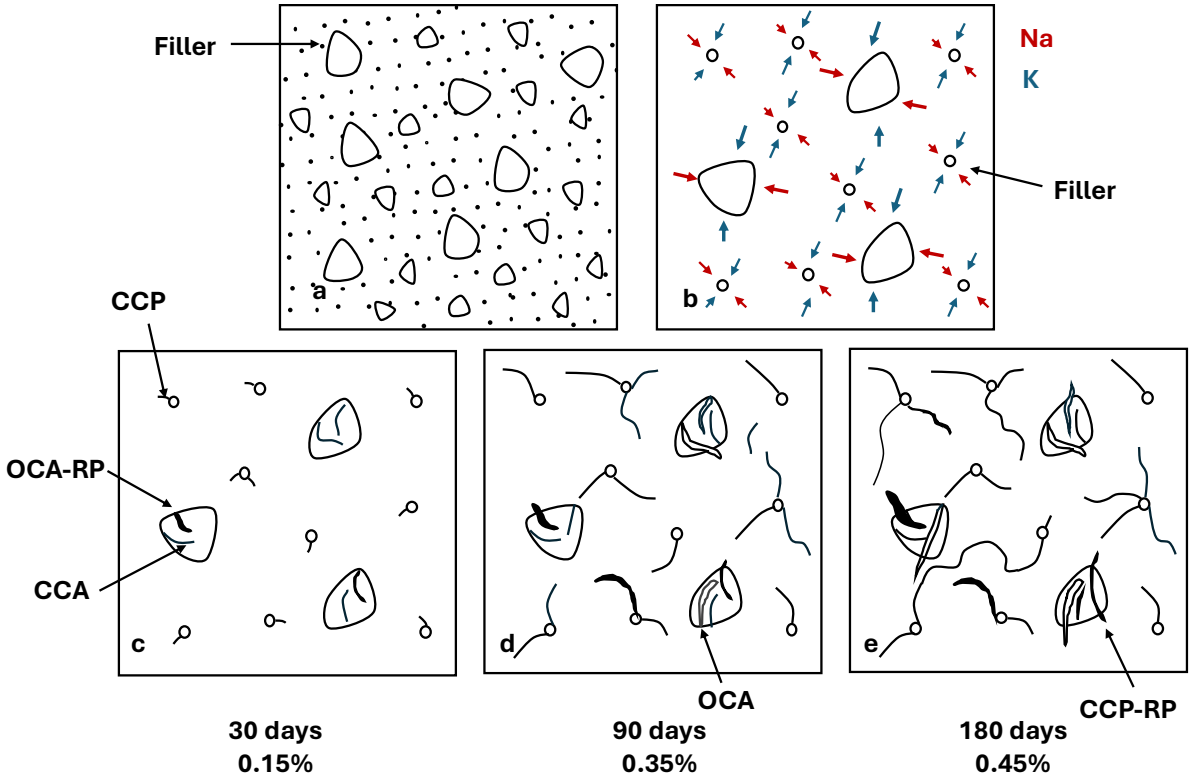

Source: Author (2025).

For mixtures with reactive fine aggregates, the kinetics were different compared to the system with reactive coarse aggregates. For coarse aggregates, the expansion rate

was reduced in the first 30 days, whereas for fine aggregates, the expansion rate increased. This is probably a result of the difference in SSA between the aggregates. With coarse aggregates, the reaction occurs preferentially with the fillers surrounding the aggregate and less alkalis react with the particle. For the fine aggregates, the SSA is larger and more alkalis react with the particles despite the filler particles around them (Figure 5.23(b)). Therefore, the reaction is intense in the aggregate particles, evidenced by the cracks with reaction product as opposed to samples with no reactive AMFs. Moreover, the cracks formed in the paste are probably thin and short and, thus, not counted in the DRI.

The maximum expansion rate occurs at approximately 30 days, after which the contribution of ASR-reactive AMFs is considered to reduce (Figure 5.23(c)). The reaction proceeds, with more cracks formed in the aggregate and some cracks extending to the cement paste at 90 days (i.e., 3 months, Figure 5.23(d)). At 180 days (i.e., 6 months), more cracks are observed in the cement paste, mostly as cracks in the aggregates extend to the paste, as the reactive AMF action is reduced (Figure 5.23(e)). Overall, the lower expansion and number of cracks resulting in lower DRI number for mixtures with fillers is a result of the delay in lengthening of cracks in aggregate particles in the first 30 days, because they preferentially react with the fillers, and the formation of short thin cracks uniformly distributed in the cementitious matrix. As the cracks are thin, they do not translate into expansions, but they influence the mechanical properties, as evidenced by the continuous increase in SDI values and reduction of modulus of elasticity. For this mixture, the percentage was an influential parameter. A lower percentage (10%) led to higher expansions, which is in agreement with the proposed, indicating that the higher the content of filler, the more the influence on the results as more fillers will lead to less alkalis available to the aggregate particles, delaying more the lengthening of cracks.

5.7 CONCLUSION

This study evaluated the impact of ASR-reactive AMFs on the expansion and deterioration progress of concrete containing either reactive coarse or fine aggregates. Two types of reactive AMFs (i.e., a highly reactive greywacke and a moderately reactive mylonite) were incorporated at two PSDs (i.e., <150 μm and <75 μm) and two replacement levels (i.e., 10% and 20%) in cementitious systems. The CPT was used

to monitor expansion, and the multilevel assessment (i.e., DRI and SDT) was applied to assess the deterioration progress.

The main conclusions drawn from this study are as follows:

- The use of ASR-reactive AMFs influenced expansion kinetics, particularly in the first 60 days, and damage development, particularly in systems containing reactive fine aggregates. In these systems, the presence of AMFs accelerated early expansion but led to earlier stabilization, likely due to rapid alkali consumption;
- In mixtures with reactive coarse aggregates, the reactive fillers delayed the onset of expansion. The alkalis appeared to react preferentially with the filler particles, reducing availability around the aggregate particles and thus slowing deterioration. Similar expansion values, microstructural and mechanical degradation were obtained for all combinations analyzed. Moreover, the parameters assessed (type of fillers, PSD, percentage) did not significantly influence the results;
- DRI values for both reactive systems were found to be lower than those for reactive systems with no fillers at equivalent expansion levels. However, the SDI values were consistent with the damage in systems with no fillers. This can be related to the cracks induced by the reaction between alkalis and fillers to be thin and short, often below the DRI detection threshold. These microcracks may have contributed to increased SDI values. However, given the lower number of cracks in the aggregate particles, the modulus of elasticity loss was reduced compared to a system without ASR-reactive AMFs;
- Percentage and the interaction between PSD and replacement percentage had a statistically significant effect on expansion in systems with reactive fine aggregates, confirming a synergistic role;
- The CPT, in conjunction with SDT and DRI, was effective in differentiating the deterioration mechanisms across mixtures and in capturing subtle interactions between filler characteristics and ASR development.

Overall, the study demonstrates that ASR-reactive AMFs may be viable for cement replacement in blended cements, provided that their replacement percentage and PSD are considered.

Despite the promising results obtained, the present study has some limitations. The explanations provided are based on microstructural and mechanical results. Microscopic and chemical tests should be conducted to confirm the findings. The alkali release by aggregates and ASR-reactive AMFs was not considered. Moreover, the conclusions are valid for the time range and parameters analyzed.

Further studies involving other reactive aggregates and extended monitoring are recommended to validate the long-term implications of these findings and to refine the mechanistic understanding of filler-induced alkali competition in reactive systems. The alkali release by the AAR-reactive fillers should also be assessed. Moreover, tests should be conducted with systems with no reactive aggregate to understand the isolated behaviour of the filler.

CHAPTER 6 – EFFECT OF ASR-REACTIVE FILLERS IN NON-REACTIVE SYSTEMS

Yane Coutinho [1, 2, *], Leandro Sanchez [2], and Arnaldo Carneiro [1]

[1] Federal University of Pernambuco, Recife, Brazil.
[2] Department of Civil Engineering, University of Ottawa, Ottawa, Canada.

Abstract: Aggregate mineral fillers (AMFs) are an alternative to replace cement and contribute to reducing associated CO_2 emissions. However, some of the rocks used to produce AMFs may be susceptible to alkali-aggregate reaction (AAR), and their impact in concrete durability remains unclear. This study investigates the influence of alkali-silica reaction (ASR)-reactive AMFs on concrete durability when used to replace cement in systems with non-reactive aggregates. Two reactive rocks were used to produce fillers, a moderately reactive mylonite and a highly reactive greywacke, with varying particle size distributions (PSD: <150 μm and <75 μm) and used at replacement rates of 10% and 20%. The concrete prism test (CPT) was adopted to monitor induced expansion and kinetics. To evaluate the deterioration process, the multilevel assessment was applied by means of microstructural (i.e., damage rating index – DRI) and mechanical (i.e., stiffness damage test – SDT) evaluations. Results indicate that filler reactivity, PSD, and percentage significantly affect expansion behaviour, with finer PSD materials (<75 μm) promoting higher expansions. Despite developing some expansion, the values remained in general below the limit set by standards. Moreover, negligible physical damage was observed, indicating the potential for ASR-reactive fillers to be utilized in sustainable cement alternatives when the parameters evaluated are adequately considered.

Keywords: Alkali-aggregate reaction, ASR-reactive AMFs, non-reactive system, multilevel assessment, concrete durability.

6.1 INTRODUCTION

Reducing CO_2 emissions from the construction sector has become a priority considering the Net Zero target, as the cement industry is a major contributor (IEA, 2021). Cement manufacturing is estimated to generate 0.6 tons of CO_2 per ton of cement produced (IEA, 2021). The demand of concrete is expected to increase from

14 to 20 billion m^3 per year by 2050, prompting strategies to reduce cement content to improve sustainability (GCCA, 2021; IEA, 2021). This can be achieved in the short term by the partial replacement of cement by alternative materials (i.e., supplementary cementitious material (SCM) or fillers) (AMRAN *et al*., 2022; ASTM, 2020; BALLAN; PAONE, 2014; DAMTOFT *et al*., 2008; GARTNER; HIRAO, 2015; IEA, 2020; LOTHENBACH; SCRIVENER; HOOTON, 2011; LUDWIG; ZHANG, 2015; MILLER *et al*., 2021; VON GREVE-DIERFELD *et al.*, 2020). In a context where the supply of current SCMs tends to decrease, aggregate mineral fillers (AMFs) offer a promising alternative.

The American Concrete Institute defines AMFs as a finely divided inorganic material produced as a byproduct of crushing operations of rocks (ACI, 2020). The use of AMFs normally enhances concrete properties by means of improved packing (KORPA; KOWALD; TRETTIN, 2008) and introduction of nucleation sites for the precipitation of clinker hydration products (AQEL; PANESAR, 2016; LI *et al*., 2018; LOTHENBACH; SCRIVENER; HOOTON, 2011; MOOSBERG-BUSTNES; LAGERBLAD; FORSSBERG, 2004). Concrete properties in fresh and hardened states have been evaluated with the use of several AMFs, such as quartzite (CRAEYE *et al*., 2010; KADRI et al., 2010; POPPE; DE SCHUTTER, 2005; RAHHAL; TALERO, 2005), alumina (POPPE; DE SCHUTTER, 2005), basalt (DOBISZEWSKA; SCHINDLER; PICHÓR, 2018; LI *et al*., 2021; SOROKA; SETTER, 1977; XIE *et al*., 2024; ZHU *et al*., 2024), diabase (ZHU *et al*., 2024), tuff (ZHU *et al*., 2024), dolomite (SOROKA; SETTER, 1977), marble (MULTON *et al*., 2010; VARDHAN *et al*., 2015), and granite (COUTINHO, 2019; MÁRMOL *et al*., 2010; RAMOS *et al*., 2013). However, durability aspects have been insufficiently addressed.

In addition, rocks used to produce AMFs may be susceptible to alkali-aggregate reaction (AAR), a deterioration mechanism that affects the durability and serviceability of infrastructure worldwide (FOURNIER; BÉRUBÉ, 2011; SIMS; POOLE, 2017). This reaction can be classified into two main mechanisms: alkali-silica reaction (ASR), involving the interaction between metastable siliceous phases in the aggregates and hydroxyl ions in the pore solution (LEEMANN *et al.*, 2024a), and alkali-carbonate reaction (ACR), which is associated with certain dolomitic carbonate rocks and is less common (GRATTAN-BELLEW *et al.*, 2010; KATAYAMA, 1992, 2010; KATAYAMA;

GRATTAN-BELLEW, 2012; LEEMANN *et al.*, 2024b; MEDEIROS; SANCHEZ; DOS SANTOS, 2024; THOMAS; FOURNIER; FOLLIARD, 2013).

Given that AAR-reactive rocks are found globally, fillers derived from these sources are widely available and economically attractive. Nevertheless, their use raises durability concerns that must be thoroughly investigated.

6.2 AAR-REACTIVE AMFs IN CONCRETE

6.2.1 Tests for assessing AAR-induced expansion

The most commonly used tests to evaluate AAR-induced expansion are the accelerated mortar bar test (AMBT) (ABNT, 2018b; ASTM, 2023a) and the concrete prism test (CPT) (ABNT, 2018e; ASTM, 2023b; CSA, 2024). These tests provide key parameters (i.e., kinetics and ultimate expansion (SANCHEZ *et al.*, 2018)) for assessing the effects of AAR-reactive AMFs in reactive and non-reactive systems. The reliability of these tests has been debated for many years, with the CPT considered more reliable compared to the AMBT due to the more realistic storage conditions, whereas those of the AMBT are harsh (THOMAS; FOURNIER; FOLLIARD, 2013), often leading to false-positive and false-negative results (BÉRUBÉ; FOUNIER, 2003; DEMERCHANT; FOURNIER; STRANG, 2000; GOLMAKANI; HOOTON, 2016; GRATTAN-BELLEW, 1997; IDEKER *et al.*, 2012; THOMAS et al., 2006). However, some challenges such as alkali leaching remain for the CPT (IDEKER *et al.*, 2010; LINDGÅRD *et al.*, 2012).

A recent study analyzing extensive field and laboratory data indicated that AMBT and CPT have similar performances in correctly identifying aggregate reactivity (BERGMANN; SANCHEZ, 2025). However, these traditional tests were developed to assess aggregates and their effectiveness in evaluating the behaviour of AAR-reactive AMFs is still unknown. Conflicting results have been reported for the same conditions when using AMBT and CPT in systems with AAR-reactive AMFs (CASTRO *et al.*, 1997; COUTINHO; MONTEFALCO; CARNEIRO, 2024; OLIVEIRA; SALLES; ANDRIOLO, 1995; PEDERSEN, 2004; TAPAS *et al.*, 2023). This highlights the need to critically examine whether existing test methods are appropriate for assessing the impact of AAR-reactive AMFs in concrete. To address this, it is essential to complement expansion tests with deterioration evaluations in systems incorporating AAR-reactive AMFs.

6.2.2 Tests for assessing AAR-induced deterioration

AAR-induced deterioration in systems incorporating AAR-reactive AMFs has not been thoroughly investigated. Previous approaches have mainly relied on surface cracking evaluations (CARLES-GIBERGUES *et al*., 2008) and multilevel assessment (ANTUNES, 2021). While surface cracking is not the best approach considering that AAR is an internal mechanism, the multilevel assessment is promising to monitor deterioration progress over time (SANCHEZ, 2014; SANCHEZ *et al*., 2014, 2015, 2017). This approach combines advanced microscopic (i.e., damage rating index – DRI) and mechanical (i.e., stiffness damage test – SDT) evaluations.

The DRI is a petrographic procedure conducted using a stereomicroscope at 15–16× magnification in which deterioration features are counted in 1 cm^2 grids drawn on the surface of polished concrete sections (SANCHEZ, 2014). The distinct deterioration features are then multiplied by weighing factors whose purpose is to balance their respective importance towards the overall damage. At the end, the final DRI is computed by averaging the features counted multiplied by the corresponding weighting factors and normalized for an area of 100 cm^2. The SDT consists of applying five cyclic loads in compression to concrete specimens (CHRISP; WALDRON; WOOD, 1993; SANCHEZ *et al*., 2014; SMAOUI *et al*., 2004). The load applied corresponds to 40% of the compressive strength at 28 days, and the loading rate is 0.10 MPa/s (SANCHEZ *et al*., 2014). The outcomes of the test are the modulus of elasticity, stiffness damage index (SDI), and plastic deformation index (PDI). The SDI and PDI are calculated as the ratios of dissipated energy to total energy and plastic deformation to total deformation implemented in the system, respectively (SANCHEZ *et al*., 2017), whereas the modulus of elasticity is calculated as the average obtained from the second and third cycles of the SDT.

Therefore, despite the availability of established tests for assessing aggregate reactivity, there is currently no standardized or validated method specifically designed to evaluate the performance and influence of AAR-reactive AMFs in concrete. The interactions between fillers, cementitious materials, and aggregates require a more comprehensive approach, coupling expansion- and damage-induced evaluations. Developing or validating reliable methodologies to assess AAR-reactive AMFs is thus essential to ensure their safe and effective application, particularly as the use of AMFs in blended cement tends to increase.

6.2.3 Past research on AAR-reactive AMFs

The use of AMFs has been mainly evaluated in terms or AAR-mitigation capacity (ALVES *et al.*, 1997; BRAGA *et al*., 1991; CARLES-GIBERGUES *et al*., 2008; COUTINHO, 2019; CYR; RIVARD; LABRECQUE, 2009; LI; HE; HU, 2015; OLIVEIRA; SALLES; ANDRIOLO, 1995; TAPAS *et al*., 2023). In this regard, most of the studies used the AMBT to evaluate the effect of the fillers (CASTRO *et al.*, 1997; COUTINHO; MONTEFALCO; CARNEIRO, 2024; OLIVEIRA; SALLES; ANDRIOLO, 1995; PEDERSEN, 2004; TAPAS *et al*., 2023), which means reducing the aggregate to sand-sized particles. Therefore, the evaluated systems combined two AAR-reactive components: i) the filler and ii) the aggregate (i.e., coarse (CASTRO *et al*., 1997; COUTINHO; MONTEFALCO; CARNEIRO, 2024; OLIVEIRA; SALLES; ANDRIOLO, 1995; PEDERSEN, 2004; TAPAS et al., 2023) or fine (ANTUNES, 2021; TAPAS *et al*., 2023)). However, by introducing two reactive components, the evaluation of their individual contributions is hindered. Therefore, it is important to test systems with no reactive aggregates, in which the only reactive component is the filler, particularly when considering the possible application of this material in the production of blended cements.

The only study found in which a non-reactive system was assessed consisted of incorporating ASR-reactive AMFs in different percentages (i.e., 15% and 30%) and replacing simultaneously cement and sand (i.e., 50% replacing cement and 50% replacing sand) (GUÉDON-DUBIED *et al*., 2000). The results indicated an increase in the expansions with the use of the AAR-reactive AMFs, but they remained below the threshold set for one year of storage. Nonetheless, because of the choice of replacement in this study, it is not possible to understand the contribution of the fillers when replacing cement or sand individually. Therefore, to complement the findings in Paper 2 of the thesis, it is important to analyze the effect of fillers in non-reactive systems to better understand their isolated effect.

6.3 SCOPE OF THE WORK

Considering the efforts to reduce CO_2 emissions in the cement industry, AMFs have also been considered as an alternative to be used replacing cement. As rocks can be susceptible to AAR, the effect of AAR-reactive AMFs in concrete must be better understood. Studies on this topic evaluated different parameters and used different

tests, hindering the construction of a solid knowledge about the topic. In particular, systems with no reactive aggregates and AAR-reactive AMFs replacing cement to fully understand its influence with no interference of other effects have not been addressed. Moreover, it is still unclear whether current methods to evaluate aggregate reactivity can be used to assess the effect of AAR-reactive AMFs. To fill this knowledge gap, this study aims to evaluate the use of ASR-reactive AMFs replacing cement in non-reactive systems. The variables analyzed were the type of fillers (i.e., highly reactive and moderately reactive), PSD (i.e., < 150 μm and < 75 μm), and percentage (i.e., 10% and 20%). For an evaluation in concrete, the CPT was adopted and its adequacy in evaluating systems with ASR-reactive AMFs was assessed by comparing the results from the CPT with the deterioration progress observed by applying the multilevel assessment (i.e., DRI and SDT). The results of this study are expected to contribute to a better understanding of the action of ASR-reactive AMFs considering kinetics and deterioration, how the variables analyzed affect the reaction progress, and the adequacy of CPT to test systems with ASR-reactive AMFs such as to determine the potential viability of this material to be used in the production of blended cements.

6.4 EXPERIMENTAL PROGRAM

6.4.1 Materials for concrete production

A conventional Portland cement GU type (equivalent to ASTM type I) was used. There is no equivalent considering Brazilian cements, but it shares characteristics of CP-V (low percentage of additions) and CP II-F (particle size). The fillers used were produced from two reactive rocks, a moderately reactive mylonite from Brazil and a highly reactive greywacke from Canada (Springhill). The chemical composition was determined by X-ray fluorescence (XRF) using a Rigaku Supermini200 WDXRF Spectrometer. The X-ray diffraction was conducted using a Rigaku Ultima IV Diffractometer. The results of the XRF for the cement and AMFs and diffractograms of the AMFs are presented in Table 6.1 and Figure 6.1, respectively.

Table 6.1 – Chemical composition of cement and fillers.

Chemical composition	Cement (%)	Mylonite (%)	Springhill (%)
SiO_2	19.64	59.06	51.72
Al_2O_3	4.53	13.48	10.76
CaO	62.04	5.17	8.69
K_2O	0.97	3.58	2.70
Na_2O	0.42	3.45	1.45
MgO	2.64	3.22	5.59
Fe_2O_3	3.69	8.34	4.97
TiO_2	0.23	1.50	0.60
P_2O_5	0.14	0.89	0.11
MnO	0.05	0.12	0.07
Traces	1.81	0.36	0.33
L.O.I.	3.84	0.84	13.00
Na_2O_{eq}	1.06	5.80	3.23
TOTAL	100.00	100.00	100.00

Source: Author (2025).

Figure 6.1 – Diffractograms of the mylonite and Springhill fillers used.

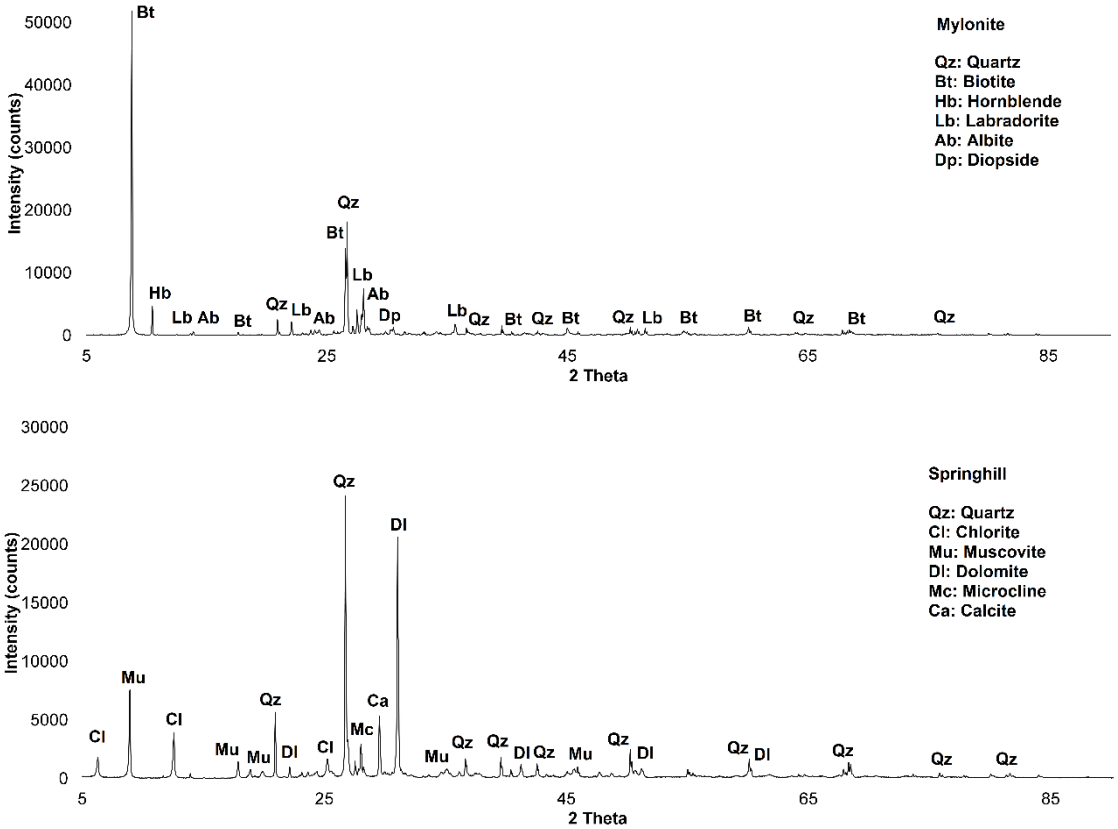

Quartz: SiO_2, Biotite: $(K(Mg,Fe)_3(AlSi_3O_{10})(F,OH)_2)$, Hornblende: $((Ca,Na)_{2-3}(Mg,Fe,Al)_5(Al,Si)_8O_{22}(OF,F)_2)$, Labradorite: $((Ca,Na)(Si,Al)_4O_8)$, Albite: $(Na,Ca)Al(Si,Al)_3O_8$, Diopside: $(MgCaSi_2O_6)$, Chlorite: $(Mg,Al)_6(Si,Al)_4O_{10}(OH)_8$, Muscovite: $(K,Na)(Al,Mg,Fe)_2(Si_{3.1}Al_{0.9})O_{10}(OH)_2$, Dolomite: $CaMg(CO_3)_2$, Microcline: $K(AlSi_3)O_8$, Calcite: $(Mg_{0.03}Ca0.97)(CO_3)$.

Source: Author (2025).

The aggregates were crushed using a jaw crusher and sieved to obtain powders passing the sieves with openings 150 μm and 75 μm. The selection of the < 150 μm fraction was based on the particle size range adopted in the AMBT (ASTM, 2023a), still extensively adopted in laboratories. In this test, the aggregates are crushed and fractions from 4.8 mm to 150 μm are used, whereas the material passing the 150-μm sieve is discarded. Thus, this fraction was selected to test the AMFs as it is indirectly produced. To further investigate the influence of filler PSD, an additional fraction passing the 75-μm sieve was also adopted. This fraction was selected based on the physical requirement for type C fillers (byproduct from aggregate crushing operations) of having ≥ 65% passing the 75-μm sieve for use in hydraulic cement concrete, as per the ASTM C1797 (ASTM, 2024). These parameters were also adopted in previous studies (CASTRO *et al.,* 1997; COUTINHO; MONTEFALCO; CARNEIRO, 2024; SALLES; OLIVEIRA; ANDRIOLO, 1997). The PSD curves of cement and fillers, obtained by laser diffraction, are shown in Figure 6.2.

Figure 6.2 – PSD of cement and fillers.

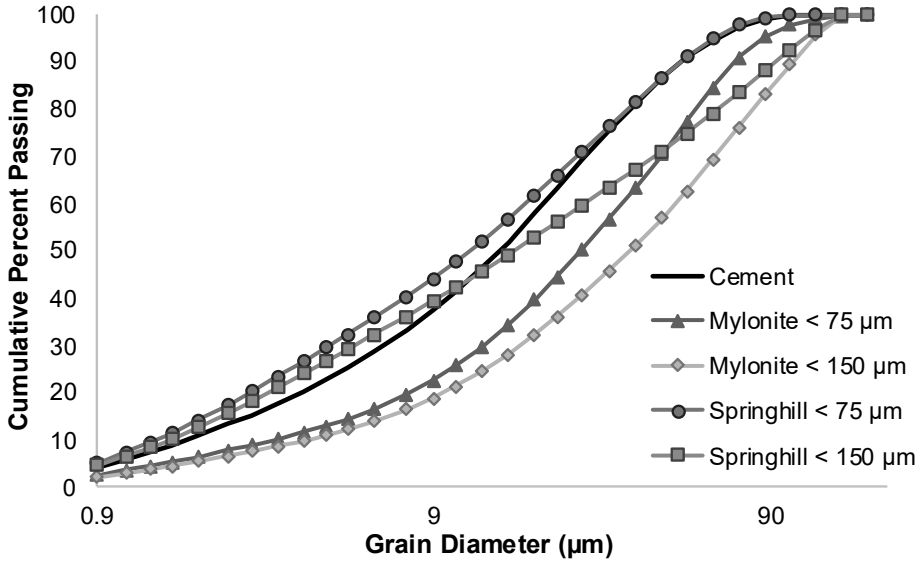

Source: Author (2025).

As observed in the figure, both mylonite fillers were coarser than Portland cement, whereas the Springhill fillers exhibited a PSD closer to that of cement. The percentages adopted were 10% and 20% based on the literature review conducted and the values used in other studies (CARLES-GIBERGUES *et al.,* 2008; COUTINHO; MONTEFALCO; CARNEIRO, 2024; LI; HE; HU, 2015). The replacement was made by

cement to reduce cement consumption considering the NetZero target. The coarse and fine aggregates adopted were non-reactive, as detailed in Table 6.2.

Table 6.2 – Coarse and fines aggregates used.

Aggregate		Reactivity	Rock Type	Specific Gravity	Absorption (%)	AMBT* (%)
Coarse	LC	NR	Crushed limestone	2.78	0.42	0.02
Fine	NS	NR	Natural sand	2.70	0.40	0.04

* Results of the AMBT as per ASTM C 1260.

Source: Author (2025).

6.4.2 Mixture proportion and production of samples

The CPT was conducted to measure ASR expansions as it allows a better representation of field concrete compared to accelerated tests. Moreover, previous studies have indicated that certain fillers of rocks containing siliceous mineral phases may exhibit pozzolanic activity at high temperatures, such as that of the AMBT (i.e., 80 ºC), making the selection of a test with a lower temperature fundamental for the scope of this study (PEDERSEN, 2004).

Concrete cylinders of 100 × 200 mm were produced in this study. The following parameters were evaluated: type of fillers (Mylonite and Springhill), PSD (< 150 µm and < 75 µm), and percentage (10% and 20%), representing 8 families. For each family, expansion measurements were conducted for 9 months and samples were at tested, 1, 3, and 6 months. Six samples were produced for each age and three additional samples for compressive strength tests, totalling 27 samples per family and 216 for the study. The nomenclature adopted consisted of the letter A representing the type of mixture followed by the type of filler (M or SP), PSD (150 or 75), and percentage (P10 or P20). Therefore, a sample named ASP75P10 would indicate a mixture with Springhill filler, PSD of 75 µm, and percentage of 10%.

The mixture design followed the requirements of ASTM C1293 (ASTM, 2023b). The concrete was boosted to reach an alkali equivalent of 5.25 kg/m^3 of concrete. The water/cement ratio adopted was 0.45 and the cement + filler content was 420 kg/m^3. The mixture proportions used are listed in

Table *6.3*.

Table 6.3 – Concrete mixture proportions.

Mixture	Filler	PSD	%	Cement (kg/m³)	Filler (kg/m³)	FA – NR* (kg/m³)	CA – NR* (kg/m³)	Water (kg/m³)
A	M	150	10	378.00	42.00	723.07	1133.44	170.10
A	M	150	20	336.00	84.00	723.07	1133.44	151.20
A	M	75	10	378.00	42.00	723.07	1133.44	170.10
A	M	75	20	336.00	84.00	723.07	1133.44	151.20
A	SP	150	10	378.00	42.00	723.07	1133.44	170.10
A	SP	150	20	336.00	84.00	723.07	1133.44	151.20
A	SP	75	10	378.00	42.00	723.07	1133.44	170.10
A	SP	75	20	336.00	84.00	723.07	1133.44	151.20

* FA: fine aggregate; CA: coarse aggregate; NR: non-reactive.
Source: Author (2025).

The ends of samples were drilled and steel gauges were positioned and fixed with the use of a fast-setting cement slurry. The samples were allowed to harden for 24 h, after which the initial measurements were taken. The samples were stored in sealed plastic buckets lined with a moist cloth at 38 ºC and 100% relative humidity (RH). The cylinders were regularly measured and taken at the ages of 1, 3, and 6 months for additional tests.

6.4.3 Assessment of the ASR development in the concrete

The kinetics and ultimate expansion, considered as the expansion at the end of the test or from which the expansion stabilize, were evaluated by measuring the expansions at given ages using a measuring arch, as per the standard ASTM C1293 (ASTM, 2023b).

6.4.3.1 Compressive Strength

The samples for compressive strength were wrapped in plastic film and stored in a chamber at 12 ºC to avoid the development of ASR, which can affect the results of the test, as AAR-reactive AMFs were used. The samples remained at this temperature for 47 days, which corresponds to 28 days at 20 ºC, as per the maturity concept by ASTM C 1074 (ASTM, 2019). This procedure was validated by Sanchez (2014) and Sanchez et al. (2016).

6.4.3.2 Damage Rating Index

The method described in Sanchez et al. (2016) was used to calculate the DRI. The samples were axially cut in half and polished using a hand polisher with diamond impregnated rubber disks (nº. 50, 100, 200, 400, 800, 1500, 3000). The analysis was conducted in a stereomicroscope (16× magnification) at the ages of 1, 3, and 6 months. The final DRI number was calculated based on the counts of features (i.e., open crack in the aggregate, closed crack in the aggregate, crack in the cement paste) multiplied by their weighting factors normalized for an area of 100 cm^2.

6.4.3.3 Stiffness Damage Test

The SDT was performed as per the procedure described in the works of Sanchez and colleagues (SANCHEZ *et al*., 2014, 2017a, 2018). It consists of applying five loading/unloading cycles at 40% of the ultimate compressive strength capacity of samples at 28 days through a loading rate of 0.10 MPa/s. The results obtained and presented are an average of three samples tested at each curing period. The outputs of the test are the stiffness damage index (SDI), plastic deformation index (PDI), and modulus of elasticity. The modulus of elasticity was calculated as the average obtained from the second and third cycles of the SDT, whereas the SDI and PDI were calculated as the ratios of dissipated energy to total energy and plastic deformation to total deformation implemented in the system, respectively (SANCHEZ *et al*., 2017).

6.4.4 Statistical Analysis

The results obtained were statistically analyzed using multi-factorial analysis of variance (ANOVA) for a significance level of 5%. Shapiro–Wilk and Barlett's tests were applied to verify the normality and homoscedasticity (equal variance) of the data.

6.5 RESULTS

6.5.1 ASR Kinetics

Figure 6.3 shows show the expansion kinetics (i.e., average value of four consecutive measurements per sample with standard deviations ranging from 0.01% to 0.06%) obtained by incorporating different types of ASR-reactive AMFs with different PSDs and percentages replacing cement in a non-reactive system. The black dashed curve

refers to the results for the combination with coarse (limestone) and fine aggregates used with no AAR-reactive AMFs as a reference.

Figure 6.3 – ASR kinetics over time. (a) Expansion and (b) mass gain for all mixtures studied.

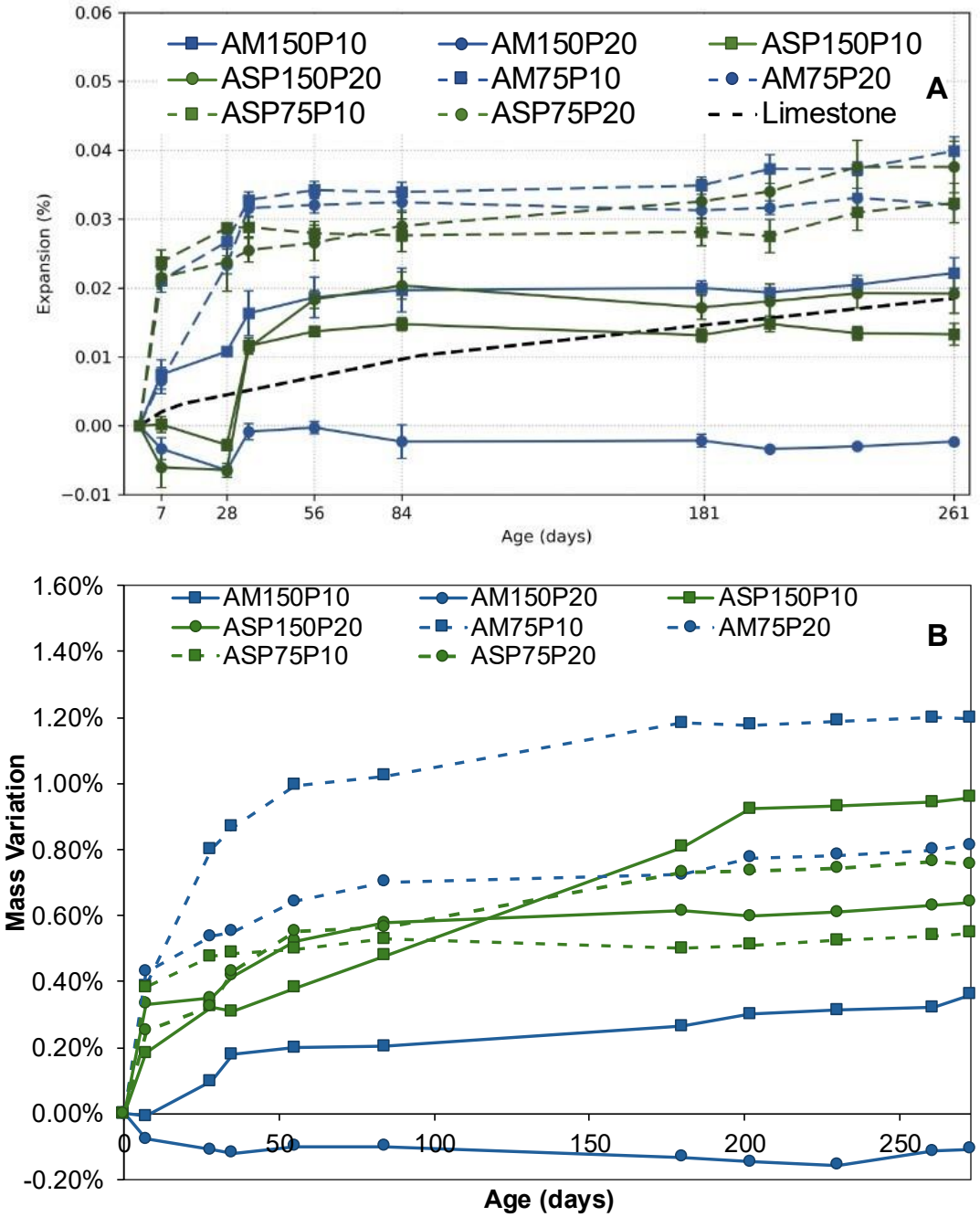

Source: Author (2025).

Distinct behaviours can be observed for the mixtures at early ages as some exhibit fast kinetics whereas others experience shrinkage followed by a fast increase in expansions. Mixtures with PSD <75 μm (i.e., dashed curves) exhibit most of the expansion development in the first 7 days. In contrast, most of the mixtures with PSD

<150 μm (i.e., solid lines) exhibit shrinkage followed but a fast increase in expansions. The expansions seem to start stabilizing after 1 month, and are all below the threshold of 0.04% set by ASTM (ASTM, 2023b) to consider a system reactive, except combination AM75P10, with an expansion slightly above this value (i.e., 0.041%). Comparing the curves with the reference one (i.e., limestone) with no ASR-reactive AMFs, only combinations ASP150P10 and AM150P20 exhibited lower expansions at the end of the period analyzed, indicating the influence of the fillers. Moreover, the kinetics are also different when no ASR-reactive fillers are incorporated, with a stable increase of expansion in contrast to the fast kinetics in the first month followed by continuous stabilization for the combinations with fillers.

The samples that experienced shrinkage were those with coarser AMFs (<150 μm), and higher expansions were achieved by combinations with finer AMFs (<75 μm). This may indicate that the ASR-expansions in mixtures with <75 μm AMFs compensated for the shrinkage. The maximum expansions ranged from -0.002% to 0.041%. The mass gain ranged from -0.11% and 1.20% at the maximum expansion and the behaviour of the mass curves was similar to that of the expansion curves.

6.5.2 Damage Rating Index

Figure 6.4 shows the DRI values (i.e., average of two specimens per combination) for mixtures A with non-reactive aggregates and AAR-reactive AMFs for the ages of 1, 3, and 6 months and for all combinations analyzed.

As observed, the DRI values varied randomly for the ages analyzed, varying from 61 to 125. No pattern was observed for the DRI values obtained because they were very low, indicating negligible level of damage, as per the classification of damage degree in concrete due to ASR proposed by Sanchez et al. (2017). Few cracks were observed in the paste, which can be from both the contribution of the fillers and shrinkage, as observed in the expansion curves in Figure 6.3.

Figure 6.4 – DRI values for non-reactive systems.

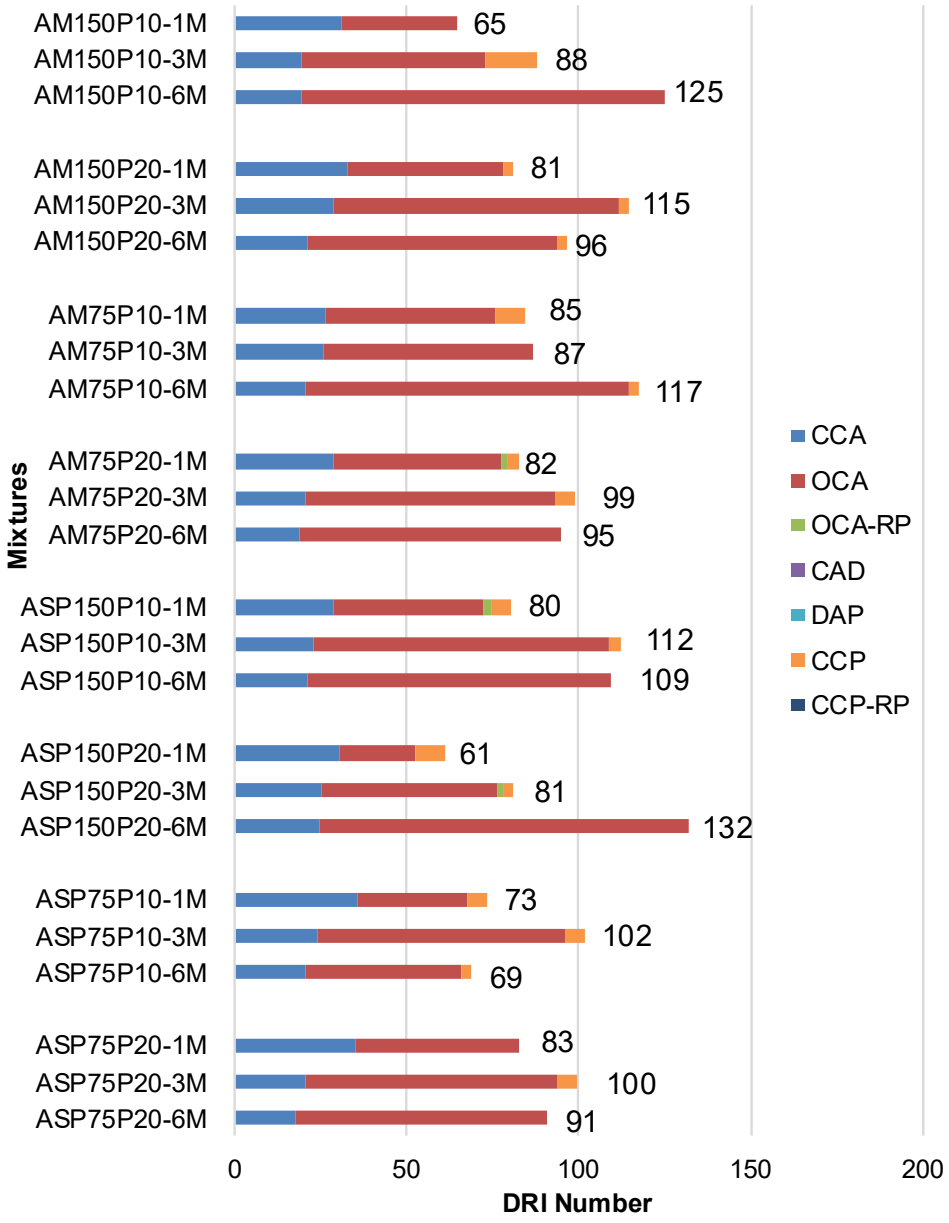

Source: Author (2025).

6.5.3 Stiffness Damage Test

The results of SDT represent the average obtained from three samples tested. Figure 6.5 shows the results of SDI, PDI, and modulus of elasticity for the ages tested for all the combinations analyzed.

Figure 6.5 – SDT results for non-reactive systems. (a) SDI. (b) PDI. (c) Modulus of elasticity.

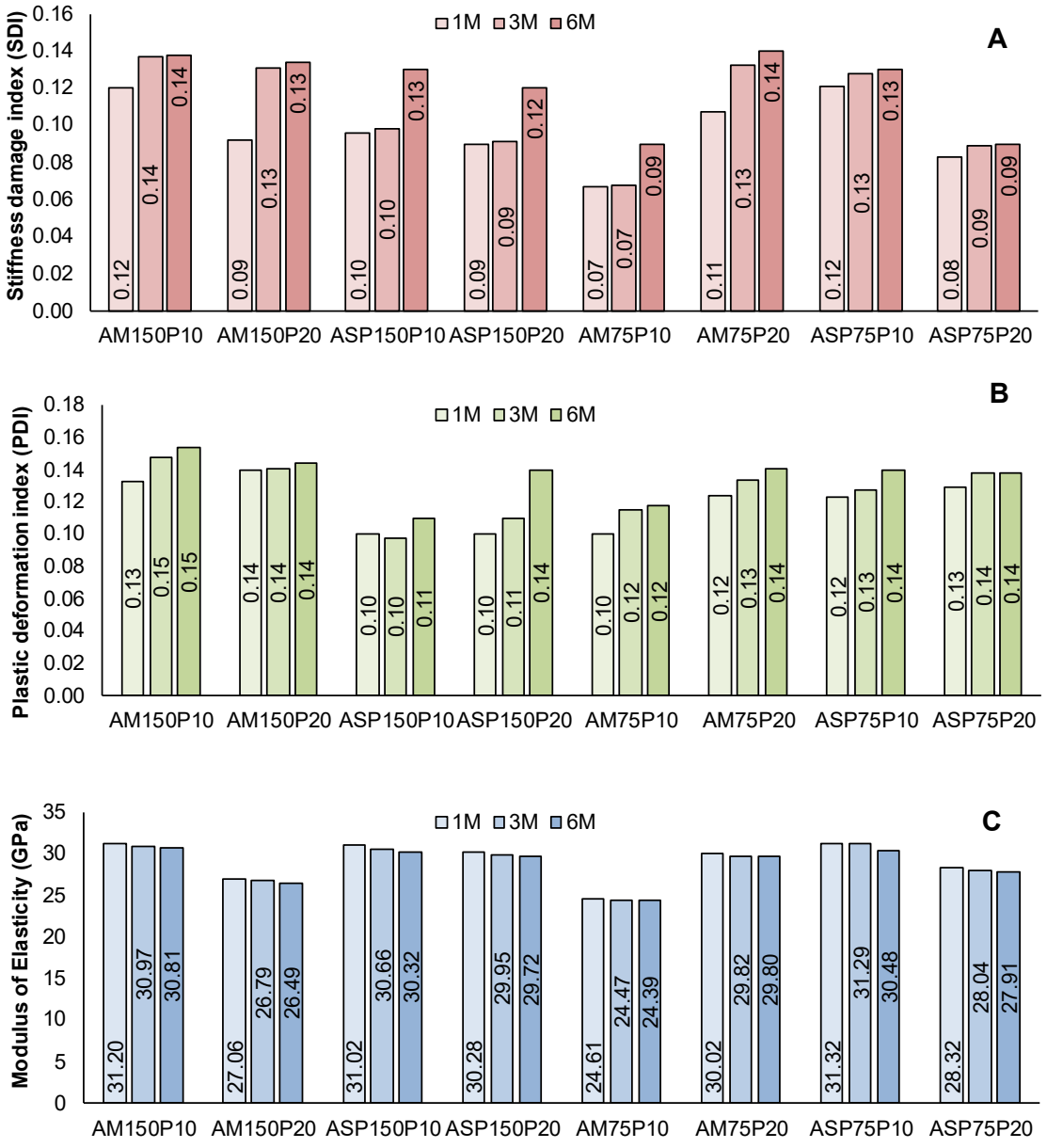

Source: Author (2025).

As observed, the SDI and PDI slightly increased over time, whereas the modulus of elasticity slightly decreased. However, the values were very similar, corresponding to negligible or marginal damage degree in concrete (SANCHEZ *et al*., 2017). The SDI values varied from 0.07 to 0.14 and the PDI values varied from 0.10 to 0.15.

6.6 DISCUSSION

6.6.1 Effect of parameters evaluated on the kinetics and maximum expansion of the reaction

In this study, ASR-reactive AMFs were evaluated replacing cement in a non-reactive system, that is, non-reactive aggregates were used. Moreover, three parameters were analyzed for each mixture: type of filler (i.e., Mylonite or Springhill), PSD (i.e., < 150 µm or < 75 µm), and percentage (i.e., 10% and 20%). Figure 6.6 shows the expansion development obtained for the combinations analyzed.

Figure 6.6 – Expansions for the combinations analyzed.

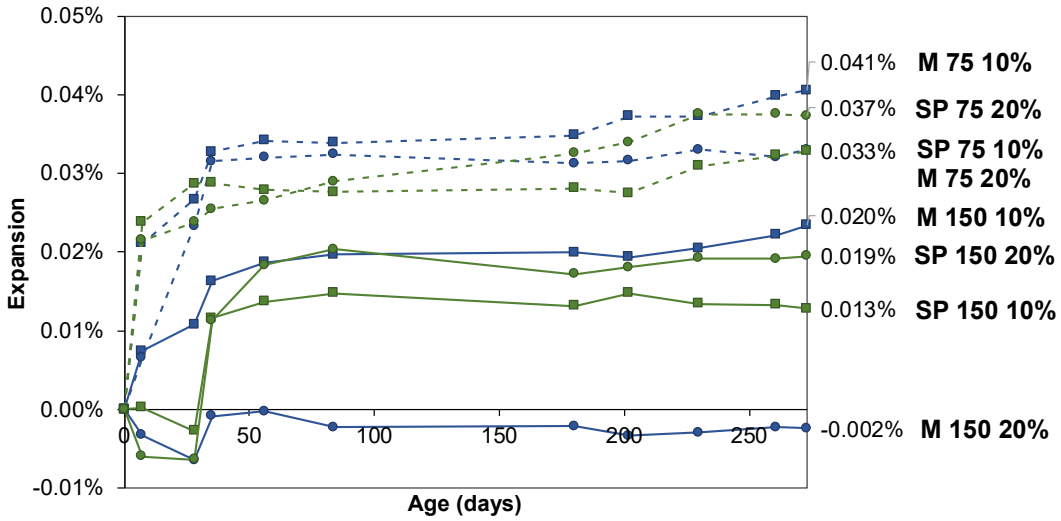

Source: Author (2025).

When analyzing separately the curves with different PSDs, distinct behaviours were observed. Mixtures with fillers with particle size <150 µm exhibited a slight shrinkage at early ages, except combination AM150P10, whereas this was not observed for mixtures with fillers with particle size <75 µm. Finer particles lead to increased drying shrinkage (MARUYAMA *et al.*, 2022). Therefore, considering that higher expansions were obtained for all combinations with PSD <75 µm, the kinetics in these combinations were sufficiently fast to compensate for the shrinkage.

To better understand the kinetics behaviour, the expansion rate curves and maximum expansion rates were calculated and are shown in Figure 6.7.

Figure 6.7 – (a) Expansion rate curves. (b) Maximum expansion rate.

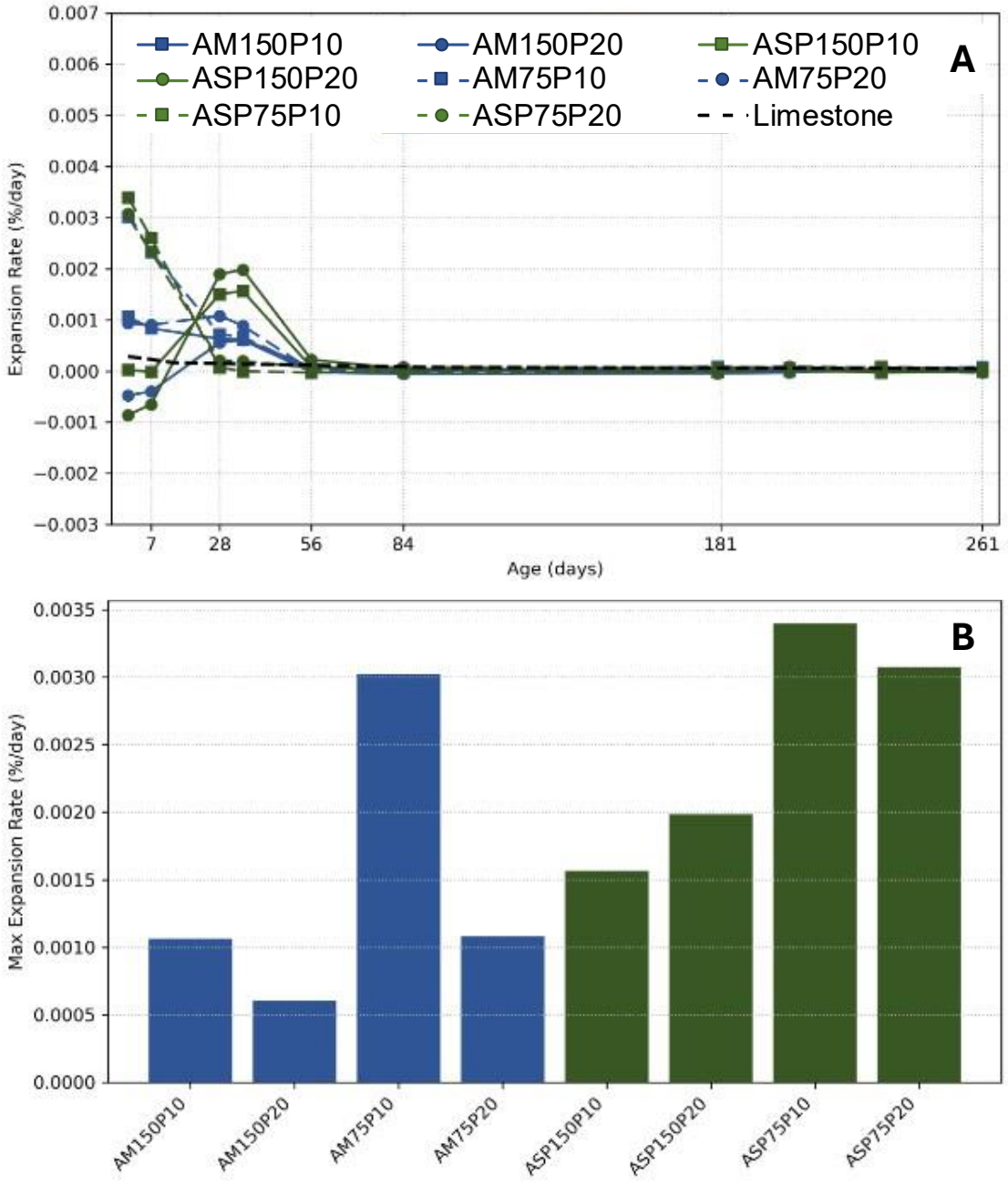

Source: Author (2025).

As observed, despite a similar behaviour for expansion, the rates differed. Moreover, the rate curve of the reference mixture with no fillers continuous, indicating that the rate was the same for the period analyzed, whereas the curves for the mixtures with fillers varied considerably in the first 60 days, highlighting the action of the fillers.

The expansions were faster in the first 60 days, with the fastest rate observed around 7 days for some combinations and 30 days for others, and ranging from 0.0006 to 0.0034 %/day. The maximum expansion rate was reached at 7 days for combinations

AM75P10, ASP75P10, and ASP75P20, indicating that the filler action was intense in the first 7 days, reducing from that point. These combinations were also the ones with higher expansion. For the other combinations with intermediate expansions and that experienced shrinkage, the maximum rate was reached at approximately 30 days. Therefore, when the expansions were sufficient to overcome shrinkage, they increased at a very fast rate. From 60 days, the rate of expansion stabilizes.

Considering the parameters analyzed, mixtures with mylonite did not exhibit a considerable difference in expansion rate, whereas mixtures with Springhill exhibited variable results. Moreover, for mixtures with the same parameters and different fillers, the ones with Springhill filler exhibited higher maximum expansion rates, indicating that the degree of reactivity influenced this aspect, as Springhill is more reactive than mylonite. When varying the PSD, mixtures with PSD <75 μm exhibited a higher maximum expansion rate. For the percentage, mixtures with 10% of filler exhibited higher maximum expansion rates compared to their counterparts with 20% filler. For mixtures with Springhill filler, higher maximum rates were obtained for the combination with 20% filler and a PSD <150 μm and for the combination with 10% filler for a PSD <75 μm.

In the following sections, the influence of each parameter analyzed in the expansion will be discussed in detail.

6.6.1.1 Effect of the type of fillers on the kinetics and maximum ASR-induced expansions

Figure 6.8 shows the maximum expansion obtained for the non-reactive system with different fillers while maintaining the other parameters. As observed, when analyzing combinations with all the variables fixed while varying the type of fillers, different behaviours were observed. Combinations containing mylonite displayed higher expansions compared to their counterparts using Springhill for the lower percentage used (10%). In contrast, when using 20% of filler, combinations with Springhill filler exhibited higher expansion. Therefore, the results indicated that the variable type of fillers should not be analyzed individually as it interacts with the variable replacement percentage.

Figure 6.8 – Maximum expansions obtained considering the type of fillers as the focus variable.

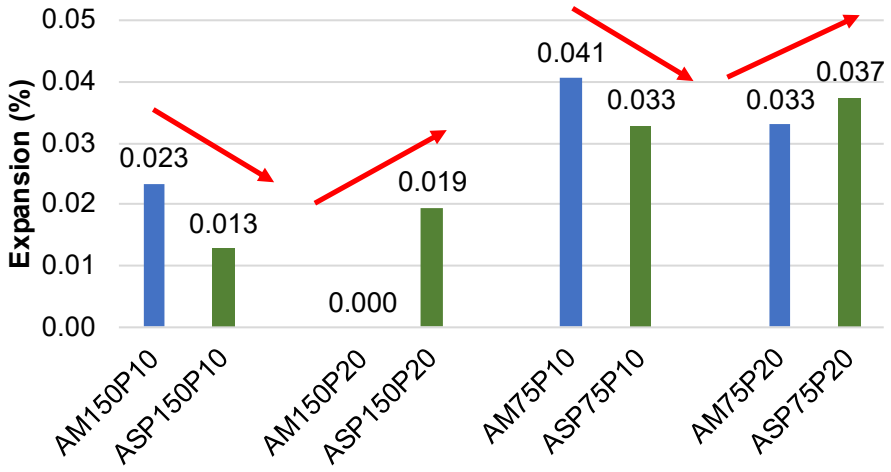

Source: Author (2025).

6.6.1.2 Effect of the fillers PSD on the kinetics and maximum ASR-induced expansions

Figure 6.9 shows the maximum expansion obtained for the combinations with different PSDs of fillers (<150 µm and <75 µm) while maintaining the other parameters fixed.

Figure 6.9 – Maximum expansions obtained considering the PSD as the focus variable.

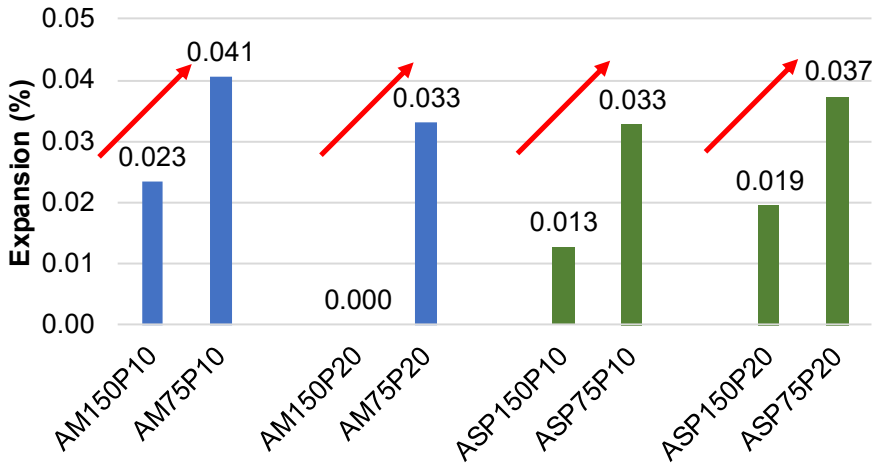

Source: Author (2025).

Comparing mixtures with same parameters and different PSDs, that a PSD < 75 µm resulted in higher ultimate expansions for all combinations analyzed. This indicates that the fineness of the fillers plays a role in intensifying the reaction, with a direct relationship. This is contrary to theories on the action of the reactive fillers in the literature, in which finer particles would react fast and the reaction product would

dissipate in the cementitious matrix (DYER, 2014). This particular behaviour can be related to the pessimum effect, which is the intensification of the reaction in a certain size range, whereas above and below this content expansions reduce (QIU *et al.*, 2022).

6.6.1.3 Effect of replacement percentage of fillers on the kinetics and maximum ASR-induced expansions

Figure 6.10 shows the maximum expansion obtained for the non-reactive system with different percentages of fillers replacing cement (10% and 20%) while maintaining the other parameters fixed.

Figure 6.10 – Maximum expansions obtained considering the percentage as the focus variable.

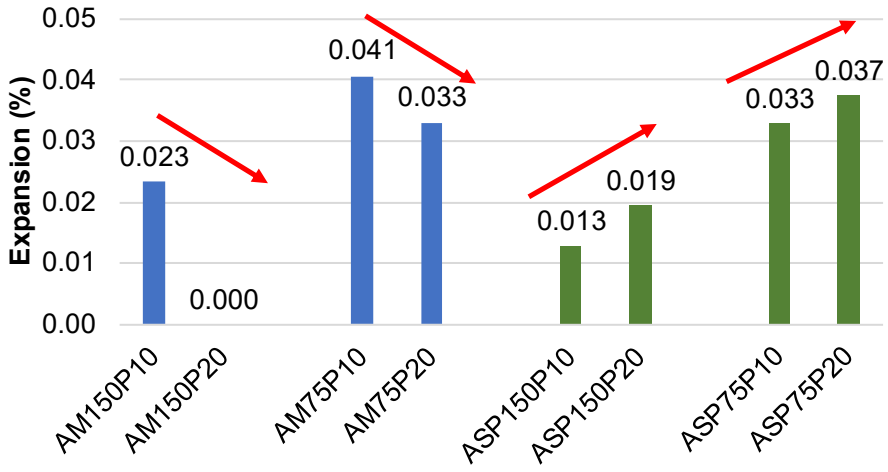

Source: Author (2025).

In this analysis, the relationship between type of fillers and percentage is once more emphasized. Combinations with mylonite fillers exhibited lower expansions for higher filler percentages. In contrast, combinations with Springhill fillers exhibited increased expansions when increasing the percentage used (20%).

Table 6.4 summarizes the effect of each parameter on the expansions, as discussed in previous sections.

Table 6.4 – Summary of the effect of different parameters on expansions.

	Expansion
Type of fillers	10%: M > SP 20% SP > M
PSD	75 µm > 150 µm
Percentage	M: 10% > 20% SP: 10% < 20%

Source: Author (2025).

6.6.2 Multilevel assessment

6.6.2.1 Microscopic assessment

The petrographic deterioration features were analyzed in absolute counts and in percentage of main damage features to evaluate the progress of the ASR-induced damage, as shown in Figure 6.11. The features were arranged in three groups: Group I, consisting of closed cracks in the aggregate (CCA), Group II, consisting of open cracks in the aggregate (OCA and OCA-RP), with and without reaction product, and Group III, consisting of cracks in the cement paste, with or without reaction product (CCP and CCP-RP).

Figure 6.11 – Microscopic deterioration features normalized by 100 cm^2 for the combinations analyzed. (a) Counts. (b) Percentage.

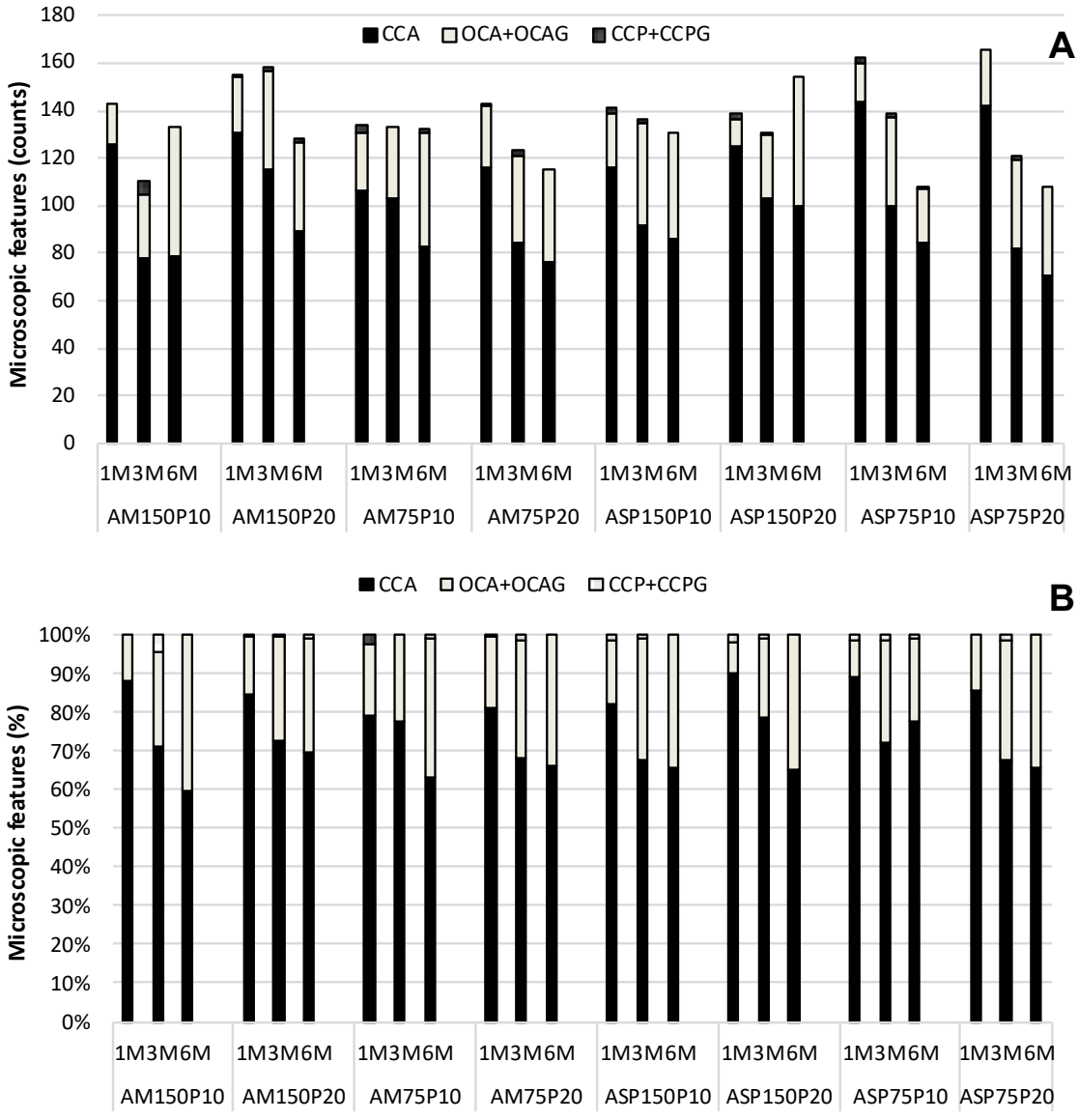

Source: Author (2025).

As previously indicated, the DRI numbers obtained for all combinations ranged from 61 to 125, being below 150, which indicates negligible damage as per the classification of damage degree in concrete due to ASR proposed by Sanchez et al. (2017). The count and percentage of microscopic features in Figure 6.11 indicate that the main deterioration feature observed was CCA, which is probably a result of processing operations of the aggregate. The number of cracks in group II also remained similar, indicating that the deterioration is not progressing or is progressing in extremely slow kinetics. Very few cracks in the CCP were observed, and even those may have also been generated owing to shrinkage.

6.6.2.2 Mechanical assessment

Figure 6.12 shows the (a) SDI and expansion values; (b) modulus of elasticity reduction and expansion values for the combinations analyzed.

Figure 6.12 – (a) SDI vs expansion and (b) Modulus of elasticity reduction vs expansion for combinations with reactive fillers in non-reactive systems.

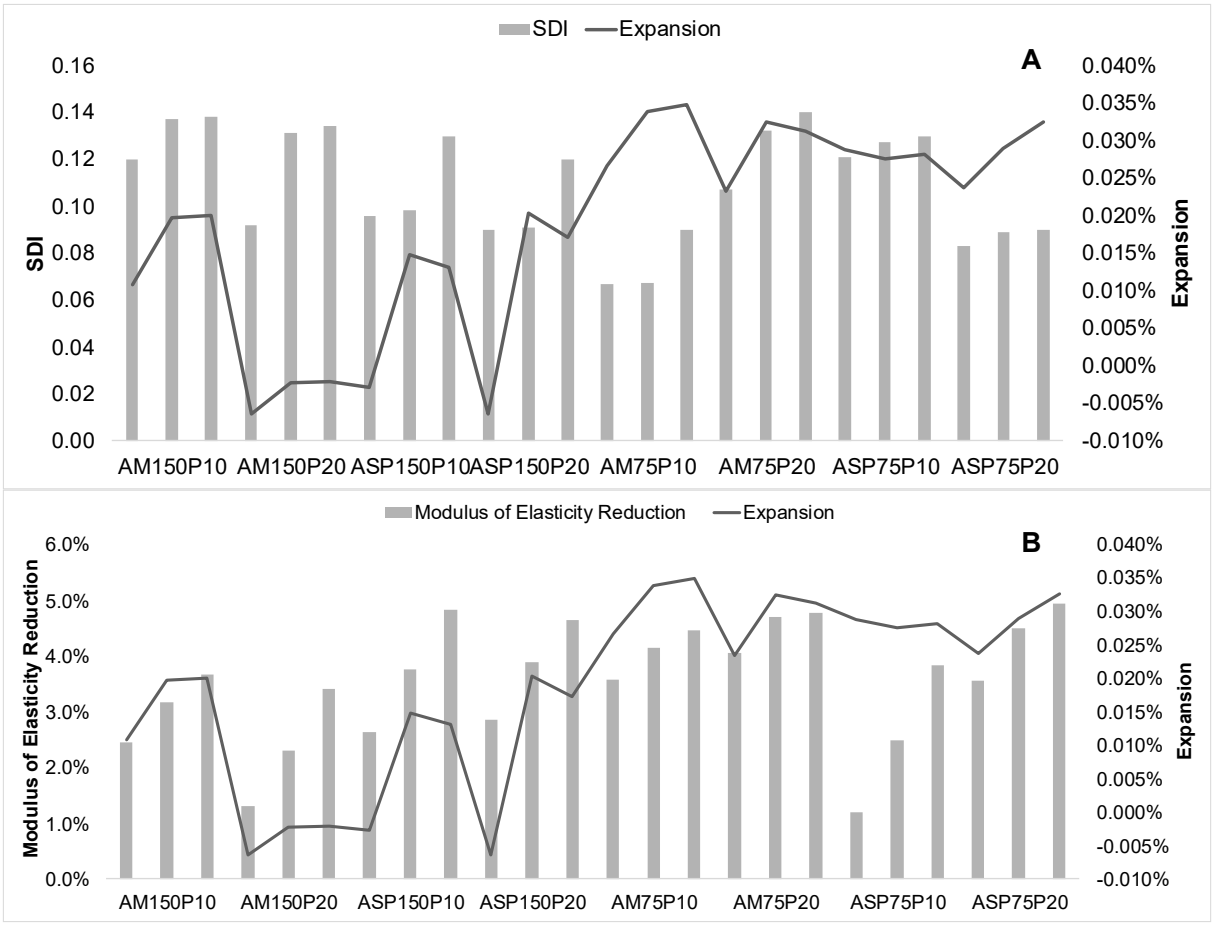

Source: Author (2025)

No relationship is observed between SDI values and expansions, as well as modulus of elasticity reduction and expansions, which is because of the negligible damage observed. The modulus of elasticity is observed to reduce with time, but the value remains below 5%, which is also an acceptable variability of the test. The SDI values ranged from 0.07 (0.03% expansion) to 0.14 (0.03% expansion). As for the modulus of elasticity, the reduction ranged from 1.2% to 4.9%.

An important factor that was not assessed but could potentially influence the results is the contribution of alkalis from the aggregates (LEEMANN; HOLZER, 2005), particularly from the ASR-reactive AMFs used, as the alkali release in influenced by the particle size (SOARES *et al.,* 2016). Considering the alkali contribution of ASR-reactive filler is essential to better understand the individual action of this material.

6.6.2.3 Statistical analysis

The results obtained were also assessed to determine whether the differences observed were statistically significant. Multi-factorial ANOVA was conducted with a significance level of 5%, and the corresponding results are listed in Table 6.5.

Table 6.5 – ANOVA considering expansion results for mixtures B and C.

Parameter	SQ	DF	MQ	F	F 0.05	p-value	Signif.*
Type of fillers	$7.38\ 10^{-7}$	1	$7.38\ 10^{-7}$	9.837	4.013	0.003	S
PSD	$1.36\ 10^{-6}$	1	$1.36\ 10^{-6}$	18.124	4.013	$7.969\ 10^{-5}$	S
Percentage	$7.71\ 10^{-7}$	1	$7.71\ 10^{-7}$	10.279	4.013	0.002	S
Fillers *vs* Percentage	$-5.9\ 10^{-7}$	1	$-5.9\ 10^{-7}$	-7.284	4.013	1.000	NS
Fillers *vs* PSD	$-7.2\ 10^{-7}$	1	$-7.2\ 10^{-7}$	-9.573	4.013	1.000	NS
Percentage *vs* PSD	$-7.1\ 10^{-7}$	1	$-7.1\ 10^{-7}$	-9.513	4.013	1.000	NS
Fillers *vs* PSD *vs* Percentage	$7.64\ 10^{-7}$	1	$7.64\ 10^{-7}$	10.189	4.013	0.002	S
Residue	$4.2\ 10^{-6}$	56	$2.57\ 10^{-7}$				
Total	$5.81\ 10^{-6}$	63					

*S: Significant; NS: Not significant.

Source: Author (2025).

As observed, all the parameters had a significative impact on the results. In particular, by comparing the p-values, the PSD was the parameter that had the most impact, which could be inferred based on the curves in Figure 6.3, with a clear distinction between combinations with PSD 150 µm and 75 µm. Moreover, although the coupled effect of any two parameters did not have a statistically significant effect, the interaction

between the three parameters was statistically significant, indicating that they must be considered carefully.

6.7 CONCLUSION

This study evaluated the impact of ASR-reactive fillers on the expansion and deterioration progress of concrete containing non-reactive aggregates. Two types of reactive fillers (i.e., a highly reactive greywacke and a moderately reactive mylonite) were incorporated at two PSDs (i.e., <150 μm and <75 μm) and two replacement levels (i.e., 10% and 20%) in cementitious systems. The CPT was used to monitor expansion, and the multilevel assessment (i.e., DRI and SDT) was applied to assess the deterioration progress.

The main conclusions drawn from this study are as follows:

- The action of the filler was concentrated in the first 30 days. Fillers with PSD <75 μm reacted fast in the first 7 days, after which the expansion rate reduced. Fillers with PSD <150 μm in general experienced shrinkage, leading to slower expansion rate in the beginning that increased until reaching maximum values at 30 days. After 30 days, the expansion rate reduced and expansions stabilized at 60 days;
- Finer fillers (<75 μm) led to higher expansions, opposite to theories on the action of AAR- reactive fillers in the literature, in which finer particles would react fast and the reaction product would dissipate in the cementitious matrix. This behaviour is probably related to the “pessimum effect”, where certain particle sizes maximize expansion;
- Despite some expansion, SDT and DRI results indicate negligible internal damage in all combinations analyzed;
- All analyzed parameters (type of filler, PSD, and replacement percentage) significantly influenced ASR expansion. Moreover, the interactions between these parameters also were significant to the expansion behaviour;
- The CPT showed adequacy in evaluating these systems, revealing that ASR-reactive fillers can be used without compromising concrete durability, provided proportions and PSD are well controlled.

Overall, the study demonstrates that ASR-reactive fillers may be viable for cement replacement in blended cements, provided that the reactivity, fineness, and percentage of replacement are considered.

Despite the promising results obtained, the study has some limitations that should be considered. First, the analysis was based on microstructural and mechanical results. Microscopic and chemical tests should be conducted to confirm the findings. The alkali release by aggregates and ASR-reactive AMFs was not considered. Moreover, the conclusions are valid for the time range and parameters analyzed.

Further studies involving other reactive aggregates and extended monitoring are recommended to validate the long-term implications of these findings and to better understand the action of the filler in the cementitious matrix.

CHAPTER 7 – CONCLUSION AND RECOMMENDATIONS

7.1 CONCLUSION

This study addressed the effect of AAR-reactive AMFs in reactive and non-reactive systems, focusing on the mesoscale. The main conclusions, valid for the conditions and materials studied, are presented as follows, considering the objectives proposed initially.

- **Current state of the art**

Since the discovery of AAR in the 1940s, some studies throughout the years have addressed the use of AAR-reactive AMFs. However, the effect of this material in concrete remains unclear. This can be related to the various tests and parameters adopted, which to vary owing to the different standards applied. Therefore, even when using the same test, the results are not comparable, as the standards and the specifications are different. Moreover, an important aspect that may have hindered the development of knowledge in this topic is the nomenclature, as the term used to refer to reactive fillers varies across studies. This study proposes the term AAR-reactive AMFs (which could be ASR- or ACR-reactive AMFs) for clarity.

Several tests have been used to assess the effect of AAR-reactive AMFs in mortar and concrete. In general, accelerated results indicated a reduction in expansion with the use of AMFs, whereas longer tests indicated the same or slightly increased expansions. Based on the results analyzed, the kinetics and ultimate expansion of systems containing AAR-reactive AMFs vary depending on the test used and the mortar/concrete system (e.g., containing reactive coarse aggregates, reactive fine aggregates, or non-reactive aggregates). Therefore, the evaluation of the same AMF in different types of systems and using a long-term test would be beneficial to better understand the influence of AMFs. Moreover, the progress of deterioration has barely been addressed in previous studies, and it has been evaluated only at the ultimate expansion. Thus, evaluating at different ages would be beneficial to understand the deterioration progress over time.

Several parameters were analyzed in studies, among which the role of mineralogy, PSD, and replacement strategy were considerably influential and discussed in details. The mineralogy of the source rock needs to be considered when evaluating the use of

AAR-reactive AMFs, such as the crushing process, which influences the dispersion of mineral grains and morphology of particles, and the alkali release. The effect of the PSD has not been completely understood, as results are conflicting. One hypothesis to explain such behaviour is the pessimum effect, which has also been studied, with some models proposed to explain it. When considering the studies in which AAR-reactive AMFs were used, different parameters were adopted as a measure of particle size, which hinders comparison. Considering the percentage of cement replaced, in general, the expansions reduce when the percentage increases, whereas the opposite occurs when the sand is replaced.

The knowledge gaps identified were the basis for the development of the experimental program developed in this study.

- **Use of ASR-reactive AMFs in reactive systems**

The impact of ASR-reactive AMFs on the expansion and deterioration progress of concrete containing either reactive coarse or fine aggregates was evaluated. The type of filler, PSD, and replacement percentage were varied to analyze the corresponding effect.

Based on the results, the use of ASR-reactive AMFs influenced expansion kinetics, particularly in the first 60 days, and damage development, particularly in systems containing reactive fine aggregates. In these systems, the presence of AMFs accelerated early expansion but led to earlier stabilization, likely due to rapid alkali consumption. In mixtures with reactive coarse aggregates, the reactive fillers delayed the onset of expansion. The alkalis appeared to react preferentially with the filler particles, reducing availability around the aggregate particles and thus slowing deterioration. Similar expansion values, microstructural and mechanical degradation were obtained for all combinations analyzed. Moreover, the parameters assessed (type of fillers, PSD, percentage) did not significantly influence the results for systems with reactive coarse aggregate. In contrast, percentage and the interaction between PSD and replacement percentage had a statistically significant effect on expansion in systems with reactive fine aggregates, confirming a synergistic role.

DRI values for both reactive systems were found to be lower than those for reactive systems with no fillers at equivalent expansion levels. However, the SDI values were consistent with the damage in systems with no fillers. This can be related to the cracks

induced by the reaction between alkalis and fillers to be thin and short, often below the DRI detection threshold. These microcracks may have contributed to increased SDI values. However, given the lower number of cracks in the aggregate particles, the modulus of elasticity loss was reduced compared to a system without ASR-reactive AMFs.

The CPT, in conjunction with SDT and DRI, was effective in differentiating the deterioration mechanisms across mixtures and in capturing subtle interactions between filler characteristics and ASR development.

Overall, the study demonstrates that ASR-reactive AMFs may be viable for cement replacement in reactive systems, considering the conditions that were applied in this study.

Despite the promising results obtained, the present study has some limitations. The explanations provided are based on microstructural and mechanical results. Microscopic and chemical tests should be conducted to confirm the findings. The alkali release by aggregates and ASR-reactive AMFs was not considered. Moreover, the conclusions are valid for the time range and parameters analyzed.

Further studies involving other reactive aggregates and extended monitoring are recommended to validate the long-term implications of these findings and to refine the mechanistic understanding of filler-induced alkali competition in reactive systems. The alkali release by the AAR-reactive fillers should also be assessed. Moreover, tests should be conducted with systems with no reactive aggregate to understand the isolated behaviour of the filler.

- **Use of ASR-reactive AMFs in non-reactive systems**

The effect of ASR-reactive AMFs on the ASR-induced expansion and deterioration in a non-reactive system was evaluated to identify the individual contribution of the filers. The results indicated that the action of the ASR-reactive AMFs was concentrated in the first 30 days. Fillers with PSD <75 μm reacted fast in the first 7 days, after which the expansion rate reduced. Fillers with PSD <150 μm in general experienced shrinkage, leading to slower expansion rate in the beginning that increased until reaching maximum values at 30 days. After 30 days, the expansion rate reduced and expansions stabilized at 60 days.

Finer fillers (<75 μm) led to higher expansions, opposite to theories on the action of AAR- reactive fillers in the literature, in which finer particles would react fast and the reaction product would dissipate in the cementitious matrix. This behaviour is probably related to the “pessimum effect”, where certain particle sizes maximize expansion

Despite some expansion, SDT and DRI results indicate negligible internal damage in all combinations analyzed. Moreover, all analyzed parameters (i.e., type of filler, PSD, and replacement percentage) significantly influenced ASR expansion. The interactions between these parameters also were significant to the expansion behaviour.

The CPT coupled with the multilevel assessment has showed to be an effective approach to analyze systems with ASR-reactive fillers, revealing that this material has potential to be used without compromising concrete durability, provided that the type of filler, fineness, and percentage of replacement are considered.

7.2 RECOMMENDATIONS FOR FUTURE STUDIES

Based on the results obtained and considering the aspects that need further analysis, the following topics are suggested for future studies:

- Extended monitoring of expansions and corresponding deterioration for reactive and non-reactive systems;
- Application of the extended DRI to analyze the length and width of cracks to confirm the hypothesis proposed in this study;
- Analysis of the alkali release by AAR-reactive AMFs in non-reactive systems;
- Analysis of the contribution of alkalis by both AAR-reactive AMFs and aggregates in reactive systems;
- Performance of microstructural/chemical tests for further analysis of the effect of AAR-reactive AMFs, such as evaluation of reaction product composition;
- Modelling of reactive and non-reactive systems with AAR-reactive AMFs;
- Evaluation of the structural behavior of concrete produced with AAR-reactive AMFs.

REFERENCES

ABD ELMOATY, A. E. M. Mechanical properties and corrosion resistance of concrete modified with granite dust. **Construction and Building Materials**, v. 47, p. 743–752, 2013.

ÅKESSON, U.; STIGH, J.; LINDQVIST, J. E.; GÖRANSSON, M. The influence of foliation on the fragility of granitic rocks, image analysis and quantitative microscopy. **Engineering Geology**, v. 68, p. 275–288, 2003.

ALVES, E. F. R.; CARMO, J. B. M.; SANTOS, M. C.; TRABOULSI, M. A. Comparative study on the expansion of molded concrete and mortar. *In*: Simpósio Sobre Reatividade Álcali-Agregado em Estruturas de Concreto, 1997, Goiânia. [...]. Goiânia: 1997.

AMERICAN ASSOCIATION OF STATE HIGHWAY AND TRANSPORTATION OFFICIALS. **AASHTO. T 380-22:** Standard Method of Test for Potential Alkali Reactivity of Aggregates and Effectiveness of ASR Mitigation Measures (Miniature Concrete Prism Test, MCPT). (AASHTO), 2022.

AMERICAN CONCRETE INSTITUTE. **Guide to durable concrete - ACI 201.2R-16**. Concrete Institute, 2016.

____. **Guide for Proportioning Concrete Mixtures with Ground Calcium Carbonate and Other Mineral Fillers**. 2020.

AMRAN, M.; MAKUL, N.; FEDIUK, R.; LEE, Y. H.; VATIN, N. I.; LEE, Y. Y.; MOHAMMED, K. Global carbon recoverability experiences from the cement industry. **Case Studies in Construction Materials**, v. 17, 1, 2022.

ANTUNES, L. R. **The Influence of Alternative Materials on Alkali Aggregate Reaction (AAR) Induced Development in Concrete**. Master's Thesis. University of Ottawa, Ottawa, 2021.

AQEL, M.; PANESAR, D. K. Hydration kinetics and compressive strength of steam-cured cement pastes and mortars containing limestone filler. **Construction and Building Materials**, v. 113, p. 359–368, 2016.

ASSOCIAÇÃO BRASILEIRA DE NORMAS TÉCNICAS. **ABNT NBR 16697:** Portland cement – Requirements. Rio de Janeiro. ABNT, 2018a.

____. **NBR 15577-4: Aggregates –Alkali-aggregate reactivity. Part 4:** Determination of expansion on mortar bars by accelerated mortar bar method. Rio de Janeiro. ABNT, 2018b.

____. **NBR 15577-6:** Aggregates –Alkali-aggregate reactivity. Part 6: Determination of mitigation of expansion on concrete prisms. Rio de Janeiro. ABNT, 2018c.

____. **NBR 15577-7:** Aggregates –Alkali-aggregate reactivity. Part 7: Determination of concrete prism by accelerated method. 2018d.

____. **NBR 15577-1**: Aggregates –Alkali-aggregate reactivity. Part 1: Guide for the evaluation of potential reactivity of aggregates and preventive measures for its use in concrete. Rio de Janeiro. ABNT, 2018e.

ASTM. **Practice for Estimating Concrete Strength by the Maturity Method**. West Conshohocken, PA: ASTM International, 2019.

ASTM. **ASTM C219:** Hydraulic and Other Inorganic Cements. West Conshohocken, PA: ASTM International, 2020.

ASTM. **C1260:** Test Method for Potential Alkali Reactivity of Aggregates (Mortar-Bar Method). West Conshohocken, PA. ASTM International, 2023a.

ASTM. **C1293:** Test Method for Determination of Length Change of Concrete Due to Alkali-Silica Reaction. West Conshohocken, PA. ASTM International, 2023b.

ASTM. **ASTM C1797:** Specification for Ground Calcium Carbonate and Aggregate Mineral Fillers for use in Hydraulic Cement Concrete**.** West Conshohocken, PA. ASTM International, 2024.

BALLAN, J.; PAONE, P. Supplementary Cementitious Materials: Concepts for the Treatment of Raw Materials. **IEEE Industry Applications Magazine**, v. 20, 2014.

BAŽANT, Z. P.; ZI, G.; MEYER, C. Fracture Mechanics of ASR in Concretes with Waste Glass Particles of Different Sizes. **Journal of Engineering Mechanics**, v. 126, n. 3, p. 226–232, 2000.

BEKTAS, F.; TURANLI, L.; TOPAL, T.; GONCUOGLU, M. C. Alkali reactivity of mortars containing chert and incorporating moderate-calcium fly ash. **Cement and Concrete Research**, v. 34, n. 12, p. 2209–2214, 2004.

BENTZ, D. P.; WEISS, W. J. Limestone Fillers Conserve Cement Part 2: Durability Issues and the Effects of Limestone Fineness on Mixtures. **Concrete International**, v. 31, n. 11, p. 35–46, 2009.

BERGMANN, A.; MEDEIROS, R.; OLAJIDE, O.; XIA, Z.; SANCHEZ, L. Performance of Conventional AAR-Reactivity Testing Methods to Evaluate Portland Limestone Cement Mixtures. *In*: SANCHEZ, L.; TROTTIER, C. **ICAAR 2024, RILEM Bookseries**. 1. ed. Springer, 2024. p. 229–238.

BERGMANN, A.; SANCHEZ, L. F. M. Assessing the reliability of laboratory test procedures for predicting concrete field performance against alkali-aggregate reaction (AAR). **Cement**, v. 19, p. 100133, 2025.

BERUBÉ, M. A.; DUCHESNE, J.; DORION, J. F.; RIVEST, M. Laboratory assessment of alkali contribution by aggregates to concrete and application to concrete structures affected by alkali – silica reactivity. **Cement and Concrete Research**, v. 32, p. 1215–1227, 2002.

BÉRUBÉ, M.; FOUNIER, B. Canadian experience with testing for alkali-aggregate reactivity in concrete. **Cement and Concrete Composites**, v. 15, n. 1–2, p. 27–47, 2003.

BEZERRA, A. **The Use of Artificial Intelligence for Assessing Damage in Concrete Affected by Alkali-Silica Reaction (ASR)**. Master's Thesis. University of Ottawa, Ottawa, 2021.

BODDY, A. M.; HOOTON, R. D.; THOMAS, M. D. A. The effect of the silica content of silica fume on its ability to control alkali–silica reaction. **Cement and Concrete Research**, v. 33, n. 8, p. 1263–1268, 2003.

BONAVETTI, V. L.; RAHHAL, V. F.; IRASSAR, E. F. Studies on the carboaluminate formation in limestone filler-blended cements. **Cement and Concrete Research**, v. 31, n. 6, p. 853–859, 2001.

BOUASKER, M.; MOUNANGA, P.; TURCRY, P.; LOUKILI, A.; KHELIDJ, A. Chemical shrinkage of cement pastes and mortars at very early age: Effect of limestone filler and granular inclusions. **Cement and Concrete Composites**, v. 30, n. 1, p. 13–22, 2008.

BOUQUETY, M. N.; DESCANTES, Y. Experimental study of crushed aggregate shape. **Construction and Building Materials**, v. 21, p. 865–872, 2007.

BRAGA, J. A.; ZANELLA, M. R.; ZALESKI, J. M.; ANDRIOLO, F. R. Use of rolled concrete - Capanda project - Angola - Special tests. *In*: XIX Seminário Nacional de Grandes Barragens, 1991, Aracaju. [...]. Aracaju: 1991. p. 353–385.

CAC, Cement Association of Canada, **Technical introduction to portland-limestone cement for municipal and provincial construction specifications**. 2023.

CARLES-GIBERGUES, A.; CYR, M.; MOISSON, M.; RINGOT, E. A simple way to mitigate alkali-silica reaction. **Materials and Structures/Materiaux et Constructions**, v. 41, n. 1, p. 73–83, 2008.

CASTRO, C. H.; SANTOS, M. C.; TRABOULSI, M. A.; BITTENCOURT, R. M. Influência do agregado pulverizado na reação álcali-agregado. Em: Simpósio Sobre Reatividade Álcali-Agregado em estruturas de Concreto, 1997, Goiânia. [...]. Goiânia: 1997.

CHRISP, T. M.; WALDRON, P.; WOOD, J. G. M. Development of a non-destructive test to quantify damage in deteriorated concrete. **Magazine of Concrete Research**, v. 45, n. 165, p. 247–256, 1993.

CHRISP, T. M.; WOOD, J. G. M.; NORRIS, P. Towards quantification of microstructural damage in AAR deteriorated concrete. (S. P. Shah, S. E. Swartz, B. Barr) *In*: International Conference on Recent Developments on the Fracture of Concrete and Rock, 1993, [...]. Taylor & Francis, 1993.

COUTINHO, Y. **Influence of the grinding process of aggregates on AAR expansions (in Portuguese)**. 2019. Master's Thesis. Universidade Federal de Pernambuco, 2019.

COUTINHO, Y.; MONTEFALCO, L.; CARNEIRO, A. Influence of aggregate crushing on the results of accelerated alkali-silica reactivity tests. **Construction and Building Materials**, v. 325, 28 mar. 2022.

COUTINHO, Y.; MONTEFALCO, L.; CARNEIRO, A. Evaluation of ASR-Reactive Aggregate Powder on ASR Expansions of Mortars and Concretes Using AMBT and MCPT. *In*: SANCHEZ, L. F.; TROTTIER, C. **Proceedings of the 17th International Conference on Alkali-Aggregate Reaction in Concrete. ICAAR 2024.** [s.l.] Springer, 2024. p. 604–611.

CRAEYE, B.; DE SCHUTTER, G.; DESMET, B.; VANTOMME, J.; HEIRMAN, G.; VANDEWALLE, L.; CIZER, Ö.; AGGOUN, S.; KADRI, E. H. Effect of mineral filler type on autogenous shrinkage of self-compacting concrete. **Cement and Concrete Research**, v. 40, n. 6, p. 908–913, 2010.

CSA. **A23.1:24/CSA A23.2:24 Concrete materials and methods of concrete construction/Test Methods and Standard Practices for concrete.** 2024.

CYR, M.; RIVARD, P.; LABRECQUE, F. Reduction of ASR-expansion using powders ground from various sources of reactive aggregates. **Cement and Concrete Composites**, v. 31, n. 7, p. 438–446, 2009.

DAMTOFT, J. S.; LUKASIK, J.; HERFORT, D.; SORRENTINO, D.; GARTNER, E. M. Sustainable development and climate change initiatives. **Cement and Concrete Research**, v. 38, n. 2, p. 115–127, 2008.

DE GRAZIA, M. T. **Short and long-term performance of eco-efficient concrete mixtures**. 2023. PhD Thesis. University of Ottawa, Ottawa, 2023.

DE GRAZIA, M. T.; SANCHEZ, L. F. M. “Enhancing the Journey towards Concrete Net Zero: The Role of Eco-Efficient Concrete, Particle Packing Models, and Limestone Fillers”. *In*: SP-362: ICCM2024, 2024, [...]. American Concrete Institute, 2024. p. 901–915.

DE SOUZA, D. J.; SANCHEZ, L. F. M.; BIPARVA, A. Assessment of the efficiency of distinct surface treatments to mitigate ASR-induced development. **Construction and Building Materials**, v. 456, 20, 2024.

DE WEERDT, K.; HAHA, M. Ben; LE SAOUT, G.; KJELLSEN, K. O.; JUSTNES, H.; LOTHENBACH, B. Hydration mechanisms of ternary Portland cements containing limestone powder and fly ash. **Cement and Concrete Research**, v. 41, n. 3, p. 279–291, 2011.

DEMERCHANT, D. P.; FOURNIER, B.; STRANG, F. Alkali-aggregate research in New Brunswick. **Canadian Journal of Civil Engineering**, v. 27, p. 212–225, 2000.

DIAMOND, S. Alkali Silica Reactions-Some Paradoxes. **Cement and Concrete Composites**, v. 19, p. 391–401, 1997.

DIAMOND, S.; THAULOW, N. A study of expansion due to alkali - silica reaction as conditioned by the grain size of the reactive aggregate. **Cement and Concrete Research**, v. 4, p. 591–607, 1974.

DIÓGENES, L.; MAIA, R.; BESSA, I.; CASTELO BRANCO, V.; NOGUEIRA NETO, J.; SILVA, F. The influence of crushing processes and mineralogy of aggregates on their shape properties and susceptibility to degradation. **Construction and Building Materials**, v. 284, 2021.

DOBISZEWSKA, M.; SCHINDLER, A. K.; PICHÓR, W. Mechanical properties and interfacial transition zone microstructure of concrete with waste basalt powder addition. **Construction and Building Materials**, v. 177, p. 222–229, 2018.

DU, H.; PANG, S. D. High-performance concrete incorporating calcined kaolin clay and limestone as cement substitute. **Construction and Building Materials**, v. 264, p. 120152, 2020.

DYER, T. **Concrete Durability**. Boca Raton: CRC Press, 2014. 43 p.

EUROPEAN CEMENT RESEARCH ACADEMY. **CSI/ECRA - Technology Papers 2017 Development of State of the Art Techniques in Cement Manufacturing: Trying to Look Ahead**. 2017.

FERRAZ, A. R.; FERNANDES, I.; SOARES, D.; SILVA, A. S.; QUINTA-FERREIRA, M. Assessment of the Alteration of Granitic Rocks and its Influence on Alkalis Release. **IOP Conference Series: Earth and Environmental Science**, v. 95, 2017.

FIGUEIRÔA, J. P.; ANDRADE, T. **O Ataque da Reação Álcali-Agregado sobre as Estruturas de Concreto**. Recife: Editora Universitária UFPE, 2007. 228 p.

FOURNIER, B.; BÉRUBÉ, M. Alkali-aggregate reaction in concrete: a review of basic concepts and engineering implications. **Canadian Journal of Civil Engineering**, v. 27, n. 2, p. 167–191, 2011.

FOURNIER, B.; BERUBÉ, M. A. Alkali-aggregate reaction in concrete: A review of basic concepts and engineering implications. **Canadian Journal of Civil Engineering**, v. 27, p. 167–191, 2000.

GARTNER, E.; HIRAO, H. A review of alternative approaches to the reduction of CO_2 emissions associated with the manufacture of the binder phase in concrete. **Cement and Concrete Research**, v. 78, p. 126–142, 2015.

GCCA. **Concrete Future - The GCCA 2050 Cement and Concrete Industry Roadmap for Net Zero Concrete**. 2021.

GOLMAKANI, F.; HOOTON, R. D. Comparison of laboratory performance tests used to assess alkali-silica reactivity. *In*: Annual Conference - Canadian Society for Civil Engineering, 2016, [...]. 2016. v. 2, p. 1–7.

GOLTERMANN, P. Mechanical Predictions of Concrete Deterioration-Part 2: Classification of Crack Patterns. **ACI Materials Journal**, v. 92, n. 1, p. 58–62, 1995.

GRATTAN-BELLEW, P. E.; DANAY, A. Comparison of laboratory and field evaluation of alkali-silica reaction in large dams. **Collection: NRC Publications Archive/ Archives des publications du CNRC**, p. 1–25, 1992.

GRATTAN-BELLEW, P. E. A critical review of ultra-accelerated alkali-silica reactivity. **Cement and Concrete Composites**, v. 19, p. 403–414, 1997.

GRATTAN-BELLEW, P. E.; MITCHELL, L. D.; MARGESON, J.; MIN, D. Is alkali – carbonate reaction just a variant of alkali – silica reaction ACR = ASR? **Cement and Concrete Research**, v. 40, n. 4, p. 556–562, 2010.

GUDMUNDSSON, G.; OLAFSSON, H. Alkali-silica reactions and silica fume: 20 years of experience in Iceland. **Cement and Concrete Research**, v. 29, n. 8, p. 1289–1297, 1999.

GUÉDON-DUBIED, J.-S.; CADORET, G.; DURIEUX, V.; MARTINEAU, F.; FASSEU, P.; VAN OVERBEKE, V. Étude du calcaire Tournaisien de la carrière Cimescaut à Antoing (Belgique) Analyse pétrographique et chimique et réactivité aux alcalins. **Bull. Lab. Ponts et Chaussées**, v. 226, p. 57–66, 2000.

HANZIC, L.; HO, J. C. M. Multi-sized fillers to improve strength and flowability of concrete. **Advances in Cement Research**, v. 29, n. 3, p. 112–124, 2017.

HOBBS, D. W.; GUTTERIDGE, W. A. Particle size of aggregate and its influence upon the expansion caused by the alkali-silica reaction. **Magazine of Concrete Research**, v. 31, n. 109, p. 235–242, 1979.

HOU, X.; STRUBLE, L. J.; KIRKPATRICK, R. J. Formation of ASR gel and the roles of C-S-H and portlandite. **Cement and Concrete Research**, v. 34, n. 9, p. 1683–1696, 2004.

IDEKER, J. H.; BENTIVEGNA, A. F.; FOLLIARD, K. J.; JUENGER, M. C. G. Do current laboratory test methods accurately predict alkali-silica reactivity? **ACI Materials Journal**, v. 109, n. 4, p. 395–402, 2012.

IDEKER, J. H.; EAST, B. L.; FOLLIARD, K. J.; THOMAS, M. D. A.; FOURNIER, B. The current state of the accelerated concrete prism test. **Cement and Concrete Research**, v. 40, n. 4, p. 550–555, 2010.

IEA. **Energy Technology Perspectives 2020**. 2020.

IEA. **Net Zero by 2050 - A Roadmap for the Global Energy Sector**. 2021.

JOHN, V. M.; DAMINELI, B. L.; QUATTRONE, M.; PILEGGI, R. G. Fillers in cementitious materials — Experience, recent advances and future potential. **Cement and Concrete Research,** v. 114, p. 65–78, 2018.

KADRI, E. H.; AGGOUN, S.; DE SCHUTTER, G.; EZZIANE, K. Combined effect of chemical nature and fineness of mineral powders on Portland cement hydration. **Materials and Structures/Materiaux et Constructions**, v. 43, n. 5, p. 665–673, 2010.

KATAYAMA, T. A critical review of carbonate rock reactions — is their reactivity useful or harmful? *In*: Proceedings of the 9th International Conference on Alkali-Aggregate Reaction, 1992, [...]. 1992. p. 508–517.

KATAYAMA, T. The so-called alkali-carbonate reaction (ACR) - Its mineralogical and geochemical details, with special reference to ASR. **Cement and Concrete Research**, v. 40, n. 4, p. 643–675, 2010.

KATAYAMA, T.; GRATTAN-BELLEW, P. E. Petrography of the Kingston Experimental Sidewalk at Age 22 Years - ASR as the Cause of Deleteriously Expansive, So-called Alkali-Carbonate Reaction. *In*: Proceedings of the 14th International Conference on Alkali-Aggregate Reaction in Concrete, 2012, Austin, Texas, USA. [...]. Austin, Texas, USA: 2012.

KOMBA, J.; MGANGIRA, M. B.; MOHALE, L. Investigation of the effects of the type of crusher on coarse aggregate shape properties using the three-dimensional laser scanning technique. **Geo-China**, p. 125–132, 2016.

KORPA, A.; KOWALD, T.; TRETTIN, R. Hydration behaviour, structure and morphology of hydration phases in advanced cement-based systems containing micro and nanoscale pozzolanic additives. **Cement and Concrete Research**, v. 38, n. 7, p. 955–962, 2008.

KUMAR, A.; OEY, T.; KIM, S.; THOMAS, D.; BADRAN, S.; LI, J.; FERNANDES, F.; NEITHALATH, N.; SANT, G. Simple methods to estimate the influence of limestone fillers on reaction and property evolution in cementitious materials. **Cement and Concrete Composites**, v. 42, p. 20–29, 2013.

KUO, W. Ten; SHU, C. Y. Effect of particle size and curing temperature on expansion reaction in electric arc furnace oxidizing slag aggregate concrete. **Construction and Building Materials**, v. 94, p. 488–493, 2015.

LEEMANN, A.; GÓRA, M.; LOTHENBACH, B.; HEUBERGER, M. Alkali silica reaction in concrete - Revealing the expansion mechanism by surface force measurements. **Cement and Concrete Research**, v. 176, p. 107392, 1 fev. 2024a.

LEEMANN, A.; HOLZER, L. Alkali-aggregate reaction-identifying reactive silicates in complex aggregates by ESEM observation of dissolution features. **Cement and Concrete Composites**, v. 27, p. 796–801, 2005.

LEEMANN, A.; LOTHENBACH, B. The influence of potassium–sodium ratio in cement on concrete expansion due to alkali-aggregate reaction. **Cement and Concrete Research**, v. 38, n. 10, p. 1162–1168, 1 out. 2008.

LEEMANN, A.; MÜNCH, B.; TROTTIER, C.; SANCHEZ, L. Microstructural Consequences of Alkali-Carbonate Reaction. *Em*: SANCHEZ, L.; TROTTIER, C. **Proceedings of the 17th International Conference on Alkali-Aggregate Reaction in Concrete**. RILEM Bookseries, Springer, 2024b. p. 87–94.

LI, C.; JIANG, L.; XU, N.; JIANG, S. Pore structure and permeability of concrete with high volume of limestone powder addition. **Powder Technology**, v. 338, p. 416–424, 2018.

LI, Y.; HE, Z.; HU, S. Mechanism of suppressing ASR using ground reactive sandstone powders instead of cement. **Journal Wuhan University of Technology, Materials Science Edition**, v. 30, n. 2, p. 344–351, 2015.

LI, Y.; ZENG, X.; ZHOU, J.; SHI, Y.; UMAR, H. A.; LONG, G.; XIE, Y. Development of an eco-friendly ultra-high performance concrete based on waste basalt powder for Sichuan-Tibet Railway. **Journal of Cleaner Production**, v. 312, p. 127775, 2021.

LINDGÅRD, J.; ANDIÇ-ÇAKIR, Ö.; BORCHERS, I.; BROEKMANS, M.; BROUARD, E.; FERNANDES, I.; GIEBSON, C.; PEDERSEN, B.; PIERRE, C.; RØNNING, T. F.; THOMAS, M. D. A.; WIGUM, J. **RILEM TC 219-ACS-P: Literature survey on performance testing** (J. Lindgård). 2011.

LINDGÅRD, J.; ANDIÇ-ÇAKIR, Ö.; FERNANDES, I.; RØNNING, T. F.; THOMAS, M. D. A. Alkali–silica reactions (ASR): Literature review on parameters influencing laboratory performance testing. **Cement and Concrete Research**, v. 42, n. 2, p. 223–243, 2012.

LOTHENBACH, B.; MATSCHEI, T.; MÖSCHNER, G.; GLASSER, F. P. Thermodynamic modelling of the effect of temperature on the hydration and porosity of Portland cement. **Cement and Concrete Research**, v. 38, n. 1, p. 1–18, 2008.

LOTHENBACH, B.; SCRIVENER, K.; HOOTON, R. D. Supplementary cementitious materials. **Cement and Concrete Research**, v. 41, n. 12, p. 1244–1256, 2011.

LUDWIG, H. M.; ZHANG, W. Research review of cement clinker chemistry. **Cement and Concrete Research**, v. 78, p. 24–37, 2015.

Mactaquac Dam. Available at: <https://mynewbrunswick.ca/mactaquac-dam/>. Access: 16 February 2025.

MÁRMOL, I.; BALLESTER, P.; CERRO, S.; MONRÓS, G.; MORALES, J.; SÁNCHEZ, L. Use of granite sludge wastes for the production of coloured cement-based mortars. **Cement and Concrete Composites**, v. 32, n. 8, p. 617–622, 2010.

MARUSIN, S. L.; SHOTWELL, L. B. Alkali-Silica Reaction in Concrete Caused by Densified Silica Fume Lumps: A Case Study. **Ceent, Concrete, and Aggregates**, v. 20, n. 2, p. 90–94, 2000.

MARUYAMA, I.; SUGIMOTO, H.; UMEKI, S.; KURIHARA, R. Effect of fineness of cement on drying shrinkage. **Cement and Concrete Research**, v. 161, p. 106961, 2022.

MAYFIELD, L. L. Limestone Additions to Portland Cement Old Controversy Revisited*. *In*: KLIEGER, P.; HOOTON, R. D. **Carbonate Additions to Cement, ASTMSTP 1064**. Philadelphia: American Society for Testing and Materials, 1990. p. 3–13.

MEDEIROS, R.; SANCHEZ, L.; DOS SANTOS, A. C. Assessing Alkali-Carbonate Reaction-Induced Damage in Critical Concrete Infrastructure: The First ACR-Affected Field Structure Reported in Brazil. *In*: SANCHEZ, L.; TROTTIER, C. **Proceedings of the 17th International Conference on Alkali-Aggregate Reaction in Concrete. ICAAR 2024.** Springer, 2024. p. 445–452.

MEISSNER, H. S. Pozzolans used in mass concrete. (T. Stanton, R. Blanks) *In*: Symp. Use Pozzolanic Mater. Mortars Concr., 1950, West Conshohocken. [...]. West Conshohocken: ASTM International, 1950. p. 16–30.

MENÉNDEZ, E.; SANTOS-SILVA, A.; FERNANDES, I.; DUCHESNE, J.; BERRA, M.; DE WEERDT, K.; SALEM, Y.; GARCÍA-ROVÉS, R.; SOARES, D.; FOURNIER, B.; MANGIALARDI, T.; LINDGÅRD, J. RILEM TC 258-AAA Round Robin Test: Alkali release from aggregates and petrographic analysis. Critical review of the test method AAR-8. **Materiales de Construcción**, v. 72, n. 346, e279, 2022. https://doi.org/10.3989/mc.2022.17021.

MILLER, S. A.; HABERT, G.; MYERS, R. J.; HARVEY, J. T. Achieving net zero greenhouse gas emissions in the cement industry via value chain mitigation strategies. **One Earth**, v. 4, n. 10, p. 1398–1411, 2021.

MOHAMMADI, A.; GHIASVAND, E.; NILI, M. Relation between mechanical properties of concrete and alkali-silica reaction (ASR): A review. **Construction and Building Materials**, v. 258, p. 119567, 2020.

MOOSBERG-BUSTNES, H.; LAGERBLAD, B.; FORSSBERG, E. **The function of fillers in concrete**. Materials and Structures, v. 34, p. 74–81, 2004.

MULTON, S.; CYR, M.; SELLIER, A.; DIEDERICH, P.; PETIT, L. Effects of aggregate size and alkali content on ASR expansion. **Cement and Concrete Research**, v. 40, p. 508–516, 2010.

NIXON, P. J.; SIMS, I. **RILEM Recommendations for the Prevention of Damage by Alkali-Aggregate Reactions in New Concrete Structures. State-of-the-Art-Report of the RILEM Technical Committee 219 ACS.** Springer, 2016.

OLIVEIRA, P. J.; SALLES, F. M.; ANDRIOLO, F. R. Crushed powder filler - The use on RCC and the reduction of expansion due to the alkali-aggregate reaction. *In*: International Symposium of Roller Compacted Concrete Dams, 1995, Santander - Spain. [...]. Santander - Spain: 1995.

PALM, S.; PROSKE, T.; REZVANI, M.; HAINER, S.; MÜLLER, C.; GRAUBNER, C. A. Cements with a high limestone content - Mechanical properties, durability and ecological characteristics of the concrete. **Construction and Building Materials**, v. 119, p. 308–318, 2016.

PANG, L.; WU, S.; ZHU, J.; WAN, L. Relationship between Petrographical and Physical Properties of Aggregates. **Journal of Wuhan University of Technology-Mater. Sci.**, v. 25, n. 4, p. 678–681, 2010.

PEDERSEN, B. **Alkali-reactive and inert fillers in Concrete. Rheology of fresh Mixtures and expansive Reactions.** 2004. Norwegian University of Science and Technology, 2004.

PEDERSEN, B. M.; WIGUM, B. J.; LINDGÅRD, J. Influence of Aggregate Particle Size on The Alkali-Silica Reaction-A Literature Review. (H. M. Bernardes, N. Hasparyk) *In*: 15th International Conference on Alkali Aggregate Reaction in Concrete, 2016, São Paulo, Brazil. [...]. São Paulo, Brazil: 2016.

POPPE, A. M.; DE SCHUTTER, G. Cement hydration in the presence of high filler contents. **Cement and Concrete Research**, v. 35, n. 12, p. 2290–2299, 2005.

QINGHAN, B.; XUEQUAN, W.; MINGSHU, T.; NISHIBAYASHI, S.; KURODA, T.; TIECHENG, W. Effect of Reactive Aggregate Powder on Suppressing Expansion due to Alkali-Silica Reaction. *In*: Proceedings of the 10th International Conference on AAR in concrete, 1996, Melbourne, Australia. [...]. Melbourne, Australia: 1996. p. 546–553.

QIU, X.; CHEN, J.; YE, G.; DE SCHUTTER, G. Insights in the chemical fundamentals of ASR and the role of calcium in the early stage based on a 3D reactive transport model. **Cement and Concrete Research**, v. 157, 2022.

RAHHAL, V.; TALERO, R. Early hydration of portland cement with crystalline mineral additions. **Cement and Concrete Research**, v. 35, n. 7, p. 1285–1291, 2005.

RÄISÄNEN, M.; MERTAMO, M. An evaluation of the procedure and results of laboratory crushing in quality assessment of rock aggregate raw materials. **Bulletin of Engineering Geology and the Environment**, v. 63, n. 1, p. 33–39, 2004.

RAMOS, T.; MATOS, A. M.; SCHMIDT, B.; RIO, J.; SOUSA-COUTINHO, J. Granitic quarry sludge waste in mortar: Effect on strength and durability. **Construction and Building Materials**, v. 47, p. 1001–1009, 2013.

RAMYAR, K.; TOPAL, A.; ANDIÇ, Ö. Effects of aggregate size and angularity on alkali–silica reaction. **Cement and Concrete Research**, v. 35, n. 11, p. 2165–2169, 2005.

REZAIEH, A. Z. **Evaluating ASR physicochemical process under distinct restraint conditions for a better assessment of affected concrete infrastructure**. PhD Thesis. University of Ottawa, Ottawa, 2021.

SALLES, F. M.; OLIVEIRA, P. J. R.; ANDRIOLO, F. R. Use of crushing fines to reduce AAR-expansions (in Portuguese). *In*: Simpósio Sobre Reatividade Álcali-Agregado em Estruturas de Concreto, 1997, Goiânia. [...]. Goiânia: 1997.

SANCHEZ, L. **Contribution to the assessment of damage in aging concrete infrastructures affected by alkali-aggregate reaction**. PhD Thesis. Université Laval, 2014.

SANCHEZ, L. F. M.; DRIMALAS, T.; FOURNIER, B.; MITCHELL, D.; BASTIEN, J. Comprehensive damage assessment in concrete affected by different internal swelling reaction (ISR) mechanisms. **Cement and Concrete Research**, v. 107, p. 284–303, 2018.

SANCHEZ, L. F. M.; FOURNIER, B.; JOLIN, M.; BASTIEN, J. Evaluation of the stiffness damage test (SDT) as a tool for assessing damage in concrete due to ASR: Test loading and output responses for concretes incorporating fine or coarse reactive aggregates. **Cement and Concrete Research**, v. 56, p. 213–229, 2014.

SANCHEZ, L. F. M.; FOURNIER, B.; JOLIN, M.; BEDOYA, M. A. B.; BASTIEN, J.; DUCHESNE, J. Use of Damage Rating Index to quantify alkali-silica reaction damage in concrete: Fine versus coarse aggregate. **ACI Materials Journal**, v. 113, n. 4, p. 395–407, 2016.

SANCHEZ, L. F. M.; FOURNIER, B.; JOLIN, M.; DUCHESNE, J. Reliable quantification of AAR damage through assessment of the Damage Rating Index (DRI). **Cement and Concrete Research**, v. 67, p. 74–92, 2015.

SANCHEZ, L. F. M.; FOURNIER, B.; JOLIN, M.; MITCHELL, D.; BASTIEN, J. Overall assessment of Alkali-Aggregate Reaction (AAR) in concretes presenting different strengths and incorporating a wide range of reactive aggregate types and natures. **Cement and Concrete Research**, v. 93, p. 17–31, 2017.

SCRIVENER, K.; JOHN, V.; GARTNER, E. Eco-efficient cements: Potential economically viable solutions for a low-CO2 cement-based materials industry. **Cement and Concrete Research**, v. 114, n. February, p. 2–26, 2018.

SCRIVENER, K.; MARTIRENA, F.; BISHNOI, S.; MAITY, S. Calcined clay limestone cements (LC3). **Cement and Concrete Research**, v. 114, p. 49–56, 2018.

SEKRANE, N. Z.; ASROUN, A. Modelling the effects of aggregate size on alkali aggregate reaction expansion. **Technology & Applied Science Research**, v. 4, n. 3, p. 656–661, 2014.

SHAFAATIAN, S. M. H.; AKHAVAN, A.; MARAGHECHI, H.; RAJABIPOUR, F. How does fly ash mitigate alkali-silica reaction (ASR) in accelerated mortar bar test (ASTM C1567)? **Cement and Concrete Composites**, v. 37, n. 1, p. 143–153, mar. 2013.

SHAO, Y.; LEFORT, T.; MORAS, S.; RODRIGUEZ, D. Studies on concrete containing ground waste glass. **Cement and Concrete Research**, v. 30, n. 1, p. 91–100, 2000.

SHAYAN, A. The “Pessimum” Effect in an Accelerated Mortar Bar Test Using 1M NaOH Solution at 80°C. **Cement & Concrete Composites**, v. 14, p. 249–255, 1992.

SIMS, I.; POOLE, A. **Alkali-Aggregate Reaction in Concrete - A World Review**. London: CRC Press, 2017. 768 p.

SMAOUI, N.; BÉRUBÉ, M.-A.; FOURNIER, B.; BISSONNETTE, B.; DURAND, B. Evaluation of the expansion attained to date by concrete affected by alkali–silica reaction. Part I: Experimental study. **Canadian Journal of Civil Engineering**, v. 31, n. 5, p. 826–845, 2004.

SOARES, D.; SILVA, A. S.; MIRÃO, J.; FERNANDES, I.; MENÉNDEZ, E. Study on the factors affecting alkalis release from aggregates into ASR. (N. P. HASPARYK, H. M. BERNARDES) *In*: The 15th Conference on Alkali-Aggregate Reaction in Concrete, 2016, São Paulo. [...]. São Paulo: 2016.

SOROKA, I.; SETTER, N. The effect of fillers on strength of cement mortars. **Cement and Concrete Research**, v. 7, n. 4, p. 449–456, 1977.

SOUZA, D. J. **Avoiding & mitigating alkali-aggregate reaction (AAR) in concrete structures**. PhD Thesis. University of Ottawa, Ottawa, 2022.

STANTON, T. Expansion of Concrete through Reaction between Cement and Aggregate. **Proceedings of American Society of Civil Engineers**, v. 66, n. 10, p. 1781–1811, 1940.

SUWITO, A.; JIN, W.; XI, Y.; MEYER, C. A Mathematical Model for the Pessimum Size Effect of ASR in Concrete. **Concrete Science and Engineering**, v. 4, n. 13, p. 23–34, 2002.

TAPAS, M. J.; THOMAS, P.; VESSALAS, K.; NSIAH-BAAFI, E.; MARTIN, L.; SIRIVIVATNANON, V. Comparative study of the efficacy of fly ash and reactive aggregate powders in mitigating alkali-silica reaction. **Journal of Building Engineering**, v. 63, 2023.

TAYLOR, H. F. W. **Cement chemistry**. 2. ed. London: Thomas Telford, 1997. 469 p.

THOMAS, M. The effect of supplementary cementing materials on alkali-silica reaction: A review. **Cement and Concrete Research**, v. 41, n. 12, p. 1224–1231, 2011.

THOMAS, M. D. A.; FOURNIER, B.; FOLLIARD, K. J. **Alkali-Aggregate Reactivity (AAR) Facts Book**. Federal Highway Administration. 2013.

THOMAS, M.; FOURNIER, B.; FOLLIARD, K.; IDEKER, J.; SHEHATA, M. Test methods for evaluating preventive measures for controlling expansion due to alkali-silica reaction in concrete. **Cement and Concrete Research**, v. 36, p. 1842–1856, 2006.

TIA, M.; CHUNG, H.-W.; SUBGRANON, T. **Phase II - Reducing Portland Cement Content and Improving Concrete Durability**. University of Florida. 2021.

US BUREAU OF RECLAMATION. **Elephant Butte Dam**. Available at: <https://www.usbr.gov/projects/index.php?id=94>. Access: 23 October 2024a.

US BUREAU OF RECLAMATION. **Arrowrock Dam**. Available at: <https://www.usbr.gov/projects/index.php?id=6>. Access: 23 October 2024b.

VALDUGA, L. **Influence of procedure conditions of ASTM C 1260 in the verification of alkali-aggregate reation (in Portuguese)**. PhD Thesis. Universidade Federal do Rio Grande do Sul, 2007.

VARDHAN, K.; GOYAL, S.; SIDDIQUE, R.; SINGH, M. Mechanical properties and microstructural analysis of cement mortar incorporating marble powder as partial replacement of cement. **Construction and Building Materials**, v. 96, p. 615–621, 2015.

VILLENEUVE, V. **Détermination de l'endommagement du béton par méthode pétrographique quantitative**. Master's Thesis, Université Laval, 2011.

VIVIAN, H. E. Studies in cement-aggregate reaction. XIX: The effect on mortar expansion of the particle size of the reactive component in the aggregate. **Australian Journal of Applied Science**, v. 2, n. 4, p. 488–494, 1951.

VON GREVE-DIERFELD, S.; LOTHENBACH, B.; VOLLPRACHT, A.; WU, B.; HUET, B.; ANDRADE, C.; MEDINA, C.; THIEL, C.; GRUYAERT, E.; VANOUTRIVE, H.; SAÉZ DEL BOSQUE, I.; IGNJATOVIC, I.; ELSEN, J.; PROVIS, J. L.; SCRIVENER, K.; THIENEL, K.; SIDERIS, K.; ZAJAC, M.; ALDERETE, N.; CIZER, Ö.; VAN DEN HEEDE, P.; HOOTON, R.; KAMALI-BERNARD, S.; BERNAL, S.; ZHAO, Z.; SHI, Z.; DE BELIE, N. Understanding the carbonation of concrete with supplementary cementitious materials: a critical review by RILEM TC 281-CCC. **Materials and Structures/Materiaux et Constructions**, v. 53, n. 6, 2020.

WALSH, J. B. The effect of cracks on the uniaxial elastic compression of rocks. **Journal of Geophysical Research**, v. 70, n. 2, p. 399–411, 1965.

WANG, D.; SHI, C.; FARZADNIA, N.; SHI, Z.; JIA, H. A review on effects of limestone powder on the properties of concrete. **Construction and Building Materials**, v. 192, p. 153–166, 2018.

WANG, Y.; YU, G.; DENG, M.; TANG, M.; LU, D. The use of thermodynamic analysis in assessing alkali contribution by alkaline minerals in concrete. **Cement and Concrete Composites**, v. 30, p. 353–359, 2008.

XIA, Z.; BERGMANN, A.; SANCHEZ, L. Assessment of Alkali-Silica Reaction Development in High Limestone Replacement Portland-Limestone Mortar and Concrete. *In*: SANCHEZ, L.; TROTTIER, C. **ICAAR 2024, Rilem Bookseries**. Springer, 2024. p. 710–717.

XIE, D.; LIU, Q.; ZHOU, Z.; GAO, J.; LIU, C. Rheology and hardened properties of eco-friendly ultra-high performance concrete paste: Role of waste stone powder fillers. **Construction and Building Materials**, v. 447, p. 138163, 2024.

YE, G.; LIU, X.; DE SCHUTTER, G.; POPPE, A. M.; TAERWE, L. Influence of limestone powder used as filler in SCC on hydration and microstructure of cement pastes. **Cement and Concrete Composites**, v. 29, n. 2, p. 94–102, 2007.

ZHANG, C.; WANG, A.; TANG, M.; WU, B.; ZHANG, N. Influence of aggregate size and aggregate size grading on ASR expansion. **Cement and Concrete Research**, v. 29, p. 1393–1396, 1999.

ZHANG, X.; GRAVEST, G. W. The alkali-silica reaction in OPe/silica glass mortar with particular reference to pessimum effects. **Advances in Cement Research**, v. 3, n. 9, p. 9–13, 1990.

ZHU, Y.; WANG, P.; GUO, H.; LOU, R.; YE, W.; LIU, Y.; LIU, K. Effect of dry process manufactured sands dust on the mechanical property and durability of recycled concrete. **Journal of Building Engineering**, v. 87, p. 108942, 2024.

ZHU, Y.; ZAHEDI, A.; SANCHEZ, L. F. M.; FOURNIER, B.; BEAUCHEMIN, S. Overall assessment of alkali-silica reaction affected recycled concrete aggregate mixtures derived from construction and demolition waste. **Cement and Concrete Research**, v. 142, p. 106350, 2021.

ZUBAIDA, N. **Evaluation of the potential of residual expansion of concrete affected by alkali aggregate reaction**. Master's Thesis. University of Ottawa, Ottawa, 2020.

APPENDIX A

In this appendix, some tables that summarize data collected in this study are provided as additional support.

Table A1 summarizes the ultimate expansion results and important conditions of the studies evaluated.

Table A1 – Summary of ultimate expansions in the studies assessed.

	Ultimate expansion	Reduction	Test	Condition
Greywacke (TAPAS *et al.*, 2023)	0.11 (coarse)	77%	AMBT	25% replacing cement Systems with coarse and fine reactive aggregates
	0.12 (fine)	74%		
Dacite (TAPAS *et al.*, 2023)	0.21	56%	AMBT	25% replacing cement
Sandstone Capanda (CASTRO *et al.*, 1997)	0.17 (20%)	7%	NBRI method modified	Replacement of cement
	0.11 (40%)	39%		
	0.05 (60%)	72%		
Sandstone Formosa (CASTRO *et al.*, 1997)	0.40 (20%)	19%	NBRI method modified	Replacement of cement
	0.28 (40%)	43%		
	0.11 (60%)	77%		
	0.04 (80%)	91%		
Orthogneiss (COUTINHO; MONTEFALCO; CARNEIRO, 2024)	0.12 (10%)	65%	AMBT	Replacement of cement
	0.09 (20%)	74%		
Basalt (OLIVEIRA; SALLES; ANDRIOLO, 1995)	0.35 (10%)	24%	NBRI method	Replacement of cement
	0.28 (20%)	39%		
	0.18 (30%)	61%		
Greywacke (ANTUNES, 2021)	0.41 (15% sand – coarse)	-14% (increment)	Accelerated CPT	Replacement of sand and cement. Systems with coarse and fine reactive aggregates
	0.38 (15% cement – coarse)	-6% (increment)		
	0.57 (15% sand – fine)	-14% (increment)		
	0.47 (15% sand – fine)	6%		

	Ultimate expansion	Reduction	Test	Condition
Dolomitic argillaceous limestone (ANTUNES, 2021)	0.37 (coarse)	-3% (increment)	Accelerated CPT	15% replacing sand. Systems with coarse and fine reactive aggregates
	0.53 (fine)	-6% (increment)		
Siliceous limestone (GUÉDON-DUBIED *et al.*, 2000)	0.03 (15%)	49%	CPT (French standard)	50% replacing cement and 50% replacing sand
	0.03 (30%	55%		
Metaquartzite (CARLES-GIBERGUES *et al.*, 2008)	0.03	89%	CPT (French standard)	20% replacing sand Blaine fineness: 400 m^2/kg
Siliceous limestone (CARLES-GIBERGUES *et al.*, 2008)	0.128	36%	CPT (French standard)	20% replacing sand Blaine fineness: 600 m^2/kg
Opaline aggregate (CARLES-GIBERGUES *et al.*, 2008)	0.01	96%	CPT (French standard)	20% replacing sand Blaine fineness: 650 m^2/kg Only 36% of the aggregate used was opal, the remainder was non-reactive aggregate.
Mylonite (PEDERSEN, 2004)	0.311 (10% 0–20)	46%	AMBT (Norwegian standard)	When not mentioned, the coarse aggregate is mylonite
	0.158 (20% 0–20)	72%		
	0.212 (20% 10–30)	63%		
	0.109 (Gran. Agg. 20% 0–125)	51%		
	0.286 (20% 20–125)	50%		
	0.166 (Cat. Agg. 20% 0–20)	68%		
	0.427 (10% 0–125)	26%		
	0.263 (20% 0–125)	54%		
Cataclasite (PEDERSEN, 2004)	0.314 (10% 0–20)	45%	AMBT (Norwegian standard)	Replacement of sand The coarse aggregate is mylonite.
	0.141 (20% 0–20)	75%		
	0.265 (20% 10–40)	54%		
Icelandic Rhyolite (PEDERSEN, 2004)	0.264 (10% 0–125)	54%	AMBT (Norwegian standard)	Replacement of sand The coarse aggregate is mylonite.
	0.041 (20% 0–20)	93%		
	0.088 (20% 10–40)	85%		
	0.126 (20% 0–125)	78%		

	Ultimate expansion	Reduction	Test	Condition
Mylonite (PEDERSEN, 2004)	0.210 (5% 0–20)	-17% (increment)	CPT (Norwegian standard)	Replacement of sand The coarse aggregate is mylonite.
	0.193 (5% 10–30)	-8% (increment)		
	0.202 (5% 0–125)	-13% (increment)		
	0.200 (10% 0–125)	-12% (increment)		
Cataclasite (PEDERSEN, 2004)	0.191 (5% 0–125)	-7% (increment)	CPT (Norwegian standard)	Replacement of sand The coarse aggregate is mylonite.
Icelandic Rhyolite (PEDERSEN, 2004)	0.041 (5% 0–125)	77%	CPT (Norwegian standard)	Replacement of sand The coarse aggregate is mylonite.

Table A2 lists PSD values according to different parameters provided.

Table A2 – Parameters used in studies as a measure of particle size.

	Maximum dimension/ Range	D10 (μm)	D50 (μm)	D90 (μm)	Blaine fineness (m²/kg)	BET (m²/kg)
Greywacke filler (TAPAS *et al.*, 2023)	–	2.44	30.50	99.21	–	–
Dacite filler (TAPAS *et al.*, 2023)	–	2.14	41.19	96.22	–	–
Orthogneiss (COUTINHO, 2019; COUTINHO; MONTEFALCO; CARNEIRO, 2024)	<150 μm	41.84	105.36	200.01	173.79	1892.4
Greywacke (ANTUNES, 2021)	–	–	30.00	–	–	–
Dolomitic argillaceous limestone (ANTUNES, 2021)	–	–	19.00	–	–	–
Siliceous limestone (GUÉDON-DUBIED *et al.*, 2000)	<100 μm	–	~16.00	–	450	–
Metaquartzite (CARLES-GIBERGUES *et al.*, 2008)	80 μm	–	–	–	100, 200, and 400	–
Siliceous limestone (CARLES-GIBERGUES *et al.*, 2008)	80 μm	–	–	–	200, 400, and 600	–
Opaline aggregate (CARLES-GIBERGUES *et al.*, 2008)	80 μm	–	–	–	200, 400, and 650	–
Sandstone (LI; HE; HU, 2015)	–	–	–	–	210, 400, 610, and 860	–
Andesite (QINGHAN et al., 1996)	–	–	–	–	780	–
Basalt (SALLES; OLIVEIRA; ANDRIOLO, 1997)	<75 μm	–	–	–	170–200	–
Mylonite (PEDERSEN, 2004)	0–20, 10–30, 20–125, 0–125 μm	–	–	–	–	–

	Maximum dimension/ Range	D10 (μm)	D50 (μm)	D90 (μm)	Blaine fineness (m²/kg)	BET (m²/kg)
Cataclasite (PEDERSEN, 2004)	0–20, 10–40, 0–125 μm	–	–	–	–	–
Icelandic Rhyolite (PEDERSEN, 2004)	0–20, 10–40, 0–125 μm	–	–	–	–	–

Table A3 lists the chemical composition of AMFs used in studies.

Table A3 – Chemical composition of AAR-reactive AMFs used in studies.

Oxide	**Siliceous limestone** (GUÉDON-DUBIED *et al.*, 2000)	**Andesite** (QINGHAN et al., 1996)	**Greywacke** (TAPAS *et al.*, 2023)	**Dacite** (TAPAS *et al.*, 2023)	**Orthogneiss** (COUTINHO; MONTEFALCO; CARNEIRO, 2024)	**Greywacke** (ANTUNES, 2021)	**Dolomitic argillaceous limestone** (ANTUNES, 2021)	**Sandstone** (LI; HE; HU, 2015)	**Metaquartzite** (CARLES-GIBERGUES *et al.*, 2008)	**Siliceous limestone** (CARLES-GIBERGUES *et al.*, 2008)	**Opaline aggregate** (CARLES-GIBERGUES *et al.*, 2008)
SiO_2	16.15	66.20	66.85	68.40	58.15	60.45	9.47	63.04	87.70	15.70	92.70
Al_2O_3	1.71	16.10	14.24	13.30	15.89	12.17	2.66	10.65	4.00	1.70	0.00
Fe_2O_3	0.76	3.40	3.80	3.30	7.44	5.21	0.90	3.23	1.00	1.10	0.30
CaO	43.12	3.30	1.94	2.40	5.19	5.21	41.51	8.78	0.40	43.6	0.20
K_2O	0.58	2.60	3.11	3.80	4.26	2.67	0.82	1.97	0.90	0.50	0.10
Na_2O	0.05	3.50	4.25	2.40	3.16	1.41	0.17	1.54	0.10	0.50	0.20
MgO	1.29	2.00	1.58	1.30	2.47	3.50	5.48	2.56	0.20	1.50	0.10
Traces	1.18	1.00	1.94	1.00	2.72	1.13	0.41	7.33	0.10	0.20	1.10
Na_2O_{eq}	0.43	5.21	6.30	4.90	5.96	3.17	0.71	2.84	0.69	0.83	0.23
L.O.I.	35.16	1.90	2.29	4.10	0.70	8.25	38.58	–	1.10	34.90	6.00